

C–H Activation for Sustainable Synthesis: Base Metal- and Electro-Catalysis

Dissertation

for the award of the degree

“Doctor rerum naturalium”

of the Georg-August-University of Göttingen



within the doctoral program

„Catalysis for Sustainable Synthesis” (CaSuS)

of the Georg-August-University School of Science (GAUSS)

submitted by

Nicolas Sauermann

from Lindlar

Göttingen, 2018

Thesis Committee

Prof. Dr. Lutz Ackermann, Institute of Organic and Biomolecular Chemistry, Göttingen

Prof. Dr. Konrad Koszinowski, Institute of Organic and Biomolecular Chemistry,
Göttingen

Prof. Dr. Matthias Tamm, Institute for Inorganic and Analytical Chemistry,
Braunschweig

Examination Board

Reviewer: Prof. Dr. Lutz Ackermann, Institute of Organic and Biomolecular Chemistry

Second Reviewer: Prof. Dr. Konrad Koszinowski, Institute of Organic and Biomolecular
Chemistry

Further Members of the Examination Board

Prof. Dr. Dietmar Stalke, Institute of Inorganic Chemistry

PD Dr. Alexander Breder, Institute of Organic and Biomolecular Chemistry

Dr. Shoubhik Das, Institute of Organic and Biomolecular Chemistry

Dr. Franziska Thomas, Institute of Organic and Biomolecular Chemistry

Date of the Oral Examination: 03.07.2018, 10.30.

Acknowledgement

Zuallererst gebührt an dieser Stelle Dank meinem Doktorvater Professor Lutz Ackermann für die Möglichkeit die vorliegende Arbeit unter seiner Anleitung anzufertigen. Neben der stets freundlichen und fachlich exzellenten Beratung sowie der Sicherstellung einer optimalen Ausstattung, ist es vor allem seine Art und Weise eine große, internationale Gruppe zu einem Team zu formen die erwähnt werden sollte.

Weiterhin danke ich Prof. Konrad Koszinowski und Prof. Matthias Tamm für die Bereitschaft die Betreuung dieser Arbeit im Rahmen des CaSuS Promotionsprogramms zu übernehmen sowie Prof. Dietmar Stalke, Dr. Alexander Breder, Dr. Shoubhik Das und Dr. Franziska Thomas für ihre Teilnahme im Rahmen der Prüfungskommission.

Auch bei den analytischen Abteilungen hier im Haus möchte ich mich für die gewissenhafte Bearbeitung aller Messaufträge bedanken, ebenso wie für die kompetente Beratung bei analytischen Problemen jeder Art.

Ich danke dem gesamten AK Ackermann für die überragende Arbeitsatmosphäre und die vielen kleinen Dinge, die die letzten Jahre bereichert haben.

Vor allem Gabi, für die Hilfe bei allen bürokratischen Herausforderungen, Karsten für die zuverlässige Bereitstellung von Chemikalien und Glasgeräten sowie Stefan für die kleineren und größeren Reparaturen, die alles am Laufen halten.

Ein ganz besonderer Dank gebührt allen Kollegen, mit denen ich die letzten Jahre verbringen durfte, allen voran Marc, Svenja, Ralf, Torben, Julian, Thomas, Alan und Tjark. Auch ein herzlicher Dank geht an Maria und Elisabetta, für die gemeinsamen Projekte. Leo, Julian, Valentin, Torben und Tjark danke ich für die äußerst gewissenhafte Korrektur dieser Arbeit.

Mein größter Dank gebührt jedoch meiner Familie, die mich während der Studienzeit und auch in der Promotion immer bedingungslos unterstützt hat und ohne die dies alles nie möglich gewesen wäre. Zum Schluss danke ich noch meiner liebsten Jasmin, für die stete Unterstützung, Geduld und ihre Liebe

Contents

1 Introduction	1
1.1 Transition Metal-Catalyzed C–H Activation	1
1.2 Cobalt-Catalyzed C–H Activation	5
1.2.1 C–H Activation with Well-Defined Cobalt Complexes	6
1.2.2 C–H Activation using Low-Valent Cobalt Catalysis	8
1.2.3 C–H Activation using High-Valent Cobalt Catalysis	15
1.2.4 Oxidative C–H Activation using Cobalt Salts.....	21
1.3 Manganese-Catalyzed C–H Activation	27
1.4 Electrochemical Transition Metal-Catalyzed C–H Activation.....	31
1.4.1 Palladium-Catalyzed Transformations	33
1.4.2 Transformations Catalyzed by other Transition Metals	37
2 Objectives	40
3 Results and Discussion	43
3.1 Cobalt-Catalyzed Alkenylation under Triazolylidene-Assistance by C–H/C–O Cleavage	43
3.1.1 Optimization	44
3.1.2 Scope of the Cobalt-Catalyzed Alkenylation using Alkenyl Phosphates ...	46
3.1.3 Scope of the Cobalt-Catalyzed Alkenylation using Alkenyl Acetates	49
3.1.4 Mechanism of the Cobalt-Catalyzed Alkenylation	54
3.2 Cobalt-Catalyzed Allylation using Allyl Acetates.....	55
3.2.1 Optimization and Scope	56
3.3 Base Metal-Catalyzed C–H Alkynylation	58
3.3.1 Optimization of the Cobalt-Catalyzed C–H Alkynylation.....	58
3.3.2 Scope of the Cobalt-Catalyzed C–H Alkynylation	60
3.3.3 Mechanistic Studies	64
3.3.4 Proposed Catalytic Cycle	65
3.3.5 Diversification of the Alkynylated Indoles	66
3.3.6 Optimization of the Manganese-Catalyzed C–H Alkynylation	67
3.3.7 Scope of the Manganese-Catalyzed C–H Alkynylation	70
3.3.8 Mechanistic Studies for the Manganese-Catalyzed Alkynylation	75
3.4 Electrochemical Cobalt-Catalyzed C–H Oxygenation	79
3.4.1 Optimization of the Cobalt-Catalyzed Electrochemical C–H Oxygenation	79
3.4.2 Scope of the Cobalt-Catalyzed Electrochemical C–H Oxygenation	84

3.4.3 Mechanistic Studies and Proposed Mechanism.....	92
3.5 Electrochemical Cobalt-Catalyzed C–H Amination.....	97
3.5.1 Optimization of the Cobalt-Catalyzed Electrochemical C–H Amination.....	97
3.5.2 Scope of the Electrochemical Cobalt-Catalyzed C–H Amination	102
3.5.3 Mechanistic Studies and Proposed Mechanism.....	109
3.6 Mechanistic Studies on Transition Metal-Catalyzed Electrochemical C–H Activation.....	114
3.6.1 Cobalt-Catalyzed Electrochemical Annulation of Terminal and Internal Alkynes using an Electrocleavable Directing Group.....	115
3.6.2 Rhodium-Catalyzed C–H/O–H Annulation of Benzoic Acids.....	119
4 Summary and Outlook	122
5 Experimental Part	127
5.1 General Remarks	127
5.1.1 Vacuum.....	127
5.1.2 Chromatography	127
5.1.3 Gas Chromatography.....	127
5.1.4 Nuclear Magnetic Resonance	128
5.1.5 Mass Spectrometry	128
5.1.6 Melting Points.....	128
5.1.7 Infrared Spectroscopy	128
5.1.8 Electrochemistry.....	129
5.1.9 Solvents	129
5.1.10 Chemicals	129
5.2 General Procedures	130
5.3 Cobalt-Catalyzed C–H Alkenylation under Triazole Assistance	133
5.3.1 Analytical Data and Experimental Procedures	133
5.4 Cobalt-Catalyzed Allylation of Indoles	146
5.4.1 Analytical Data and Experimental Procedures	146
5.5 Base-Metal Catalyzed C–H Alkynylation	149
5.5.1 Analytical Data and Experimental Procedures	149
5.5.2 Mechanistic Experiments for the Cobalt Catalysis	165
5.5.3 Mechanistic Experiments for the Manganese Catalysis	167
5.6 Electrochemical Cobalt-Catalyzed C–H Oxygenation	177
5.6.1 Analytical Data and Experimental Procedures	177
5.6.2 Mechanistic Studies	189

5.7 Electrochemical Cobalt-catalyzed C–H Amination	199
5.7.1 Analytical Data and Experimental Procedures	199
5.7.2 Mechanistic Studies	209
5.8 Mechanistic Experiments for Electrochemical C–H Activation.....	215
6 References	223

List of Abbreviations

Ac	acetyl
acac	acetylacetonate
Alk	alkyl
AMLA	ambiphilic metal-ligand activation
aq	aqueous
Ar	aryl
atm	atmospheric pressure
BIES	base-assisted internal electrophilic substitution
Bn	benzyl
Boc	<i>tert</i> -butyloxycarbonyl
Bu	butyl
calc.	calculated
cat.	catalytic
CCE	constant current electrolysis
CMD	concerted metalation deprotonation
Cp	cyclopentadienyl
Cp*	pentamethylcyclopentadienyl
CV	Cyclic voltammetry
Cy	cyclohexyl
δ	chemical shift
d	doublet
DCE	1,2-dichloroethane

dd	doublet of doublets
DG	directing group
DMF	<i>N,N</i> -dimethylformamide
DMSO	dimethylsulfoxide
dt	doublet of triplets
ee	enantiomeric excess
EI	electron ionization
equiv	equivalent
ESI	electrospray ionization
Et	ethyl
g	gram
GC	gas chromatography
h	hour
HFIP	1,1,1,3,3,3-hexafluoro-2-propanol
HRMS	high resolution mass spectrometry
Hz	Hertz
<i>i</i>	<i>iso</i>
IMes	1,3-bis(2,4,6-trimethylphenyl)imidazole-2-ylidene
IPr	1,3-bis(2,6- <i>iso</i> -propylphenyl)imidazole-2-ylidene
IR	infrared spectroscopy
<i>J</i>	coupling constant
KIE	kinetic isotope effect
L	ligand
<i>m</i>	<i>meta</i>
m	multiplet

M	molar
[M] ⁺	molecular ion peak
mA	milliampere
Me	methyl
Mes	mesityl
mg	milligram
MHz	megahertz
min	minute
mL	milliliter
mmol	millimole
M. p.	melting point
MS	mass spectrometry
<i>m/z</i>	mass to charge ratio
napht	naphthenate
NCTS	<i>N</i> -cyano-4-methyl- <i>N</i> -phenyl-benzenesulfonamide
NHC	N-heterocyclic carbene
NMR	nuclear magnetic resonance
<i>o</i>	<i>ortho</i>
ox	oxalate
<i>p</i>	<i>para</i>
Ph	phenyl
PIP	(2-pyridin-2-yl)isopropylamine
Piv	pivaloyl
ppm	parts per million
Pr	propyl

Py	pyridyl
PyO	pyridine- <i>N</i> -oxide
q	quartet
Q	8-aminoquinoline
RT	room temperature
RVC	Reticulated vitreous carbon
s	singlet and second
SET	single electron transfer
SPS	solvent purification system
<i>t</i>	<i>tert</i>
t	triplet
<i>T</i>	temperature
TEMPO	2,2,6,6-tetramethylpiperidine- <i>N</i> -oxide
TFE	2,2,2-trifluoroethanol
THF	tetrahydrofuran
TIPS	tri- <i>iso</i> -propylsilyl
TLC	thin layer chromatography
TM	transition metal
TMS	trimethylsilyl
TS	transition state
V	Volt
X	(pseudo-)halide

1 Introduction

In the last century, organic synthesis has made tremendous progress, which has affected the daily lives of billions of people. Valuable products of organic synthesis are used for a wide range of applications ranging from pharmaceuticals and crop-protection agents to functional materials, such as OLEDs, coloring agents and polymers.^[1] Although these products unarguably present a huge benefit in their diverse applications, their synthesis is associated with a number of drawbacks, for example a huge amount of toxic waste, the depletion of limited natural resources and overall high energy consumption.^[2]

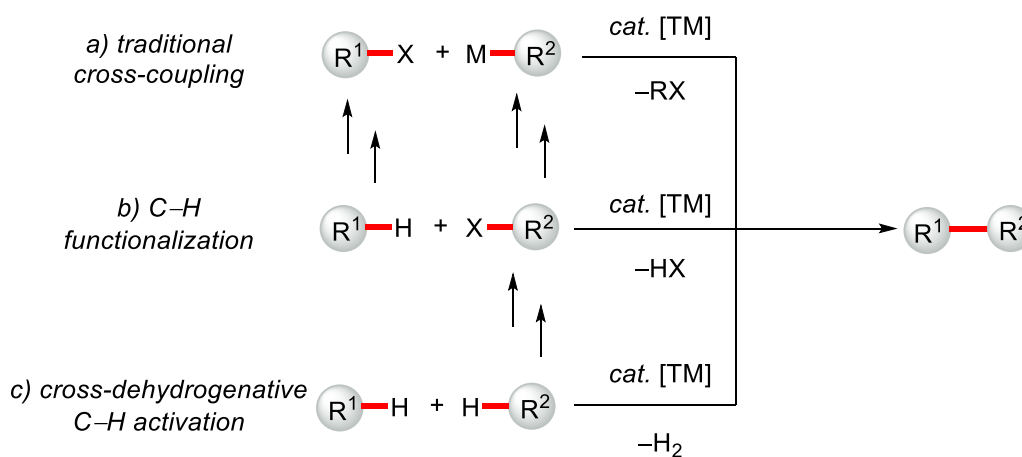
Therefore, in 1998, Anastas and Warner proposed their *12 Principles of green chemistry*,^[3] which outlined ways to reduce the ecological footprint of organic synthesis and minimize the amounts of byproducts and waste. Among them are the use of catalytic transformations, avoidance of unnecessary prefunctionalization and auxiliaries to increase the atom economy, use of mild reaction conditions (e.g. ambient temperature) and renewable sources for chemicals and the use of nontoxic reagents and solvents.

1.1 Transition Metal-Catalyzed C–H Activation

Although the beginnings of transition metal-catalyzed coupling chemistry^[4] can be traced back to *inter alia* the early copper-catalyzed reactions by Glaser^[5] and Ullmann,^[6] it was not until the discovery of palladium-catalyzed cross-couplings that these transformations found considerable use in organic synthesis.^[7] However, once established, palladium-catalyzed cross-coupling chemistry soon became the benchmark process for the formation of C–C and C–Het bonds. In time, a wide range of methods using different organometallic coupling partners were realized, resulting in a range of well-known named reactions, such as Suzuki-Miyaura,^[8] Negishi,^[9] Kumada-Corriu,^[10] Hiyama,^[11] Stille^[12] and Sonogashira-Hagihara^[13] cross coupling reactions. Furthermore, although not a cross coupling reaction its traditional sense, the Mizoroki-Heck^[14] reaction and the Buchwald-Hartwig amination^[15] should be mentioned as milestones in palladium-catalyzed chemistry. These important

contributions were recognized with the award of the Chemistry Nobel Prize to Heck, Negishi and Suzuki in 2010.^[16]

Despite recent efforts to render cross-coupling chemistry more environmentally benign and cost effective by the use of earth-abundant metals, such as iron^[17] or nickel,^[18] and the use of renewable solvents,^[19] the major drawback of cross-coupling chemistry remains, namely the need for prefunctionalized starting materials. Moreover, these materials are in most cases either not stable under ambient conditions (Grignard reagents, organolithium and organozinc compounds) or toxic (organotin compounds). Therefore, the direct functionalizations of C–H bonds is extremely desirable in terms of the step- and atom-economy of organic syntheses (Scheme 1.1).^[20]



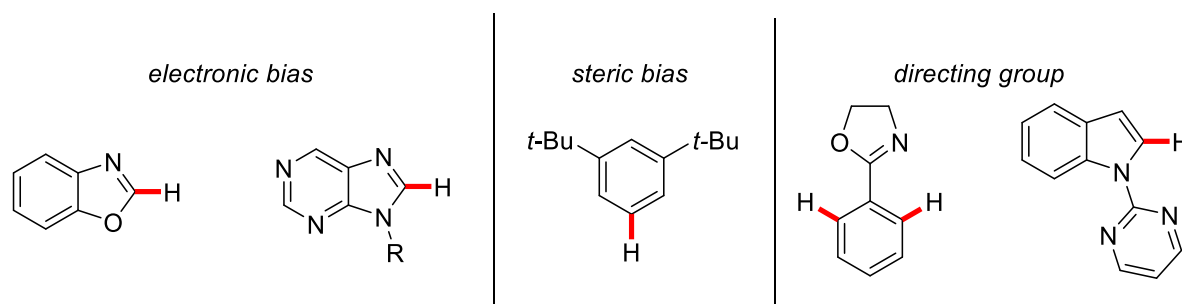
Scheme 1.1. Comparison of traditional cross-coupling chemistry versus C–H activation.

While the most atom efficient reaction is in principle the cross-dehydrogenative C–H activation, which formally only generates hydrogen as a byproduct, these reactions suffer from the need for a stoichiometric oxidant, resulting in additional waste (Scheme 1.1.c). Moreover, common oxidants include expensive and toxic silver(I) and copper(II) salts. While direct C–H functionalization using organic electrophiles requires a degree of prefunctionalization in one coupling partner (Scheme 1.1.b), the substance classes most often employed, organic halides and phenol derivatives are accessible within a reasonable number of steps and largely stable under ambient conditions.^[21] Traditional cross-coupling meanwhile (Scheme 1.1.a) does not only require an electrophilic coupling partner, but also an additional nucleophilic organometallic reagent.

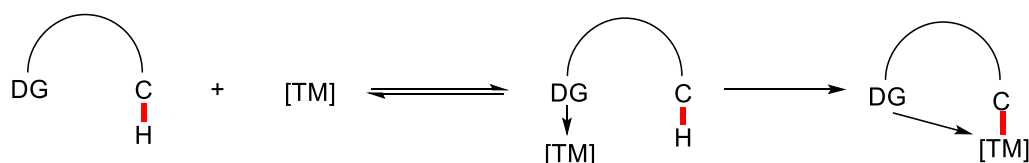
In contrast to traditional cross-coupling reactions, C–H functionalization faces an additional challenge besides the activation of otherwise inert C–H bonds. While the new connection in cross-coupling chemistry is clearly defined by the substitution

pattern of the electrophile and nucleophile, organic molecules contain a large number of C–H bonds with similar bond dissociation energies (113.5 kcal/mol for C(sp²)–H bonds in benzene).^[22] This problem can be overcome in mainly three ways: (i) the use of electronically activated substrates, where one C–H bond has a higher kinetic acidity than the others, (ii) steric shielding of C–H bonds where the reaction is undesired and (iii) the use of lewis-basic directing groups (DG) to coordinate to the transition metal catalyst in close proximity to the C–H bond to be functionalized (Scheme 1.2).^[23]

a) Differentiation of C–H bonds



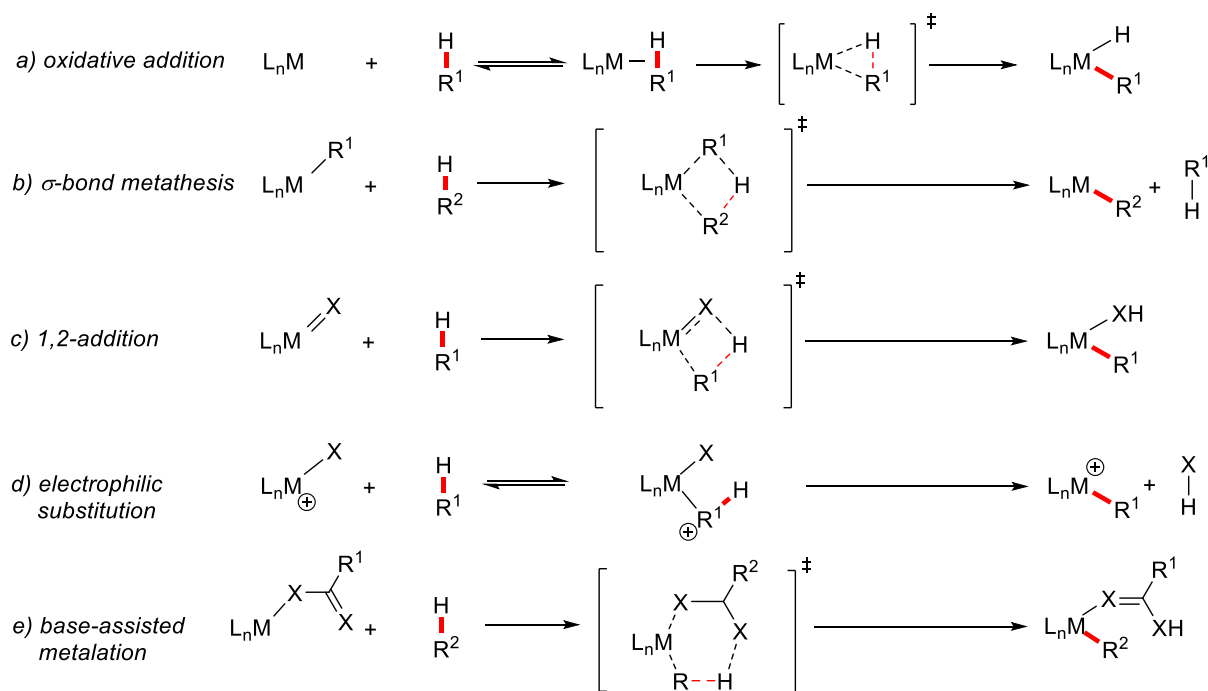
b) Influence of the directing group (DG)



Scheme 1.2. a) Differentiation of C–H bonds. b) Influence of the directing group.

While the first two options are severely limited in substrate scope, the directing group approach shows tremendous potential. This holds especially true if the directing group is an important building block of the target molecule or is easily removed or modified.^[24]

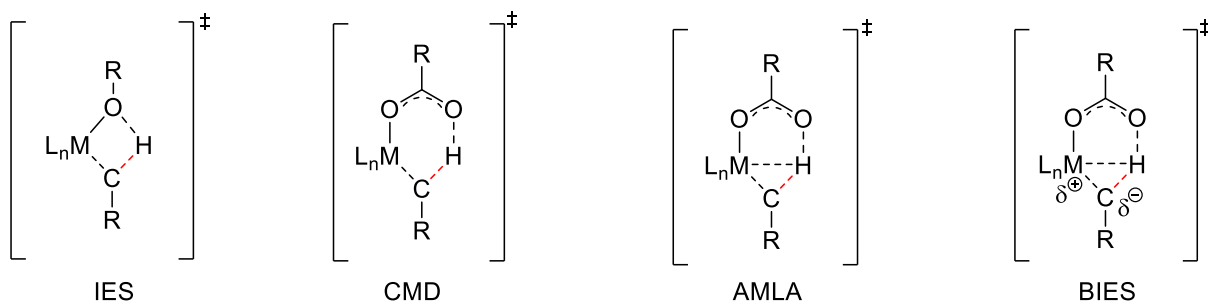
The key step for C–H functionalization reactions is often the cleavage of the C–H bond itself. Therefore, C–H bond cleavage was and still is studied in close detail, resulting in different modes of action being identified (Scheme 1.3).^[25]



Scheme 1.3. Modes of action for various C–H cleavage mechanisms under transition metal assistance.

Oxidative addition to cleave C–H bonds was mostly observed with electron-rich complexes of late transition metals.^[25a] For early transition metals with d^0 -configuration, this mode of action is obviously not feasible. In contrast, σ -bond metathesis and 1,2-addition are possible ways to achieve C–H activation with early transition metals,^[25b] while electrophilic substitution was proposed for cationic complexes of late transition metals.^[25c] In recent years, base-assisted C–H activation has gained traction as a model for C–H cleavage in C–H functionalizations using basic additives.^[25a]

This base-assisted C–H cleavage was the object of further research, resulting in the proposal of several transition states (Scheme 1.4).



Scheme 1.4. Transition state models for base-assisted C–H metalation.

Intramolecular electrophilic substitution (IES),^[26] the mechanism for alkoxide bases relies on a highly strained, thus high-energy four-membered ring transition state.

Concerted metalation-deprotonation (CMD)^[27] and ambiphillic metal-ligand activation (AMLA)^[28] were disclosed independently and describe the interaction of metal, carboxylate-ligand and C–H bond especially for electron-deficient substrates. In contrast, base-assisted internal substitution (BIES)^[29] was proposed to explain the preferred reactivity of electron-rich substrates in several transformations.

Despite tremendous progress in the recent decades regarding C–H activation,^[4, 30] most of these advances were realized using cost-intensive and toxic 4d and 5d transition metals, such as rhodium,^[31] iridium,^[32] palladium^[33] and ruthenium.^[34] Here, new opportunities remain for the development of 3d transition metal-catalyzed C–H activation with possible benefits due to the significantly lower toxicity, abundance and lower price of the employed metal catalysts.

1.2 Cobalt-Catalyzed C–H Activation

Cobalt is one of the more abundant elements in the earth crust, with a concentration of approximately 25 ppm, compared to 1 ppb for noble metals, such as iridium and rhodium.^[35] The result is a relatively low price for cobalt salts, which makes the use of cobalt as a catalyst quite attractive.^[36]

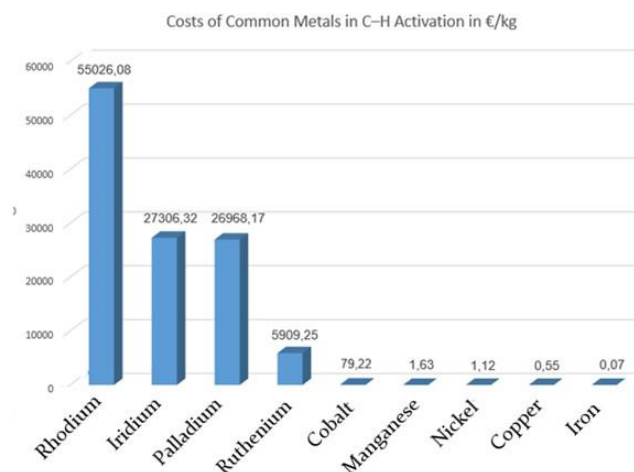
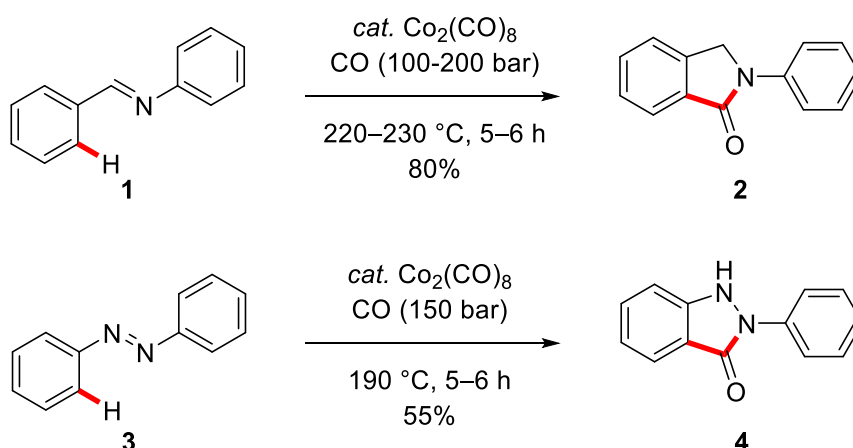


Figure 1.1. Prices of metals in C–H activation.

Therefore, a wide range of transformations are known employing cobalt catalysis, such as hydroformylation,^[37] the Bönnemann pyridine synthesis,^[38] the Pauson-Khand reaction,^[39] the Jacobsen kinetic resolution of epoxides^[40] and the coupling of Grignard reagents in the Kharash-coupling,^[41] to name a few examples.

Indeed, even cobalt-catalyzed C–H activation is not a new concept, and the groundbreaking work published by Murahashi in 1955 is not only the first catalytic C–H activation with cobalt, but among the first examples of C–H activation in general (Scheme 1.5).^[42] Although the reaction proceeded under harsh conditions and the scope was severely limited, it highlighted the use of simple and stable cobalt complexes as catalysts.

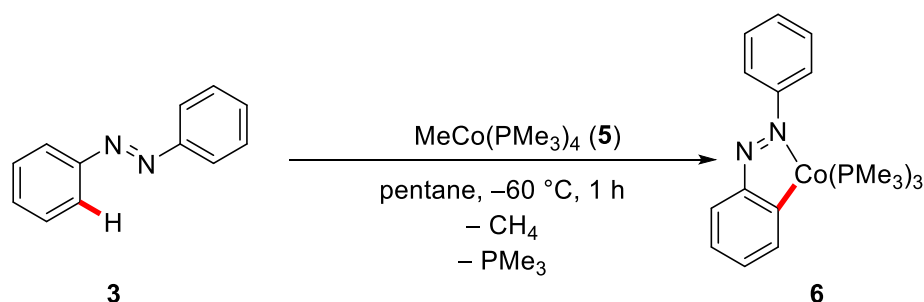


Scheme 1.5. Murahashis cobalt-catalyzed carbonylation of benzaldimine **1** and azobenzene **3**.^[42]

Despite these early advances, cobalt-catalyzed C–H activation did not receive much attention for the next decades. The recent progress in the field will be discussed in the next chapters. For this thesis, cobalt-catalyzed C–H activation will be divided into four parts: (i) C–H activation with well-defined complexes, (ii) low-valent cobalt-catalyzed C–H activation, (iii) $\text{Cp}^*\text{Co}(\text{III})$ -catalyzed C–H activation and (iv) oxidative C–H activation using simple cobalt salts.

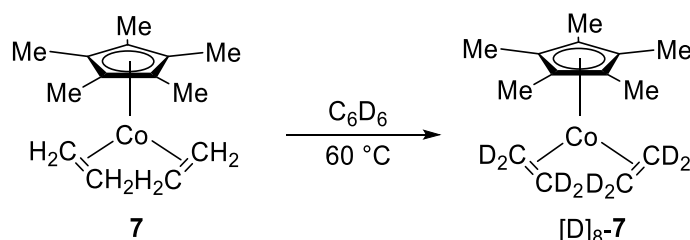
1.2.1 C–H Activation with Well-Defined Cobalt Complexes

In the early 1990s, Klein showed in a stoichiometric reaction that the cobalt phosphine complex **5** was able to metalate C–H bonds of several substrates (Scheme 1.6).^[43] Besides the depicted five-membered species,^[43a-d, 43f] four-^[43e] and six-membered^[43d] rings could also be obtained.



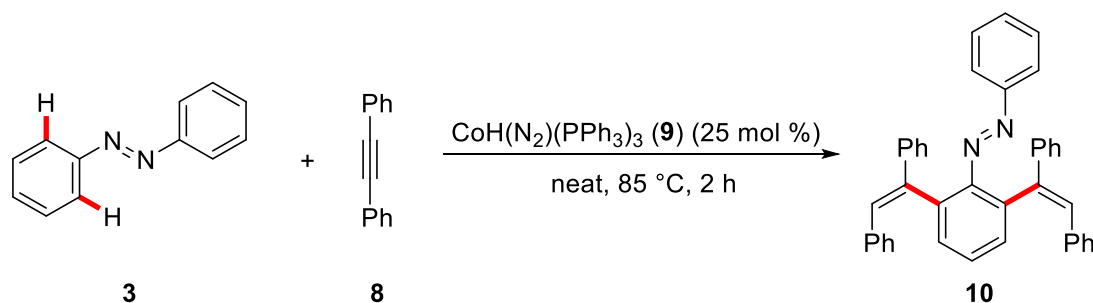
Scheme 1.6. Stoichiometric C–H metalation using complex **5**.^[43f]

Furthermore, Brookhart disclosed that well-defined cobalt ethylene complex **7** enabled deuterium scrambling if heated in benzene- d_6 . Through various steps of insertion and elimination, the completely deuterated complex $[\text{D}]_8\text{-7}$ was thereby available (Scheme 1.7).^[44]



Scheme 1.7: H/D scrambling in Brookhart's complex **7**.^[44]

In a groundbreaking contribution, Kisch reported on the hydroarylation of alkynes **8** with catalytic amounts of cobalt-hydride complex **9**.^[45] Although limited in scope and practicability, this work presented the first substoichiometric use of a well-defined cobalt(I) complex in C–H activation (Scheme 1.8).

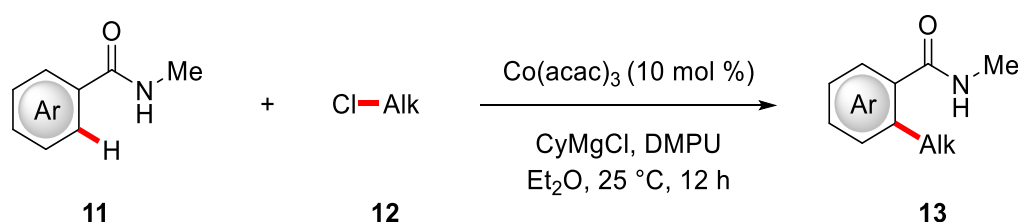


Scheme 1.8: Hydroarylation of toluene **8** using Kisch's complex **9**.^[45]

Subsequently, similar work in this field was performed in the 2010s by Petit. However so far, these systems remain limited to the addition of C–H bonds to C–C double or triple bonds.^[46]

1.2.2 C–H Activation using Low-Valent Cobalt Catalysis

While the early work by Kisch highlighted the potential of low-valent complexes for C–H activation,^[45] their instability towards air and moisture makes their handling rather difficult. In reference to the Kharash coupling,^[41] Nakamura and coworkers proposed the generation of a low-valent cobalt species *in situ* from a cobalt salt and a Grignard reagent (Scheme 1.9).^[47] Hence, a combination of $\text{Co}(\text{acac})_3$ and cyclohexylmagnesiumchloride was able to catalyze the hydroarylation as well as the direct alkylation of benzamides **11**.



Scheme 1.9. Alkylation of benzamides **11** by Nakamura.^[47]

Besides the fact that this method is more user-friendly than the direct use of cobalt(I) or cobalt(0) species, its biggest benefit may be the highly modular approach to optimizing the reaction conditions. After Nakamura's initial report, this flexibility was shown in subsequent reports by Ackermann and Yoshikai, among others.^[48] A List of ligands commonly employed in low-valent cobalt catalysis is shown below (Figure 1.2). It should be noted, that most reactions are highly specific to the substitution pattern of the ligand, and even small changes can shut down the observed reactivity.

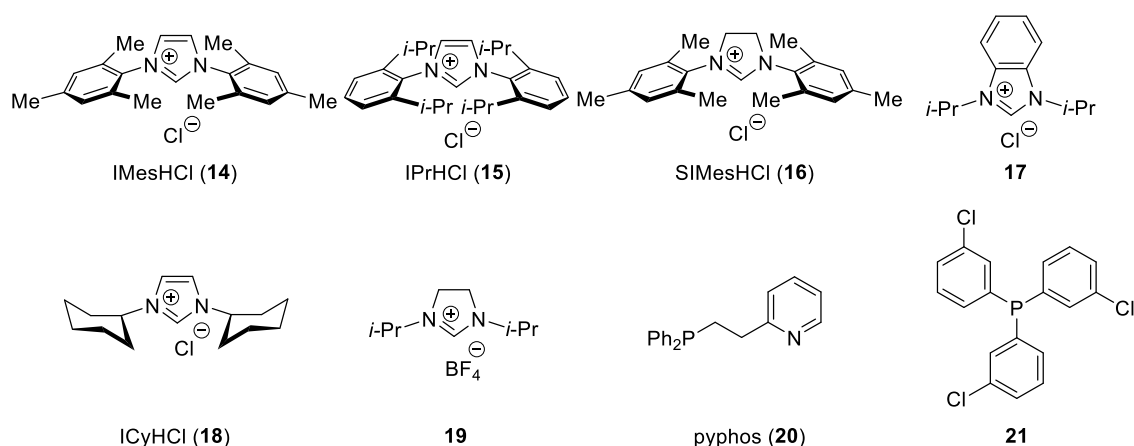
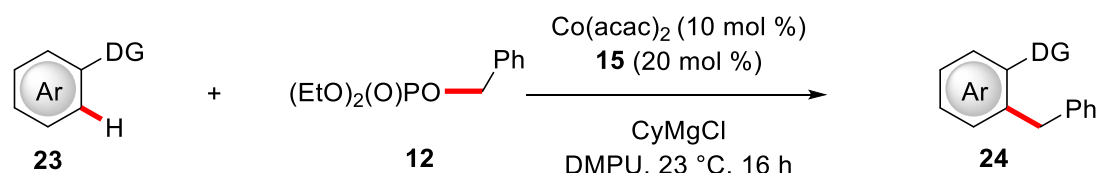


Figure 1.2. Common (pre)ligands in cobalt-catalyzed C–H activation.

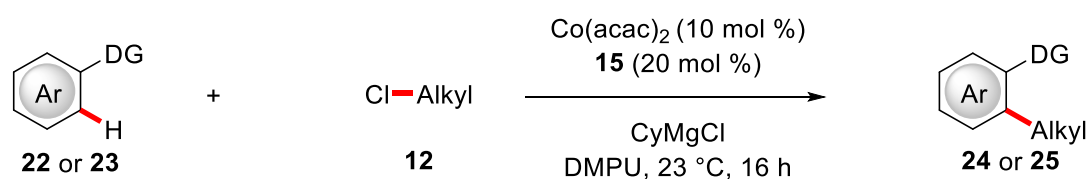
In contrast to the reactions published using well-defined complexes,^[45-46] this approach also enables coupling-type chemistry besides simple hydrofunctionalization.

Ackermann^[49] disclosed the alkylation of 2-arylpyridines **22** and pyrimidylindoles **23**, with a report from Yoshikai^[50] broadening the scope of directing groups to ketimines **26** (Scheme 1.10).

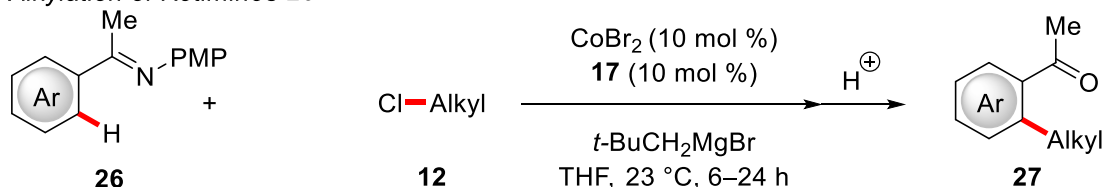
a) C–H Benzylation



b) C–H Alkylation of Arylpyridines **22** and Pyrimidines **23**



c) C–H Alkylation of Ketimines **26**

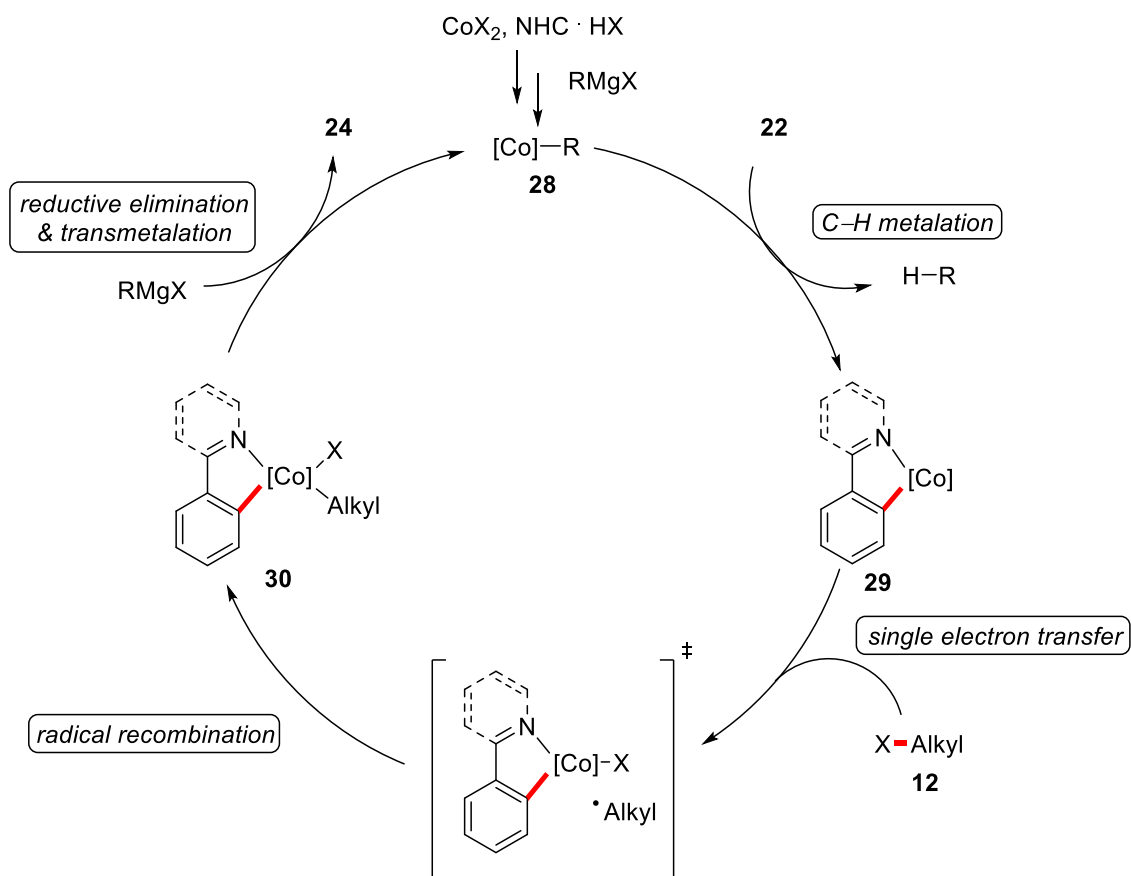


Scheme 1.10. Cobalt-catalyzed primary and secondary C–H alkylations.^[49-50]

Both reports showed the possibility to utilize primary as well as secondary alkyl chlorides **12**. Although the reaction conditions are somewhat similar, it should be noted, that CyMgCl is more cost effective than the corresponding neopentylmagnesiumbromide.^[51] Along the same lines, an unprecedented benzylation was published by Ackermann (Scheme 1.10a).^[52]

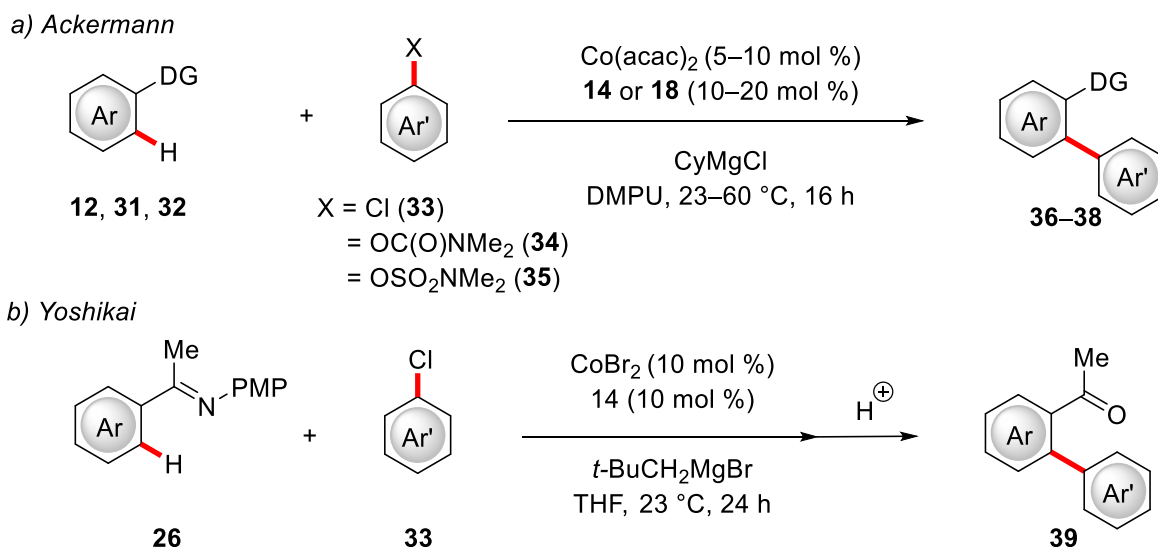
Based on mechanistic experiments performed to gain insight into the mode of action of the low-valent cobalt-catalyzed alkylation, a plausible catalytic cycle was proposed (Scheme 1.11).^[48d] The reaction is initiated by the formation of the ill-defined active species **28** from the cobalt salt, NHC (pre-)ligand and the Grignard reagent. This species can perform C–H metalation, either by oxidative addition of the C–H bond due to the electron-rich cobalt species or by ligand to ligand hydrogen transfer (LLHT).^[48a] Subsequently, the alkyl halide **12** is activated by single electron transfer,^[48d] followed by radical recombination to generate intermediate **30**. Reductive elimination of the product **24** and transmetalation with another equivalent of the Grignard reagent regenerates the catalytically active species **28**.

Besides alkylations, also C–H arylation reactions have been reported using this approach, beginning with Ackermann in 2012^[49, 52] (Scheme 1.12). A variety of substrates, such as ketimines **26**,^[50] benzamides **12** and tetrazoles **31**^[53] as well as oxazolines **32**^[54] have here been utilized, highlighting the versatility of this strategy.



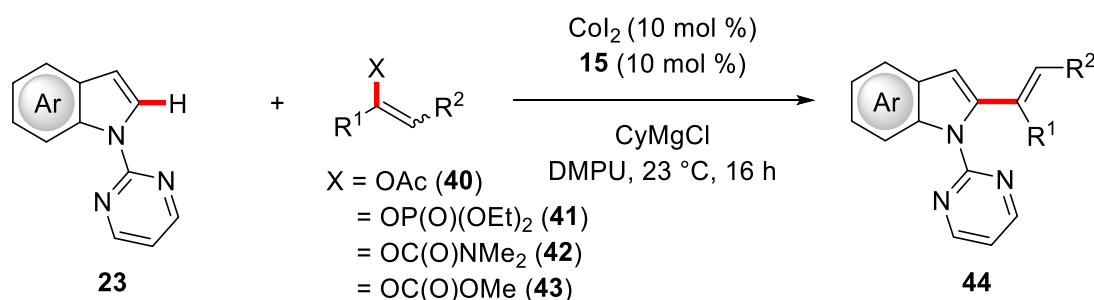
Scheme 1.11. Plausible catalytic cycle for the cobalt-catalyzed C–H alkylation.^[48d]

The mechanism of low-valent cobalt-catalyzed C–H arylations is rationalized to be similar to the related alkylations.^[48d] Additionally, besides halides **33**, phenol derivatives **34** and **35** also proved to efficiently yield the desired products **36–38**.



Scheme 1.12. Cobalt-catalyzed C–H arylations.^[49-50, 52-54]

Related electrophiles, enol acetates **40**, phosphates **41**, carbamates **42** and carbonates **43**, which are easily accessible from the related ketones,^[55] were shown by Ackermann to be viable substrates in cobalt-catalyzed direct C–H alkenylations (Scheme 1.13).^[56]



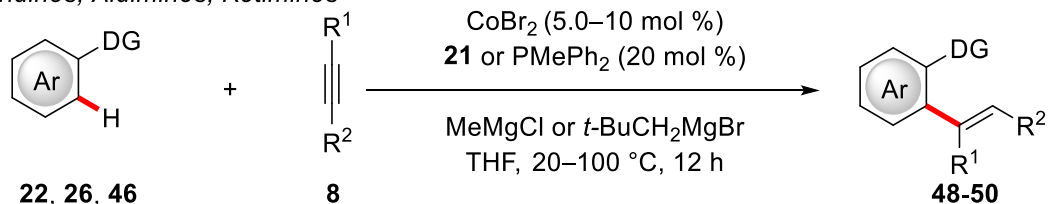
Scheme 1.13. Cobalt-catalyzed C–H alkenylation of indoles **23**.^[56]

Advantages of this method are the excellent regioselectivity in cases of unsymmetrical substrates **40** and the possibility to use cyclic enol electrophiles **40-43**, both of which are usually not achieved in alkyne hydroarylation.^[48a] Indeed, for low-valent cobalt-catalyzed C–H activation, several hydroarylation reactions are known. For alkynes **8**, Yoshikai disclosed examples using simple phosphines as ligands and various directing groups, such as phenylpyridines **22**,^[57] indoles **23** and imidazoles **45**^[58] as well as aldimines **46** and ketimines **26** (Scheme 1.14).^[59] Additionally, when alkenes **47** were used instead of arenes, heterocycle synthesis by hydro-functionalization proved possible.^[60] Furthermore, Yoshikai also developed hydroarylations of alkynes **8** using the inherent kinetic acidity of heterocycles.^[61] A catalytic cycle was rationalized to

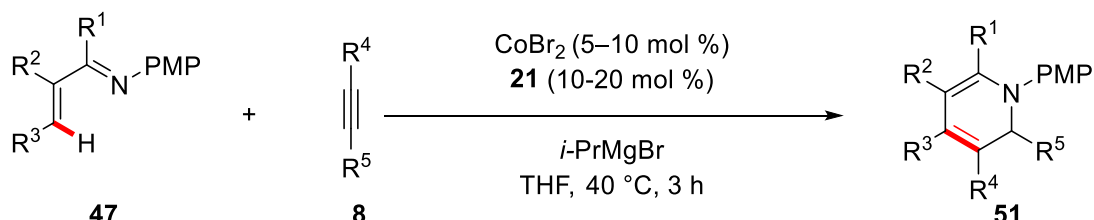
include the generation of the active cobalt species **56**, followed by precoordination of alkyne **8** to the metal center (Scheme 1.15).^[48c] Then, C–H activation takes place, most probably by oxidative addition of the C–H bond. After cyclometallation, migratory insertion of alkyne **8** into the Co–H bond yields vinylic cobalt species **59**, furnishing the desired product **49** via reductive elimination.

Besides alkynes **8**, also alkenes **60** were identified as viable substrates. Here, the possibility of branched or linear selectivity offers a further challenge. Beginning with work from Nakamura, who explored hydroarylation of unactivated alkenes **60**,^[47] Yoshikai broadened the field of cobalt-catalyzed alkene hydroarylation by the use of phenylpyridines **22**^[62] and imines **26** and **46**^[63] using activated alkenes **60** (Scheme 1.16). It is noteworthy, that linear/branched products **61** and **62** could be selectively accessed using different combinations of ligand and Grignard reagents.

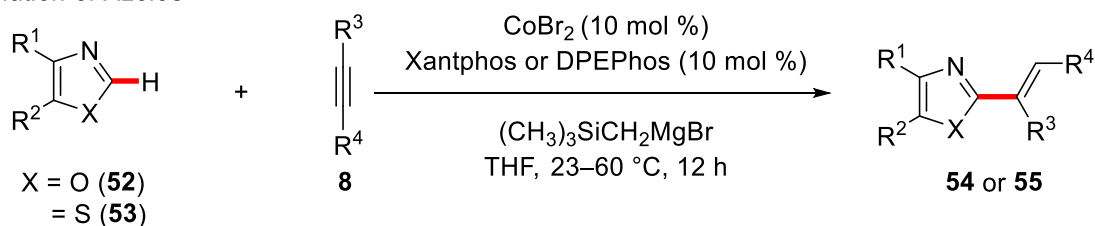
a) Phenylpyridines, Aldimines, Ketimines



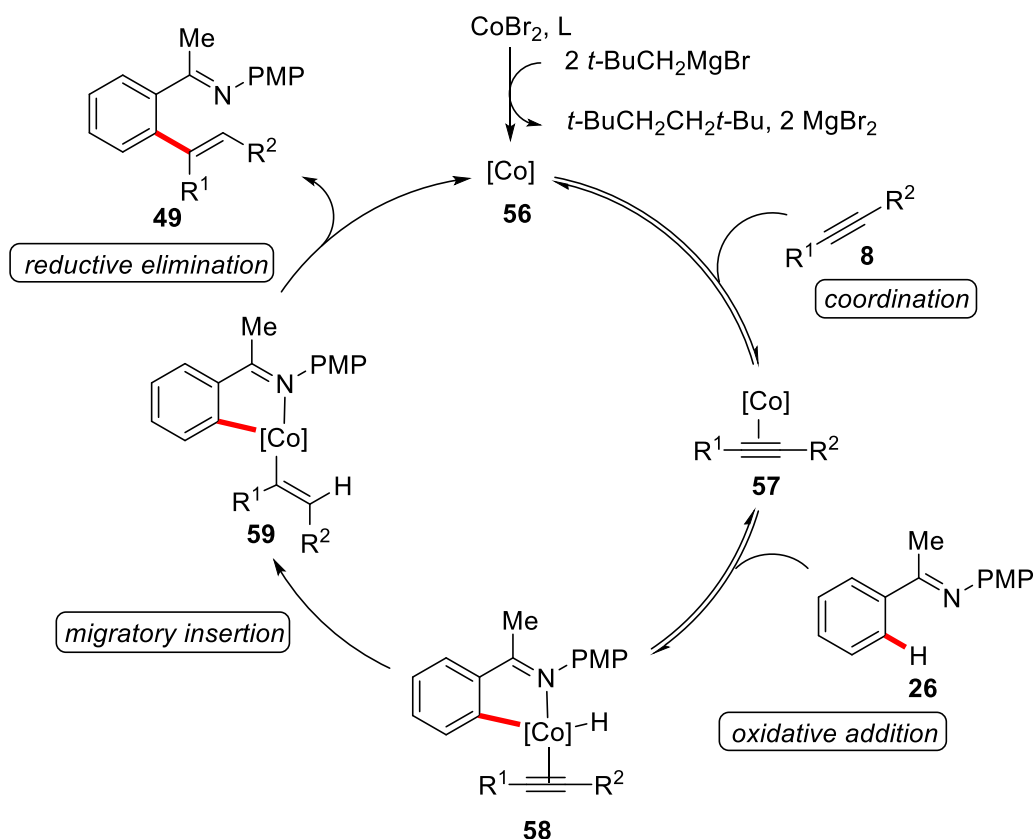
b) C–H activation of Alkenes



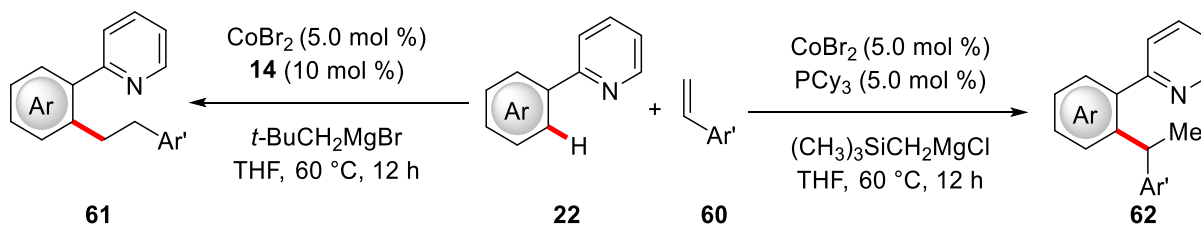
c) Hydroarylation of Azoles



Scheme 1.14. Hydroarylation of alkynes **8**.^[57-61]



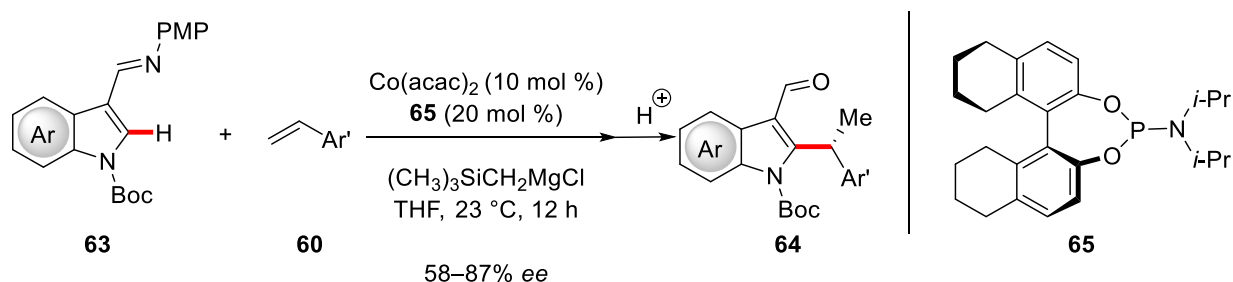
Scheme 1.15. Proposed catalytic cycle for alkyne hydroarylation.^[48c]



Scheme 1.16. Hydroarylation of alkenes **60** with switchable selectivity.^[62]

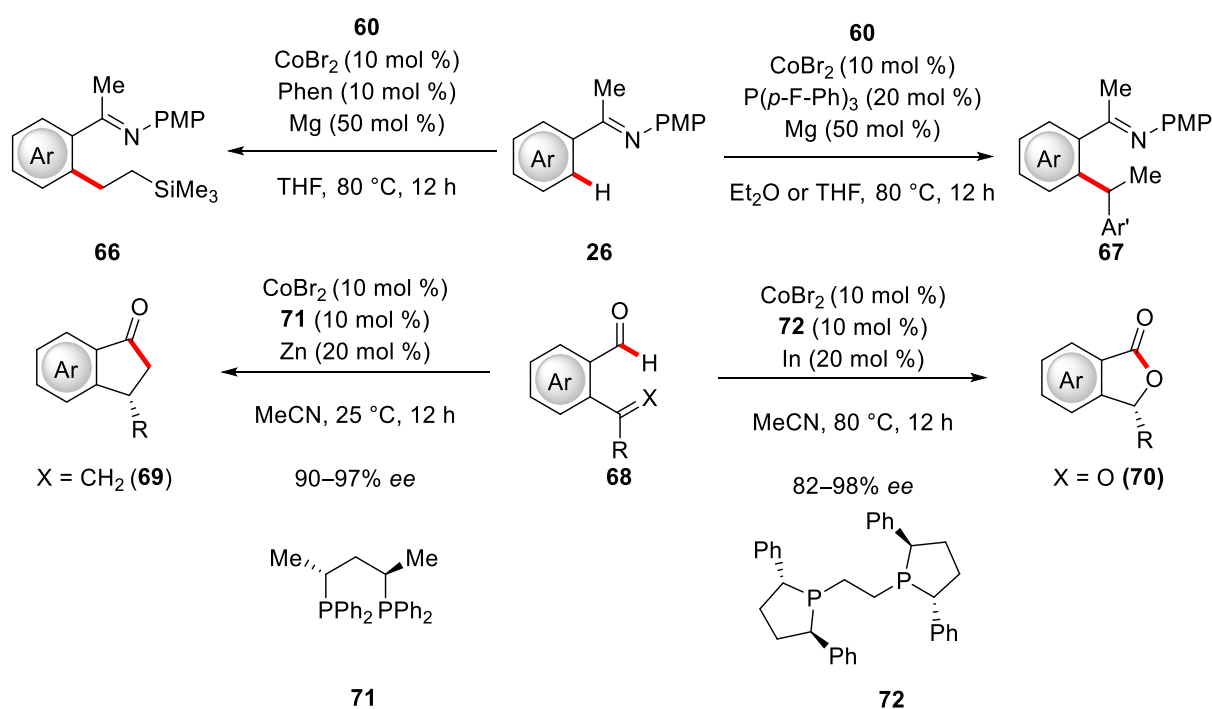
The proposed mechanism was generally comparable to the mechanism proposed for the hydroarylation of alkynes **8**.^[48c]

The branched-selective hydroarylation of alkenes **60** offers the potential to conduct these reactions in an enantioselective fashion. Indeed, Yoshikai disclosed a cobalt-catalyzed asymmetric C–H alkylation by the use of $\text{Co}(\text{acac})_2$ and ligand **65** (Scheme 1.17).^[64]



Scheme 1.17. Enantioselective hydroarylation of styrenes **60**.^[64]

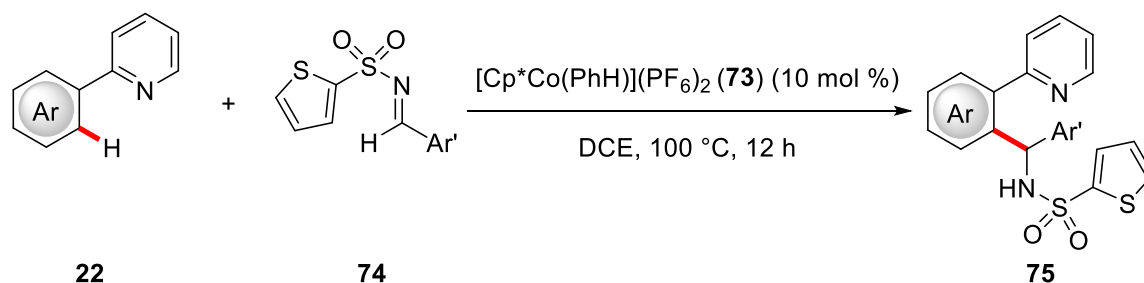
While the majority of low-valent cobalt-catalyzed C–H functionalizations are based on the use of Grignard reagents, there are inherent drawbacks associated; for instance, limited tolerance for electrophilic functional groups, such as cyano groups and aldehydes. Therefore, the substitution of the Grignard reagent with another reductant would be beneficial. To this end, magnesium, zinc or indium were identified as viable reductants, however these reactions remain limited to simple hydrofunctionalizations.^[65] Thus, hydroacylations were achieved in an intramolecular, enantioselective fashion by assistance of a chiral phosphines **71** and **72** (Scheme 1.18). Although the first contributions using a metal reductant were reported in 2014, progress in this field has been limited, and the diversity of the disclosed reactions cannot be compared to that of low-valent cobalt catalysis employing Grignard-reagents.



Scheme 1.18. Low-valent cobalt-catalyzed C–H activation using metal reductants.^[65]

1.2.3 C–H Activation using High-Valent Cobalt Catalysis

Despite tremendous progress by low-valent cobalt catalysis under rather mild conditions,^[48b, 48d] these transformations suffer from a lack of functional group tolerance. Especially the functionalization of molecules containing sensitive or protic functional groups, such as aldehydes, ketones, esters, nitro- and hydroxyl-groups are difficult or impossible. Therefore, demand for an air-stable, easy to handle and robust cobalt catalyst grew. Inspired by the Brookhart contributions,^[44] this demand was met in an important work from Matsunaga and Kanai, establishing the known Cp*Co(III)-complex **73**^[66] as a competent catalyst in the hydroarylation of imines **74** with phenylpyridines **22**^[67] (Scheme 1.19) and later pyrimidylindoles **23**.^[68]



Scheme 1.19. Hydroarylation of imines **74** using Cp*Co(III).^[67]

While the reaction temperatures were mostly higher than in the low-valent cobalt catalysis, the catalyst is generally more stable and robust and therefore offers a larger functional group tolerance. Furthermore, the Cp*Co(III)-catalysis generally offers a wide range of C–X bond formations,^[48a, 69] being somewhat orthogonal in reactivity to the low-valent systems. Over time, a variety of Cp*-derived Co(III)-complexes have been synthesized, the structures of which are summarized below (Figure 1.3).^[48a] However, simple Cp*Co(CO)₂ (**81**) is by far the most commonly employed complex in Co(III)-catalysis.

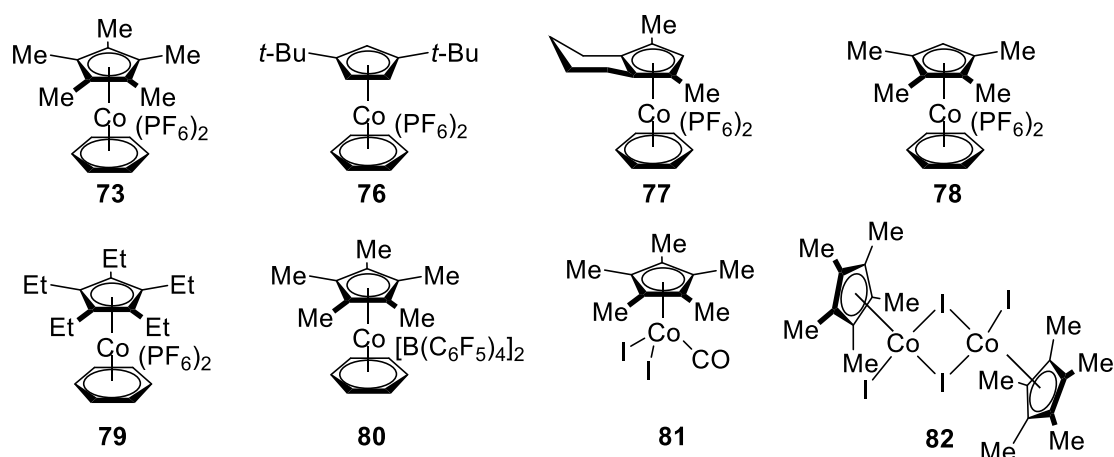
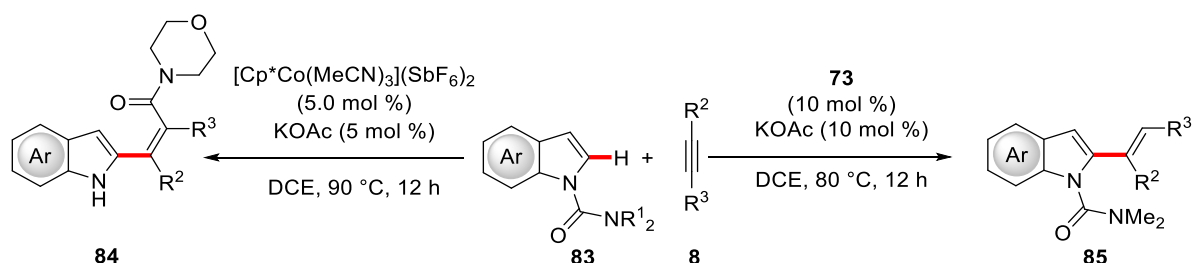


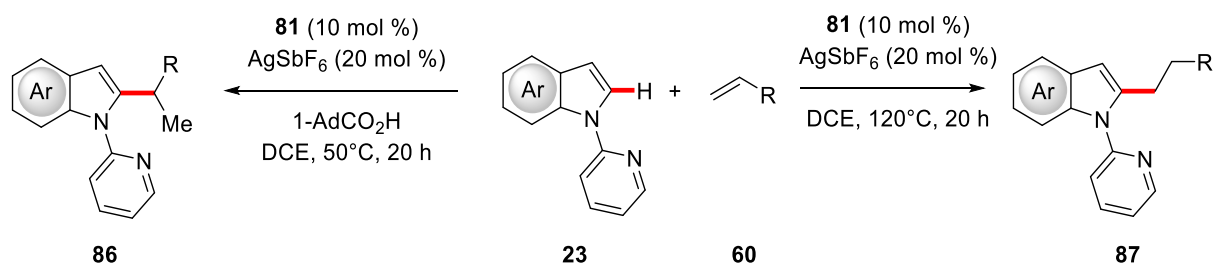
Figure 1.3. Common complexes in Cp*Co(III)-catalyzed C–H activation.^[48a]

Cp*Co(III)-catalyzed hydroarylation was not limited to imines **74**, as also a variety of other C–C and C–X multiple bonds reacted readily. Matsunaga established two protocols for alkyne hydroarylation of indoles **83** using carbamates as the directing group (Scheme 1.20). Simple dimethylcarbamates yielded the hydroarylation product **85**,^[70] whereas morpholine substituted carbamates underwent directing group migration to yield the α,β -unsaturated compound **84**.^[71] The former protocol was later extended to include the mono-functionalization of 3-substituted pyrroles using the same directing group.^[72]



Scheme 1.20. Hydroarylation of alkynes **8** using 2-carbamoylindoles **83**.^[70-71]

Besides alkynes **8**, also alkenes **60** were employed in hydroarylation reactions. Ackermann reported on a switchable Markovnikov/*anti*-Markovnikov hydroarylation of alkenes **60**, dependent on the nature of the additive (Scheme 1.21).^[29b] Extensive mechanistic studies and theoretical calculations revealed that the change in selectivity is based on an underlying change in the reaction mechanism. While the use of bulky adamantanecarboxylic acid promoted the BIES-type^[29] mechanism, resulting in the branched product, the linear was furnished in the absence of further additives by ligand to ligand hydrogen transfer (LLHT, Scheme 1.21).^[29b]

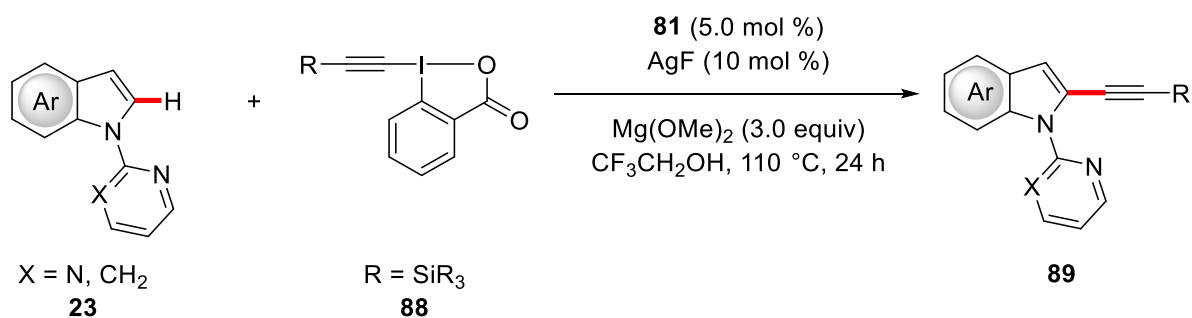


Scheme 1.21. Switchable selectivity in C–H hydroarylation of alkenes **60**.^[29b]

Further progress in Cp*Co(III)-catalysis for hydroarylation reactions was witnessed by Ackermann using challenging allenes,^[73] as well as Li and coworkers using activated alkenes and maleimides.^[74]

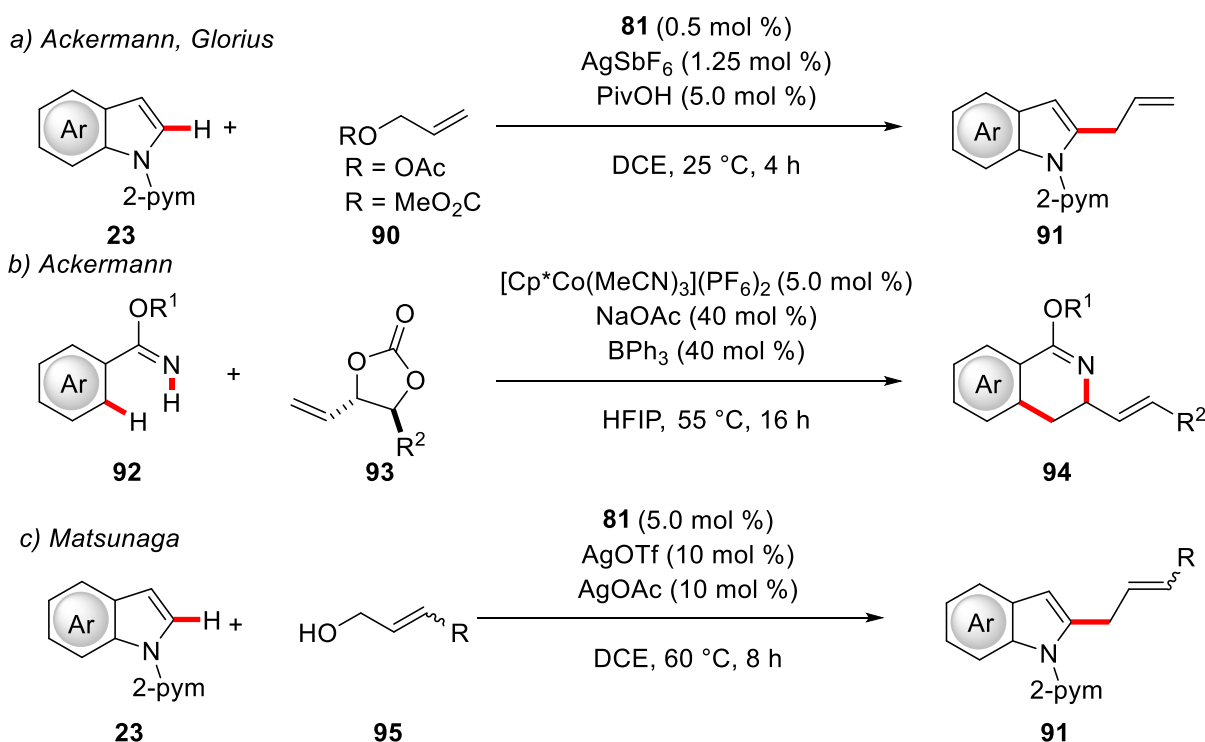
Additionally, protocols for the synthesis of heterocycles were developed for Cp*Co(III)-catalysts, ranging from indazoles and furanes,^[75] isoquinolines^[76] to indoles,^[29c] and isoquinolines.^[77]

Further C–C forming reactions besides hydroarylations are also known for Cp*Co(III) complexes. A cobalt(III)-catalyzed alkylation was published by Shi employing pyrimidylindoles **23** and hypervalent iodine based reagent TIPS-EBX (**88**) (Scheme 22).^[78] This method for cobalt-catalyzed C–H alkylation suffers from poor functional group tolerance and harsh reaction conditions, that is the use of a strong alcoholate base, resulting in a limited scope.



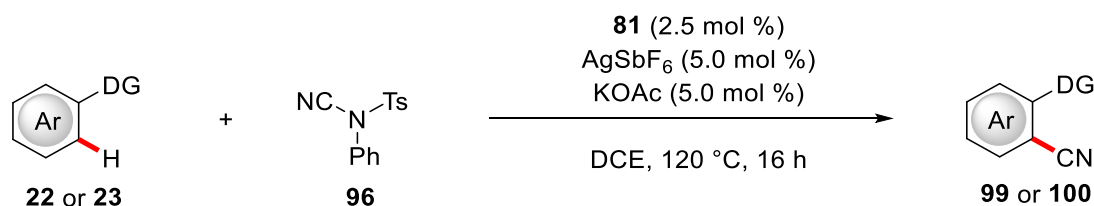
Scheme 1.22. Alkylation using hypervalent iodine reagent **88**.^[78]

Moreover, allylations have been established with different allylating reagents (Scheme 1.23). Beginning with work from Glorius and Ackermann using pyrimidylindoles **23** and allylic electrophiles **90**,^[79] this field was extended among others^[80] by Ackermann using cyclic carbonates **93**^[81] and Matsunaga who was able to directly utilize allylic alcohols **95** as a coupling agent^[82] and thus increased atom efficiency.



Scheme 1.23. Cp*Co(III)-catalyzed C–H allylations.^[78, 79b, 81-83]

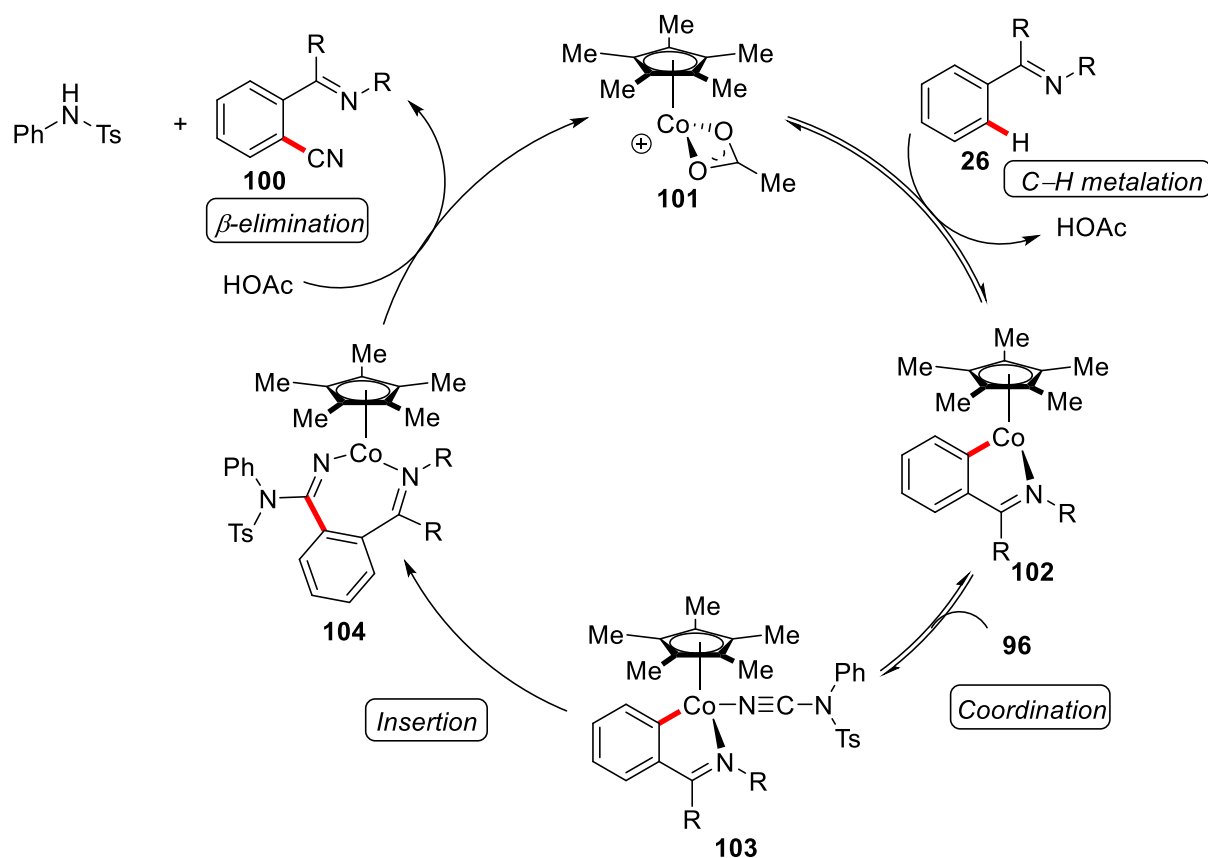
Besides C–C forming transformations, the strength of Cp*Co(III) catalysts lies in the formation of C–X bonds, and here in particular (pseudo-)halogenations and C–N forming reactions. Beginning with reports on the cyanation of (hetero)aromatic C–H bonds by Ackermann (Scheme 1.24)^[84] and a publication by Glorius using NCTS (**96**)^[79b] the field was extended by Chang to include arylpurines **97** and *N*-cyanosuccinimide (**98**) as cyanating reagent.^[85]



Scheme 1.24. Cp*Co(III)-catalyzed C–H cyanation by Ackermann.^[84]

In his report, Ackermann also rationalized a catalytic cycle to explain the product formation (Scheme 1.25).^[84] After the *in-situ* generation of the cationic cobalt complex **101**, a BIES-type C–H metalation^[29] results in the formation of cobaltacycle **102**, which can coordinate the cyanating reagent **96**.^[84] The key intermediate, seven-membered cobaltacycle **104** is generated by insertion of the C–N triple bond into the Co–C bond.

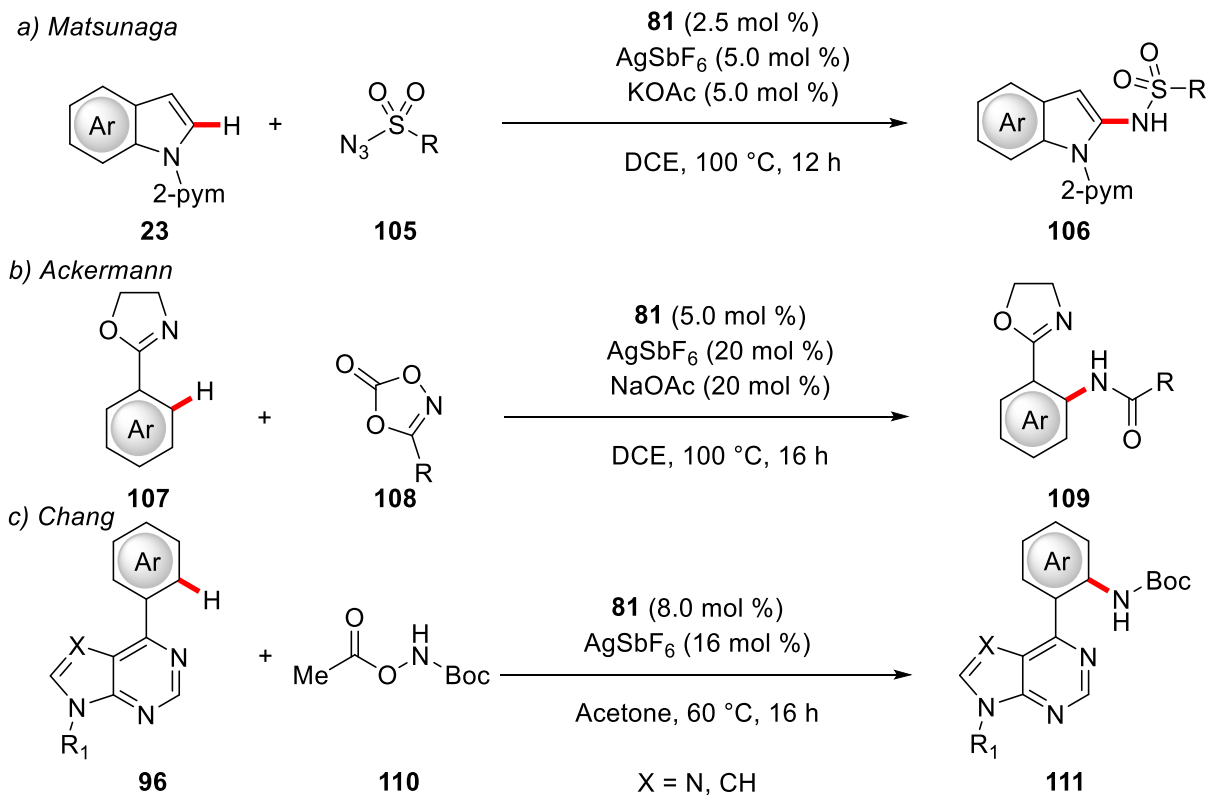
Subsequently, a β -elimination releases the product **100** and regenerates the active catalyst **101**.



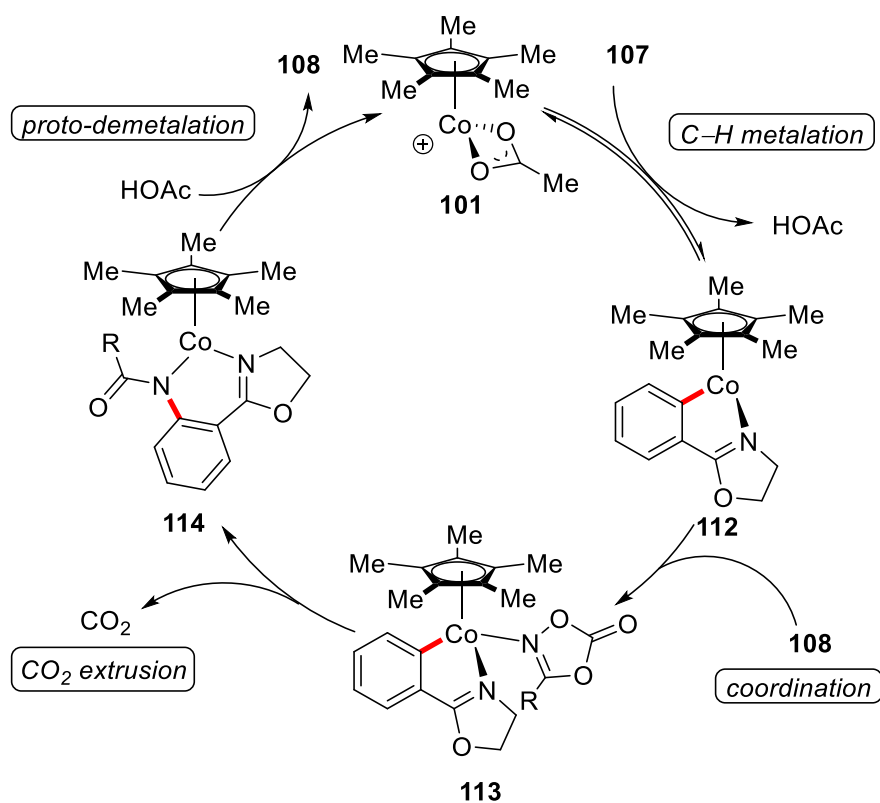
Scheme 1.25. Plausible mechanism for the cobalt-catalyzed C-H cyanation.^[84]

Along the same lines, C-H halogenations were reported using Cp*Co(III) complexes by Glorius,^[79b] and Pawar.^[86]

Beginning with a report by Matsunaga using sulfonylazides **105** as amidating reagents in 2014,^[87] also C-N formation by cobalt(III) catalysis has seen significant advances. Ackermann^[29e] and Jiao^[88] reported that cyclic carbamates **108** were viable amidating reagents, while Chang disclosed a protocol using acetoxycarbamates **110** (Scheme 1.26).^[89] Plausible mechanisms have been proposed, and the reaction is explained using as an example the reaction shown in 1.26b (Scheme 1.27). After generation of the active catalyst **101**, a BIES-type C-H metalation^[29] affords the five membered cobaltacycle **112**. Coordination of the dioxazolone **108** is followed by extrusion of CO₂, which yields intermediate **114**,^[29e] which itself can release the final product **109** upon proto-demetalation by acetic acid, thus regenerating the active catalyst **101**.



Scheme 1.26. Cp*Co(III)-catalyzed amidations.^[29e, 87, 89]



Scheme 1.27. Plausible catalytic cycle for the C-H amidation.^[29e]

1.2.4 Oxidative C–H Activation using Cobalt Salts

As mentioned before, the use of high valent cobalt catalysts in C–H activation greatly enhances the simplicity of the experimental setup and user-friendliness. However, the most simple setup would be the direct use of air-stable cobalt(II) salts as the (pre)catalyst. In 2005, Daugulis popularized the use of bidentate, monoanionic directing groups in the form of 8-aminoquinoline (Q) benzamides for palladium-catalyzed C–H activation.^[90] This concept was applied to include other metals and directing groups, such as TAM,^[91] PIP^[92] and PyO^[93] (Figure 1.3).

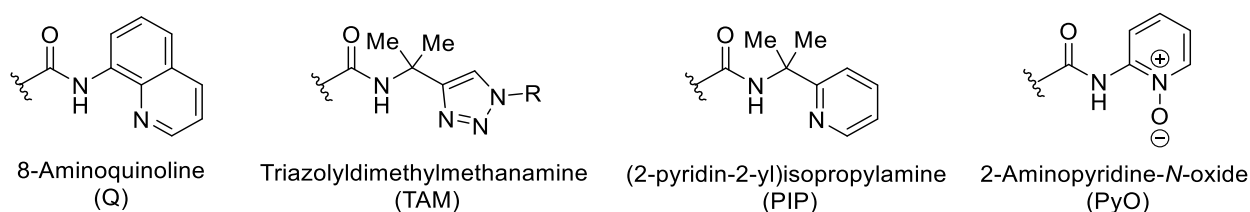
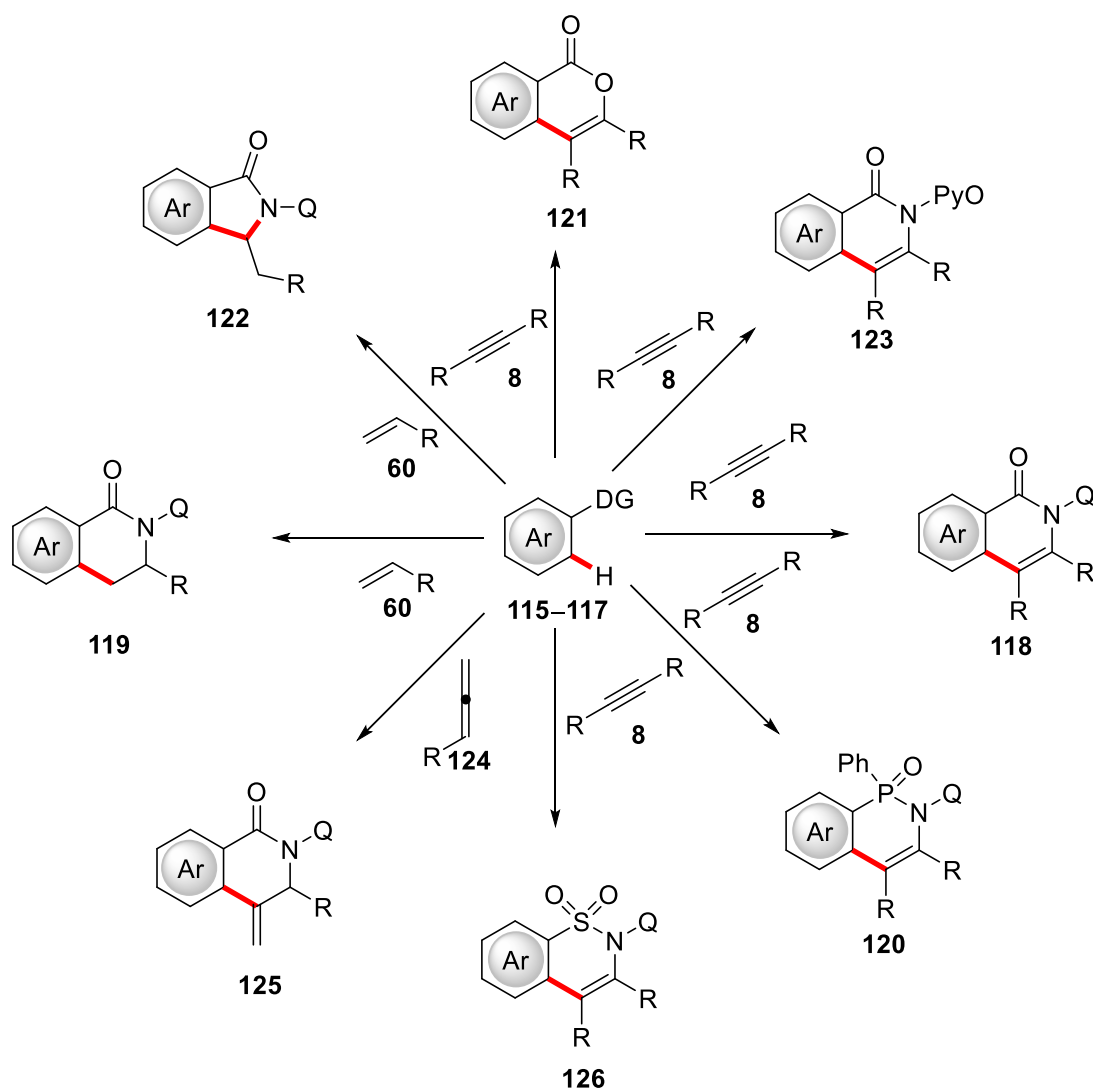


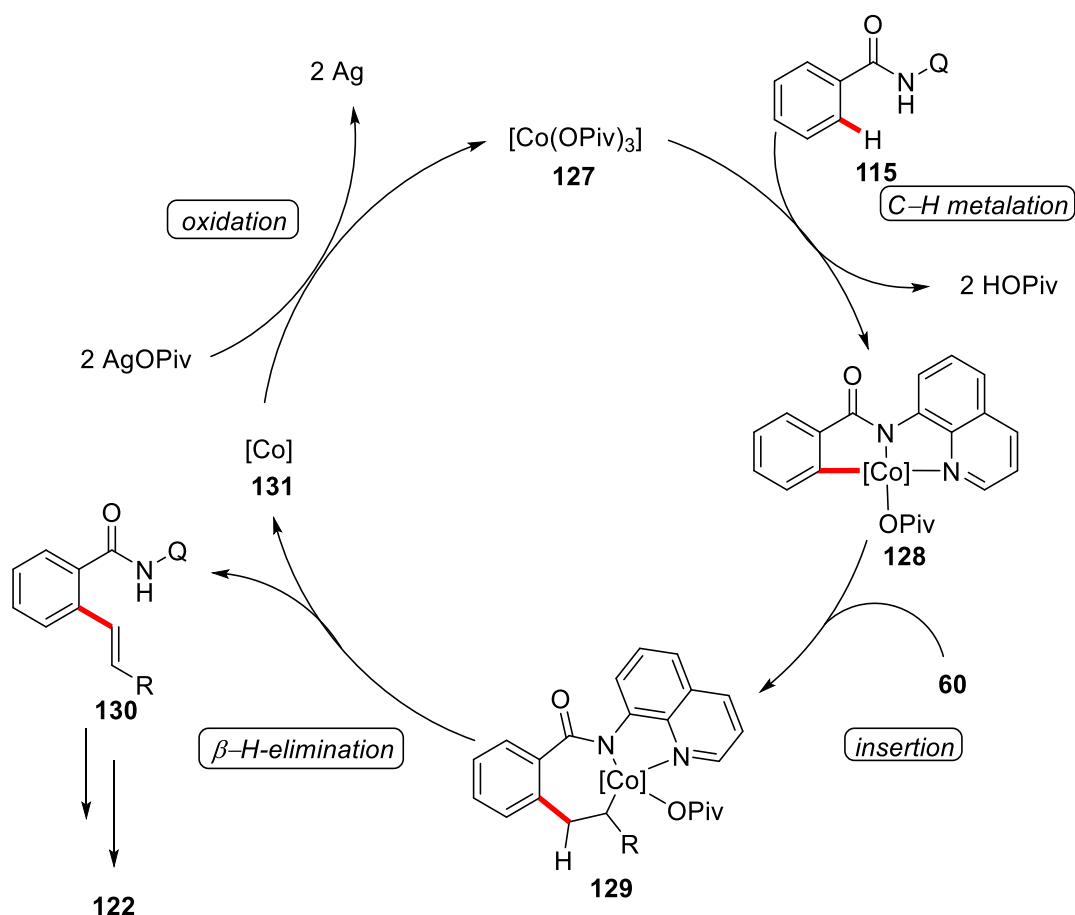
Figure 1.4 Common bidentate directing groups in catalyzed C–H activation.

However, it took nearly 10 years, before the 8-aminoquinoline directing group was applied to cobalt catalysis. Daugulis disclosed a cobalt-catalyzed C–H/N–H annulation of quinolinebenzamides **115** and alkynes **8** to generate isoquinolones **118** (Scheme 1.28a).^[94] It soon became apparent, that heterocycle formation by C–H/X–H annulation was one strength of oxidative cobalt-catalyzed C–H activation. Further heterocycle syntheses followed soon by the same group regarding tetrahydroisoquinolones **119**,^[95] cyclic phosphoramides **120**^[96] and isocoumarines **121** from benzoic acids **116** (Scheme 1.28e, 1.28h, 1.28c).^[97] Important contributions were also disclosed by Ackermann, establishing the formation of isoindolones **122** (Scheme 1.28d),^[98] and furthermore the first use of molecular oxygen as a competent terminal oxidant for this reaction employing PyO substituted benzamide **117** (Scheme 1.28b).^[99] Besides alkenes **60** and alkynes **8**, also allenes **124** were shown to be reactive by Volla and Maiti.^[100] Finally, the synthesis of sultam motifs **126** by cobalt catalysis was disclosed independently by Ribas and Sundararaju under identical conditions (Scheme 1.28g).^[101]



Scheme 1.28 Heterocycle formation by C–H/X–H annulation.

All the above-mentioned C–H/X–H annulation protocols generally follow similar mechanistic pathways, which should be explained with the example of the cobalt catalyzed isoindolone synthesis (Scheme 1.29).^[98] The initial step of the mechanism is proposed to be the base-assisted C–H activation of the chelating substrate-catalyst complex to form five membered cobaltacycle **128**. This intermediate is reactive towards unsaturated multiple bonds and can undergo migratory insertion. The resulting seven-membered intermediate **129** reacts by β -hydride elimination to yield the final product **122**. Subsequently, the cobalt species **131** is reoxidized to regenerate the active species **127**.

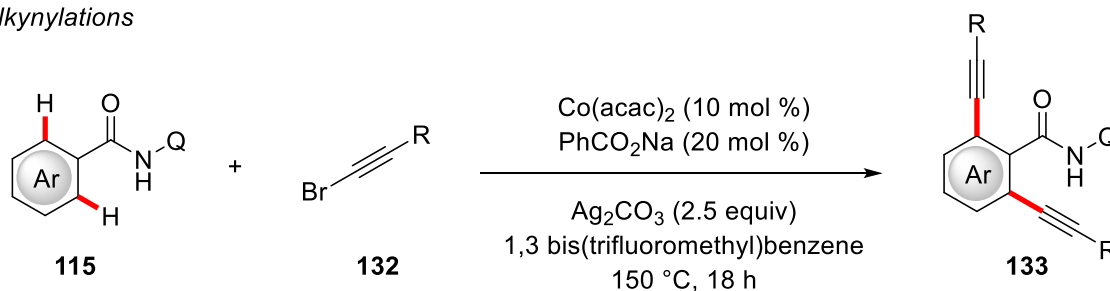


Scheme 1.29. Proposed catalytic cycle for the cobalt-catalyzed isoindolone formation.^[98]

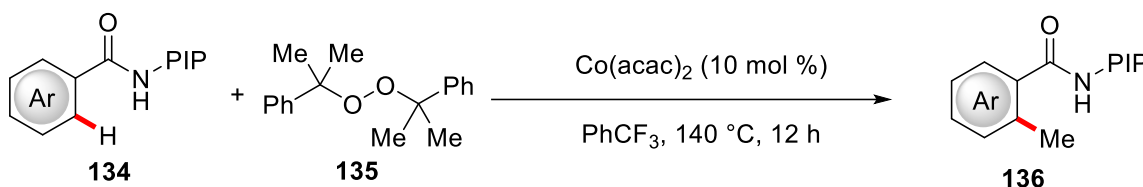
Furthermore, carbonylations have been reported as a method for heterocycle formation, for example by Daugulis in 2014.^[102]

Besides C–H/X–H annulations, C–C forming reactions have been reported. In 2016, Balaraman disclosed a cobalt-catalyzed oxidative alkynylation of benzamides **115** (Scheme 1.30a).^[103] Although the functional group tolerance on the benzamide moiety is generally good, the reaction suffers from a limited alkyne scope. In the same year, Lu and coworkers achieved a methylation under assistance of the PIP directing group in an elegant protocol using highly reactive dicumylperoxide **135** as the methylating reagent as well as the oxidant, avoiding the use of costly silver(I) salts (Scheme 1.30b).^[104] Although *ortho*-substituted benzamides **115** were used preferentially, other substitution patterns led to bis methylation. Further, Chatani reported on a cobalt-catalyzed allylation protocol using terminal alkenes **137** (Scheme 1.30c).^[105]

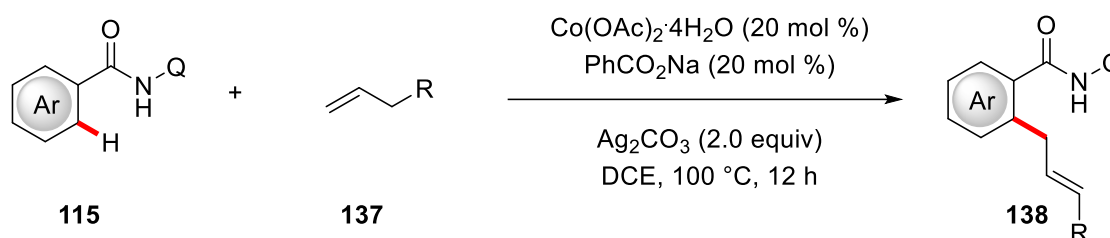
a) Alkynylations



b) Methylation



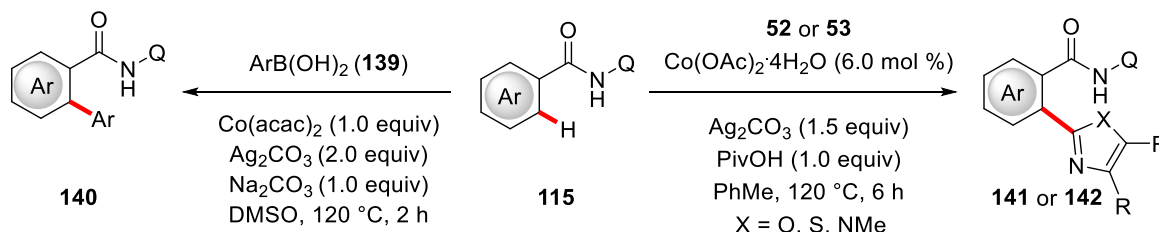
c) Allylation



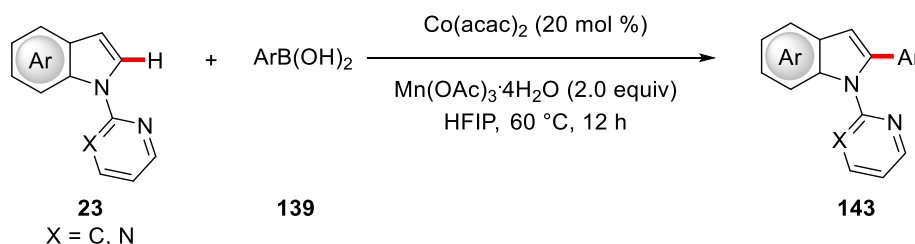
Scheme 1.30. Cobalt-catalyzed C–H activation for the formation of C–C bonds.^[103-105]

Without a doubt, the formation of biaryls is one of the most important applications of C–H activation, due to the abundance of biaryls in biologically active motifs and the deficits regarding sustainability and atom economy associated with cross coupling chemistry.^[4] In oxidative cobalt-catalyzed C–H activation, biaryl formations have been established beginning with the dimerization of quinoline benzamides **115**.^[106] This approach was elaborated by the use of different directing groups to achieve selective C–H/C–H cross-activation,^[107] while other methods used boronic acids **139** or activated heterocycles **52** or **53** (Scheme 1.31a).^[108] A noteworthy example for an oxidative cobalt-catalyzed C–H arylation was published by Song, employing indoles **23** and boronic acids **139**. While arylations of this substrate have also been achieved using low valent cobalt catalysis,^[49, 52] (*vide supra*) this example remains one of the very rare oxidative-cobalt catalyzed transformations not dependent on a bidentate directing group (Scheme 1.31b).^[109]

a) Arylations under Bidentate Assistance



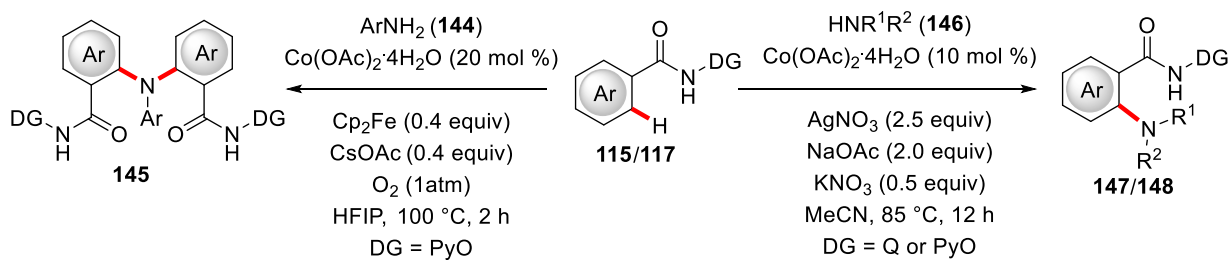
b) Arylation of Pyri(mi)dylindole



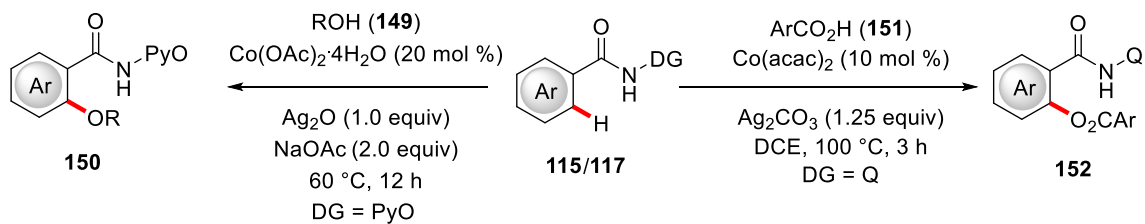
Scheme 1.31. Arylations using oxidative cobalt-catalyzed C–H activation.^[108-109]

Oxidative cobalt-catalyzed C–H activation is not limited to C–C forming reactions, as also several C–X formations have been disclosed. C–N forming transformations have been realized using 8-aminoquinoline as well as pyridine-*N*-oxide directing groups using (cyclic) secondary alkyl amines **146** as well as arylamines **144** (Scheme 1.32a).^[110] With regard to C–O bond forming reactions, both alkoxygenations and acyloxylation have been reported, by Song and recently by Chatani (Scheme 1.32b).^[111] Both reactions proceeded with good to excellent functional group tolerance and good yields. Furthermore, also alkenes were viable substrates in the presented alkoxylation protocol.^[111b] Moreover, an oxidative cobalt-catalyzed C–H halogenation was recently achieved by Chatani using molecular iodine **154** as the iodination reagent (Scheme 1.32c).^[112] While the reaction showed good functional group tolerance, the directing group had to be modified to exclude undesired side reactions. The mechanism of these transformations shall be discussed with the example of the cobalt-catalyzed C–H acyloxylation (Scheme 1.33).^[111a] After coordination of the cobalt catalyst to the deprotonated amide **115**, oxidation from cobalt(II) to cobalt(III) followed by C–H bond cleavage generates the five-membered intermediate **158**. This species can then undergo ligand exchange with the present acid to form intermediate **159**. From this complex, the product **152** can be released by reductive elimination, followed by reoxidation of the cobalt catalyst.

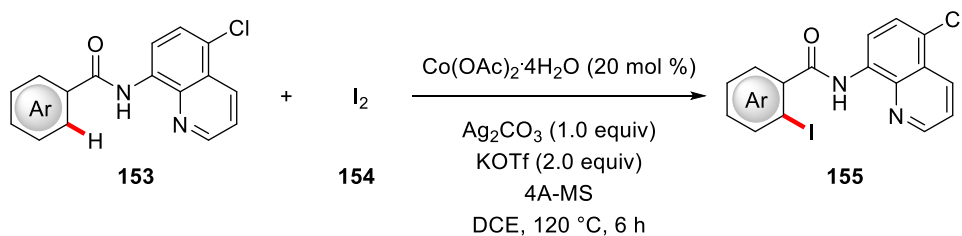
a) C–N formations



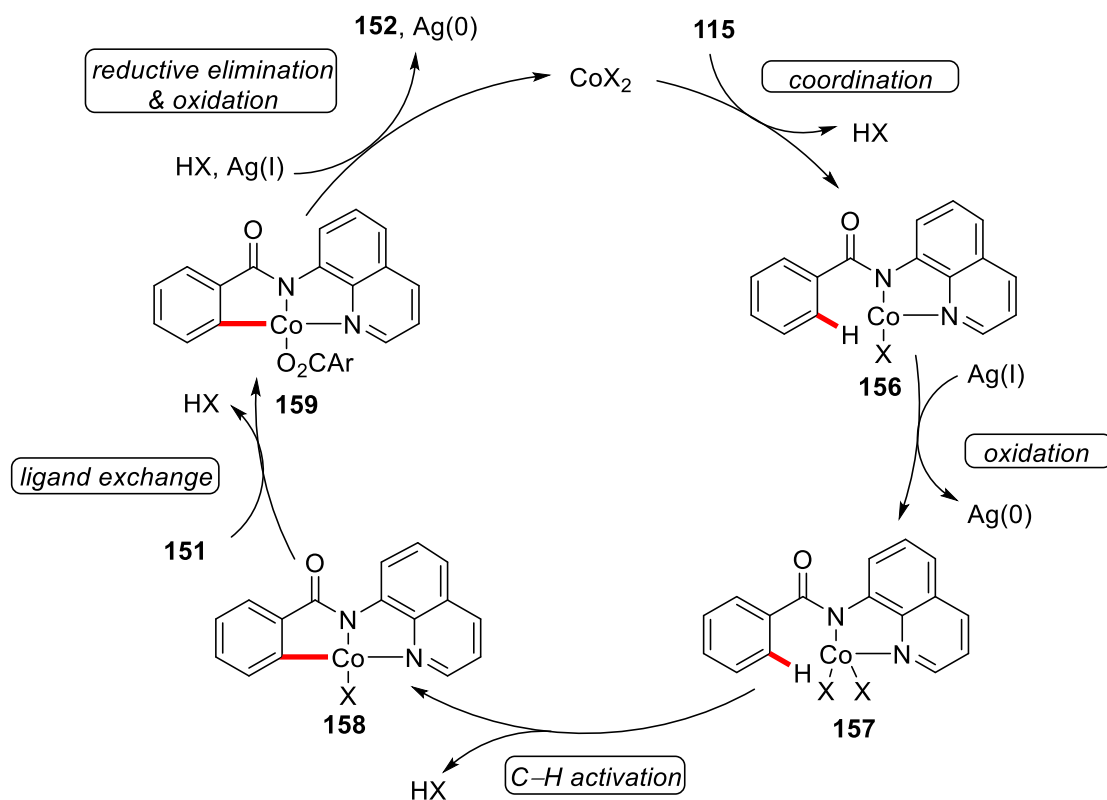
b) C–O formations



c) C–H Iodination



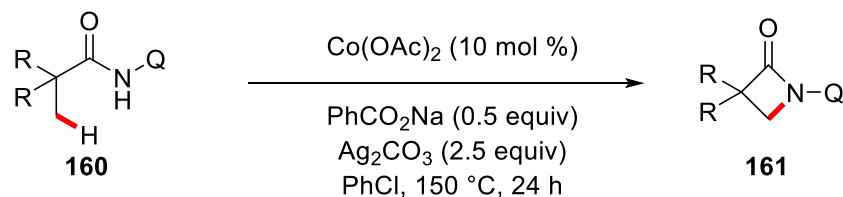
Scheme 1.32. Oxidative cobalt-catalyzed C–X formations.^[109–112]



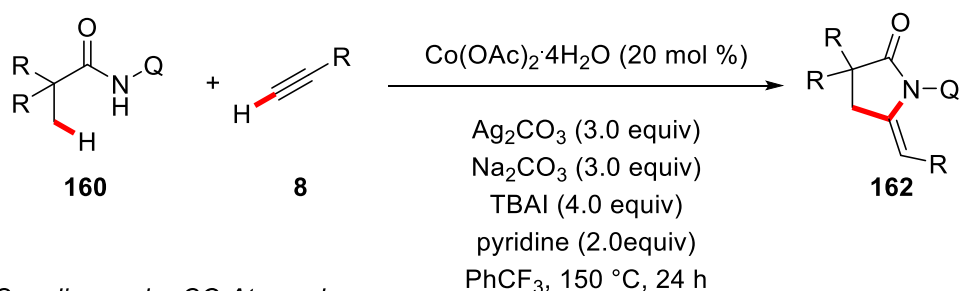
Scheme 1.33. Plausible mechanism for the cobalt-catalyzed C–H acyloxylation.^[111a]

Finally, besides the oxidative C–H activation of C(sp²)–H bonds, a few reports have highlighted the ability of cobalt to activate C(sp³)–H bonds. An intramolecular cyclization to generate small ring lactams was reported by He in 2015 (Scheme 1.34a).^[113] Intermolecular transformations using either terminal alkynes^[114] or carbonmonoxide, (Scheme 1.34c)^[115] as coupling partners were disclosed recently likewise.

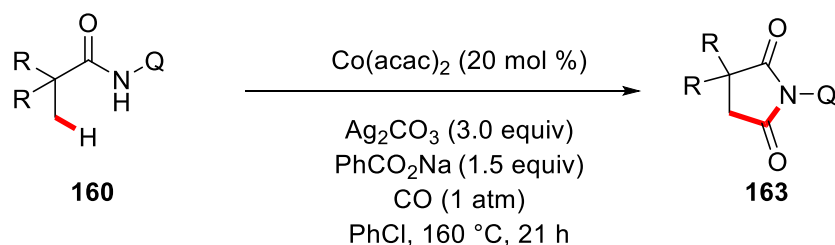
a) *Intramolecular Cyclization*



b) *Coupling with Terminal Alkynes*



c) *Coupling under CO Atmosphere*



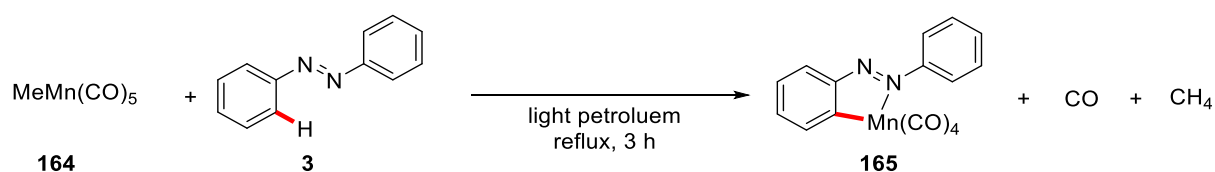
Scheme 1.34. Oxidative cobalt-catalyzed C(sp³)–H activation.^[113-115]

1.3 Manganese-Catalyzed C–H Activation

After iron and titanium, manganese is the third most abundant transition metal in the earth's crust.^[35] Hence, it represents an essential trace element for life, with manganese cores being essential for a number of enzymes in human metabolism, such as arginases and manganese-superoxide dismutases.^[116] Therefore, it is attractive as a catalyst, due to its availability, low price and low toxicity. The presence of manganese in many enzymes, led to the investigation of similar chemistry in laboratory model systems,^[116c, 117] in due course realizing C–H functionalizations by an

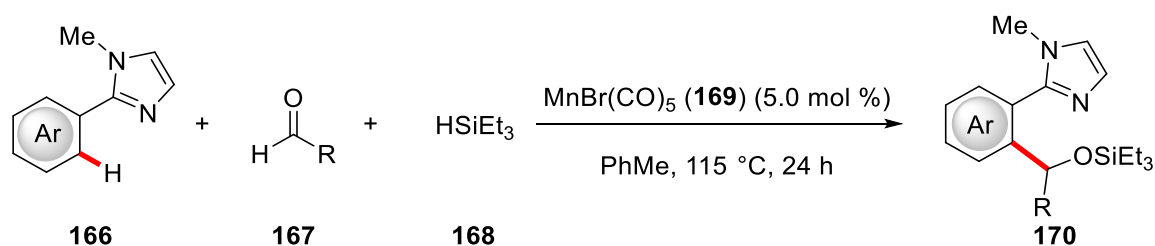
outer-sphere mechanism for a number of transformations.^[118] However, the focus of this chapter shall be manganese(I)-catalyzed organometallic C–H activation,^[119] so outer-sphere transformations and recent advances in low valent manganese chemistry^[120] will not be discussed.

An early stoichiometric C–H activation by manganese was reported by Bruce and Stone, cyclometalating azobenzene **3** with MeMn(CO)₅ (**164**) (Scheme 1.35).^[121] While the same complex **165** had been prepared two years earlier by Heck,^[122] his synthesis involved the transmetalation from palladium to manganese, and not C–H activation by manganese itself. In the following years, several cyclometalated manganese complexes were synthesized using various substrates and manganese precursors.^[123]



Scheme 1.35. Stoichiometric C–H activation with MeMn(CO)₅ (**164**).^[121]

Groundbreaking progress in catalytic C–H activation by manganese(I) was achieved by Kuninobu and Takai in 2007 (Scheme 1.36). Using simple and stable MnBr(CO)₅ (**169**) as the catalyst, *ortho* functionalization of phenylimidazoles **166** was achieved in the presence of triethylsilane **168**, albeit requiring stoichiometric silanes to ensure catalytic turnover.^[124]

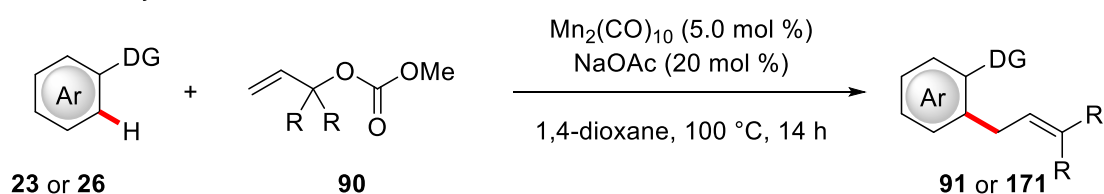


Scheme 1.36. Manganese(I)-catalyzed hydroarylation/silylation of aldehydes **167**.^[124]

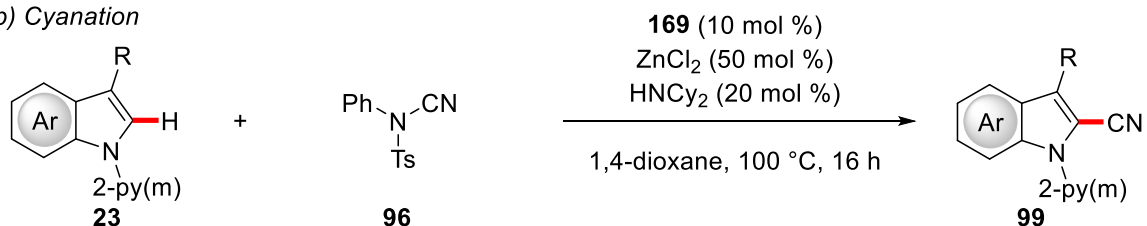
In due course, hydroarylation of C–C and C–X bonds has become a broad field of application for manganese catalysis, with notable contributions by Wang^[125] and Ackermann^[126] among others.^[127] Over time, hydroarylations have been reported by these groups for aldehydes, nitriles, imines, alkynes and activated alkenes. In addition to hydroarylations, also C–H/X–H annulations have been disclosed with diverse coupling partners to efficiently synthesize heterocycles.^[128]

Besides these addition-based reactions, a significantly smaller number of substitutive protocols in manganese(I)-catalysis is known, although these reactions offer more synthetic diversity as they are not limited to C–C or C–X multiple bonds. Ackermann disclosed the substitutive allylation of indoles **23** and ketimines **26** by the use of allylcarbonates **90** as easily accessible allylating reagents (Scheme 1.37a).^[129] A protocol for the C–H cyanation of similar substrates was reported by the same group, relying on NCTS (**96**) as a mild and safe cyanating reagent (Scheme 1.37b).^[130] Finally, Glorius applied manganese catalysis to allenylation reactions by the use of similar alkynes **172** with an ester as the leaving group (Scheme 1.37c).^[131]

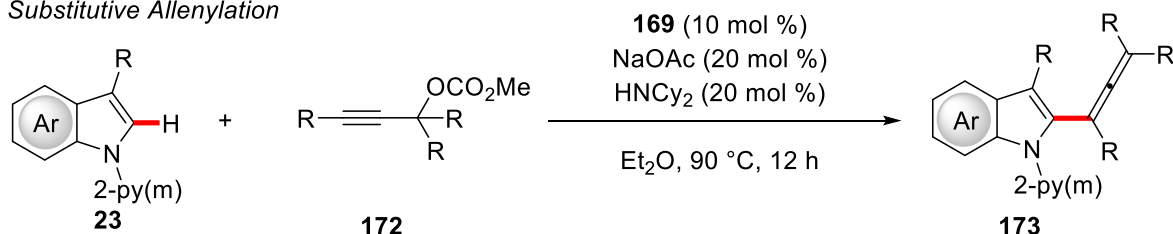
a) *Substitutive Allylation*



b) *Cyanation*

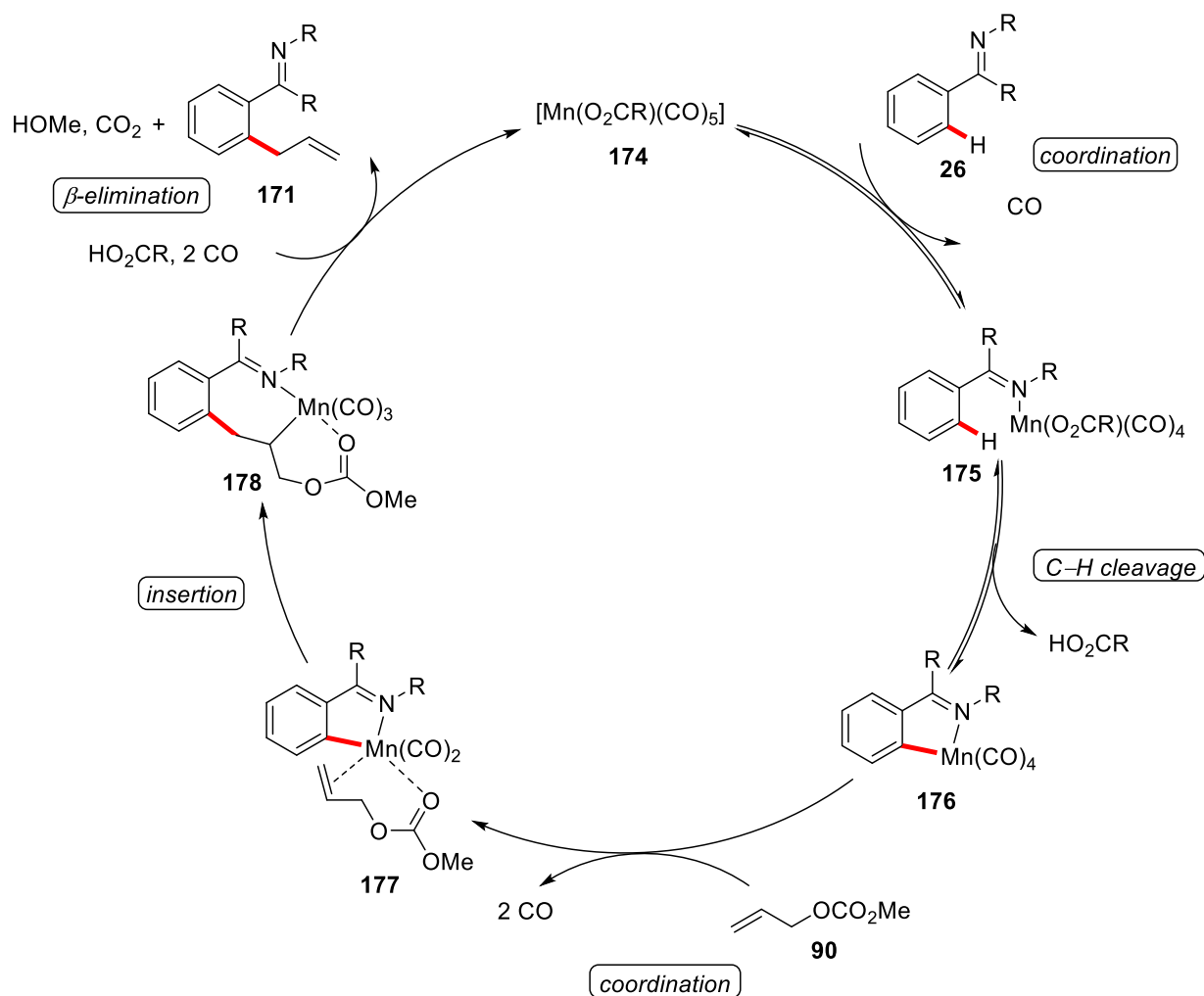


c) *Substitutive Allenylation*



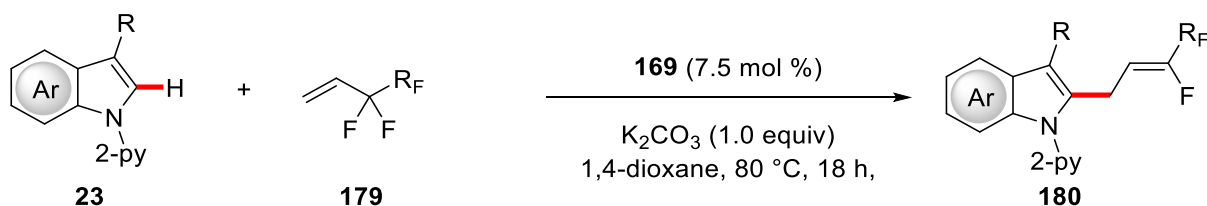
Scheme 1.37. Substitutive manganese(I)-catalyzed transformations.^[129-131]

Mechanistic proposals for these transformations were rationalized, which are discussed here with the example of the manganese-catalyzed C–H allylation (Scheme 38).^[129] The key intermediate, the five-membered manganacycle **176** is generated by a base-assisted C–H metalation. Coordination of allylcarbonate **90** in a chelating fashion sets the stage for a facile insertion of the double bond into the Mn–C bond. Subsequent β -elimination of the carbonate releases the final product **171** and regenerates the catalytically active species **174** (Scheme 1.38).^[129]



Scheme 1.38. Proposed mechanism for the manganese(I)-catalyzed C–H allylation.^[129]

Lastly, manganese(I) catalysis has been exploited to catalyze challenging C–H/C–F activation reactions. This is noteworthy, as C–F bonds are generally relatively inert due to the high bond strength and the reluctance of organofluorine compounds to coordinate to metal centers.^[132] Despite these challenges, C–H/C–F activation has been successfully employed in the manganese-catalyzed perfluoroallylation by Ackermann (Scheme 1.39)^[133] and in the monofluoroalkenylation by Ackermann^[133] and Loh^[134] in independent reports.



Scheme 1.39. C–H/C–F activation by manganese(I)-catalysis.^[133]

1.4 Electrochemical Transition Metal-Catalyzed C–H Activation

The growing demands for renewable power sources, including solar energy, hydropower and wind energy (Figure 1.5),^[135] makes the utilization of electricity to drive chemical transformations increasingly desirable.

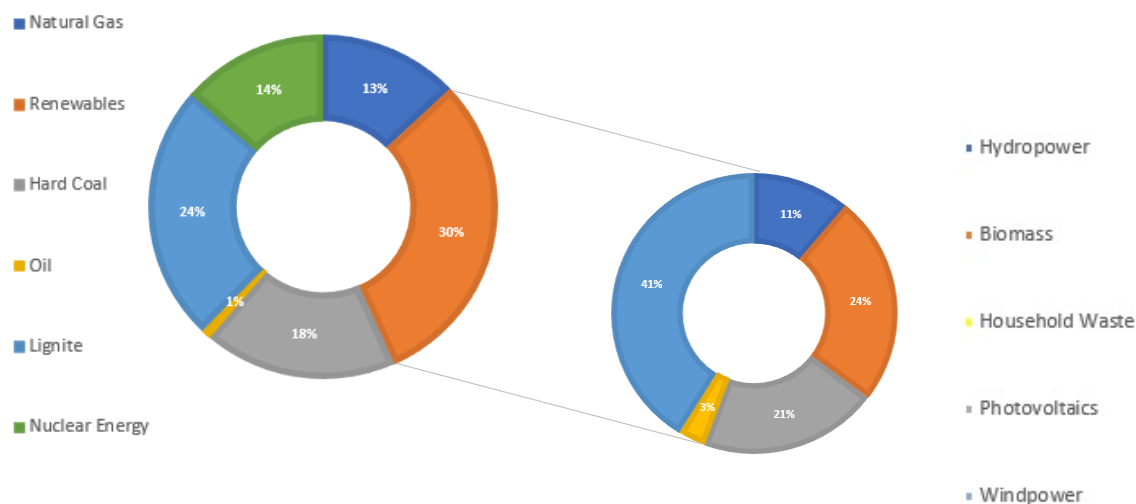


Figure 1.5. Share of energy sources of gross electricity production in Germany 2016.^[135]

Due to the increasingly sustainable energy production, the use of electricity in chemical synthesis would therefore significantly reduce the environmental footprint of molecular sciences.^[136] Furthermore, if electricity is employed to substitute costly and potentially toxic stoichiometric oxidants and reductants the cost efficiency of organic synthesis is drastically improved (Figure 1.6).^[137] Moreover, the use of electricity allows to tune the applied potential and current to a transformation, thus enabling milder conditions and potentially better selectivities. In case of chemical oxidation/reduction, the potential of the employed redox-reagent and the metal may not always overlap and thus leave room for more efficient reaction conditions by electrocatalysis (Table 1.1).^[35]

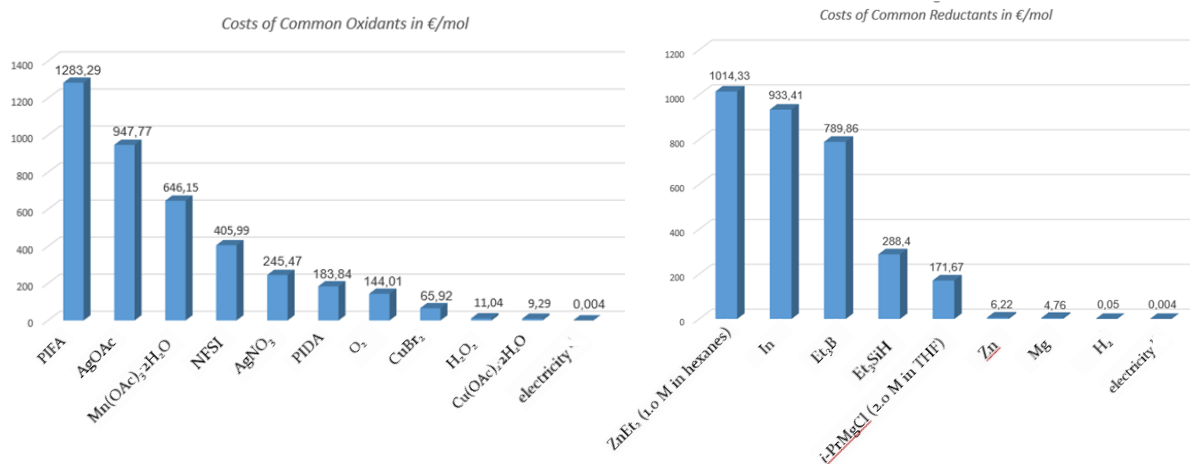


Figure 1.6. Costs of common oxidants and reductants.^[137]

Table 1.1. Standard potentials of selected redoxreagents and transition metals.^[35]

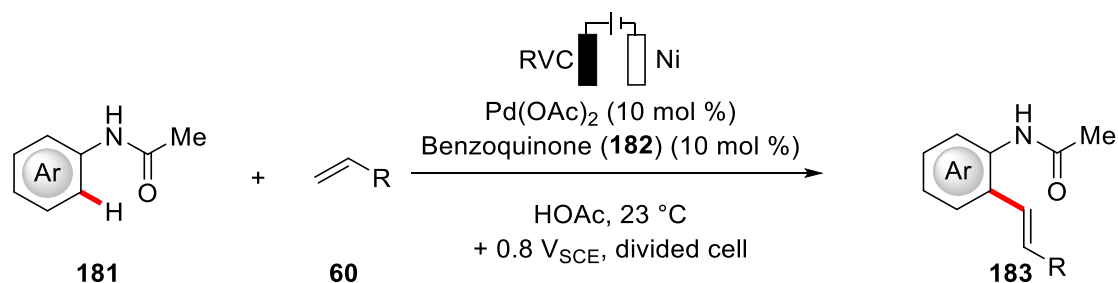
Reaction	Potential E ⁰ [V]
Oxidants	
$\text{H}_2\text{O}_2 + 2 \text{H}^+ + 2 \text{e}^- \rightarrow 2 \text{H}_2\text{O}$	1.78
$\text{Mn(III)} + \text{e}^- \rightarrow \text{Mn(II)}$	1.54
$\text{Ag(I)} + \text{e}^- \rightarrow \text{Ag(0)}$	0.79
$\text{Cu(II)} + \text{e}^- \rightarrow \text{Cu(I)}$	0.15
Reductants	
$\text{In}^{3+} + 3 \text{e}^- \rightarrow \text{In}$	-0.34
$\text{Zn}^{2+} + 2 \text{e}^- \rightarrow \text{Zn}$	-0.76
$\text{Mg}^{2+} + 2 \text{e}^- \rightarrow \text{Mg}$	-2.37
Transition Metals	
$\text{Co}^{3+} + \text{e}^- \rightarrow \text{Co}^{2+}$	1.92
$\text{Pd}^{2+} + 2 \text{e}^- \rightarrow \text{Pd}$	0.95
$\text{Ru}^{2+} + 2 \text{e}^- \rightarrow \text{Ru}$	0.46

Electro-organic synthesis has been discussed in science, since the first reports by Volta, Faraday and Kolbe.^[138] Oxidation reactions of activated substrates have been studied since the 1960s,^[139] with recent progress broadening the applicability towards a range of activated substrates,^[140] with key contributions from Waldvogel,^[141] Baran,^[142] Yoshida^[143] and Xu,^[144] among others.^[145] In contrast, the focus of this

introduction is on C–H activations catalyzed by transition metals under the assistance of electricity. Moreover, outer-sphere transformations with early reports using noble metals^[146] and recent advances towards 3d-metals^[147] will also not be discussed in detail.

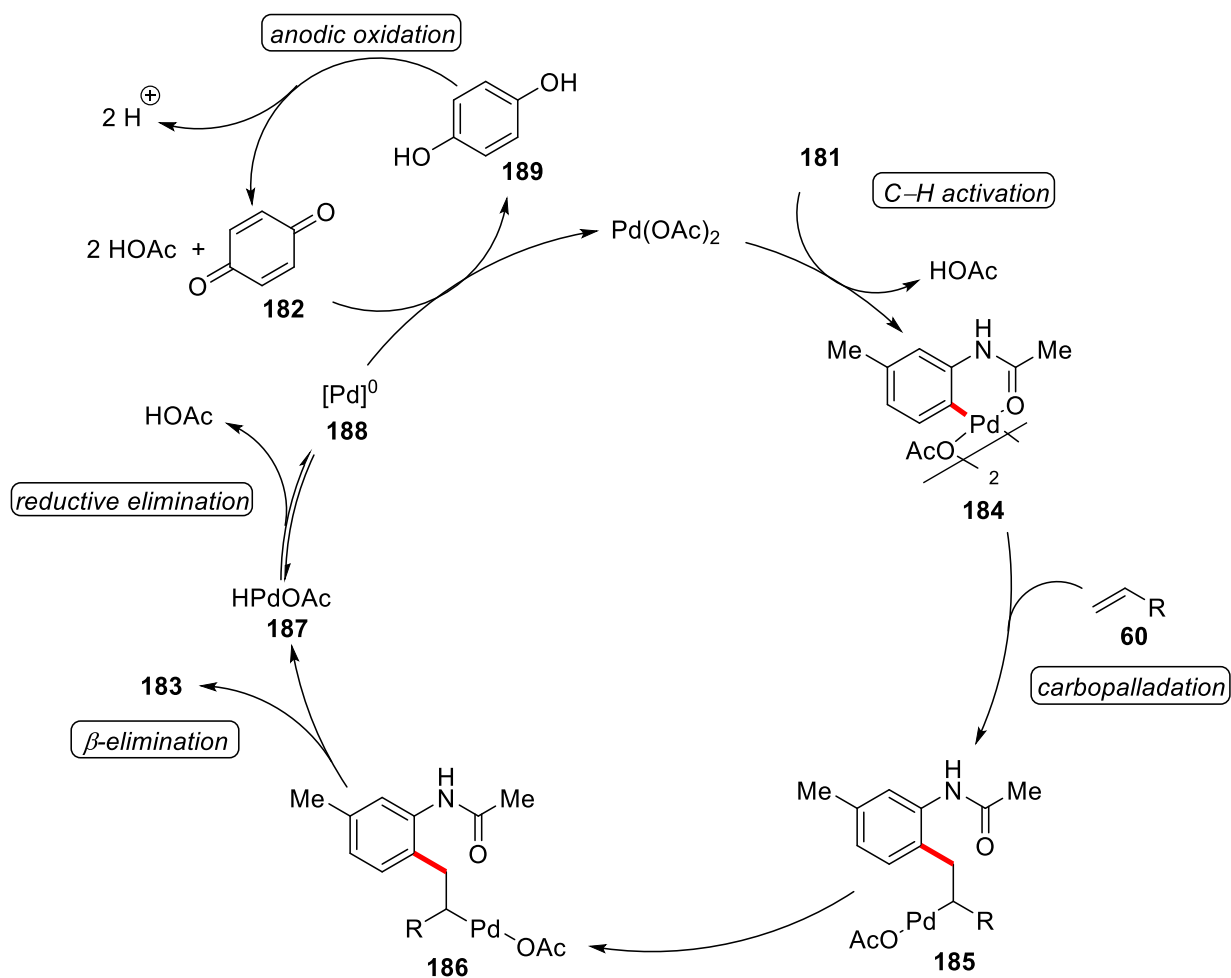
1.4.1 Palladium-Catalyzed Transformations

An elegant early example of palladium-catalyzed electrochemical C–H activation was achieved by Amatore and Jutand in 2007 (Scheme 1.40).^[148] They reported on a Fujiwara-Moritani-type reaction,^[149] using co-catalytic amounts of benzoquinone (**182**). While the reaction scope was severely limited, the authors provide a detailed mechanistic concept. The reaction is proposed to be initiated by base-assisted C–H activation, followed by an insertion of the double bond into the Pd–C bond (Scheme 1.41). A subsequent β -elimination liberates the product **183** and a reductive elimination of acetic acid generates palladium(0). Intermediate **188** is then reoxidized by benzoquinone (**182**) and the thus formed hydroquinone **189** is then oxidized again at the anode.

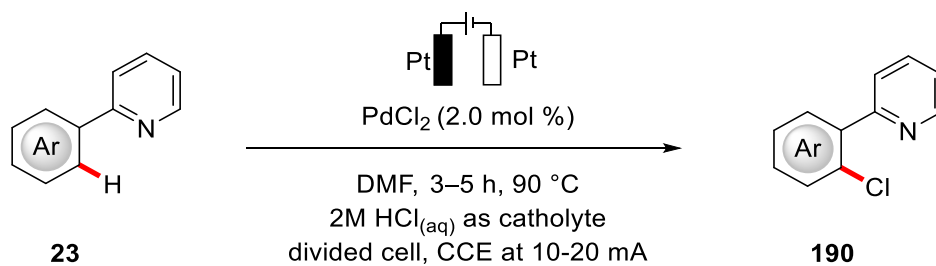


Scheme 1.40. Electrocatalytic palladium-catalyzed C–H alkenylation.^[148]

In 2009, Kakiuchi reported on a palladium-catalyzed C–H halogenation using electrochemistry (Scheme 1.42).^[150] Here, electricity was essential to generate the electrophilic halonium cation from mineral acids, which presents an elegant and cost-effective alternative to other halogenation reactions. This approach was extended to include C–H iodinations using molecular iodine (**154**) or potassium iodide.^[151] Additionally, C–H chlorinations of benzamides **153**, including the synthesis of marketed drug vismodegib,^[152] were disclosed.^[153]



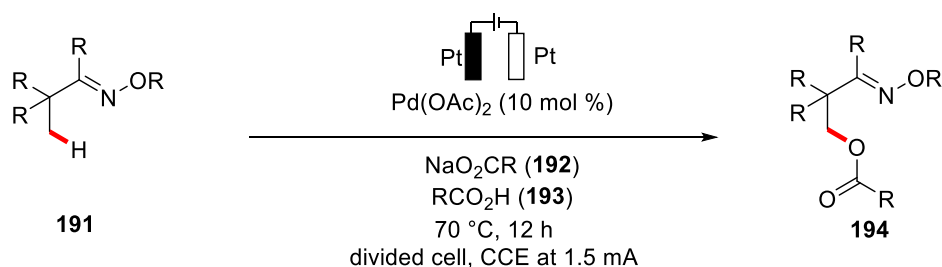
Scheme 1.41. Electrocatalytic Fujiwara-Moritani reaction.^[148]



Scheme 1.42. Electrochemical C–H halogenation of phenylpyridines **23**.^[150]

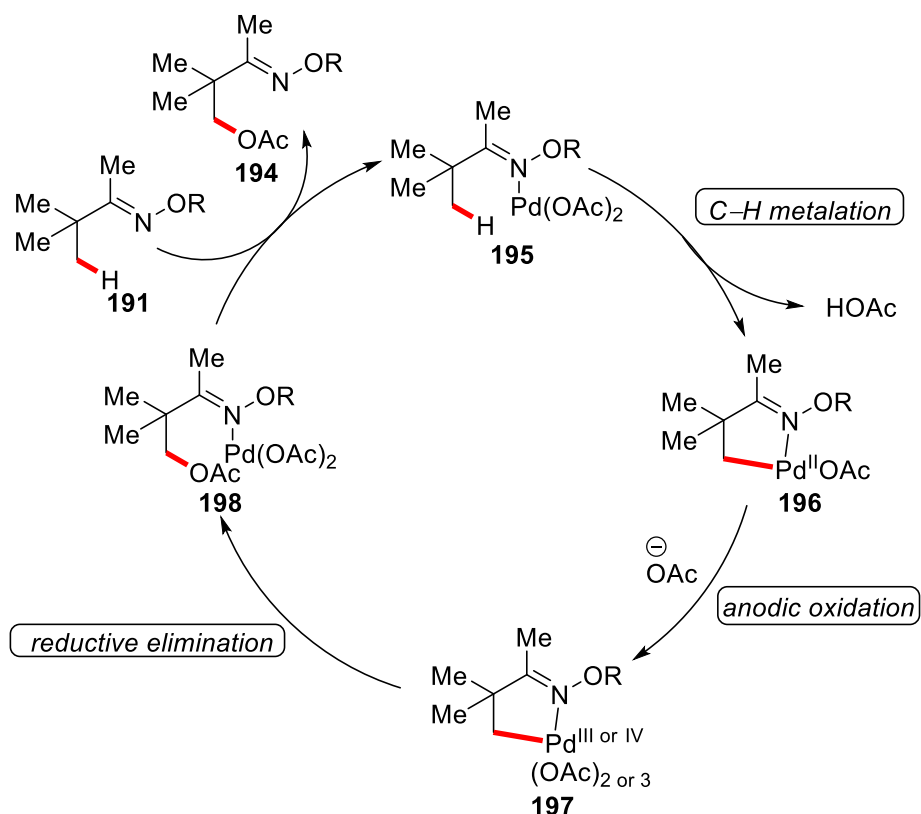
Along the same lines, Kakiuchi reported on the homodimerization of phenylpyridines **23** in the presence of stoichiometric or co-catalytic amounts of iodine (**154**).^[154]

C–H oxygenations were achieved by electrochemical transition metal-catalyzed C–H bond activation by Budnikova using palladium complexes in the coupling of perfluoroacids and phenylpyridines **23**.^[155] While the scope was limited, the authors supported their mechanistic proposal by detailed studies, including the isolation of key intermediates as well as cyclovoltammetric (CV) studies.^[156] Moreover, besides the desired perfluoroalkoxylation, at higher current also significant amounts of perfluoroalkylated product were observed. This transformation was subsequently improved to yields of more than 80%.^[157] Related transformations were also proposed in comparable yields by nickel^[158] and iron^[157a] catalysis. Recently, Mei disclosed C–H oxygenations using electrochemical palladium-catalysis.^[159] This work constitutes the first C–H activation on C(sp³)–H bonds using transition metal-catalysis and electrochemistry. The desired reaction was achieved using palladium acetate as the catalyst in a divided cell setup using carboxylic acids **192** as the solvent and the corresponding sodium salt **193** as base (Scheme 1.43).



Scheme 1.43. Palladium-catalyzed Oxygenation of C(sp³)–H bonds.^[159]

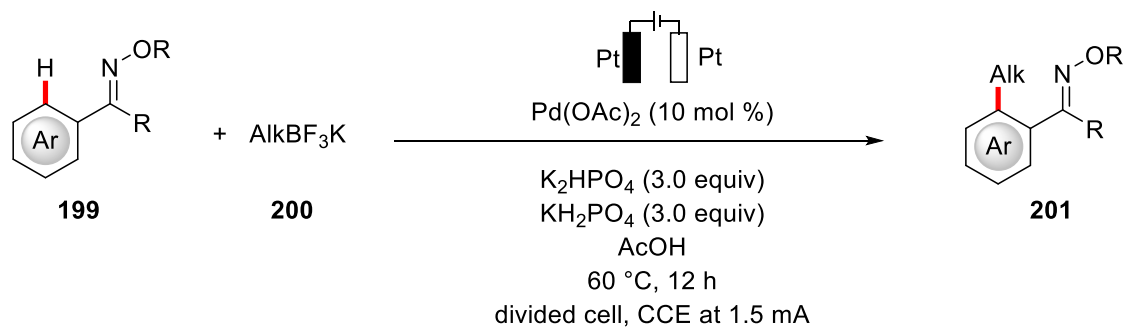
The mechanism was proposed to proceed by a proximity-induced base-assisted C–H metalation at the primary C–H bond (Scheme 1.44).^[159] The thus formed intermediate **196** is oxidized to a palladium(III) or palladium(IV) complex **197**, which then undergoes reductive elimination to form the C–O bond, followed by a ligand exchange to furnish product **194** (Scheme 1.44). In a follow-up work, Mei could show that also the oxygenation of aromatic C–H bonds was feasible with a similar catalytic system.^[160] Thereafter, Sanford disclosed a similar transformation, broadening the applicability to include quinoline and pyrazine as directing groups.^[161]



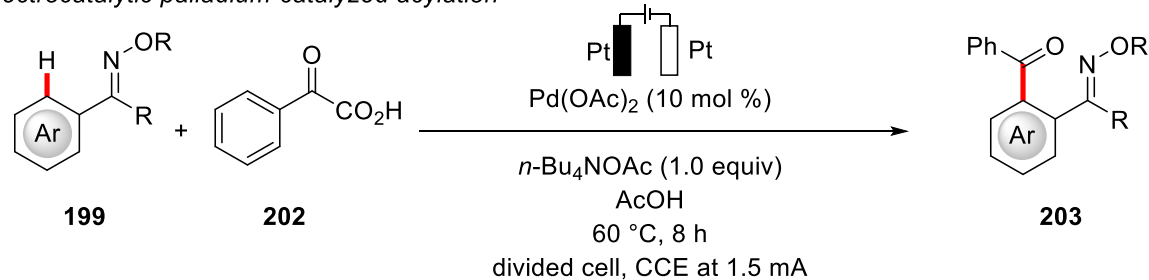
Scheme 1.44. Plausible mechanism for the palladium-catalyzed C–H oxygenation.^[159]

Additionally, Mei discovered an oxidative alkylation by palladium catalysis using alkyltrifluoroborates **200** (Scheme 1.45a).^[162] In the same report, Mei also disclosed a palladium-catalyzed benzoylation of oximes **199** (Scheme 1.45b).

a) *Electrocatalytic palladium-catalyzed methylation*



b) *Electrocatalytic palladium-catalyzed acylation*

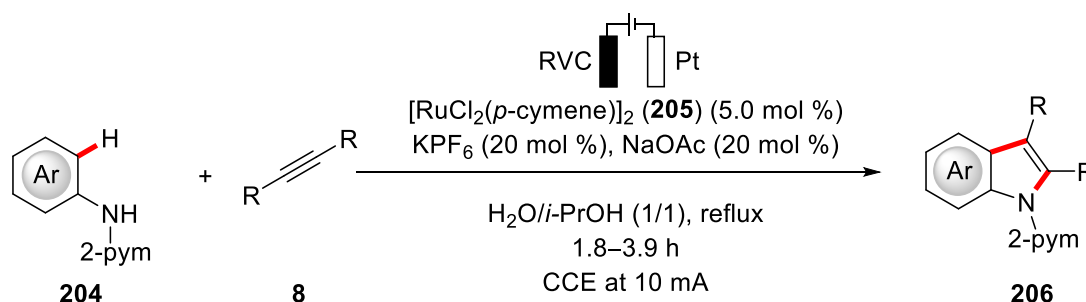


Scheme 1.45. Palladium-catalyzed alkylation and acylation.^[162]

1.4.2 Transformations Catalyzed by other Transition Metals

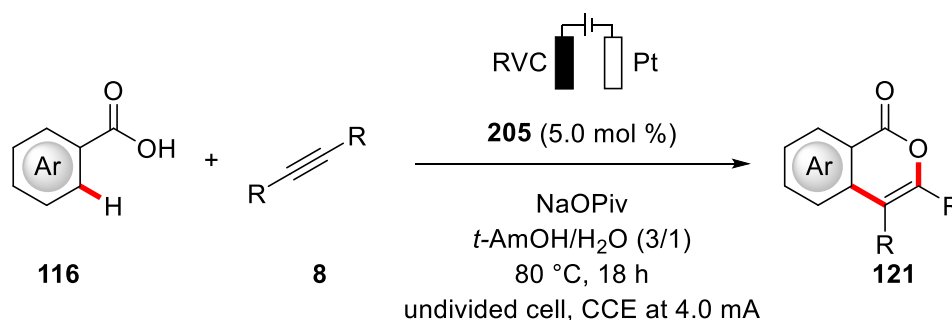
At the outset of this thesis, no electrocatalytic C–H activation was known employing metals other than palladium. However, during the course of this thesis, other reports were published, which shall be discussed in this following chapter.

Ruthenium-catalyzed C–H activation under assistance of electricity was only recently realized by Xu based on a previously reported^[163] oxidative indole synthesis (Scheme 1.46).^[164] Preliminary results also indicated that ruthenium-catalyzed [4+2] annulation of benzylamine to isoquinolines are viable.^[164]



Scheme 1.46. Ruthenium-catalyzed electrochemical indole synthesis.^[164]

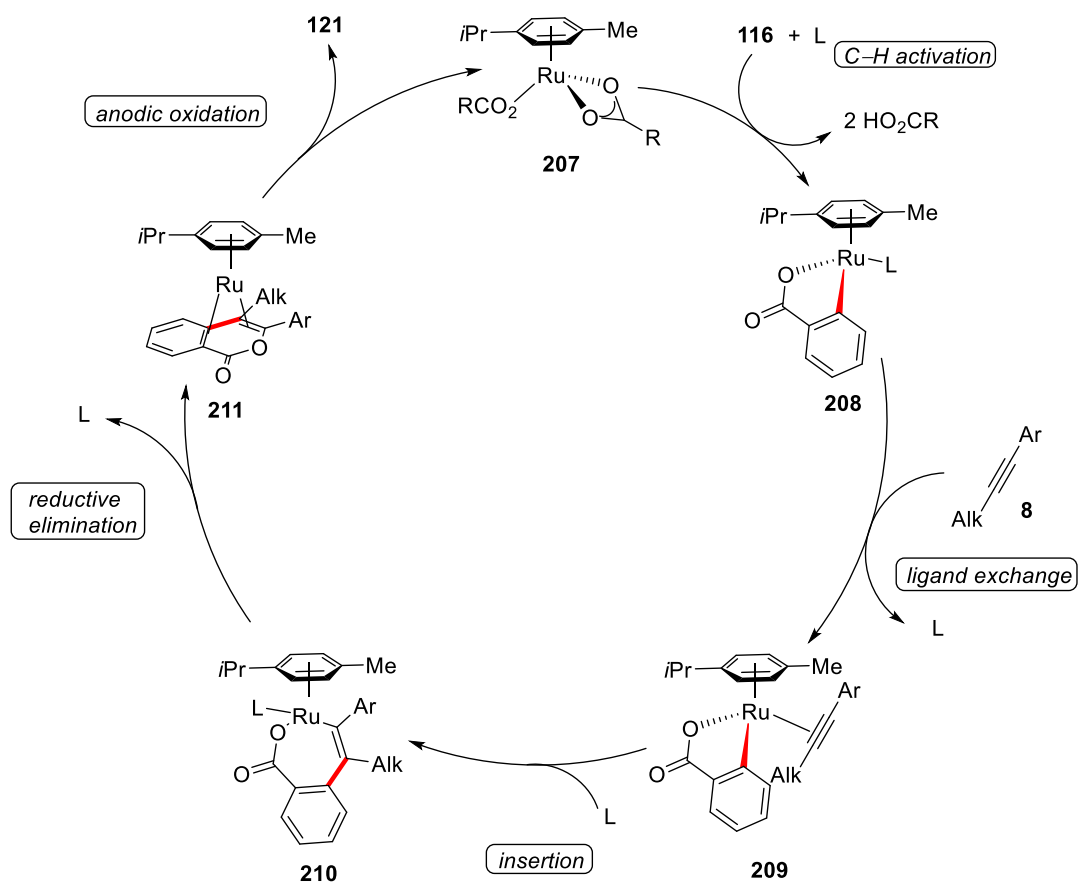
Concurrently, Ackermann developed a ruthenium-catalyzed synthesis of isocoumarines **121** by C–H/O–H annulation (Scheme 1.47).^[165] Noteworthy is the use of weakly coordinating benzoic acids **116**^[166] as substrates, showing for the first time electrochemical C–H activation by transition metals without the use of strongly coordinating nitrogen atoms.



Scheme 1.47. Ruthenium-catalyzed electrochemical C–H/O–H annulation.^[165]

Moreover, besides benzoic acids **116**, also benzamides **11** were found to be viable substrates.^[165] A plausible catalytic cycle was proposed, which includes the formation of five-membered ruthenacycle **208**, followed by coordination and migratory insertion of alkyne **8** (Scheme 1.48).^[165] From the resulting seven-membered species **210**, reductive elimination generates the product, which is still attached to the ruthenium(0)

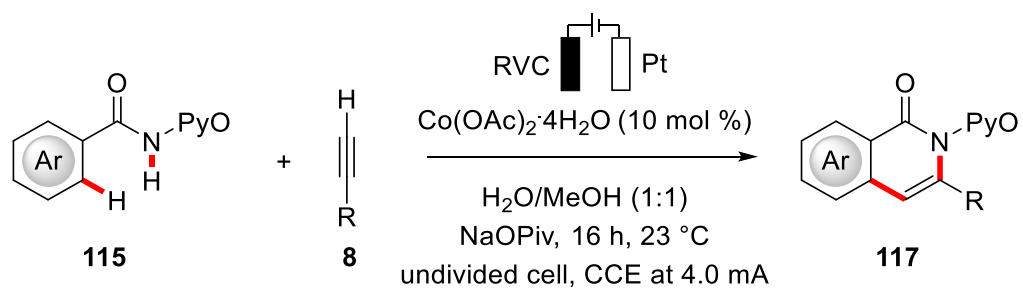
center in sandwich complex **211**. Upon anodic oxidation to regenerate ruthenium(II)-carboxylate species **207**, the desired product **121** is liberated (Scheme 1.48).



Scheme 1.48. Plausible mechanism for the ruthenium-catalyzed C-H/O-H annulation.^[165]

Cobalt-catalyzed electrochemical cross-couplings have been known for over a decade through the pioneering work from Gosmini.^[167] However, cobalt-catalyzed electrochemical C-H activation remained elusive. Although this thesis presents substantial contributions to the field of electrochemical cobalt-catalyzed C-H activation later, concurrently published contributions shall be discussed here shortly.

Recently, Ackermann reported on the electrochemical cobalt-catalyzed isoquinolone formation by assistance of the pyridine-*N*-oxide directing group (Scheme 1.49).^[168] This approach was later extended by Lei to also include the functionalization using gaseous ethylene and ethyne.^[169]

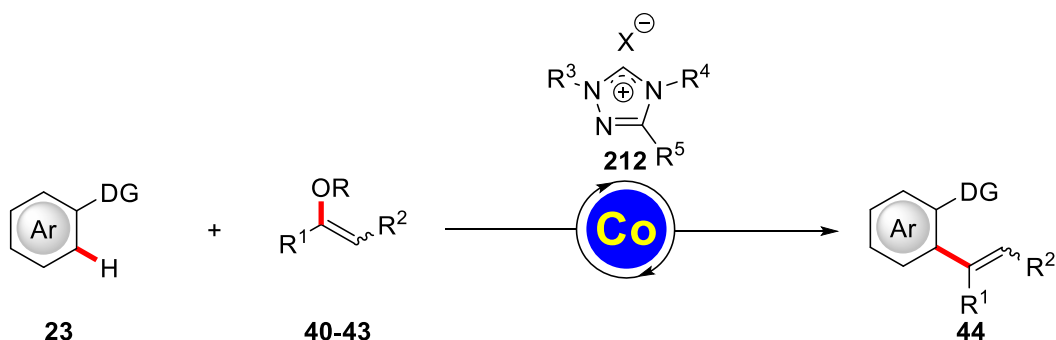


Scheme 1.49. Electrochemical cobalt-catalyzed C–H activation/annulation.^[168]

2 Objectives

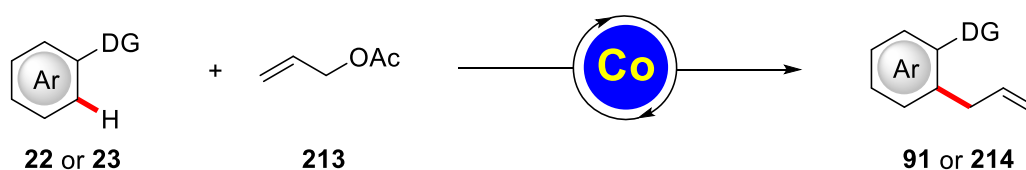
In the last decades, C–H activation exerted a significant influence on organic synthesis, as it became more efficient, cost-effective and generally applicable.^[4, 30] Also, considerable advances have been made in the use of earth-abundant 3d metals,^[18a, 119, 170] rendering these methods more suitable for sustainable organic synthesis. Especially in the field of cobalt-catalyzed reactions,^[48, 69, 171] with the use of low-valent cobalt, Cp*Co(III)-complexes and simple cobalt salts, three independent and to some degree complementary regimes of catalytic action are available.

Direct alkenylations using low-valent cobalt catalysis are known,^[56] however, these transformations are highly dependent of the ligand, as even small changes in the substitution pattern can dramatically alter the outcome. Triazolium salts were rarely used in C–H activation, but a large number of triazolium salts are available due to their prominence in organo-catalysis.^[172] Therefore, triazolium salts **212** were tested as (pre)ligands in cobalt-catalyzed alkenylations (Scheme 2.1).



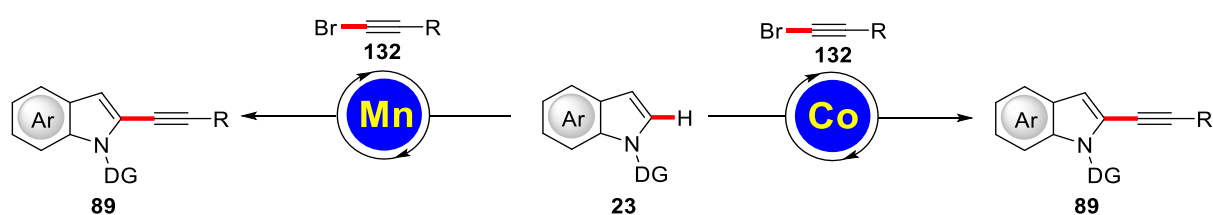
Scheme 2.1. Cobalt-catalyzed C–H alkenylation with triazolium salts **212** as (pre)ligands.

Cobalt-catalysis by Cp*Co(III)-complexes does not feature the highly modular approach of low-valent cobalt catalysis. However, the functional group tolerance is considerably higher.^[48a, 69] Allyl groups are important building blocks and offer the possibility to be functionalized in post-synthetic transformations, which makes the introduction of allyl groups by Cp*Co(III)-catalysis highly desirable (Scheme 2.2).



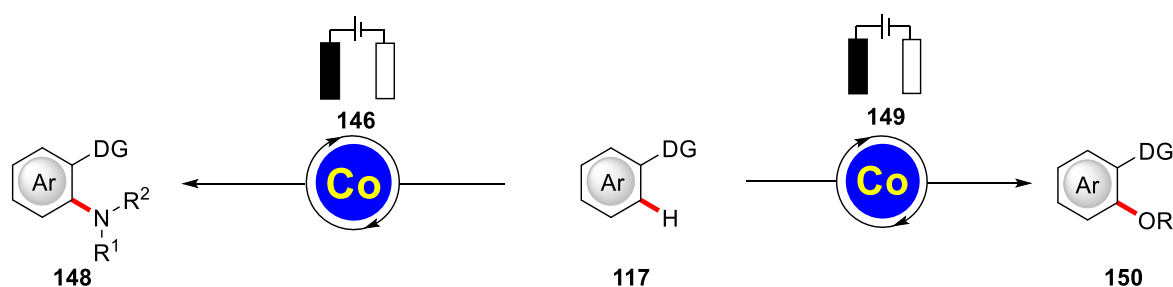
Scheme 2.2. Cobalt-catalyzed C–H allylation.

Likewise, alkynes offer huge possibilities for post-synthetic functionalizations. This is especially important given the biorthogonal nature of the alkyne moiety and possible applications in late-stage peptide ligation.^[173] Base metal-catalyzed protocols for alkynylations were at the outset of this thesis only known for cobalt using hypervalent iodine reagents **88** under harsh reaction conditions.^[78] Therefore, a cobalt-catalyzed protocol at mild conditions using bromoalkynes **132** should be developed for the alkynylation of heteroarenes. Additionally, this transformation is interesting also for manganese-catalyzed processes, as substitutive transformations for this metal are scarce (Scheme 2.3).^[119]



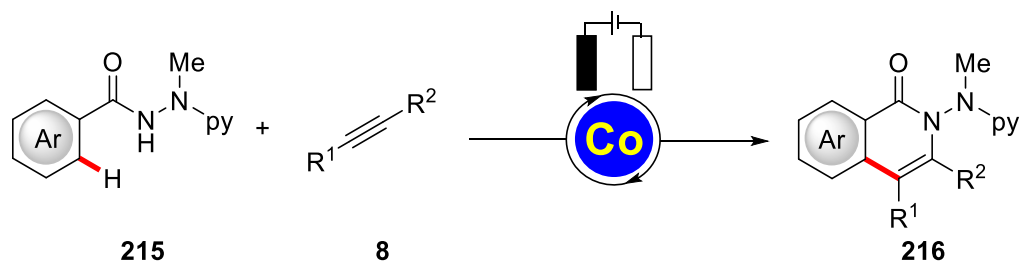
Scheme 2.3. Base metal-catalyzed C–H alkynylation.

Cross-dehydrogenative couplings present the most atom-economical transformation in C–H activation, as the formal byproduct is solely H₂.^[174] However, to achieve these transformations sacrificial oxidants are needed, which greatly reduces the atom economy of C–H activation. Furthermore, most transformations rely on expensive silver salts as oxidants, which drive the cost of the overall reaction (see Figure 1.6).^[137] Additionally, these chemical oxidants offer a specific potential associated with the redox couple, which can hardly be modified. In light of these facts, the use of electricity as the terminal oxidant would greatly increase the atom economy and reduce the associated costs of the reaction. Moreover, a modification of the potential to finely tune the reaction is possible, when needed. Here, a combination of cobalt-catalyzed C–H activation and electrocatalysis would be highly desirable in the formation of C–O and C–N bonds (Scheme 2.4).



Scheme 2.4. Electrocatalytic cobalt-catalyzed C–H oxygenations and aminations.

Finally, electro-oxidative cobalt-catalyzed C–H/N–H annulations with alkynes **8** were realized following the same principles, and the mechanism should be investigated using different methods (Scheme 2.5).



Scheme 2.5. Electro-oxidative cobalt-catalyzed C–H/N–H annulation.

3 Results and Discussion

3.1 Cobalt-Catalyzed Alkenylation under Triazolylidene-Assistance by C–H/C–O Cleavage

Based on the initial work from Yoshikai,^[57] several cobalt-catalyzed C–H alkylations,^[49-50, 52] arylations^[49, 52-54, 175] and alkenylations^[56-61] were reported. However, the majority of C–H alkenylations are based on the hydroarylation of alkynes **8**.^[57-61] This presents a major limitation, due to the poor selectivity in the conversion of unsymmetrical alkynes **8** and the absence of cyclic alkynes **8** in small and medium ring sizes.^[176]

Low-valent cobalt-catalyzed C–H functionalization reactions mainly feature two classes of ligands (see Figure 1.1), namely phosphines and NHC ligands. For NHCs, imidazole-derived IMesHCl (**14**) and IPrHCl (**15**) are the most common preligands.

In cooperation with the group of Prof. A. Berkessel from the University of Cologne, a small library of triazole derived NHCs **212** were synthesized (Figure 3.1)^[177] and tested towards their performance in cobalt-catalyzed C–H alkenylation.

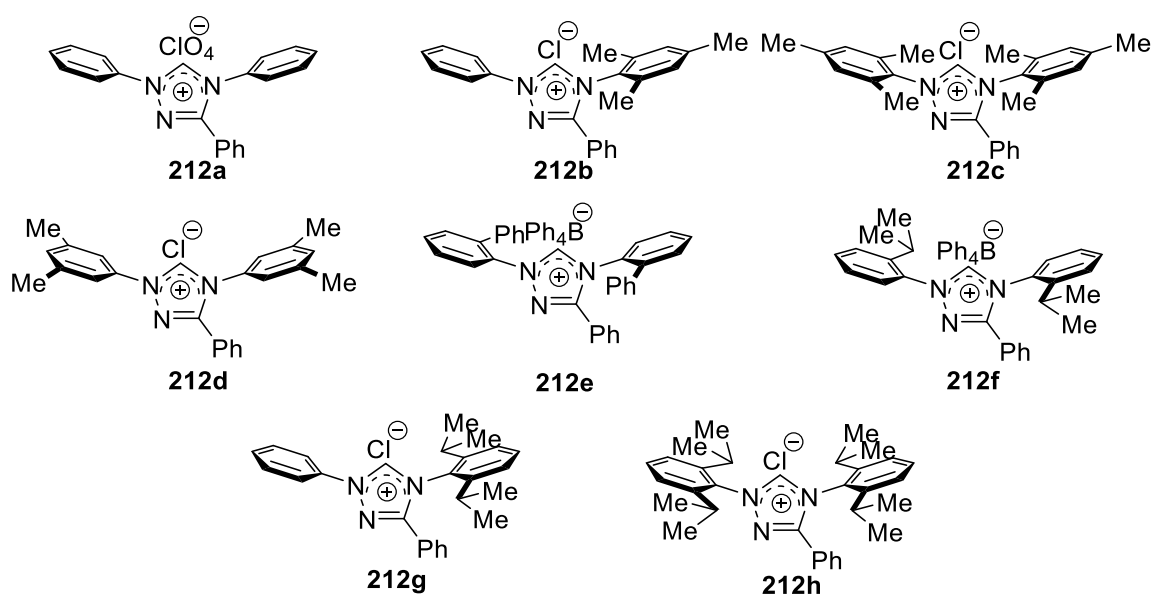


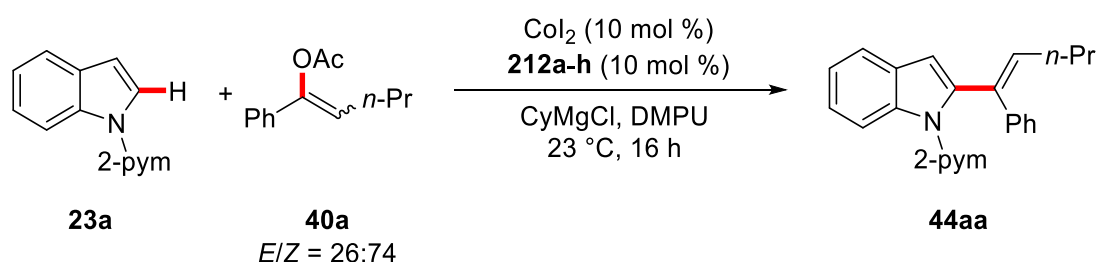
Figure 3.1. Triazolium salts **212** for the cobalt-catalyzed C–H alkenylation.

While generally employed as organocatalysts,^[172a, 178] these triazolium salts were especially interesting in terms of their lower donating abilities^[172b] and possible dispersion interactions^[179] enabled by the distal phenyl group. Moreover, their application in cobalt-catalyzed C–H activation is without precedence.

3.1.1 Optimization

Based on previous studies,^[56] initially CoI_2 , DMPU and CyMgCl were chosen as components of the ternary catalytic system. With these conditions, the preligands **212a-h** were evaluated on their ability to promote the desired reaction (Table 3.1)

Table 3.1 Ligand screening for the cobalt catalyzed C–H alkenylation under triazole assistance.^a



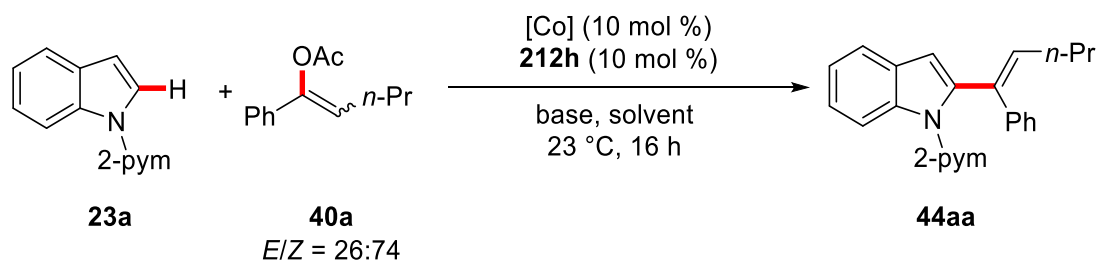
Entry	L	Yield [%]
1	---	<5
2	212a	---
3	212b	---
4	212c	14
5	212d	<5 ^b
6	212e	19
7	212f	<5
8	212g	21
9	212h	52

^a Reaction conditions: **23a** (0.25 mmol), **40a** (0.38 mmol), CoI_2 (10 mol %), **212a-h** (10 mol %), CyMgCl (0.50 mmol), DMPU (1.5 mL), 23 °C, 16 h. ^b Performed by J. Loup.

The reaction was not effective in absence of a preligand (entry 1). Ligand **212a**, as well as the *N*-phenyl-*N*-mesityl substituted triazole **212b** did not lead to improvements in efficacy (entries 2 and 3), while **212c** facilitated product formation to some extent (entry 4). *meta*-Xylene derived ligand **212d** was not effective (entry 5) while biphenyl-substituted ligand **212e** as well as 2-isopropylphenyl-substituted triazole **212g** showed improved reactivities (entries 6 and 8). Triazolium salt **212f** was not suitable (entry 7), while the best results were achieved using 2,6-diisopropylphenyl substituted triazolium salt **212h** (entry 9), which is in good agreement with the observations from our previous studies.^[56]

After the best preligand **212h** was identified, further optimization studies were performed with a focus on the cobalt source, Grignard reagent and solvent (Table 3.2).

Table 3.2 Optimization of the reaction conditions for the cobalt-catalyzed C–H alkenylation.^a



Entry	[Co]	Base	Solvent	Yield [%]
1	CoI ₂	CyMgCl	DMPU	52
2	CoBr ₂	CyMgCl	DMPU	48
3	CoCl ₂	CyMgCl	DMPU	33
4	Co(OAc) ₂	CyMgCl	DMPU	---
5	Co(acac) ₂	CyMgCl	DMPU	<5
6	CoI ₂	CyMgCl	THF	33
7	CoI ₂	CyMgCl	Et ₂ O	<5
8	CoI ₂	CyMgBr	DMPU	51
9	CoI ₂	PhMgBr	DMPU	<5
10	CoI ₂	EtMgCl	DMPU	<5
11	CoI ₂	Me ₃ SiCH ₂ MgCl	DMPU	---
12	CoI ₂	<i>t</i> -BuCH ₂ MgCl	DMPU	<5
13	CoI ₂	---	DMPU	---
14	---	CyMgCl	DMPU	---

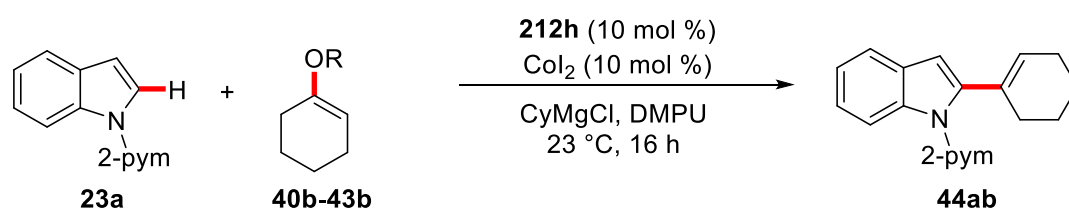
^a Reaction conditions: **23a** (0.25 mmol), **40a** (0.38 mmol), [Co] (10 mol %), **212h** (10 mol %), base (0.50 mmol), solvent (1.5 mL), 23 °C, 16 h.

The optimization commenced with a screening of various cobalt precursors. While cobalt(II) halides generally promoted the C–H alkenylation with similar efficacy (entries 1-3), cobalt(II) acetate (entry 4) and cobalt(II) acetylacetonate (entry 5) only provided trace amounts of the desired product. Besides DMPU, THF proved amenable (entry 6), while Et₂O was not a suitable reaction medium (entry 7). Regarding the Grignard reagent, a comparison between CyMgCl and CyMgBr (entry 8) revealed no significant influence of the halide, while other alkyl and phenyl derived Grignard reagents (entries

9-12) proved not suitable. This is especially noteworthy, since $\text{Me}_3\text{SiCH}_2\text{MgCl}$ and $t\text{-BuCH}_2\text{MgCl}$, which were shown to be active in cobalt catalysis before,^[57, 61-62] are quite costly compared to CyMgCl , which presents an advantage of this method. The essential nature of the base and the cobalt salt was confirmed by control experiments (entries 13 and 14).

Next, different leaving groups on the alkenyl moiety were investigated on their ability to promote the cobalt-catalyzed C–H alkenylation (Table 3.3).

Table 3.3 Leaving group performance in cobalt-catalyzed C–H alkenylation.^a



Entry	R	Yield [%]
1	Ac (40b)	80
2	$\text{P}(\text{O})(\text{OEt})_2$ (41b)	84
3	$\text{C}(\text{O})\text{OEt}$ (42b)	52
4	$\text{C}(\text{O})\text{NMe}_2$ (43b)	72

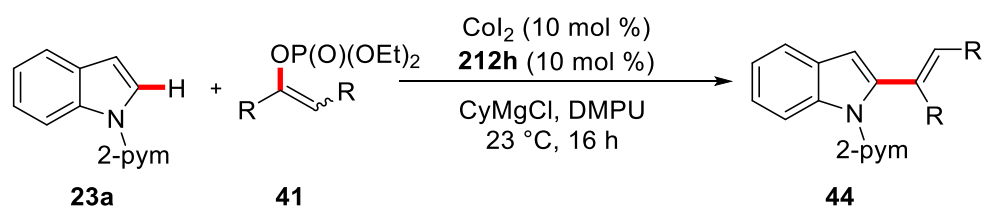
^a Reaction conditions: **23a** (0.25 mmol), **40b-43b** (0.38 mmol), Co_2 (10 mol %), **212h** (10 mol %), CyMgCl (0.50 mmol), DMPU (1.5 mL), 23 °C, 16 h.

This evaluation established alkenyl acetate **40b** and alkenyl phosphate **41b** as competent alkenylating agents (entries 1 and 2). Carbonate **42b** only showed moderate efficacy, while carbamate **43b** performed somewhat better than carbonate **42b**. Based on these results, the scope of the cobalt-catalyzed alkenylation under triazole assistance was investigated using alkenyl acetates **40** and phosphates **41** with an optimized catalytic system comprising of Co_2 , ligand **212h** and CyMgCl in DMPU as the solvent.

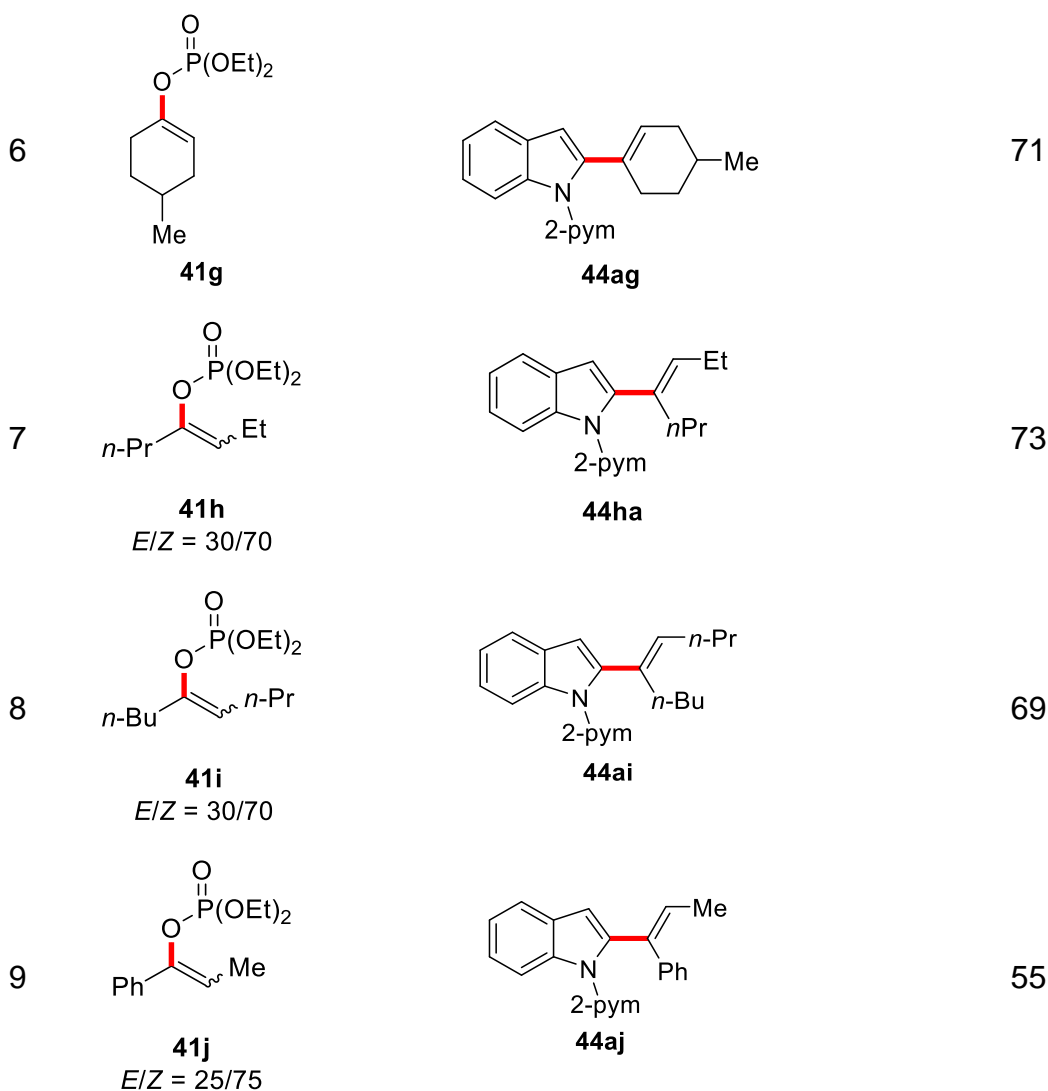
3.1.2 Scope of the Cobalt-Catalyzed Alkenylation using Alkenyl Phosphates

With the optimized conditions in hand, the scope of the reaction was examined with different alkenyl phosphates **41** (Table 3.4).

Table 3.4 Scope of the cobalt-catalyzed C–H alkenylation using alkenyl phosphates **41**.^a



Entry	Phosphate	Product	Yield [%]
1	 41b	 44ab	84
2	 41c	 44ac	81
3	 41d	 44ad	69
4	 41e	 44ae	80
5	 41af	 44af	74

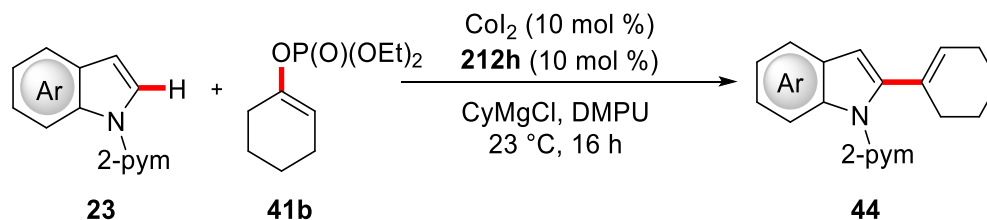


^a Reaction conditions: **23a** (0.25 mmol), **41** (0.38 mmol), CoI_2 (10 mol %), **212h** (10 mol %), CyMgCl (0.50 mmol), DMPU (1.5 mL), 23 °C, 16 h.

The reaction proceeded with moderate to excellent yields for all substrates. Comparable efficacy was achieved for cyclohexenylphosphate (**41b**) as well as 4-substituted cyclohexenylphosphates **41c-g** (entries 2-6). This is indicative of only a minor influence of the substituent in C-4 position of the alkenyl phosphate. Good yields could be observed for acyclic bisalkyl alkenyl phosphates **41h** and **41i** (entries 7 and 8), while alkenyl phosphate **41j** with mixed aryl and alkyl substituents was converted with moderate yield (entry 9). It is noteworthy, that although a mixture of *E/Z*-isomers was employed in this reaction (30/70 for entries **41h** and **41i**, 25/75 for **41j**), the *E*-product was observed exclusively, indicating a stereoconvergent process being operative here.^[56]

Furthermore, different indoles **23** were employed in the reaction using cyclohexenylphosphate (**41b**) as the alkenylating reagent (Table 3.5).

Table 3.5. Scope of the cobalt-catalyzed C–H alkenylation of indoles **23**.^a



Entry	Indole	Product	Yield [%]
1			84
2			81
3			55

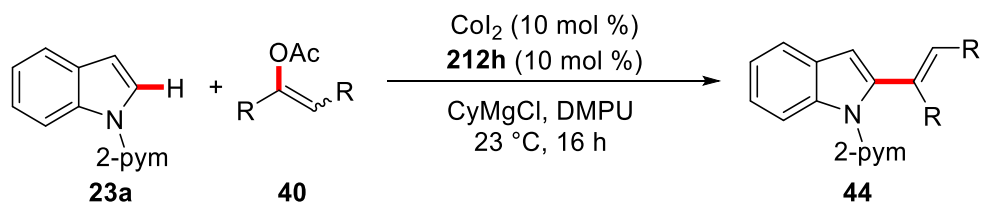
^a Reaction conditions: **23** (0.25 mmol), **41b** (0.38 mmol), CoI_2 (10 mol %), **212h** (10 mol %), CyMgCl (0.50 mmol), DMPU (1.5 mL), 23 °C, 16 h.

Unsubstituted 2-pyrimidylindole (**23a**) and 5-fluoroindole **23b** were identified as excellent substrates for the C–H alkenylation (entries 1 and 2). Remarkable was the smooth conversion of indole **23c**, because the ester group proved to be stable.^[180]

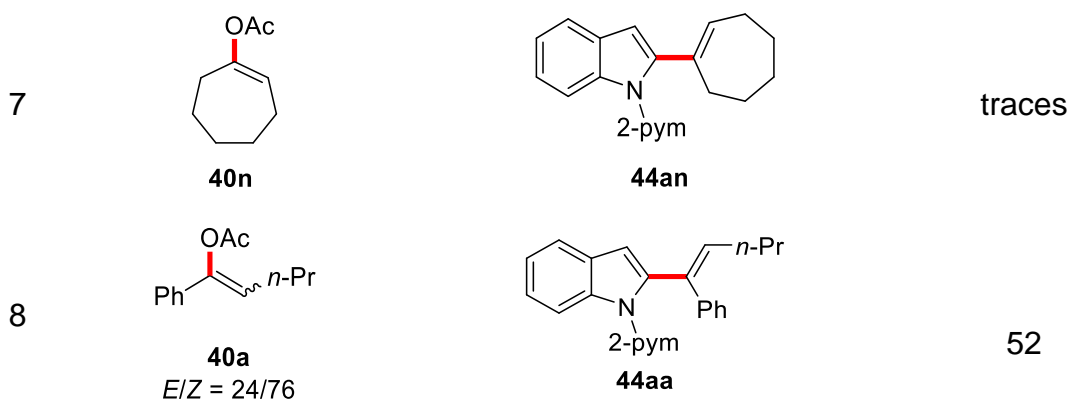
3.1.3 Scope of the Cobalt-Catalyzed Alkenylation using Alkenyl Acetates

After establishing the scope of alkenyl phosphates **41**, more atom-economical acetates **40** were investigated for their use in the cobalt-catalyzed C–H alkenylation (Table 3.6).

Table 3.6. Cobalt-catalyzed C–H alkenylation with alkenyl acetates **40**.



Entry	Acetate	Product	Yield [%]
1	 40b	 44ab	80
2	 40c	 44ac	78
3	 40e	 44ae	75
4	 40k	 44ak	71
5	 40l	 40al	---
6	 40m	 44am	traces

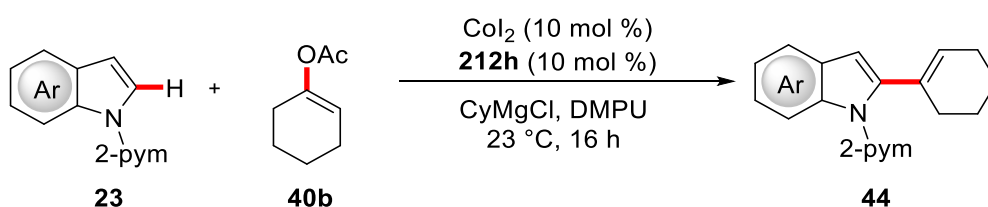


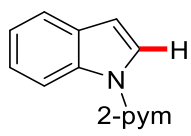
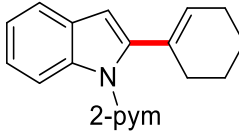
^a Reaction conditions: **23a** (0.25 mmol), **40** (0.38 mmol), CoI_2 (10 mol %), **212h** (10 mol %), CyMgCl (0.50 mmol), DMPU (1.5 mL), 23 °C, 16 h.

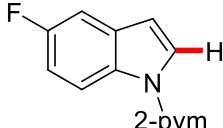
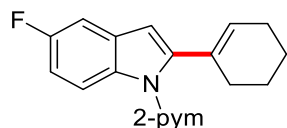
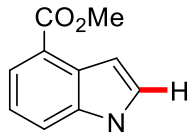
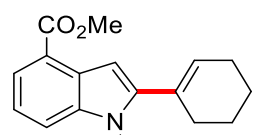
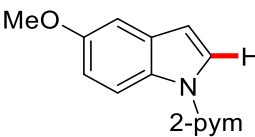
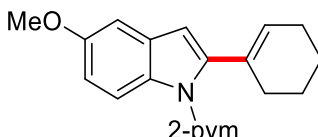
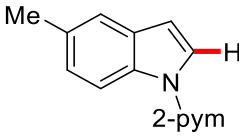
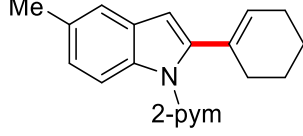
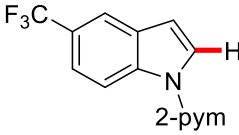
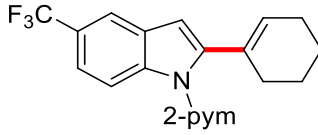
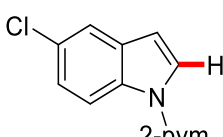
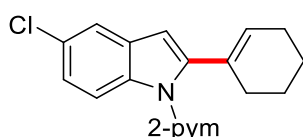
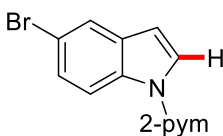
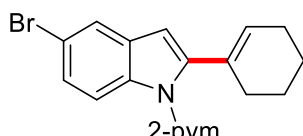
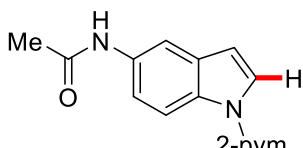
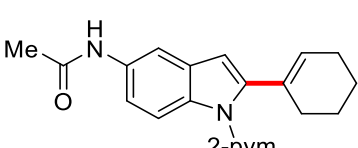
Cyclohexenylacetate (**40b**) and its substituted analogues were smoothly converted with up to 80% yield (entries 1-4). However, α -Tetralone derived acetate **40i** showed no reactivity. Smaller and larger cyclic enol acetates **40m** and **40n** (entries 6 and 7) were not suitable substrates, only resulting in traces of the desired products **44**, while acyclic acetate **40a** was converted with moderate yield, and again exclusively to the *E*-product.

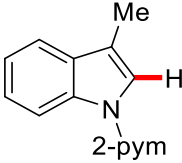
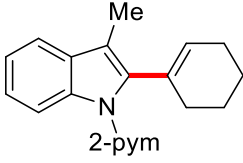
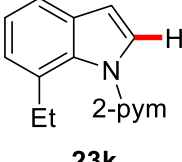
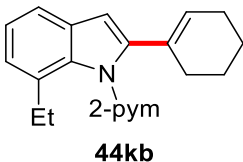
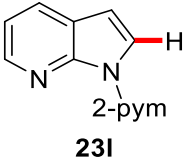
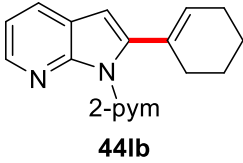
Additionally, the scope of indoles **23** was investigated using cyclohexenylacetate (**40b**) as the standard alkenylation reagent (Table 3.7).

Table 3.7. Cobalt-catalyzed C–H alkenylation of indoles **23**.



Entry	Indole	Product	Yield [%]
1	 23a	 44ab	80

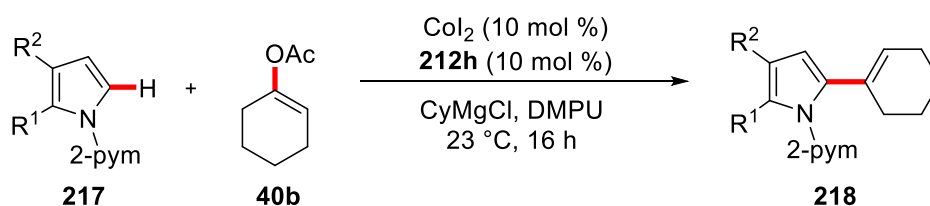
2	 23b	70
	 44bb	
3	 23c	61
	 44cb	
4	 23d	72
	 44db	
5	 23e	80
	 44eb	
6	 23f	74
	 44fb	
7	 23g	59
	 44gb	
8	 23h	---
	 44hb	
9	 23i	---
	 44ib	

10	 23j	 44jb	85
11	 23k	 44kb	74
12	 23l	 44lb	---

^a Reaction conditions: **23** (0.25 mmol), **40b** (0.38 mmol), CoI_2 (10 mol %), **212h** (10 mol %), CyMgCl (0.50 mmol), DMPU (1.5 mL), 23 °C, 16 h. ^b CyMgCl (1.00 mmol)

As shown in Table 3.7, diversely decorated indoles bearing fluoride, ester, alkyl and alkoxy substituents were amenable substrates (entries 1-6). While 5-chloroindole **23g** (entry 7) was converted with moderate yield, the corresponding 5-bromoindole **23h** (entry 8) did not show any formation of the desired product **44hb**. This can be attributed to the higher reactivity of bromo compounds in the cross coupling of bromoarenes and Grignard reagents,^[181] and indeed the formation of 5-cyclohexylindole was confirmed by GC-analysis. Acetanilide **23i** also showed no reaction, even when more base was used to account for initial deprotonation of the N–H bond which might occur under the reaction conditions (entry 9). Furthermore, sterically crowded indoles **23j** and **23k** reacted smoothly to the desired products (entries 10 and 11). Finally, 7-Azaindole derived substrate **23l** proved not suitable, maybe due to a strong chelating coordination of the cobalt-catalyst between the pyridine and pyrimidine nitrogens.

Besides indoles **23**, pyrroles **217** were also suitable substrates for this reaction (Table 3.8).

Table 3.8 Cobalt-catalyzed C–H alkenylation of pyrroles **217**.

Entry	Pyrrole	Product	Yield [%]
1	 217a	 218ab	74 ^b
2	 217b	 218bb	traces ^c
3	 217c	 218cb	53

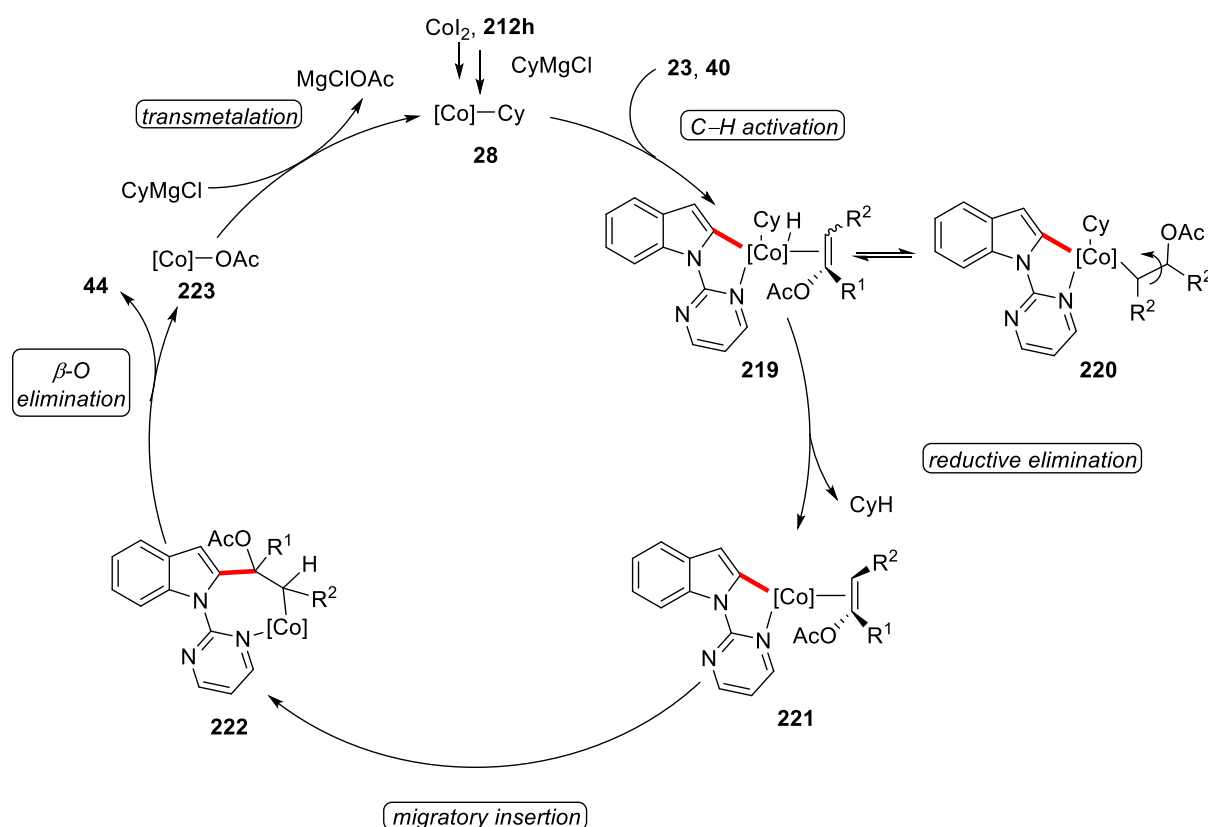
^a Reaction conditions: **217** (0.25 mmol), **40b** (0.38 mmol), Co_2 (10 mol %), **212h** (10 mol %), CyMgCl (0.50 mmol), DMPU (1.5 mL), 23 °C, 16 h. ^b **40b** (0.75 mmol) ^c 60 °C

While simple unsubstituted 2-pyridylpyrrole (**217a**) was a very good substrate, reactions using 1.50 equivalents of the alkenyl acetate resulted in mixtures of mono- and bisalkenylated products. Selective conversion to the bis-alkenylated product was achieved using 3.00 equivalents of the alkenyl acetate **40b** (entry 1). In contrast 2,4-dimethylpyrrole **217b** only provided trace amounts of product **218bb**, even at elevated temperature (entry 2). Finally, tetrahydroindolone **217c** was converted with a yield of 53%, which is remarkable given that ketones usually undergo facile addition of Grignard reagents. (entry 3).^[180]

3.1.4 Mechanism of the Cobalt-Catalyzed Alkenylation

The mechanism of the cobalt-catalyzed C–H alkenylation by triazole assistance is rationalized to be similar to the previously proposed mechanism using imidazolium

salts as preligands (Scheme 3.1).^[56, 182] After generation of the active species **28**, C-H activation occurs, and the enol reagent is coordinated. *E/Z*-isomerization takes place to give rise to the exclusively *E*-configured enol acetate or phosphate, followed by migratory insertion resulting in intermediate **222**. Subsequent β -O elimination furnished the desired product and the active species **28** is regenerated upon transmetalation.



Scheme 3.1. Proposed catalytic cycle for the cobalt-catalyzed C-H alkenylation of indoles **44**.

In summary, the first application of triazolylidenes in cobalt-catalyzed C-H activation could be realized in the C-H alkenylation of indoles **23** and pyrroles **217** using alkenyl acetates **40** and phosphates **41**. Cyclic as well as acyclic enol acetates **40** and phosphates **41** were suitable coupling partners, and for acyclic compounds, a stereoconvergent reaction was observed.

3.2 Cobalt-Catalyzed Allylation using Allyl Acetates

While a range of C-H functionalizations has been established with low-valent cobalt catalysis,^[48c, 48d] limitations exist with regard to the functional group tolerance due to

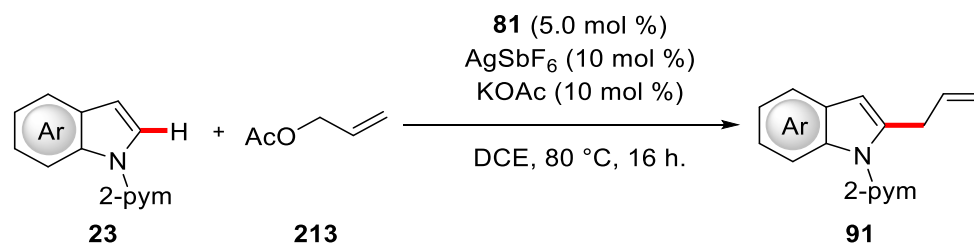
the omnipresent Grignard reagents. In this regard, Cp*Co(III)-complexes offer a versatile alternative, which should exhibit higher compatibility towards electrophilic functional groups.^[48a, 69]

Allyl groups present versatile handles for further post-synthetic diversification, for example by olefin metathesis^[183] or allylic functionalization.^[184] Therefore, the introduction of allyl groups is an interesting research area, especially using easily accessible allyl acetate **213**. Indoles are a key structural motif in many biologically active compounds,^[185] rendering them interesting substrates in C–H activation.

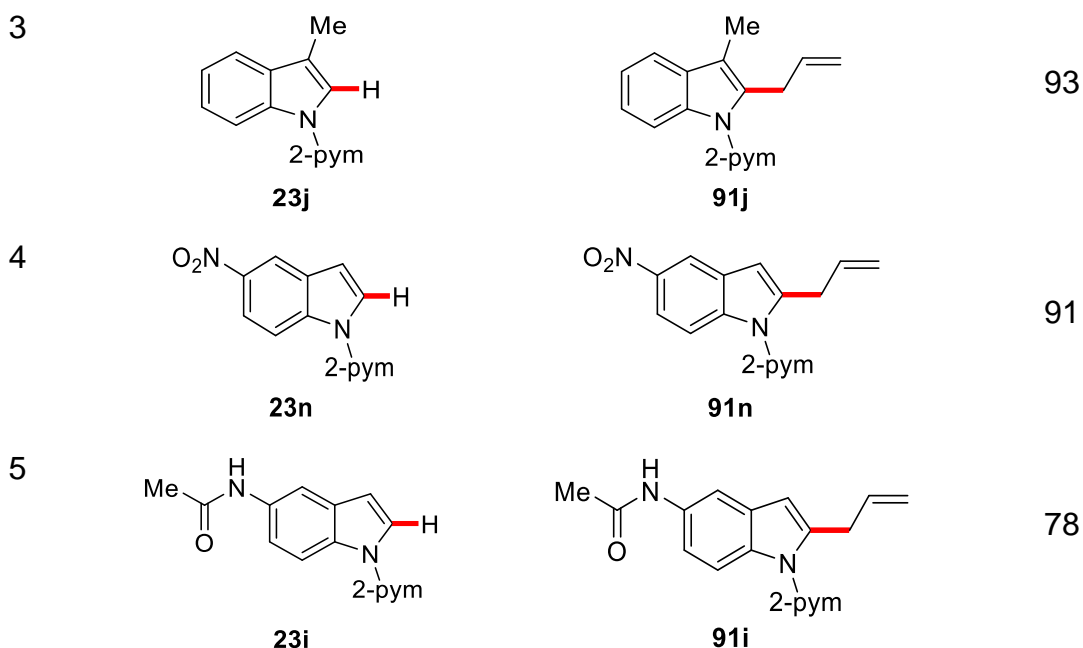
3.2.1 Optimization and Scope

Optimization studies on the cobalt(III)-catalyzed C–H allylation were conducted by M. Moselage^[182] and after testing various cobalt complexes and additives, a catalytic system comprised of Cp*Co(CO)I₂ (**81**) (5 mol %), AgSbF₆ (10 mol %) and KOAc (10 mol %) in DCE at 80 °C for 16 h was identified as optimal. With these optimized conditions in hand, the scope of the cobalt-catalyzed C–H allylation was explored regarding the indole moiety (Table 3.9).

Table 3.9 Scope of the cobalt-catalyzed allylation of indoles **23**.^a



Entry	Indole	Product	Yield [%]
1	<p>23m</p>	<p>91m</p>	89
2	<p>23f</p>	<p>91f</p>	84

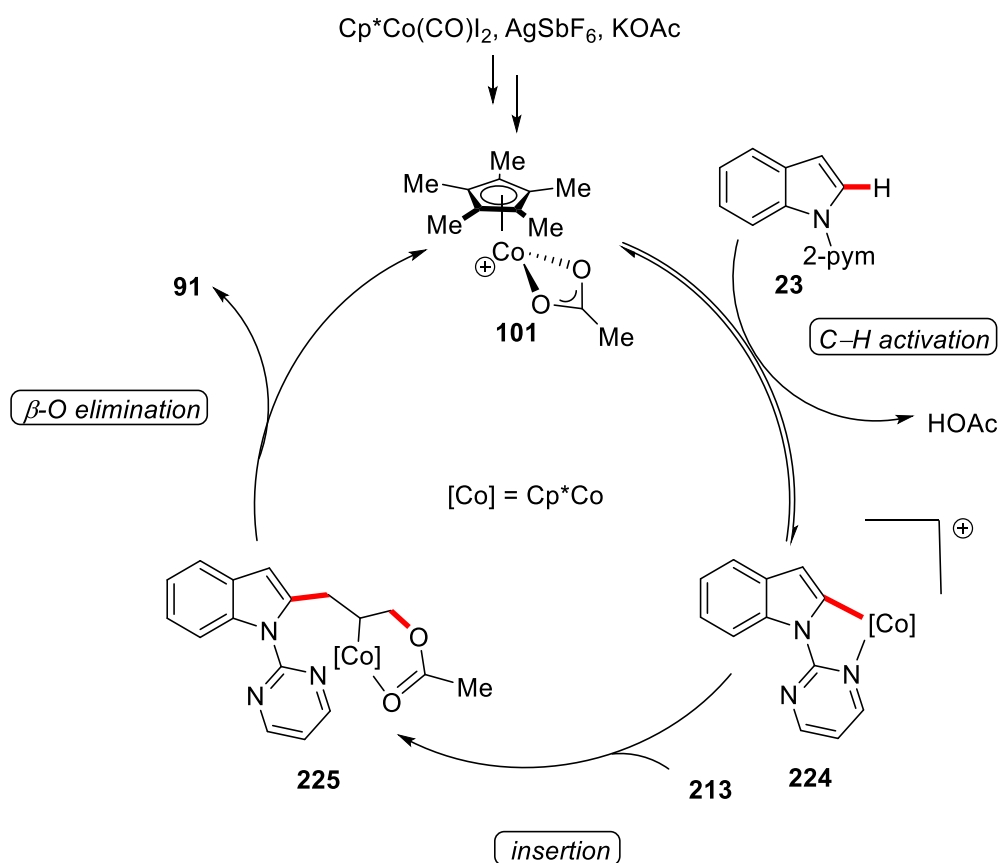


^a Reaction conditions: **23** (0.50 mmol), **213** (1.00 mmol), **81** (5.0 mol %), AgSbF₆ (10 mol %), KOAc (10 mol %), DCE (1.5 mL), 80 °C, 16 h.

The scope of indoles **23** showed a broad applicability of the cobalt(III)-catalyzed C–H allylation. Electron-rich as well as electron-deficient indoles **23** were converted (entries 1 and 2). Sterically congested indole **23j** (entry 3) was allylated with excellent yield and a nitro substituent was well tolerated (entry 4). Finally, the acetanilide containing substrate **23i** proved amenable in the cobalt(III)-catalyzed C–H allylation (entry 5).

In addition, M. Moselage established several other indoles **23** and phenyl pyri(mi)dines **22** as viable substrates, although at reduced catalytic efficiency.^[182] Experiments with substituted allyl acetates revealed a high sensitivity towards the substitution patterns, resulting in significant loss of reactivity. After considerable optimization, J. Koeller could realize an example, in which crotonylacetate was converted with an overall yield of 63% for a mixture of isomers.^[186] Finally, mechanistic studies were conducted by M. Moselage,^[182] and a catalytic cycle was rationalized.

Initial formation of the cationic complex **101** followed by reversible C–H cobaltation by BIES-type mechanism^[29] delivers five-membered intermediate **219** (Scheme 3.2). Insertion of the allylic double bond into the cobalt-carbon bond generates intermediate **220**, stabilized by coordination of the carbonyl group. From intermediate **225**, β -O elimination regenerates the active cobalt complex **101** and furnishes the desired product **91**.



Scheme 3.2 Proposed catalytic cycle for the cobalt-catalyzed C–H allylation by C–H/C–O cleavage.

3.3 Base Metal-Catalyzed C–H Alkynylation

Alkynes are versatile building blocks in organic synthesis. Possible applications include selective reductions,^[187] Sonogashira-Hagihara cross-coupling^[188] and the so-called “Click-chemistry”,^[173c, 189] among others. Therefore, alkynes represent valuable synthetic handles for further late-stage functionalization, rendering environmentally-benign and cost-effective methods to introduce alkynes into the target molecules highly desirable.

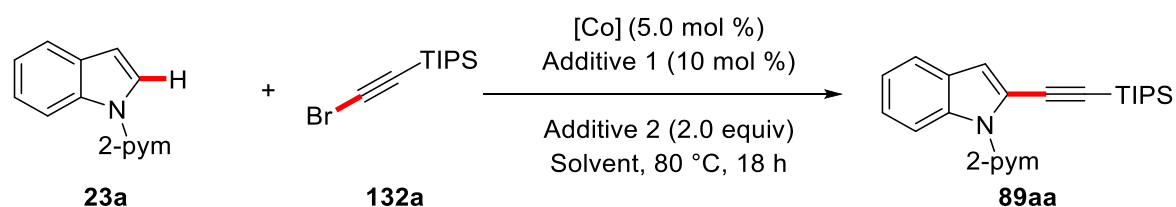
3.3.1 Optimization of the Cobalt-Catalyzed C–H Alkynylation

At the outset of this study, base metal-catalyzed C–H alkynylations were identified as a research area in need of further development. Indeed, most known methods for C–H alkynylation previously used precious and cost intensive metals, like rhodium^[190] and iridium.^[191]

During the studies presented in this thesis, Shi independently reported on a cobalt-catalyzed alkyne alkylation under harsh conditions, that is 120 °C and the use of a strong alcoholate base.^[78] Furthermore, the alkyne reagent, TIPS-EBX (**88**) requires a three-step synthesis and is not very atom-economical.^[192] Due to the desire to realize the cobalt-catalyzed alkyne alkylation efficiently under mild reaction conditions, easily accessible and more atom efficient bromoalkynes **132** were chosen as the alkyne coupling partner.

Therefore, the optimization of the envisioned cobalt-catalyzed C–H alkyne alkylation was initiated using bromoalkyne **132a**, 2-pyrimidylindole (**23a**) and Cp*Co(CO)I₂ (**81**) as the catalyst (Table 3.10).

Table 3.10 Optimization of the cobalt-catalyzed C–H alkyne alkylation using bromoalkyne **132a**.^a



Entry	[Co]	Additive 1	Additive 2	Solvent	Yield [%]
1	Cp*Co(CO)I ₂	AgSbF ₆	KOAc	MeOH	---
2	Cp*Co(CO)I ₂	AgSbF ₆	KOAc	DCE	28
3	Cp*Co(CO)I ₂	AgSbF ₆	KOAc	TFE	68
4	Cp*Co(CO)I ₂	AgSbF ₆	KOAc	HFIP	17
5	Co(OAc) ₂	AgSbF ₆	KOAc	TFE	---
6	[Cp*CoI ₂] ₂	AgSbF ₆	KOAc	TFE	75
7	[Cp*Co(C ₆ H ₆)][PF ₆] ₂	---	KOAc	TFE	---
8	[Cp*CoI ₂] ₂	AgBF ₄	KOAc	TFE	66
9	[Cp*CoI ₂] ₂	AgPF ₆	KOAc	TFE	72
10	[Cp*CoI ₂] ₂	AgNTf ₂	KOAc	TFE	58
11	[Cp*CoI ₂] ₂	Zn(OTf) ₂	KOAc	TFE	---
12	[Cp*CoI ₂] ₂	KPF ₆	KOAc	TFE	---
13	[Cp*CoI ₂] ₂	AgOTf	KOAc	TFE	---
14	[Cp*CoI ₂] ₂	AgSbF ₆	PivOH	TFE	<5
15	[Cp*CoI ₂] ₂	AgSbF ₆	K ₃ PO ₄	TFE	52
16	[Cp*CoI ₂] ₂	AgSbF ₆	KOTs	TFE	---

17	[Cp*CoI ₂] ₂	AgSbF ₆	NaOAc	TFE	69
18	[Cp*CoI ₂] ₂	AgSbF ₆	K ₂ CO ₃	TFE	91
19	[Cp*CoI ₂] ₂	AgSbF ₆	Na ₂ CO ₃	TFE	86
20	---	AgSbF ₆	K ₂ CO ₃	TFE	---
21	[Cp*CoI ₂] ₂	---	K ₂ CO ₃	TFE	---
22	[Cp*CoI ₂] ₂	AgSbF ₆	---	TFE	---
23	[Cp*CoI₂]₂	AgSbF₆	K₂CO₃	TFE	96^b

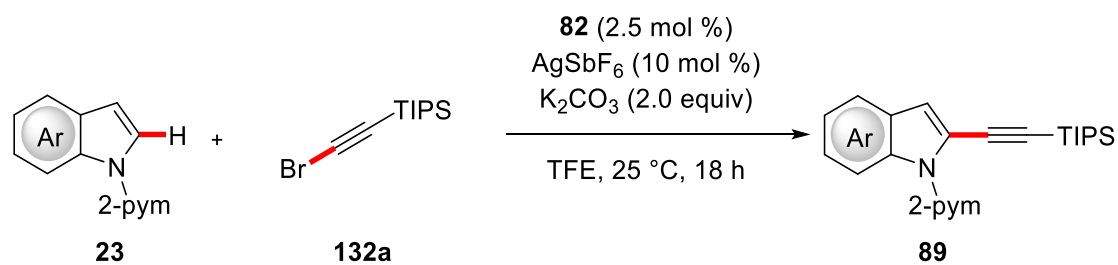
^a Reaction conditions: **23a** (0.50 mmol), **132a** (1.00 mmol), [Co] (5.0 mol %), additive 1 (10 mol %), additive 2 (1.00 mmol), solvent (2.0 mL), 80 °C, 18 h. ^b 25 °C, 18 h.

While MeOH was not a suitable reaction medium, DCE gave a promising result (entry 2), which could be further improved by the use of 2,2,2-trifluoroethanol as the solvent (entry 3). Of the screened cobalt complexes, the dimeric species [Cp*CoI₂]₂ (**82**) proved to be the most efficient catalyst (entry 6), while simple Cp*Co(CO)I₂ (**81**) gave somewhat lower yields. In contrast, simple cobalt(II) acetate and cationic sandwich complex [Cp*Co(C₆H₆)]₂[PF₆]₂ (**73**) were not competent catalysts for the C–H alkynylation (entries 5 and 7). Other silver additives with weakly coordinating counter ions^[193] showed comparable results to AgSbF₆ (entries 8-10), while additives such as zinc(II) triflate and KPF₆, were not suitable. Furthermore, among a representative set of additives, several beneficial effects were obtained (entries 14-19), with the highest efficacy observed with the mild base K₂CO₃ (entry 18). Several control experiments highlighted the essential nature of the cobalt catalyst, silver salt and base (entries 20-22). Finally, an experiment at ambient temperature of 25 °C confirmed the outstanding catalytic activity of this system, as nearly quantitative yield of **89aa** was (entry 23).

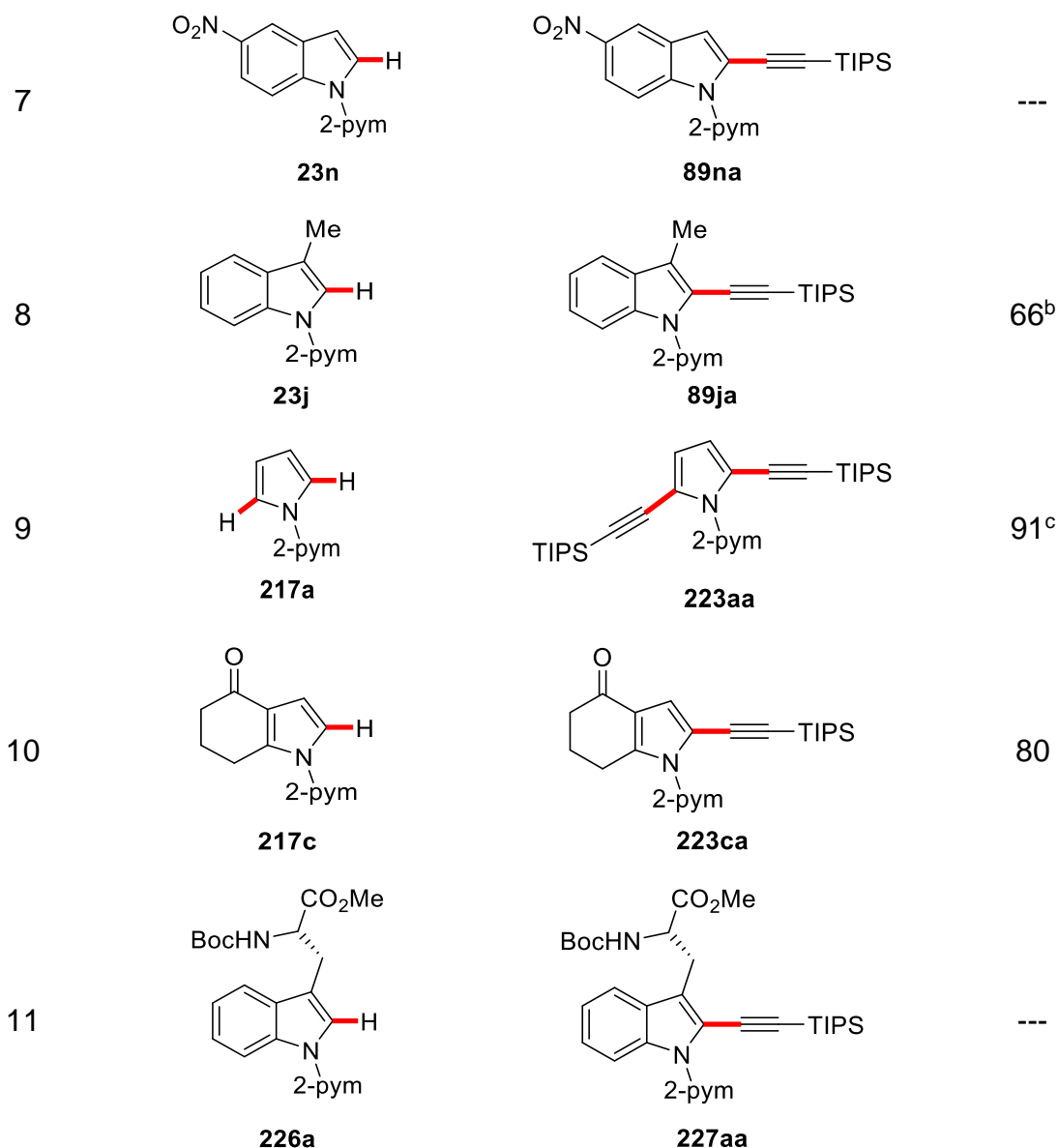
3.3.2 Scope of the Cobalt-Catalyzed C–H Alkynylation

With the optimized catalytic system in hand, the robustness of the C–H alkynylation by cobalt catalysis was evaluated towards diversely substituted indoles **23** and amino acids **226** (Table 3.11).

Table 3.11 Scope of the cobalt-catalyzed C–H alkylation of indoles **23**, pyrroles **217** and amino acid **226**.^a



Entry	Indole	Product	Yield [%]
1			96
2			91
3			94
4			82 ^b
5			92 ^b
6			87 ^b



^a Reaction conditions: **23** or **226** (0.50 mmol), **132a** (1.00 mmol), **82** (2.5 mol %), AgSbF₆ (10 mol %), K₂CO₃ (1.00 mmol), TFE (2.5 mL), 25 °C, 18 h. ^b 80 °C, 18 h. ^c **132a** (2.00 mmol).

The reaction generally proceeded with good to excellent yields. It is noteworthy, that electronically neutral or electron-rich substrates reacted efficiently at room temperature (entries 1-3), while electron-deficient substrates, such as halide substituted indoles **23o**, **23h** and **23p** (entries 4-6) required a higher reaction temperature of 80 °C. Furthermore, sterically crowded substrate **23j** was converted less efficiently (entry 8), while nitro-substrate **23n** appeared to be completely insoluble in TFE (entry 7). Simple pyrimidylpyrrole **217a** was converted with excellent yield (entry 9), however only double alkylation was achieved selectively by increasing the amount of **132a**. Lower amounts of bromoalkyne **132a** led to an inseparable mixture of mono- and


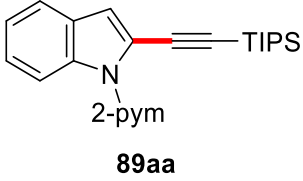
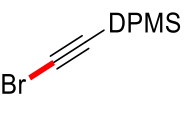
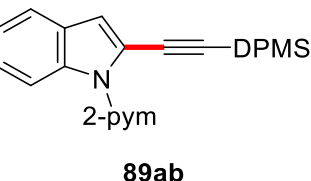

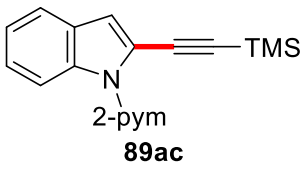
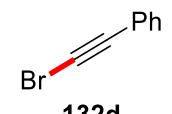
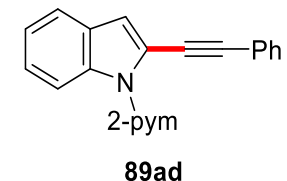
bisalkynylated products. Moreover, tetrahydroindolone **217c** was smoothly converted, once again highlighting the exceptional functional group tolerance of the cobalt catalysis (entry 10).

For tryptophan derived substrate **226a**, no reaction was observed (entry 11). Besides indoles **23**, also pyrroles **217** were investigated regarding the substrate scope

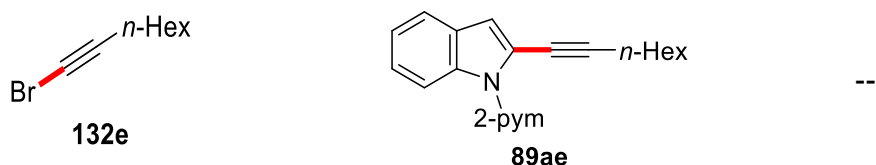
Finally, the use of different bromoalkynes **132** was tested, both regarding other silyl protecting groups as well as alkyl and aryl alkynes (Table 3.12).

Table 3.12 Scope of the cobalt-catalyzed C–H alkylation using bromoalkynes **132**.^a



Entry	Bromoalkyne	Product	Yield [%]
1	 132a	 89aa	96 ^b
2	 132b	 89ab	62
3	 132c	 89ac	73
4	 132d	 89ad	---

5

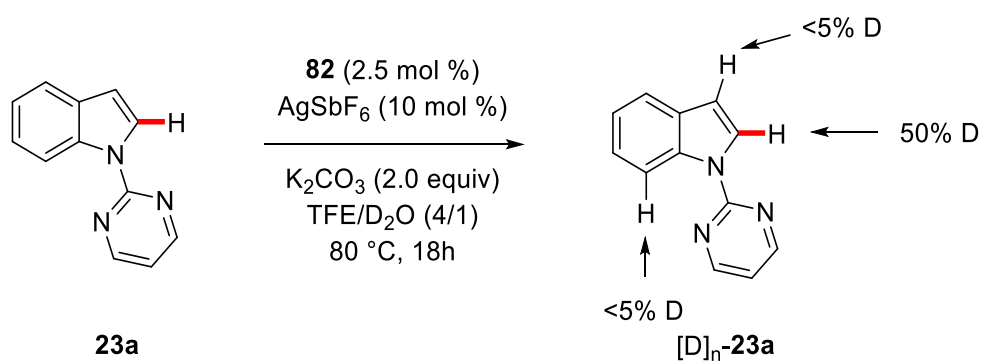


^a Reaction conditions: **23a** (0.50 mmol), **132** (1.00 mmol), **82** (2.5 mol %), AgSbF₆ (10 mol %), KOAc (1.00 mmol), TFE (2.5 mL), 25 °C, 18 h. ^b K₂CO₃ (1.00 mmol).

Besides TIPS-alkyne **132a** (entry 1), also DPMS- and TMS-alkynes **132b** and **132c** were successfully tolerated (entries 2 and 3), under a slight variation of the standard conditions. In contrast, aryl and alkyl substituted alkynes **132d** and **132e** proved to be not reactive under the reaction conditions (entries 4 and 5).

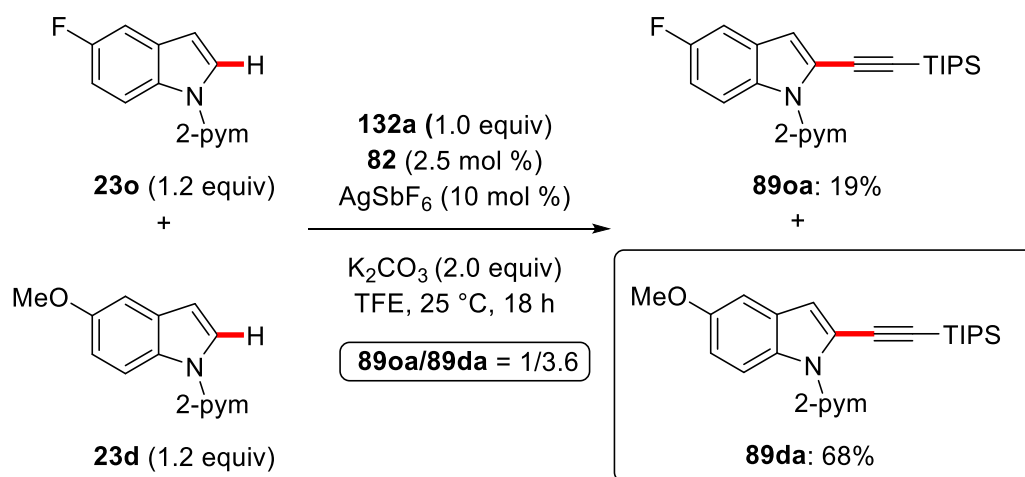
3.3.3 Mechanistic Studies

After establishing the scope of the cobalt-catalyzed C–H alkylation of indoles **23**, mechanistic experiments were conducted to gain insights into its mode of action. To this end, a reaction using D₂O as cosolvent was conducted in the absence of bromoalkyne **132a**. Starting material **23a** could be reisolated and deuterium incorporation was observed in the C-2 position with 50% deuteration. This is indicative of a reversible C–H metalation, while no deuteration could be observed in the C-3 or C-7 position (Scheme 3.3).



Scheme 3.3 H/D Exchange experiment.

Additionally, competition experiments were conducted with regard to the indole **23** (Scheme 3.4).

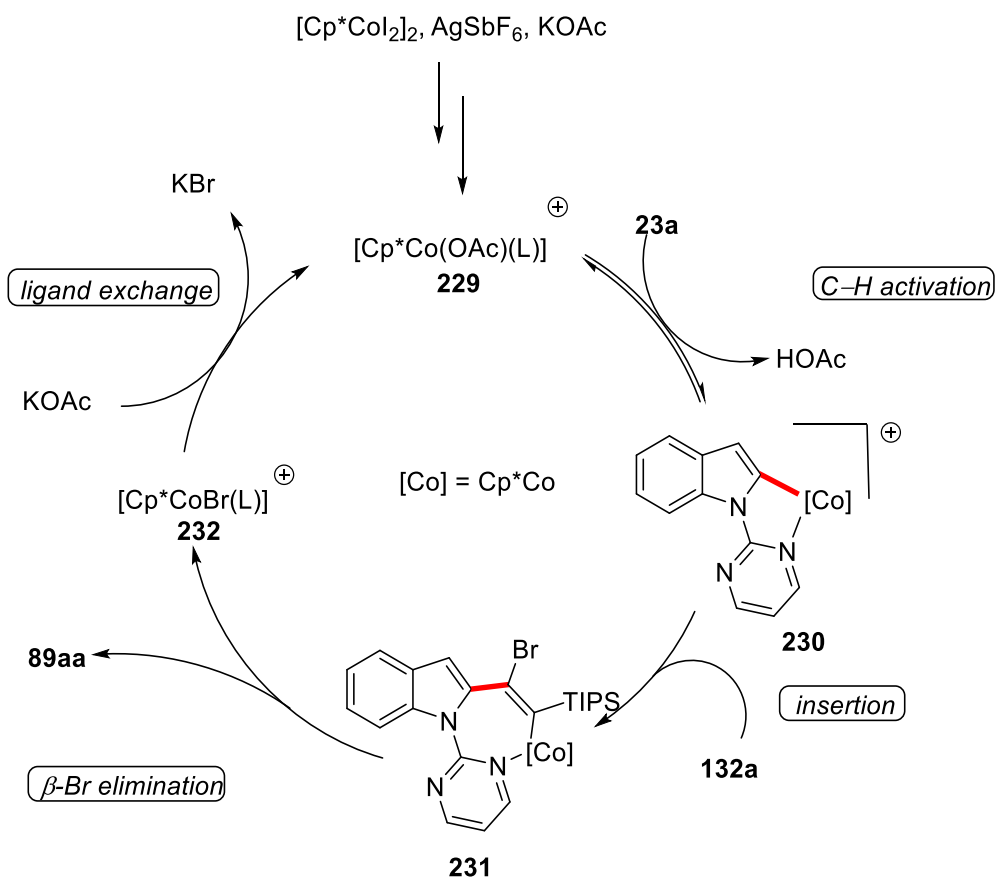


Scheme 3.4 Intermolecular competition experiment between indoles **23o** and **23d**.

The competition experiment between electron-rich and electron-deficient arenes **23d** and **23o** revealed a preferential reactivity in favor of the more electron-rich substrate **23d**. This is however not in line with a CMD/AMLA-type C–H activation,^[27-28] where a preferred reaction of the electron-deficient arene is expected, due to the higher kinetic acidity of electron deficient arenes. Therefore, a BIES C–H activation seems plausible for the cobalt-catalyzed C–H activation.^[29] Furthermore, a competition experiment between TMS-substituted alkyne **132c** and TIPS substituted alkyne **132a** was conducted by M. J. Gonzalez and showed a preference for the TMS-alkyne **132c** under the reaction conditions.^[194] This can, for example, be rationalized by a faster reaction due to steric effects of the far less bulky TMS group.

3.3.4 Proposed Catalytic Cycle

Based on these findings, a mechanistic scenario for the cobalt-catalyzed C–H alkylation of indoles **23** was proposed (Scheme 3.5). The active cobalt catalyst **229** is formed *in situ* through the cleavage of the [Cp*CoI₂]₂-dimer upon coordination of the base and abstraction of the iodide ligands. Coordination of substrate **23a** followed by a BIES C–H metalation event^[29] generates cobaltacycle **230**. Insertion of alkyne **132a** into the Co–C bond generates seven-membered cobaltacycle intermediate **226**, which can then undergo β -bromo elimination to liberate the desired product **89aa**. A subsequent ligand exchange regenerates the active cationic complex **229**.

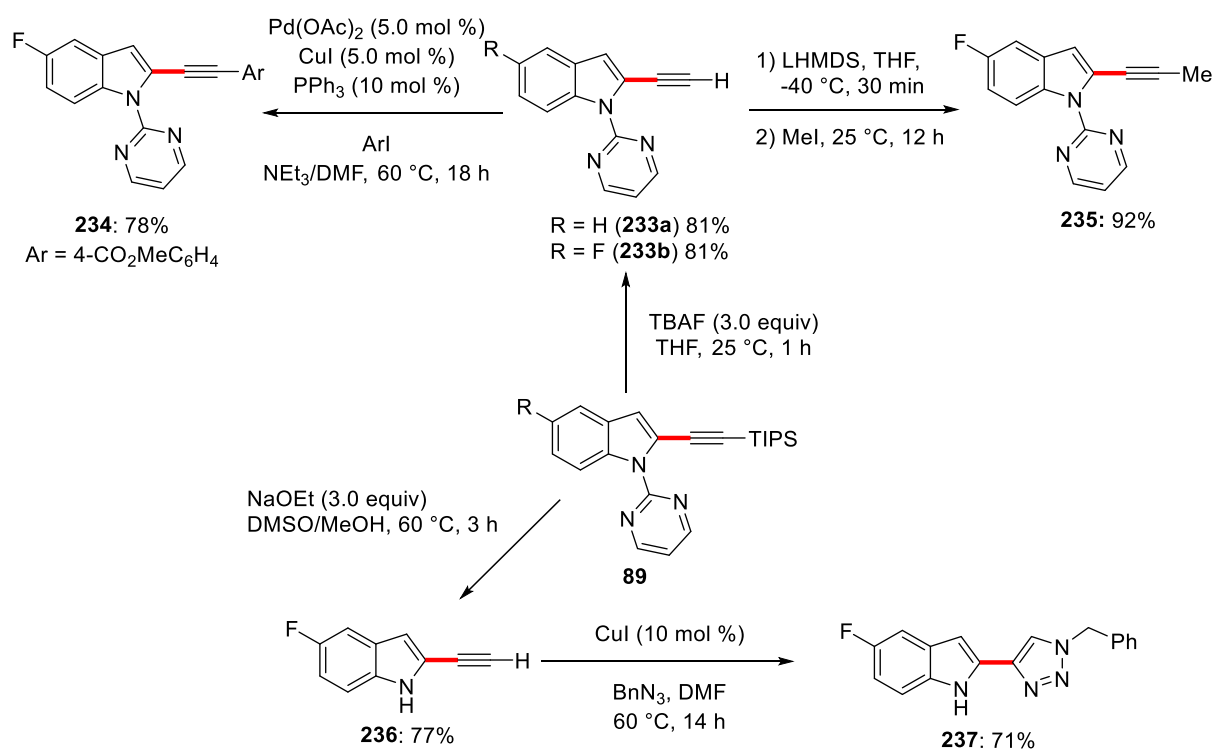


Scheme 3.5 Proposed catalytic cycle for the cobalt-catalyzed C–H alkylation.

3.3.5 Diversification of the Alkynylated Indoles

To highlight the synthetic potential of the devised cobalt-catalyzed C–H alkylation, several modifications of the isolated products **89** were performed (Scheme 3.6).

First, the selective deprotection of the silyl group was achieved using TBAF.^[195] The generated terminal alkyne **233** was subsequently alkylated by a simple deprotonation/alkylation sequence using methyl iodide^[196] or arylated by a Sonogashira-Hagihara coupling using $\text{Pd}(\text{OAc})_2$, CuI and PPh_3 as the catalytic system.^[197] Furthermore, a deprotection of both silyl group and pyrimidyl group was achieved using NaOEt in a DMSO/MeOH mixture at $60\text{ }^\circ\text{C}$.^[79a] The generated ethynylindole **236** was then utilized in a copper-catalyzed 1,3-dipolar cycloaddition to synthesize triazole **237** (Scheme 3.6, bottom).^[198]

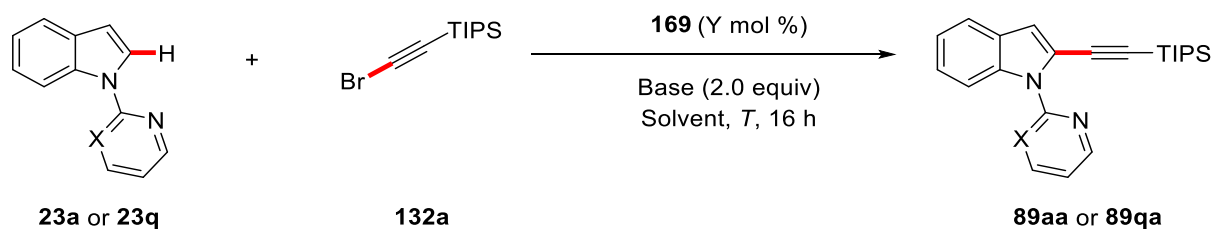


Scheme 3.6 Diversification of alkynyl indoles **89**.

Overall, the synthetic value of the alkynyl group could be highlighted by these reactions, underlining the usefulness of the novel cobalt-catalyzed C–H alkylation at exceedingly mild conditions.

3.3.6 Optimization of the Manganese-Catalyzed C–H Alkylation

In recent years, the power of manganese(I) complexes as catalysts for C–H activation was discovered and exploited for numerous transformations.^[119] Manganese is an important trace metal in living organisms, the third most abundant transition metal in the earth's crust and advantageous regarding toxicity and availability.^[35] So far a majority of transformations are hydrofunctionalizations of unsaturated C–C or C–Het multiple bonds, while substitutive transformations remained scarce.^[119] Along these lines, Z. Ruan discovered the C–H alkylation of indoles **23** using bromoalkynes **132**.^[199] While the initial reaction was already convincing with an isolated yield of 93%, further optimization studies were conducted to identify the ideal conditions (Table 3.13).

Table 3.13 Optimization of the manganese(I)-catalyzed C–H alkylation.^a

Entry	X	Y	Base	Solvent	T [°C]	Yield [%]
1	CH	10	Cy ₂ NH	1,4-dioxane	120	93 ^b
2	CH	5.0	Cy ₂ NH	1,4-dioxane	100	78 ^b
3	CH	5.0	Cy ₂ NH	DCE	80	85 ^b
4	N	10	Cy ₂ NH	1,4-dioxane	120	94
5	N	5.0	Cy ₂ NH	1,4-dioxane	120	71
6	N	5.0	NaOAc	1,4-dioxane	120	41 ^b
7	N	5.0	Na ₂ CO ₃	1,4-dioxane	120	33 ^b
8	N	5.0	Cy ₂ NH	TFE	120	15 ^b
9	N	5.0	Cy ₂ NH	DCE	120	96
10	N	2.5	Cy ₂ NH	DCE	120	71
11	N	5.0	Cy ₂ NH	DCE	100	92
12	N	5.0	Cy ₂ NH	DCE	80	95
13	N	5.0	Cy ₂ NH	DCE	60	71
14	N	5.0	Cy₂NH	DCE	80	99^{b, c}
15	N	---	Cy ₂ NH	DCE	80	---
16	N	5.0	Cy ₂ NH	DCE	80	<5

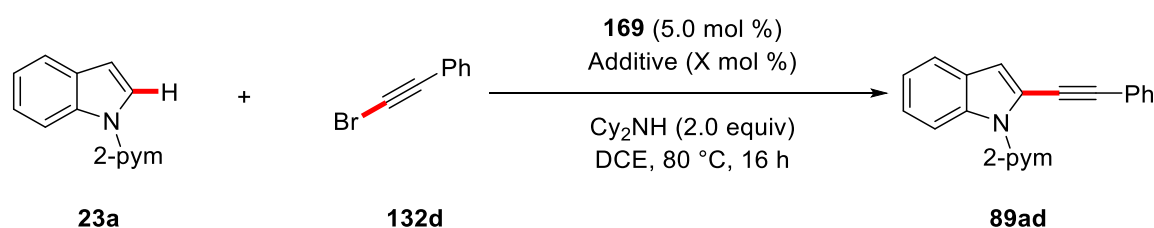
^a Reaction conditions: **23** (0.50 mmol), **132a** (0.75 mmol), **169** (Y mol %), Base (1.00 mmol), solvent (1.0 mL), T, 16 h. ^b performed by Z. Ruan. ^c **132a** (0.60 mmol).

It was observed that pyridyl as well as pyrimidyl directing groups were competent in the C–H alkylation, with the pyrimidyl group being preferred due to the easy synthesis of the pyrimidyl indoles (entries 1-4).^[200] A reduction of the catalyst loading to 5.0 mol % led to a reduced yield (entry 5), whereas bases other than dicyclohexylamine were not effective (entries 6 and 7). TFE was not suitable as the reaction medium (entry 8), however DCE showed very promising results (entry 9). Again, a further reduction of the catalyst loading led to a decrease in yield (entry 10), while the temperature could be reduced to 80 °C without a loss of reactivity (entries 11

and 12). Below 80 °C the transformation was not as efficient (entry 13). The amount of bromoalkyne **132a** could be reduced to 1.2 equivalents (entry 14) and control experiments confirmed the essential role of the manganese catalyst **169** and the base (entries 15 and 16).

Furthermore, due to the limitations known from the cobalt-catalyzed C–H alkylation regarding aryl and alkyl substituted alkynes **132**, further optimization studies using various Lewis-acidic additives were conducted (Table 3.14).

Table 3.14 Optimization of the manganese(I)-catalyzed C–H alkylation using aryl alkyne **132d**.^a



Entry	Additive	X	Yield [%]
1	---	---	--- ^b
2	BPh_3	5.0	61 ^b
3	BPh_3	5.0	--- ^{b, c}
4	CuBr_2	5.0	---
5	AlCl_3	5.0	32
6	BBr_3	5.0	56
7	ZnCl_2	5.0	<5
8	ZnBr_2	5.0	<5
9	ZnI_2	5.0	--- ^b
10	FeCl_3	2.5	--- ^b
11	MgCl_2	5.0	---
12	BPh_3	0.05	92 ^b
13	BPh_3	0.05	95^{b, d}
14	BPh_3	0.05	86 ^{b, e}

^a Reaction conditions: **23a** (0.50 mmol), **132d** (0.60 mmol), **169** (5.0 mol %), Cy_2NH (1.00 mmol), DCE (1.0 mL), 80 °C, 16 h. ^b performed by E. Manoni. ^c without **169**. ^d 1 h. ^e **169** (2.5 mol %).

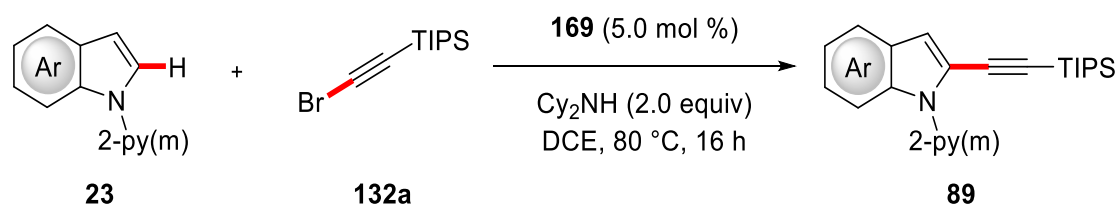
The reaction did not proceed in the absence of the additive (entry 1), while the addition of catalytic amounts of BPh_3 provided beneficial results (entry 2). A control experiment confirmed that the manganese catalyst **169** is still essential (entry 3).

Furthermore, only additives containing group 3 elements were able to promote the catalytic activity. Simple aluminumtrichloride and borontribromide led to product formation, although at reduced efficacy (entries 5 and 6), whereas other Lewis-acidic additives, such as copper(II) bromide, zinc(II) halides and iron trichloride were not effective (entries 4, 7-11). The loading of the additive could be reduced (entries 12-14). Moreover, it was possible to lower the catalyst loading and the reaction time of the transformation (entry 13).

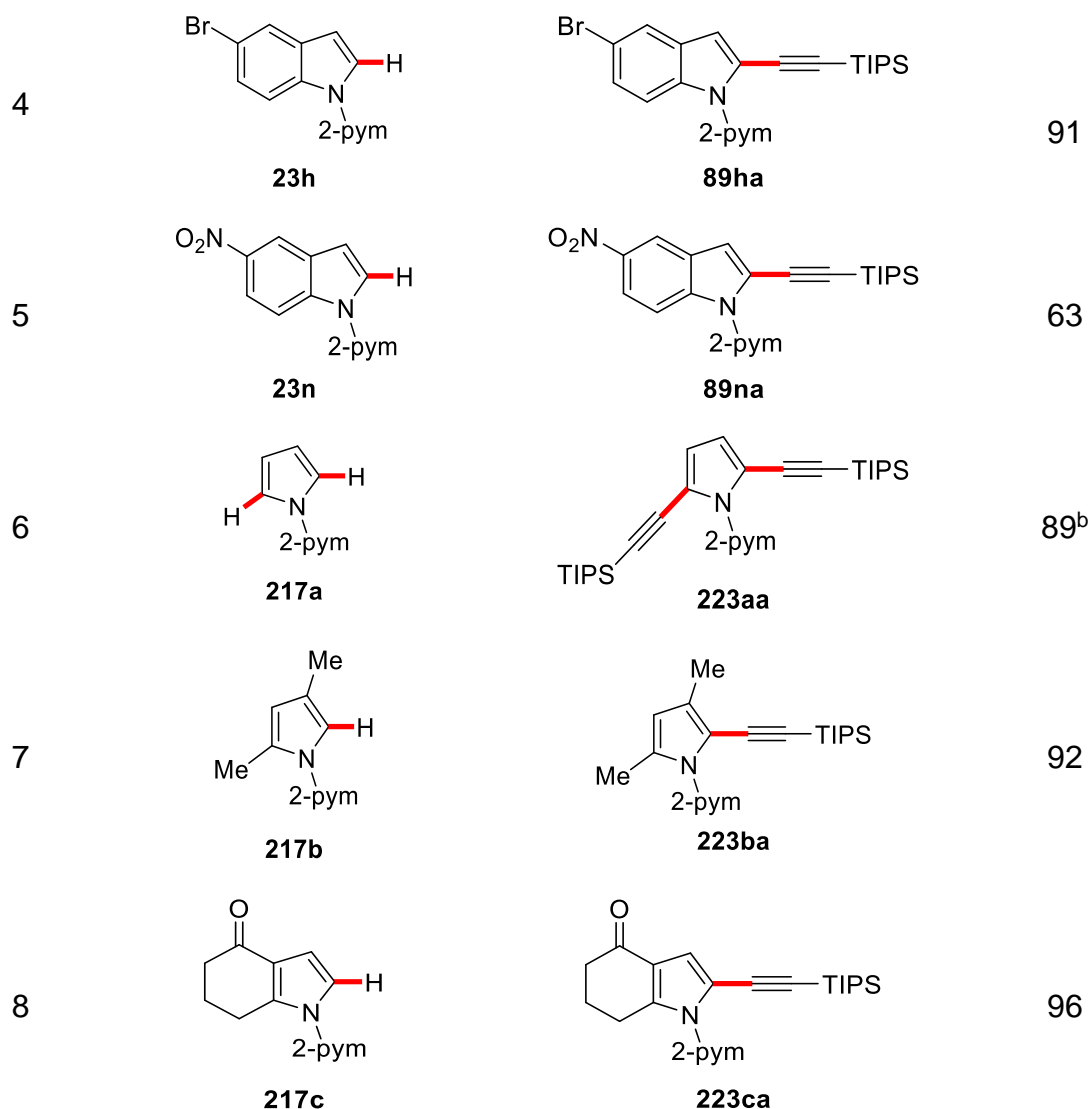
3.3.7 Scope of the Manganese-Catalyzed C–H Alkynylation

With the optimized reaction conditions being identified, the robustness of the discovered C–H alkynylation with regard to various functional groups was evaluated. First, the scope of pyrimidyl and pyridyl indoles **23** and pyrroles **217** was investigated (Table 3.15).

Table 3.15 Manganese(I)-catalyzed C–H alkynylation of indoles **23** and pyrroles **217**.



Entry	Indole	Product	Yield [%]
1	<p style="text-align: center;">23a</p>	<p style="text-align: center;">89aa</p>	99
2	<p style="text-align: center;">23d</p>	<p style="text-align: center;">89da</p>	78
3	<p style="text-align: center;">23o</p>	<p style="text-align: center;">89oa</p>	88



^a Reaction conditions: **23** or **217** (0.50 mmol), **132a** (0.6 mmol), **169** (5.0 mol %), Cy₂NH (1.00 mmol), DCE (1.0 mL), 80 °C, 16 h. ^b **132a** (1.20 mmol).

Besides the unsubstituted indole **23a**, which was transformed with excellent yield (entries 1), electron-rich 5-methoxyindole **23d** was converted with good yield (entry 2). Further indoles **23** containing valuable electrophilic functional groups, such as fluoro, bromo and nitro, were smoothly converted (entries 3-5). Also, pyrroles were investigated regarding their use in this reaction. Simple 2-pyrimidylpyrrole (**217a**) was also readily alkynylated, however an excess of bromoalkyne **132a** was necessary to ensure selective transformation to the bisalkynylated product **223aa** (entry 6). Cyclic ketone **217c** was converted with excellent yield, as was the sterically congested 2,4-dimethylpyrrole **217b**.

The scope of silyl groups on the alkyne **132** was studied exclusively by Z. Ruan and will therefore not be shown in detail.^[199] It was, however, observed that a variety of

different silylalkynes **132** reacted all with good to excellent yields of more than 85%, regardless of the steric bulk.

In addition, the scope of non-silyl substituted alkynes **132** was investigated using the optimized reaction conditions with the Lewis-acidic additive BPh₃ as co-catalyst (Table 3.16).

Table 3.16 Scope of the manganese-catalyzed C–H alkylation using bromoalkynes **132**.^a

Reaction scheme showing the manganese-catalyzed C–H alkylation of **23a** (2-pyridylindole) with bromoalkynes **132** to form products **89**. Conditions: **169** (5.0 mol %), BPh₃ (0.05 mol %), Cy₂NH (2.0 equiv), DCE, 80 °C, 16 h.

Entry	Bromoalkyne	Product	Yield [%]
1			95
2			99
3			54
4			81

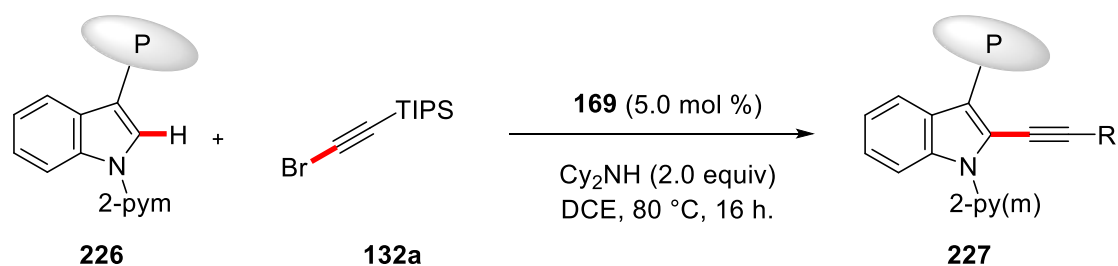
^a Reaction conditions: **23a** (0.50 mmol), **132** (0.60 mmol), **169** (5.0 mol %), BPh₃ (0.05 mol %), Cy₂NH (1.00 mmol), DCE (1.0 mL), 80 °C, 16 h.

The manganese-catalyzed C–H alkylation proved to be amenable towards variety of aryl substituted **132** with electron-rich as well as electron-deficient substituents. While

electronically neutral and electron-rich alkynes are converted very effectively (entries 1, 2, 4), electron-deficient alkyne **132g** (entry 3) was less efficient in the manganese-catalyzed C–H alkylation. Moreover, several other aryl as well as alkenyl and alkyl substituted bromoalkynes **132** were shown to be viable substrates by Z. Ruan and E. Manoni.^[201]

Finally, the C–H alkylation of readily available tryptophan derivatives **221a** and several oligopeptides **222** was investigated (Table 3.17).

Table 3.17 Scope of the manganese-catalyzed C–H alkylation of peptides **221**.^a



Entry	Peptide	Product	Yield [%]
1	 226a	 227aa	82 (>98% ee)
2	 226b	 227ba	71 (>98% ee)
3	 226c	 227ca	69

^a Reaction conditions: **226** (0.50 mmol), **132a** (0.60 mmol), **169** (5.0 mol %), Cy_2NH (1.00 mmol), DCE (1.0 mL), 80 °C, 16 h.

Simple methyl- and Boc-protected tryptophan **226a** reacted readily with bromoalkyne **132a** to alkynylated tryptophan **227aa** (entry 1). Tripeptide **226b** with the tryptophane moiety in the middle of the peptide chain (entry 2) and tripeptide **226c** with the tryptophan in terminal position (entry 3) resulted both in efficient product formation. Furthermore, peptide **226c** includes a handle for further ligation which was left intact during the transformation.

To ensure the retention of stereoconfiguration during the manganese catalysis, the products **227aa** and **227ba** were analyzed by chiral HPLC and compared to their racemic analogues, showing that no racemization occurred during the manganese catalysis (Figure 3.2 and 3.3)

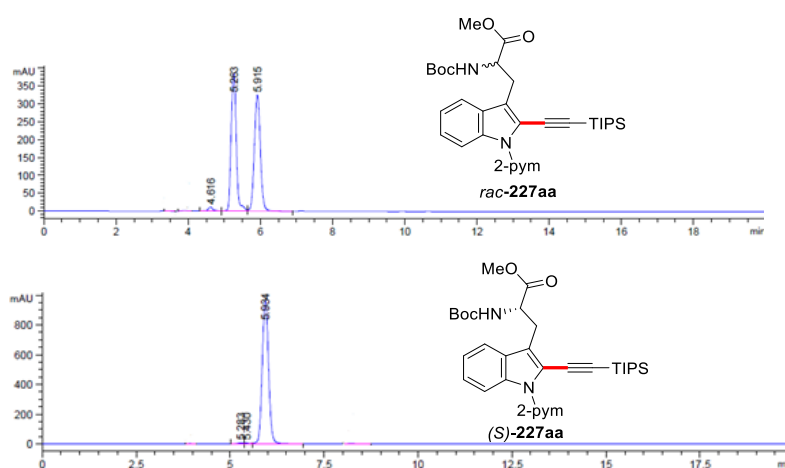


Figure 3.2 HPLC analysis of **227aa**

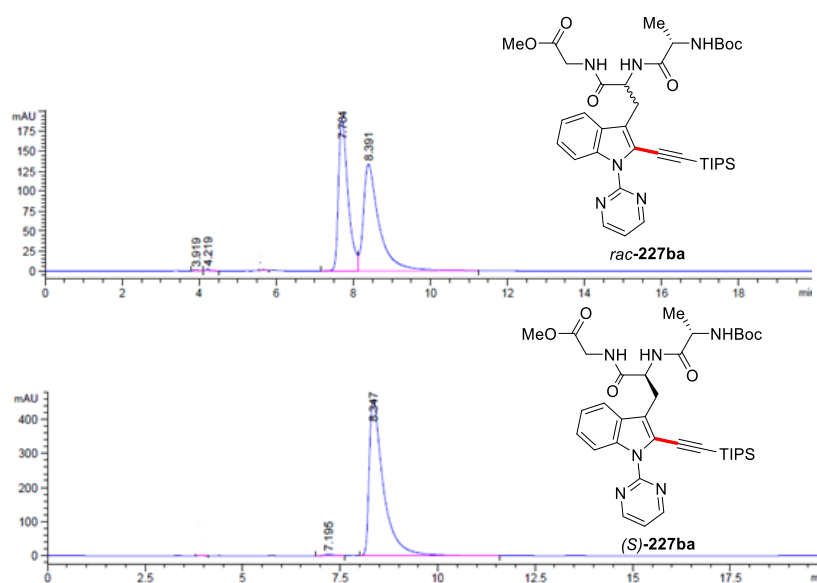
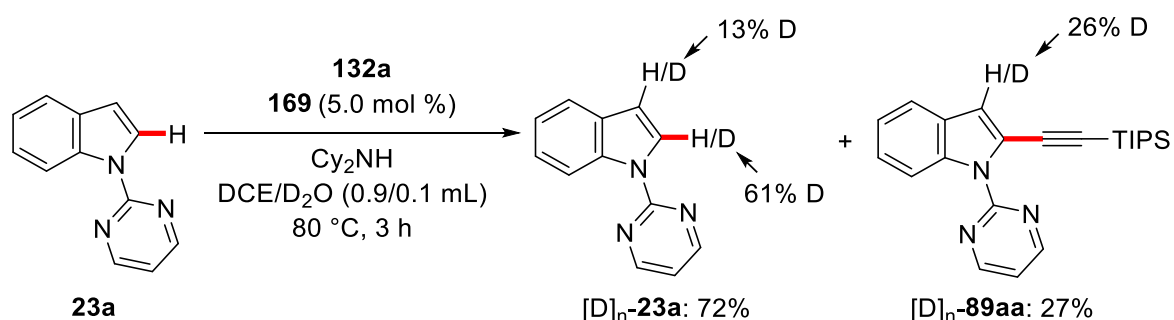


Figure 3.3 HPLC analysis of **227ba**.

3.3.8 Mechanistic Studies for the Manganese-Catalyzed Alkynylation

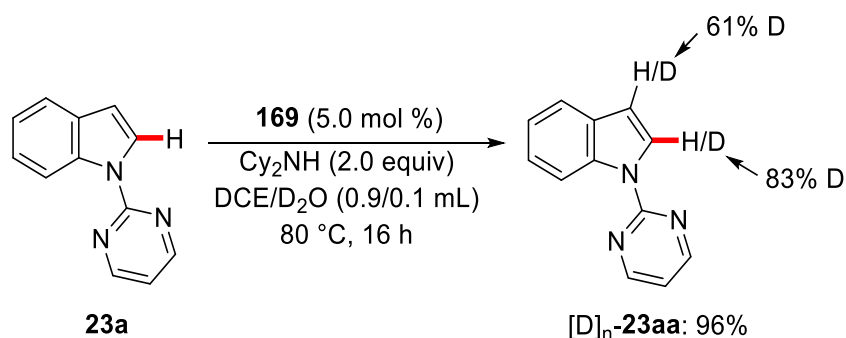
After the investigation of the scope of the manganese-catalyzed C–H alkynylation, detailed mechanistic experiments were conducted to gain insights into its mode of action.

First, deuteration studies in the presence of D₂O were conducted by Z. Ruan,^[199] revealing the incorporation of deuterium in the reisolated starting material in C-2 position of 61% and in C-3 position of 13%. Furthermore, the isolated product showed 26% deuterium incorporation in the C-3 position (Scheme 3.7).

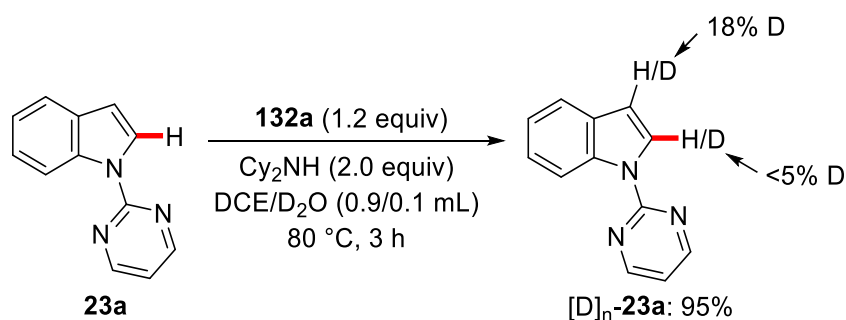


Scheme 3.7 H/D-exchange with isotopically labeled co-solvent.

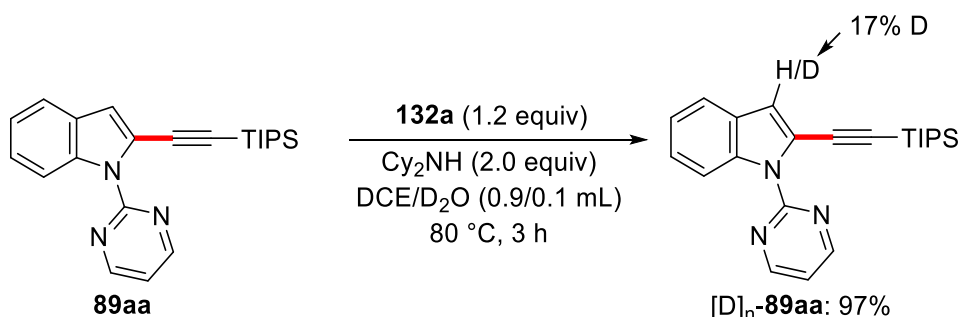
These findings are indicative of a facile and reversible C–H cleavage. To gain further insight into the C–H cleavage, additional deuteration studies in the absence of alkyne **132a** (Scheme 3.8), in the absence of $\text{MnBr}(\text{CO})_5$ (**169**) (Scheme 3.9) and for the product **89aa** under the otherwise optimized reaction conditions (Scheme 3.10) were conducted.



Scheme 3.8 H/D-exchange in the absence of bromoalkyne **132a**.



Scheme 3.9 H/D-exchange in the absence of the catalyst **169**.



Scheme 3.10 H/D-exchange of the product **89aa** in the absence of catalyst **169**.

The results of the deuteration experiments confirmed that the catalyst **169** is involved in the deuteration at the C-2 position of indole **23a**, while bromoalkyne **132a** was not essential for the deuteration. The observed deuteration in C-3 position in the reisolated starting material **23a** and product **89aa** can be attributed to an electrophilic aromatic substitution pathway,^[202] that is operative also in the absence of the manganese catalyst **169**, for both the starting material **23a** as well as the product **89aa** (Schemes 3.9 and 3.10).

A KIE experiment conducted by Z. Ruan revealed a KIE of $k_H/k_D = 1.0$,^[199] indicating that the C–H bond cleavage is not the rate-determining step of this reaction. Further reactions also conducted by Z. Ruan using various radical scavengers were inconclusive, as TEMPO did shut down the reaction nearly completely, while air and BHT reduced the catalytic efficiency, with yields over 50% could still be achieved.^[199] Finally, a slight preference for the more electron-deficient arene could be observed by Z. Ruan.^[199] However, the ratio of 1.1/1.0 showed only a minor preference.

A detailed analysis of the reaction order for indole **23a**, alkyne **132a** and manganese catalyst **169** was conducted (Figure 3.4). All orders were determined to be 1, indicating the involvement of one molecule of each component in or before the kinetically relevant steps. Furthermore, the results strongly support the hypothesis that the C–H cleavage

is not rate-determining, as the reaction order of alkyne **132a** would have been (pseudo)-zeroth order if it enters the catalytic cycle after the rate-determining step.

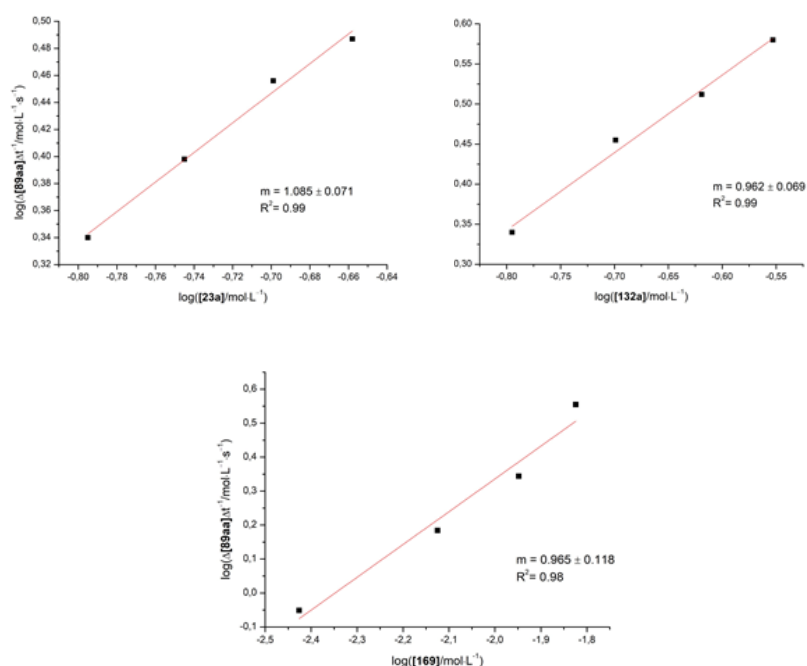
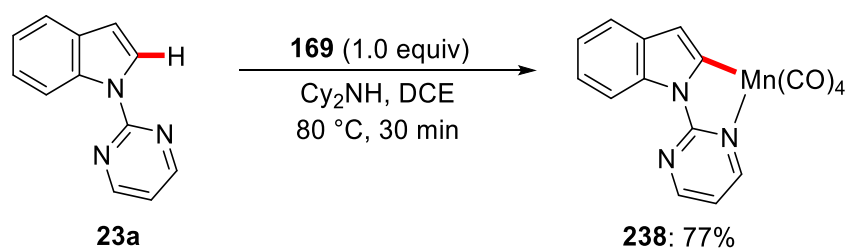


Figure 3.4 Kinetic analysis of the manganese(I)-catalyzed C–H alkylation.

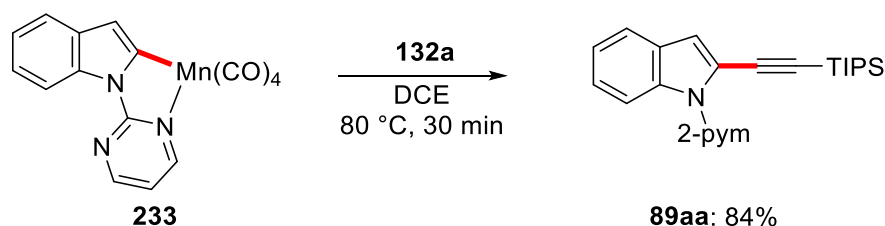
To further investigate the mechanism of the manganese(I)-catalyzed C–H alkylation, five-membered manganacycle **238**, which is proposed to be an intermediate of the catalytic cycle, was synthesized according to a modified literature procedure^[129] and characterized (Scheme 3.11).



Scheme 3.11 Stoichiometric metalation of substrate **23a**.

The stable manganacycle **238** was formed in good yield in a reaction time of 30 min, with comparable yield in the presence of catalytic amounts of BPh_3 . Upon stoichiometric reaction with bromoalkyne **132**, the desired product **89aa** could be obtained in 84% yield in the absence of base after 30 min, hinting at the role of cyclometalated complex **238** as an intermediate of the reaction (Scheme 3.12). A

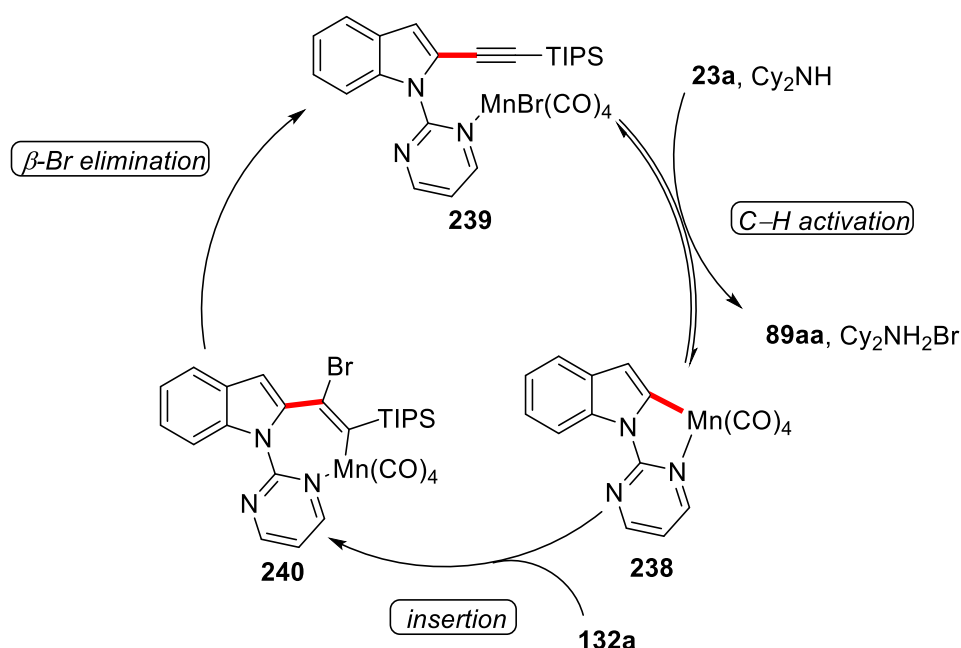
similar reaction with alkyne **132d** in the presence of BPh₃ yielded 73% of the desired product **89ad**.



Scheme 3.12 Stoichiometric alkylation of complex **233**.

Finally, to support these findings, Z. Ruan conducted a reaction with 5.0 mol % of complex **238** as the catalyst, confirming its applicability as the catalyst.^[199]

Based on the thus obtained results, a catalytic cycle was proposed, which initiates by facile and reversible C–H metalation, followed by insertion of bromoalkyne **132a** into the manganese–carbon bond to generate seven-membered intermediate **240**. From this intermediate, the catalyst is regenerated by β -bromo elimination, which furnishes the desired product **89aa** (Scheme 3.13). In case of the aryl and alkyl alkynes, the Lewis acid additive is proposed to accelerate the β -bromo elimination, which is not necessary for silyl alkynes due to the stabilization by the β -silicon effect.^[203]



Scheme 3.13 Plausible mechanism for the manganese(I)-catalyzed C–H alkylation.

In summary, two powerful methods have been developed to access alkynylated indoles **89** using base metal catalysis under mild conditions. Both protocols showed

good functional group tolerance and exclusive regioselectivity for the C-2 position of the indole. The mechanism of the manganese-catalyzed protocol was thoroughly investigated and analyzed. The applicability of this method to the modification of peptides highlights the potential of base metal catalysis for late-stage peptide diversification.

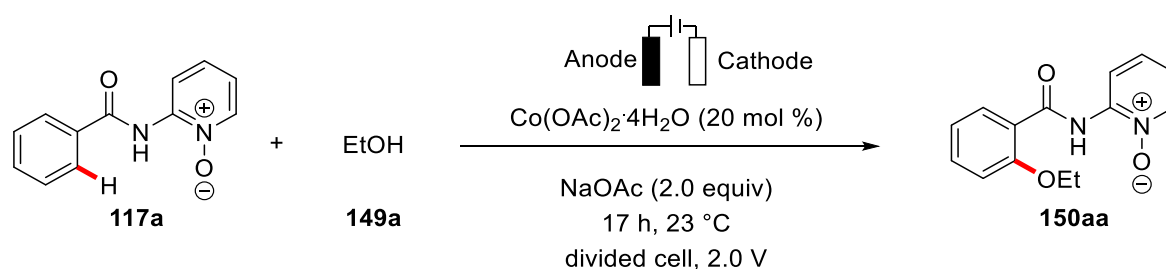
3.4 Electrochemical Cobalt-Catalyzed C–H Oxygenation

Cross-dehydrogenative transformations have great potential to realize C–H activations with formally only H₂ as the stoichiometric byproduct. However, this approach suffers from the need for expensive transition metal oxidants, such as copper(II) and silver(I) salts to achieve catalytic activity.^[174] Therefore, a merger of these C–H activations and electrochemistry would be highly desirable.^[204]

3.4.1 Optimization of the Cobalt-Catalyzed Electrochemical C–H Oxygenation

For the optimization of the cobalt-catalyzed C–H oxygenation unsubstituted benzamide **117a** was chosen as the model substrate, and a constant potential of 2.0 V vs Ag/Ag⁺ was applied in a divided cell using a constant potential setup. As the initial step of the optimization, the electrode material was investigated regarding its efficiency for the envisioned transformation (Table 3.18).

Table 3.18 Evaluation of electrode material.^a



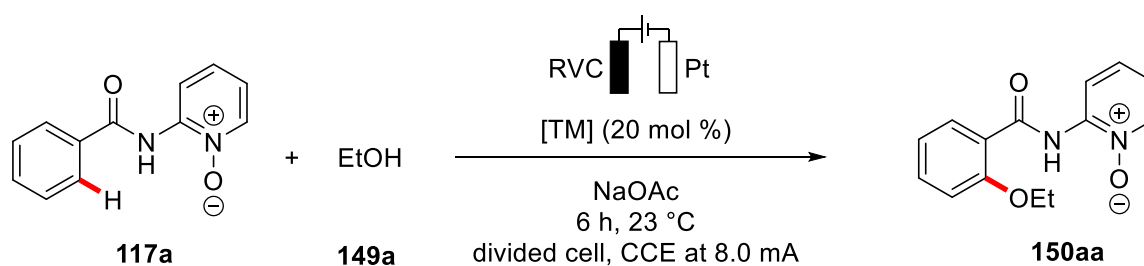
Entry	Anode	Cathode	Yield [%]
1	Pt	Pt	24 ^b
2	Pt	RVC	Traces ^b
3	RVC	Pt	58
4	RVC	Pt	65 ^c

^a Reaction conditions: divided cell, **117** (0.25 mmol), Co(OAc)₂·4H₂O (20 mol %), NaOAc (1.00 mmol each cell), **149a** (14 mL), 23 °C, 16 h, 2.0 V. ^b Performed by T. H. Meyer. ^c Constant current 4.0 mA.

A setup using only platinum electrodes showed promising conversion (entry 1), while the use of carbon as the cathode was not suitable (entry 2). However, a combination of a platinum cathode and a carbon anode proved to be the key for success (entry 3). A test reaction using constant current electrolysis (CCE) instead of constant potential revealed comparable efficacy (entry 4), thus making the constant current setup more attractive due to the much simpler equipment needed.^[140c]

For the further optimization, the reaction time was shortened to 6 h with the current increased accordingly. The reaction conditions were first investigated regarding the cobalt catalyst (Table 3.19).

Table 3.19 Optimization of the cobalt catalyst.^a

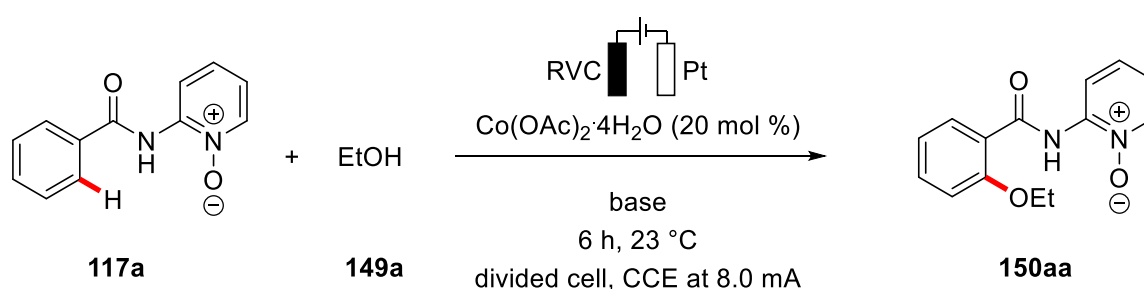


Entry	[TM]	Yield [%]
1	Co(OAc)₂·4H₂O	58
2	Co(napht) ₂	31
3	Co(oxalate) ₂	21
4	Co(acac) ₂	44
5	Co(NO ₃) ₂	13
6	CoCl ₂	64 ^{b, c}
7	CoBr ₂	55 ^{b, c}
8	Co(OAc) ₂ ·4H ₂ O	26 ^d
9	Cu(OAc) ₂	-
10	-	-

^a Reaction conditions: **117a** (0.50 mmol), [TM] (20 mol %), NaOAc (1.00 mmol) in each cell, **149a** (7.0 mL in each cell), constant current of 8 mA, 6 h. ^b Using NaOPiv (1.00 mmol) instead of NaOAc. ^c Performed by T. H. Meyer ^d [TM] (10 mol %).

The evaluation of cobalt catalysts established that common cobalt(II) salts are all competent catalysts to some extent. Cobalt(II)acetate tetrahydrate was identified as the best choice, CoCl_2 and CoBr_2 gave comparable yields, although with another base, which was later also shown to be beneficial when $\text{Co}(\text{OAc})_2$ was used (see Table 3.23). Reduced catalyst loadings of 10 mol % were not effective (entry 8), whereas copper(II)acetate did not promote the reaction at all (entry 9). The essential nature of the cobalt catalyst was highlighted by a control experiment in the absence of cobalt (entry 10).

Table 3.20 Optimization of bases.^a



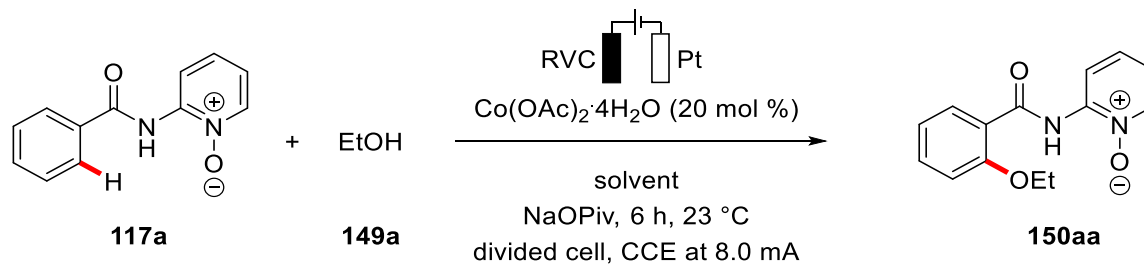
Entry	Base	Yield [%]
1	NaOAc	58
2	KOAc	57
3	CsOAc	55
4	<i>n</i> -Bu ₄ NOAc	trace
5	Na ₂ CO ₃	34 ^b
6	NaO ₂ CMes	34
7	NaOPiv	75
8	-	- ^b

^[a] Reaction conditions: **117a** (0.50 mmol), $\text{Co}(\text{OAc})_2 \cdot 4\text{H}_2\text{O}$ (20 mol %), base (1.00 mmol) in each cell, **149a** (7.0 mL in each cell), constant current of 8 mA, 6 h. ^b Performed by T. H. Meyer.

While the alkali metal cation of the base did not seem to have any significant influence (entries 1-3), carbonate and aryl carboxylate performed significantly worse (entries 5 & 6). The ideal base was identified as sodiumpivalate, yielding 75% of the desired product (entry 7). The base was found to be essential here (entry 8), probably due to the need to deprotonate the amide to facilitate coordination to the catalyst. While the use of ethanol (**149a**) as the solvent has some benefits, such as good solubility of the additive, which makes the use of costly supporting electrolytes unnecessary,^[205] this is

not true for all alcohols which might be explored in the scope. Therefore, several solvents and solvent mixtures were evaluated during the optimization as well (Table 3.21).

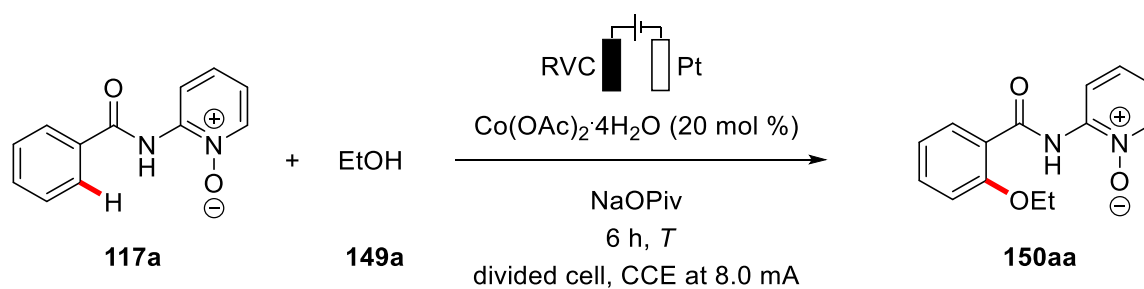
Table 3.21 Optimization of solvents^a



Entry	Solvent	Yield [%]
1	EtOH	75
2	MeCN/EtOH (16/1)	12 ^b
3	MeCN/EtOH (1/1)	19 ^b
4	DMSO/EtOH (16/1)	--- ^b
5	DMF/EtOH (16/1)	---
6	DMF/EtOH (1/1)	---
7	Aceton/EtOH (1/1)	39
8	THF/EtOH (1/1)	11
9	CH ₂ Cl ₂ /EtOH (1/1)	--- ^b

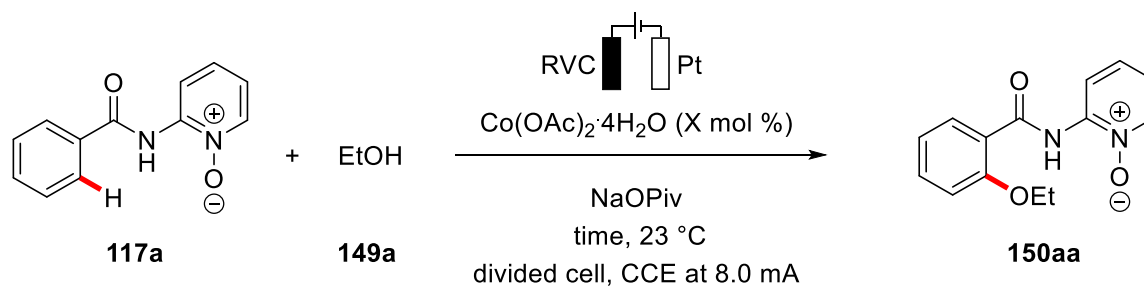
^[a] Reaction conditions: **117a** (0.50 mmol), Co(OAc)₂ (20 mol %), NaOPiv (1.00 mmol) in each cell, solvent (7.0 mL in each cell), 8 mA, 6 h. ^[b] Performed by T. H. Meyer.

While a mixture of acetone and ethanol (**149a**) seemed to support catalytic turnover (entry 7), all other evaluated mixtures showed either stoichiometric conversion or no reaction at all. Therefore, EtOH (**149a**) was kept as the sole solvent, while for other alcohols with a lower conductivity, the addition of a supporting electrolyte was identified as the ideal solution. Moreover, also the reaction temperature and time were thereafter optimized (Tables 3.22 and 3.23).

Table 3.22 Effect of reaction temperature.^a

Entry	T [°C]	Yield [%]
1	0	17
2	10	23
3	20	71
4	30	73
5	40	68 ^b
6	60	58 ^b

^a Reaction conditions: **117a** (0.50 mmol), $\text{Co}(\text{OAc})_2$ (20 mol %), NaOPiv (1.00 mmol) in each cell, **149a** (7.0 mL in each cell), 8 mA, 6 h. ^b Performed by T. H. Meyer.

Table 3.23: Optimization of catalyst loading.^a

Entry	X [mol %]	Time [h]	Current [mA]	Yield [%]
1	20	6	8	75
2	10	6	8	26
3	10	24	4	68
4	5	24	4	46

^a Reaction conditions: **117a** (0.50 mmol), $\text{Co}(\text{OAc})_2$ (X mol %), NaOPiv (1.00 mmol) in each cell, **149a** (7.0 mL in each cell), 23 °C.

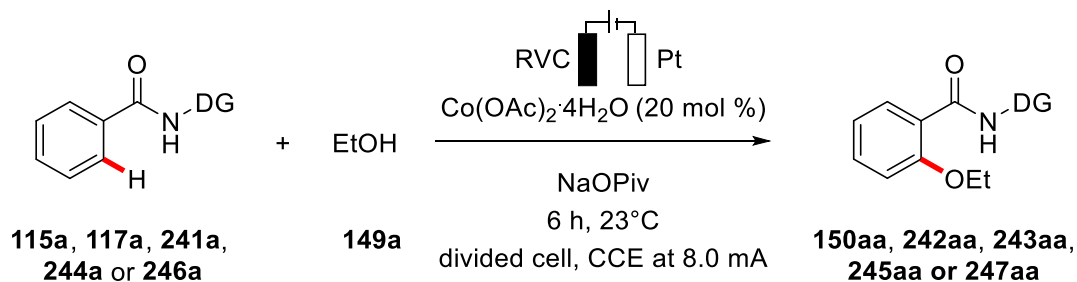
Interestingly, the reaction was operative over a wide range of reaction temperatures. While the obtained yields are rather low at 0 °C and 10 °C (entries 1 & 2), the

transformation was still ongoing, hinting at a facile C–H cleavage. Optimal yields were observed at 20 °C and 30 °C (entries 3 and 4), while a slow decrease was observed at higher temperatures. As for the catalyst loading, 20 mol % were ideal regarding the short reaction time. Yet, the yield for a lower catalyst loading could however be significantly increased with a longer reaction time (entries 3 and 4, Table 3.24).

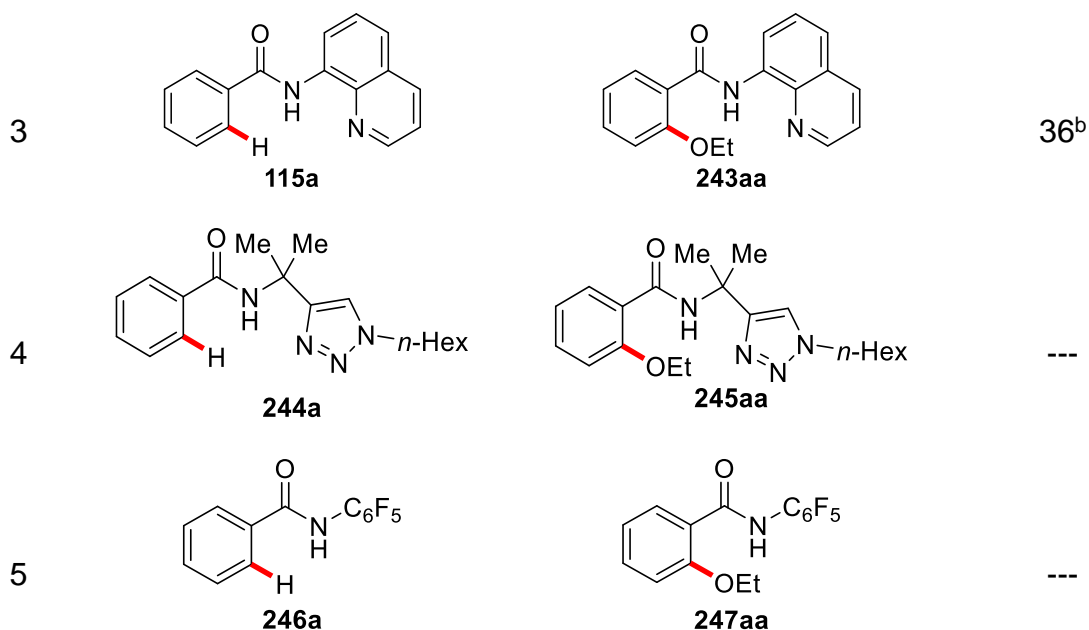
3.4.2 Scope of the Cobalt-Catalyzed Electrochemical C–H Oxygenation

With the optimized reaction conditions in hand, we became interested in exploring the scope of benzamides **117** for the electrochemical cobalt-catalyzed C–H oxygenation. In initial test reactions, several *N*-substituents were evaluated regarding their potential to promote the envisioned C–H transformation (Table 3.24).

Table 3.24 *N*-directing group effect for the electrochemical cobalt-catalyzed C–H oxygenation.^a



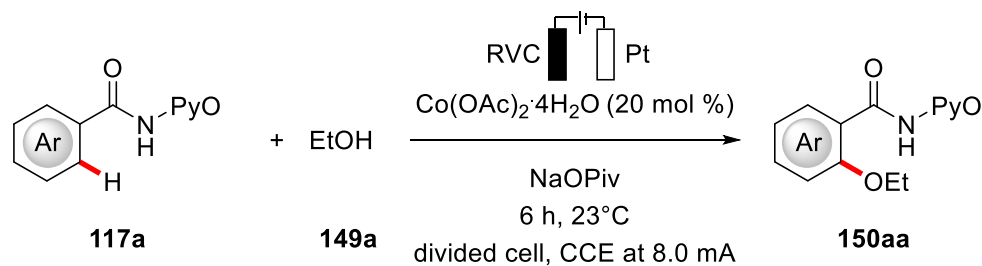
Entry	Benzamide	Product	Yield [%]
1	 117a	 150aa	75
2	 241a	 242aa	--- ^b



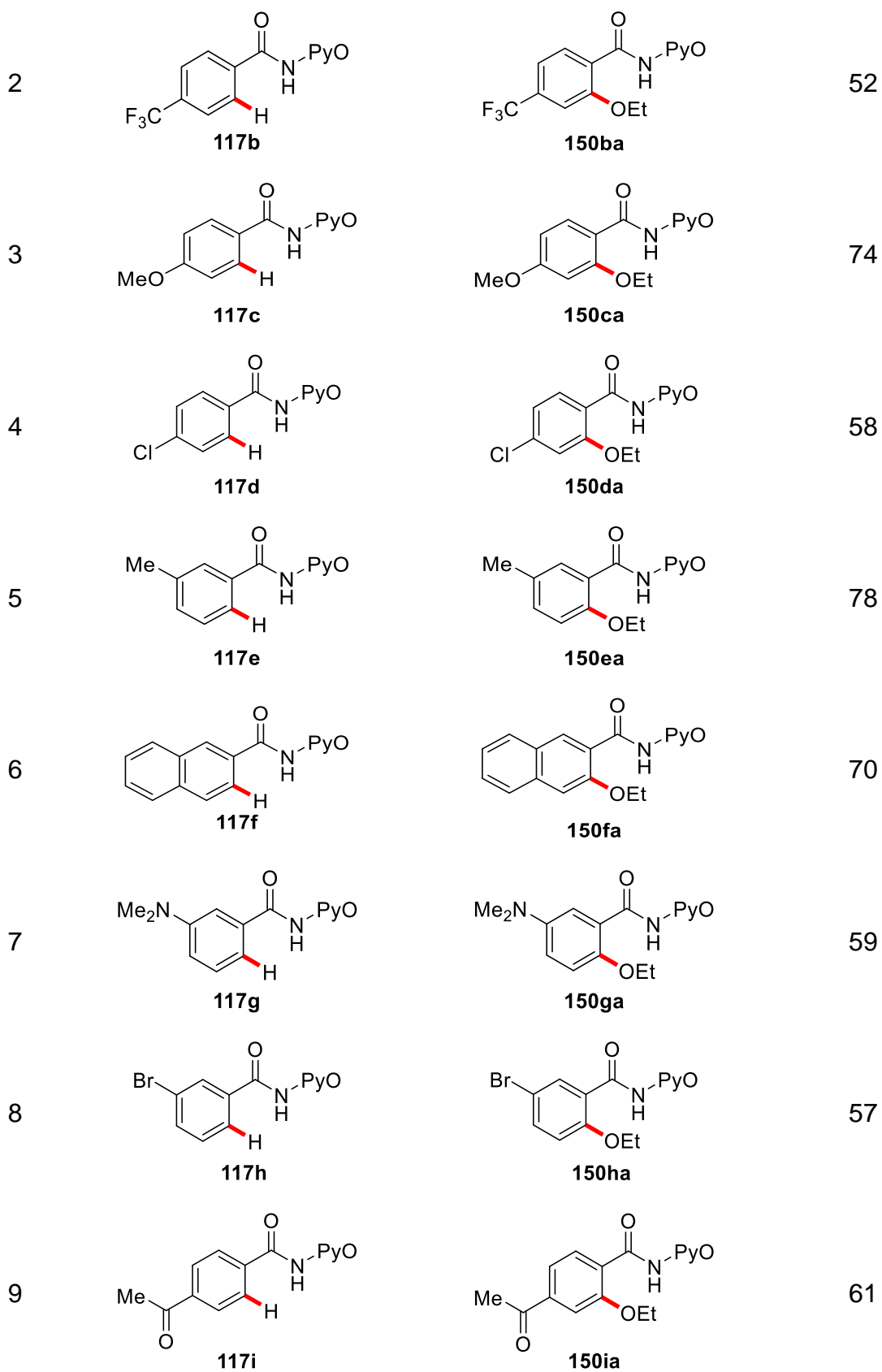
^a Reaction conditions: Benzamide (0.50 mmol), Co(OAc)₂ (20 mol %), NaOPiv (1.00 mmol in each cell), **149a** (7.0 mL in each cell), 23 °C, 8.0 mA. ^b Performed by T. H. Meyer.

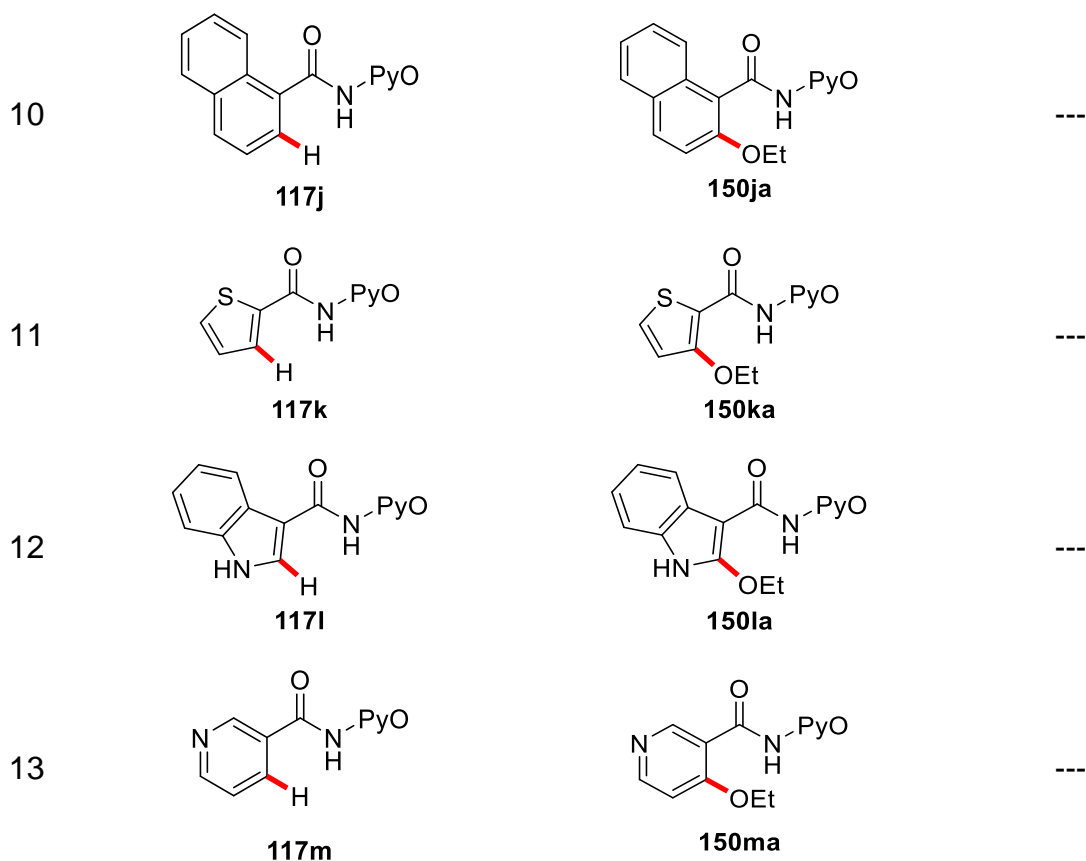
Besides pyridine-*N*-oxide, 8-aminoquinoline was able to promote the electrochemical reaction with moderate yield (entry 3),^[205] while with other directing groups no reaction could be observed. With the best *N*-substituent identified, the functional group tolerance of the C–H oxygenation was investigated (Table 3.25).

Table 3.25 Electrochemical cobalt-catalyzed C–H oxygenation of benzamides **117a**.^a



Entry	Benzamide	Product	Yield [%]
1	 117a	 150aa	75



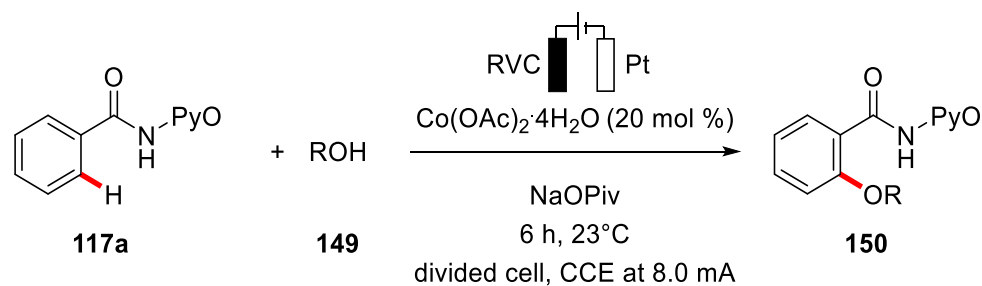


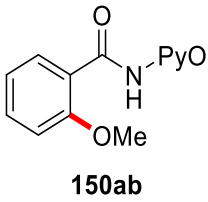
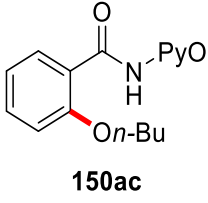
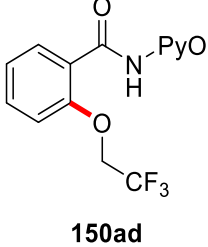
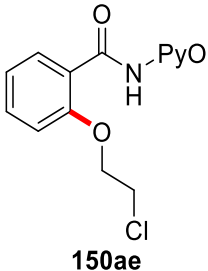
^a Reaction conditions: **117** (0.50 mmol), Co(OAc)₂ (20 mol %), NaOPiv (1.00 mmol in each cell), **149a** (7.0 mL in each cell), 23 °C, 8.0 mA.

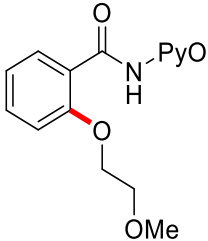
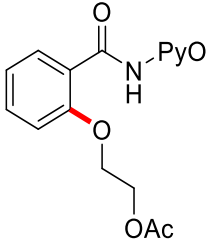
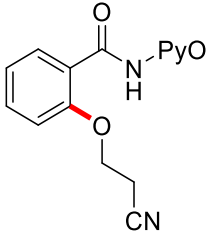
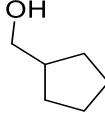
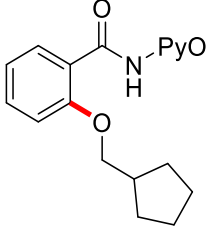
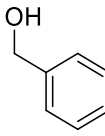
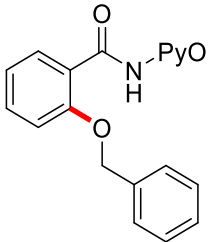
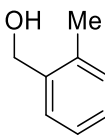
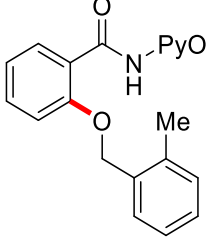
Unsubstituted benzamide **117a** (entry 1) was efficiently converted as substituents in *para*-position to the benzamide were well tolerated, while a good yield was achieved for electron-rich 4-methoxybenzamide **117c** (entry 3). Electron-deficient amide **117b** (entry 2) was not transformed as efficiently and the chloro substituent in amide **117d** was left untouched (entry 4). 3-Methylbenzamide **117e** and naphthylamide **117f** were effectively oxygenated (entries 5 and 6). *meta*-Bromo arene **117h** was well converted with moderate yield (entry 8). Tertiary amine **117g** did not reduce the catalytic efficacy (entry 7), ketone **117i** was well tolerated with moderate yield (entry 9), highlighting the mild reaction conditions of the electrochemical approach. However, also for this transformation, limitations regarding the scope remain. The use of benzamide with an *ortho*-substituent **117j** was generally not feasible, as no reaction could be observed (entry 10). This can be rationalized by steric interactions between the *ortho*-substituent and the amide in the relevant transition states of the catalysis.^[206] Moreover, also heterocyclic substrates did not show any reactivity, for both electron-rich (entry 11 and 12) as well as electron-deficient heteroarenes (entry 13), as solely the remaining starting material could be observed.

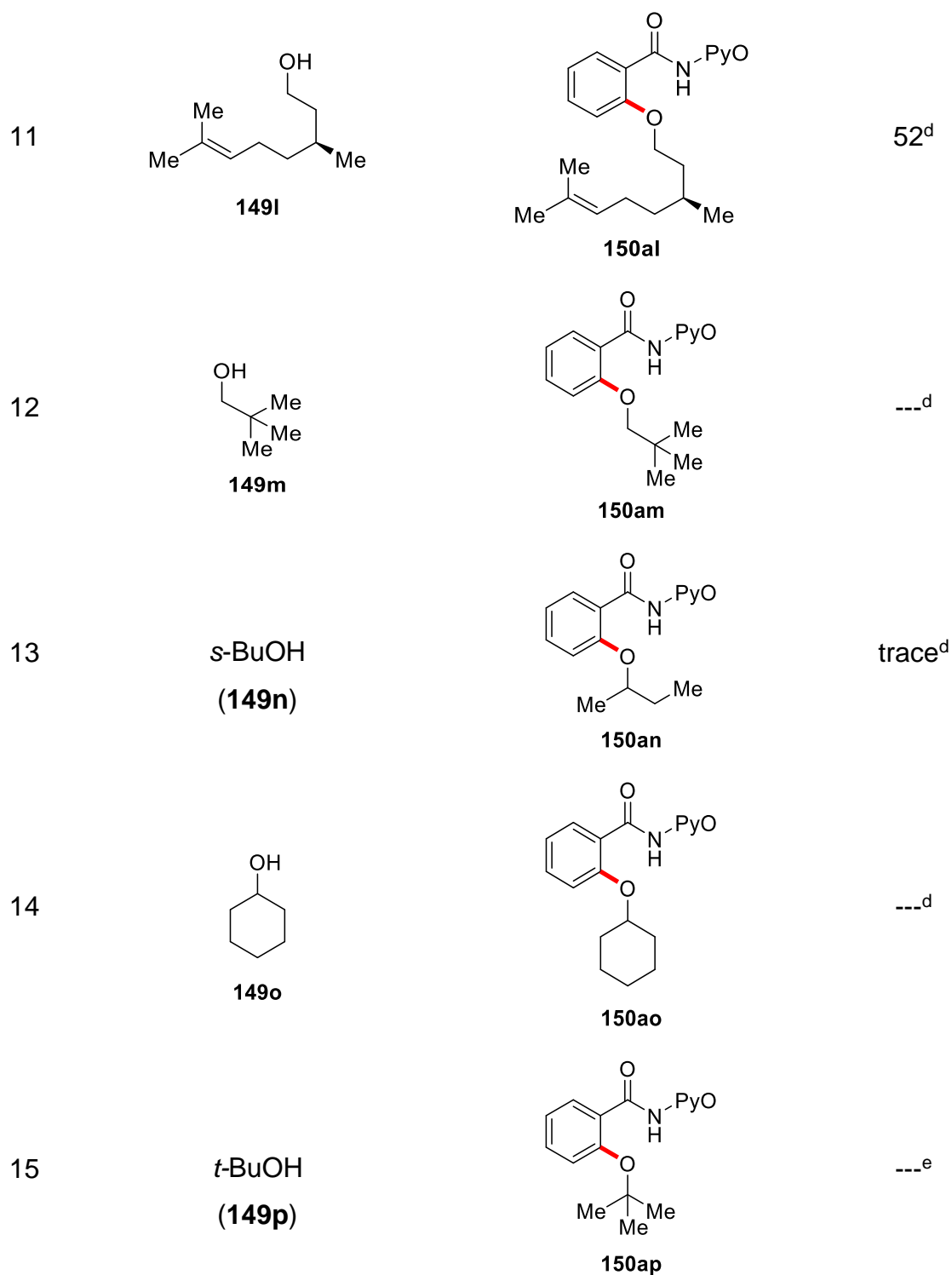
With the scope of benzamides **117** established, the use of different alcohols **149** as coupling partners was explored for the cobalt-catalyzed C–H oxygenation under electrochemical conditions (Table 3.26).

Table 3.26 Electrochemical cobalt-catalyzed C–H oxygenation using alcohols **149**.^a



Entry	Alcohol	Product	Yield [%]
1	MeOH (149b)	 150ab	71
2	<i>n</i> -BuOH (149c)	 150ac	52 ^b
3	CF ₃ CH ₂ OH (149d)	 150ad	62 ^c
4	ClCH ₂ CH ₂ OH (149e)	 150ae	76

5	<p>MeOCH₂CH₂OH (149f)</p>	 <p>150af</p>	64
6	<p>AcOCH₂CH₂OH (149g)</p>	 <p>150ag</p>	54 ^d
7	<p>NCCH₂CH₂OH (149h)</p>	 <p>150ah</p>	61 ^d
8	 <p>149i</p>	 <p>150ai</p>	78 ^d
9	 <p>149j</p>	 <p>150aj</p>	74 ^d
10	 <p>149k</p>	 <p>150ak</p>	68 ^d



^a Reaction conditions: **117a** (0.50 mmol), Co(OAc)₂ (20 mol %), NaOPiv (1.00 mmol in each cell), **149** (7.0 mL in each cell), 23 °C, 8.0 mA. ^b *n*-Bu₄NOAc (1.0 mmol in each cell) ^c 60 °C. ^d in MeCN and *n*-Bu₄NPF₆ (0.3 M).

Simple methanol (**149b**) enabled the reaction efficiently (entry 1), while in *n*-butanol (**149c**) the conductivity was low, and no conversion was observed under standard conditions. However, upon addition of *n*-Bu₄NOAc in each cell as supporting electrolyte, the reaction proceeded smoothly (entry 2). Trifluoroethanol (**149d**) was

converted with moderate yield at an increased temperature of 60 °C (entry 3), while ethanol derivatives **149e** and **149f** were converted under the standard conditions efficiently (entries 4 and 5). Ethanol derivatives **149g** and **149h** containing valuable functional groups, such as ester and nitrile (entries 6 and 7), were smoothly oxygenated. However, the addition of acetonitrile and a supporting electrolyte were necessary to ensure a sufficient conductivity. Especially noteworthy was the C–H oxygenation using benzylic alcohol **149j** (entry 9) and its derivate **149k** (entry 10), as these alcohols should be more prone to oxidation than the aliphatic alcohols.^[206] (S)-Citronellol (**149l**) could be employed upon the addition of a supporting electrolyte without racemization of the stereogenic center, as confirmed by HPLC analysis (Figure 3.5). Finally, neopentyl alcohol (**149m**) (entry 13) was used, however no catalytic activity was observed. Besides primary alcohols, secondary alcohols were also evaluated towards this reaction. While *s*-BuOH (**149n**) showed only traces of the desired product, cyclohexyl alcohol **149o** did not exhibit any reactivity (entries 13 and 14). Finally, also tertiary alcohol *t*-BuOH (**149p**) was tested, but no reaction could be observed (entry 16).

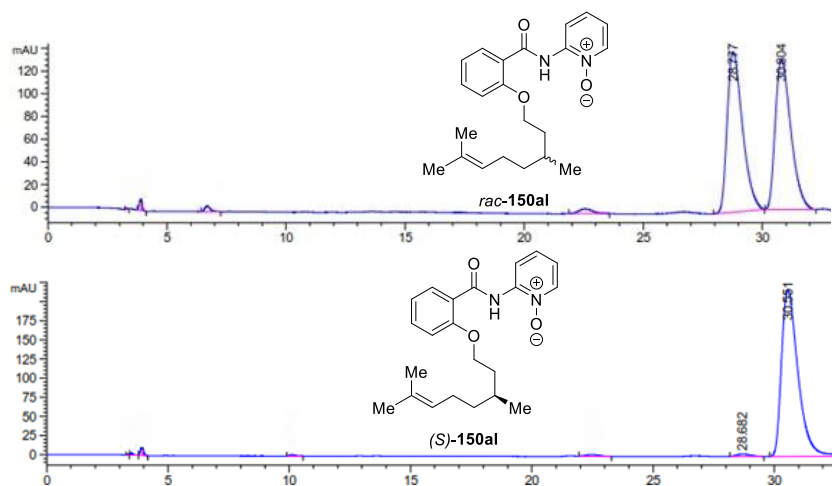
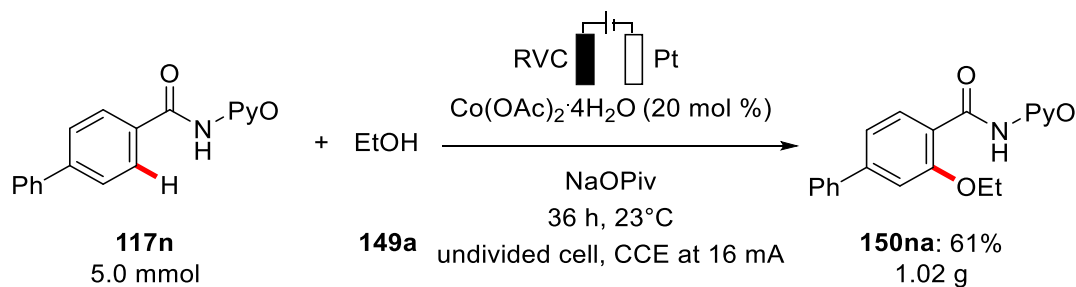


Figure 3.5: HPLC-Chromatogram of (*rac*)-150al and (S)-150al.

Besides the scope of benzamides **117**, T. H. Meyer could also show that alkenes are viable substrates for the cobalt-catalyzed C–H oxygenation.^[208]

Finally, a gram scale reaction was performed to highlight the easy upscaling and convenient electrochemical setup. For reasons of simplicity, an undivided cell was used, as no divided cells of the necessary size were available at this point (Scheme 3.14).



Scheme 3.14 Gram scale reaction.

3.4.3 Mechanistic Studies and Proposed Mechanism

To get insight into the *modus operandi* of the electrochemical cobalt catalyzed C–H oxygenation, detailed mechanistic studies were conducted.

To begin with, the Faradaic efficacy of the reaction was calculated. This can be done based on the observed yield.

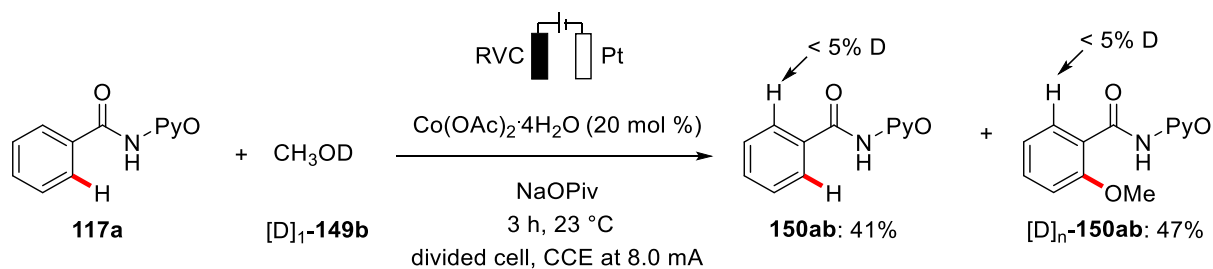
$$\text{Efficacy} = \frac{n * y * z * F}{t * I} \quad (1)$$

In equation (1), n is the amount of starting material in mol, y is the yield observed for a given reaction, z the number of electrons needed to achieve turnover, F is the Faraday constant, t is the reaction time in seconds and I the applied current in ampere (coulomb per second). Based on equation (1), the electron efficacy was calculated for the C–H oxygenation of benzamide **117a**:

$$\frac{0.0005 \text{ mol} * 0.75 * 2 * 96485 \text{ C/mol}}{21600 \text{ s} * 0.008 \text{ C/s}} = 0.418 \quad (2)$$

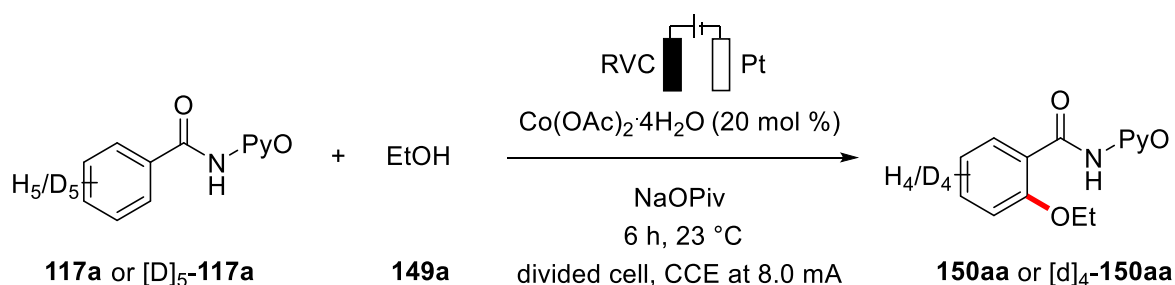
The electron efficacy for the given reaction was thus calculated to be 42%, which is corresponding to a charge of 3.58 F passed through the solution per each mole of substrate **117a**.

Furthermore, deuteration studies using $[D]_1$ -methanol ($[D]_1$ -**149b**) as the solvent showed no significant H/D-incorporation in either the reisolated starting material nor in the product, suggesting an irreversible C–H activation event (Scheme 3.15).



Scheme 3.15 H/D Exchange experiment.

Additionally, the kinetic isotope effect was studied by a comparison of the deuterated benzamide **[D]₅-117a** and the standard substrate **117a** in independent reactions. A minor KIE of $k_H/k_D \approx 1.05$ suggests a facile C–H activation, which is not the rate determining step of the overall transformation (Scheme 3.16).



Scheme 3.16 Measurement of the kinetic isotope effect.

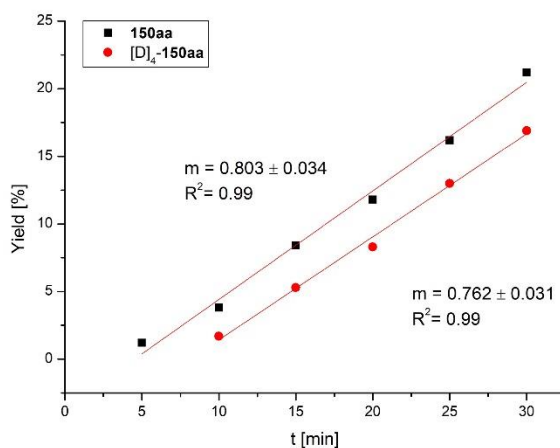
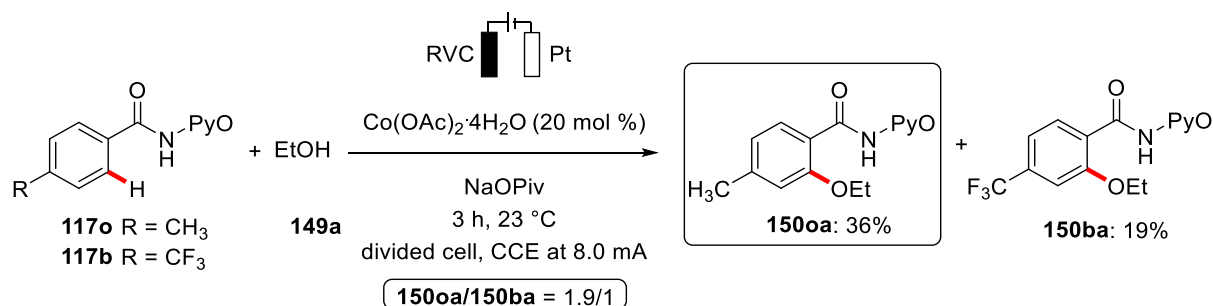


Figure 3.6 Initial rates analysis of **150aa** and **[D]₄-150aa**.

To gain further insight into the reaction mechanism, competition experiments of electron-rich and electron-deficient arenes **117** as well as electron-rich and electron-deficient alcohols **149** were conducted. For benzamides **117**, a competition experiment of 4-methyl benzamide **117o** and 4-trifluoromethyl benzamide **117b** displayed a clear

preference for the more electron-rich benzamide **117** with a ratio of 1.9/1 in favor of the 4-methyl substituted arene **117o** (Scheme 3.17 and Figure 3.7). This finding was further substantiated by a qualitative analysis of the initial rates for both substrates, which highlighted a faster initial reaction for the electron rich substrate (Figure 3.7).



Scheme 3.17 Competition experiment of arenes **117o** and **117b**.

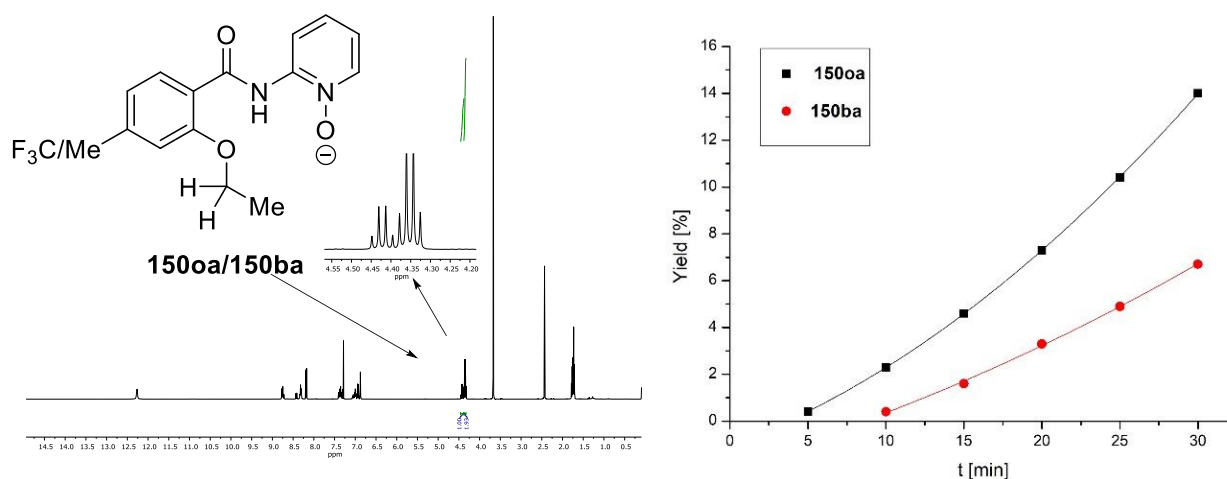
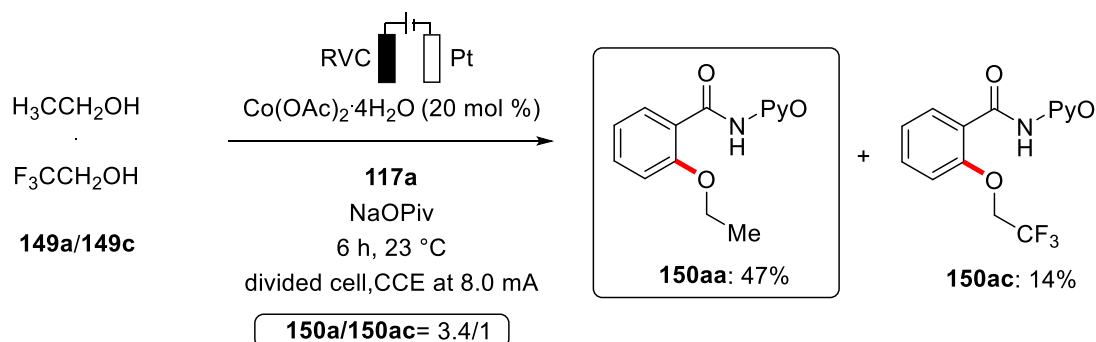


Figure 3.7. $^1\text{H-NMR}$ spectra of the mixture of **150oa** and **150ba** and qualitative analysis of the initial rates.

For the alcohol coupling partner **149**, a similar competition experiment was conducted, showing a clear preference for electron-rich ethanol (**149a**) over trifluoroethanol (**149c**) (Scheme 3.18).



Scheme 3.18 Competition experiment of different alcohols **149**.

Finally, a kinetic profile of the catalysis was recorded under the electrochemical conditions, as well as under the chemical conditions reported by Song and coworkers (Figure 3.8).^[111b] As can be seen in the figure, the overall shape of the kinetic profile is somewhat similar for both reactions, slowing down after approximately 3 h.

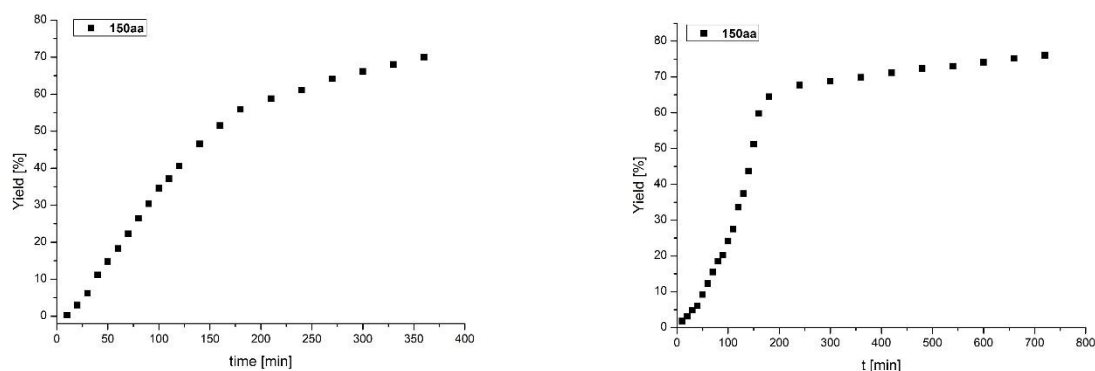


Figure 3.8 Kinetic profile for the electrochemical (left) and chemical (right) oxidation.

In addition, together with T. H. Meyer, detailed cyclic voltammometric studies were conducted in methanol as well as acetonitrile.^[144d] In methanol (**149b**), the oxidation of cobalt(II) acetate in the presence of sodiumpivalate was observed in the absence or presence of the substrate at a potential of 1.19 V_{SCE}. In contrast, the substrate **117a** alone was oxidized at a much higher potential of 1.51 V_{SCE}, being suggestive of a facile initial oxidation of cobalt(II) to cobalt(III) under the reaction conditions. In acetonitrile, similar potentials were observed. Furthermore, quenching experiments indicated the formation of a cyclometalated species which reacted in the presence of ethanol (**149a**) but is relatively stable in its absence (Figure 3.9).

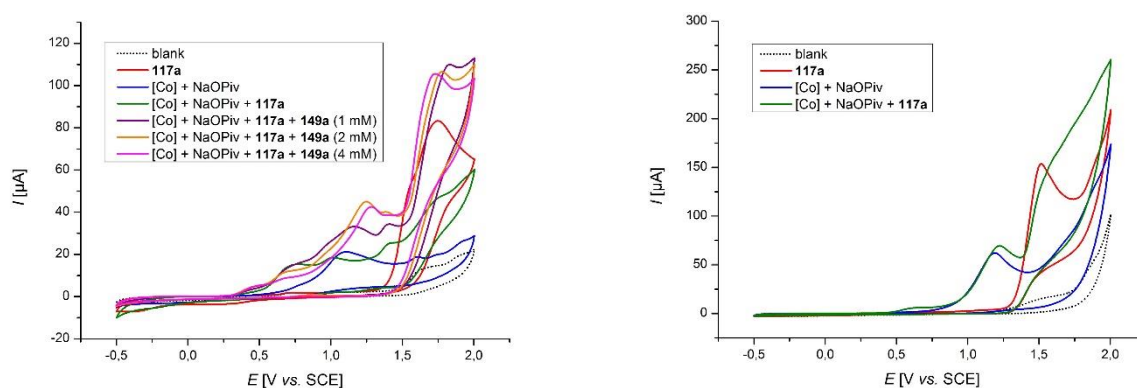
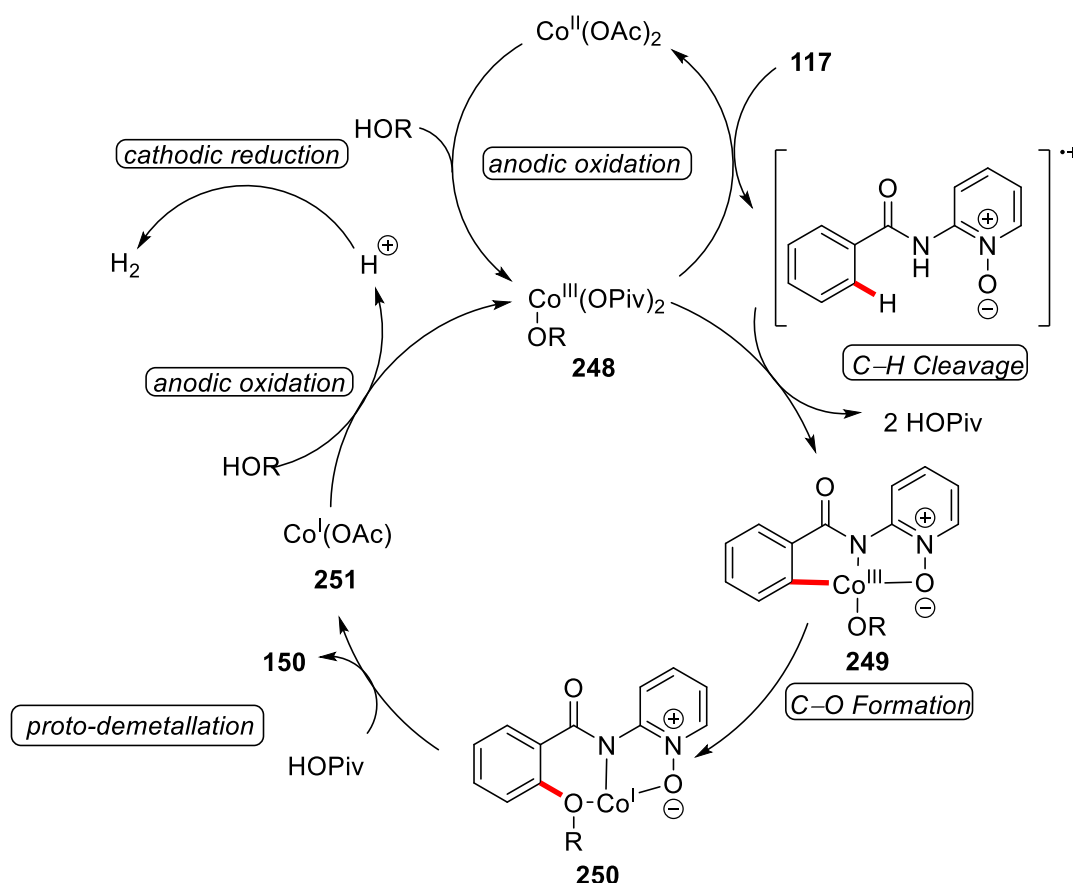


Figure 3.9 Cyclic voltammograms in MeCN (left) and MeOH (right).

From the data obtained by the aforementioned experiments, a plausible catalytic cycle can be proposed (Scheme 3.19). The reaction is initiated by the facile formation of the active cobalt(III) species **248** by anodic oxidation. Coordination to the deprotonated substrate **117** and facile BIES^[29] C–H activation results in a five-membered intermediate **249**. However, as shown in scheme 3.19, also one electron oxidation of **117** seems possible based on CV data, although C–H activation of the radical cation would result in an open shell intermediate **249**. Formation of the C–O bond occurs presumably by reductive elimination, resulting in a cobalt(I) species **250**, from which product **150** is liberated by proto-demetalation. Finally, the active species **248** is regenerated by anodic oxidation.



Scheme 3.19 Proposed catalytic cycle.

In summary, the first oxidative cobalt-catalyzed C–H activation under electrochemical conditions was realized in the form of an electrocatalytic cobalt-catalyzed C–H oxygenation of benzamides **117**. The protocol features exceedingly mild conditions, a broad and robust scope of functional groups and the possibility to perform an easy upscaling. Additionally, the unprecedented electrocatalytic cobalt catalysis was mechanistically investigated regarding its mode of action.

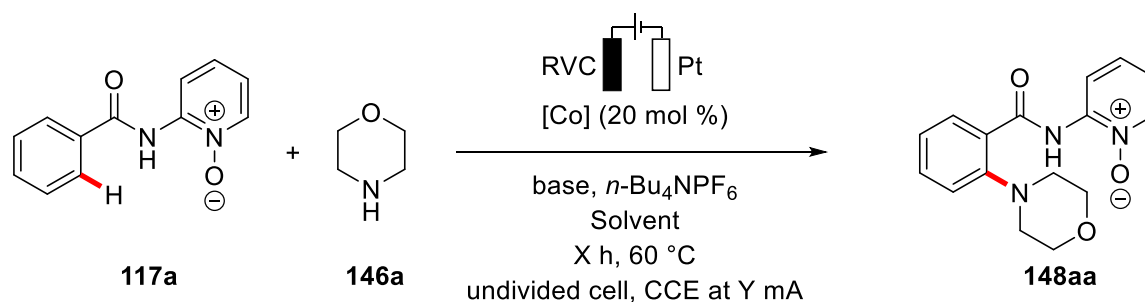
3.5 Electrochemical Cobalt-Catalyzed C–H Amination

Inspired by the success of the electrochemical cobalt-catalyzed C–H oxygenations,^[206] the formation of other C–X bonds became a next target. In the meantime, C–N formations were realized as part of a C–H/N–H annulation,^[168] making also the intermolecular direct C–H/N–H cross-coupling highly desirable.

3.5.1 Optimization of the Cobalt-Catalyzed Electrochemical C–H Amination

Based on previous reports on cobalt-catalyzed amination,^[110b, 110c] initially, an undivided cell setup using cobalt(II)acetate tetrahydrate, sodium acetate, and acetonitrile with a supporting electrolyte and a temperature of 60 °C were chosen as the starting conditions (Table 3.27).

Table 3.27 Optimization of the cobalt catalyzed amination.^a



Entry	[Co]	Base	X	Y	Solvent	Yield [%]
1	Co(OAc) ₂ ·4H ₂ O	NaOAc	4.5	12	MeCN	41
2	Co(OAc) ₂ ·4H ₂ O	NaOAc	4.5	12	DCE	16
3	Co(OAc) ₂ ·4H ₂ O	NaOAc	4.5	12	HFIP	---
4	Co(OAc)₂·4H₂O	NaOAc	12	6	MeCN	54
5	Co(acac) ₂	NaOAc	12	6	MeCN	21
6	Co(acac) ₃	NaOAc	12	6	MeCN	33
7	Co(ClO ₄) ₂	NaOAc	12	6	MeCN	41
8	Co(oxalate) ₂	NaOAc	12	6	MeCN	12
9	CoI ₂	NaOAc	12	6	MeCN	49
10	[Co(NH ₃) ₆]Cl ₃	NaOAc	12	6	MeCN	---
11	Co(OAc) ₂ ·4H ₂ O	KOAc	12	6	MeCN	37
12	Co(OAc) ₂ ·4H ₂ O	CsOAc	12	6	MeCN	29

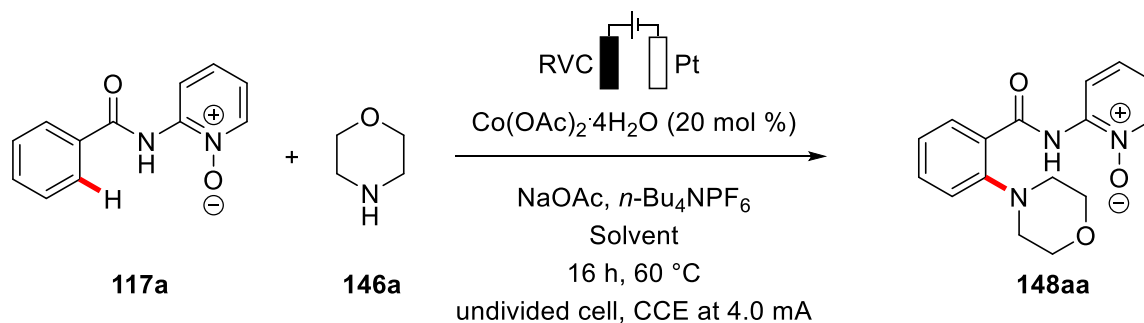
13	Co(OAc) ₂ ·4H ₂ O	Na ₂ CO ₃	12	6	MeCN	31
14	Co(OAc) ₂ ·4H ₂ O	Na ₃ PO ₄	12	6	MeCN	15
15	Co(OAc) ₂ ·4H ₂ O	NaOAc	12	6	MeCN	30 ^b
16	---	NaOAc	12	6	MeCN	-

^a Reaction conditions: **117a** (0.50 mmol), [Co] (20 mol %), base (1.50 mmol), *n*-Bu₄NPF₆ (0.50 mmol) and **146a** (1.00 mmol) in solvent (2.0 mL), time, constant current, 60 °C. ^b [Co] 10 mol %.

The initial results of the chosen reaction conditions were promising (entry 1), while other solvents (entries 2 and 3) failed to deliver the desired product **148**. An increase of the reaction time coupled with a decrease in applied current led to a significant improvement of the yield (entry 4). A representative set of cobalt salts were evaluated based on their catalytic ability (entries 5-10). Although several cobalt salts promoted the C–N bond formation with comparable efficacy, Co(OAc)₂·4H₂O was identified as ideal. Based on these results, the effect of different bases was tested (entries 11-14), which established NaOAc as the base of choice. Finally, a reaction using a reduced catalyst loading resulted in a reduced yield, while a control experiment without catalyst did not provide any product (entries 15 and 16).

Due to the relatively low yields observed during the optimization of the reaction in acetonitrile, it seemed improbable to find significantly improved conditions based on this solvent. Therefore, a careful evaluation of the reaction parameters, especially of the solvent was conducted again (Table 3.28). Furthermore, the reaction time was once more increased to 16 h and the current reduced to 4.0 mA.

Table 3.28 Optimization of solvents.^a



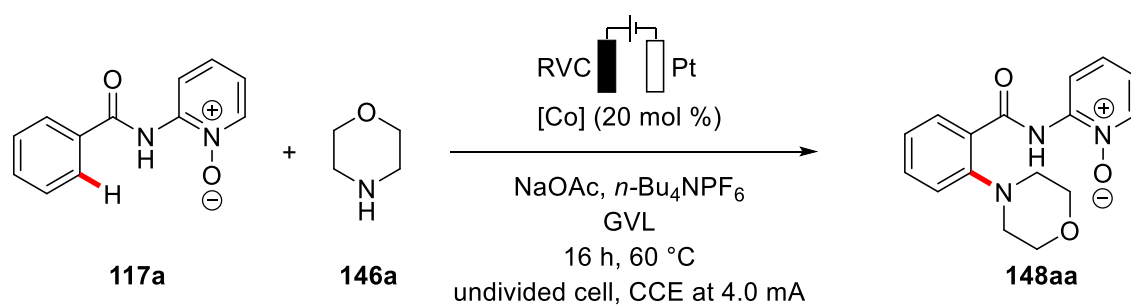
Entry	Solvent	Yield [%]
1	MeCN	41
2	DCE	11
3	HFIP	---

4	DMF	---
5	DMSO	---
6	<i>i</i> -PrOH/H ₂ O 3:1	---
7	GVL	65
8	GVL/H ₂ O 3:1	---
9	2-MeTHF	---
10	H ₂ O	---

^a Reaction conditions: **117a** (0.50 mmol), Co(OAc)₂·4H₂O (20 mol %), NaOAc (1.50 mmol), *n*-Bu₄NPF₆ (0.50 mmol) and **146a** (1.00 mmol) in solvent (2.0 mL), constant current of 4.0 mA, 16 h.

Clearly, the results for acetonitrile, DCE and HFIP are comparable to those obtained before. Polar solvents DMF and DMSO did not promote the reaction, which was also true for an *i*-PrOH/H₂O mixture (entries 4-6). Surprisingly, a significant increase in yield could be observed upon the use of γ -valerolactone as the solvent (entry 7), while a mixture with water was not a viable solvent (entry 8). Due to its possible synthesis from renewable biomass,^[19, 208] GVL as the solvent also improved the sustainability of the electrocatalysis. Further renewable biomass derived solvent 2-methyl-THF was tested as well, however, no catalytic activity was achieved in this solvent. Finally, water as the sole solvent was also not suitable for this reaction (entry 10). Based on these new information, the remaining reaction parameters were optimized again, this time with GVL as the solvent (Table 3.29).

Table 3.29 Optimization of cobalt catalyst.^a



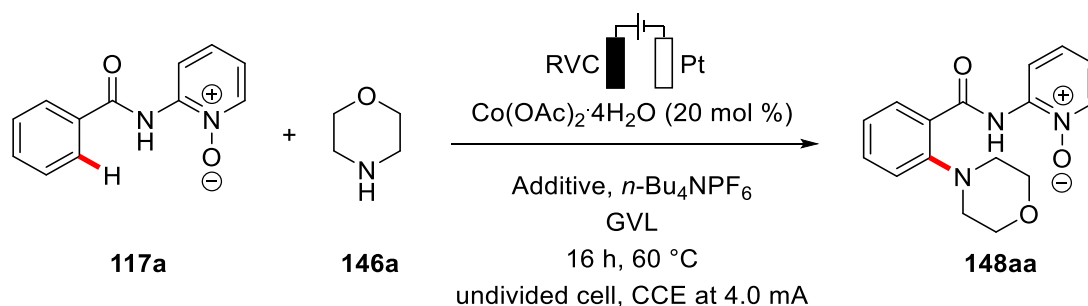
Entry	[Co]	Yield [%]
1	Co(OAc)₂·4H₂O	65
2	Co(ClO ₄) ₂	58
3	Co(acac) ₂	19
4	Co(acac) ₃	35

5	[Co(NH ₃) ₆]Cl ₃	---
6	CoI ₂	49
7	Co(oxalate) ₂	15
8	---	---

^[a] Reaction conditions: **117a** (0.50 mmol), [Co] (20 mol %), NaOAc (1.50 mmol), *n*-Bu₄NPF₆ (0.50 mmol) and **146a** (1.00 mmol) in GVL (2.0 mL), constant current of 4.0 mA, 16 h

It could be shown, that cobalt(II)acetate (entry 1) remained the best choice. However, cobalt(II)perchlorate gave a comparable yield (entry 2). The results for the other salts were comparable to those obtained in MeCN as the solvent (entries 3-7). Finally, a control experiment confirmed the essential nature of the cobalt catalyst for the reaction also in GVL (entry 8). With the solvent and cobalt salt being optimized, the additive was investigated again (Table 3.30).

Table 3.30 Optimization of the additive.^a



Entry	Additive	Yield [%]
1	NaOAc	65
2	NaOPiv	51
3	Na ₂ CO ₃	31
4	KOAc	68
5	K ₂ CO ₃	30
6	K ₃ PO ₄	15
7	---	---

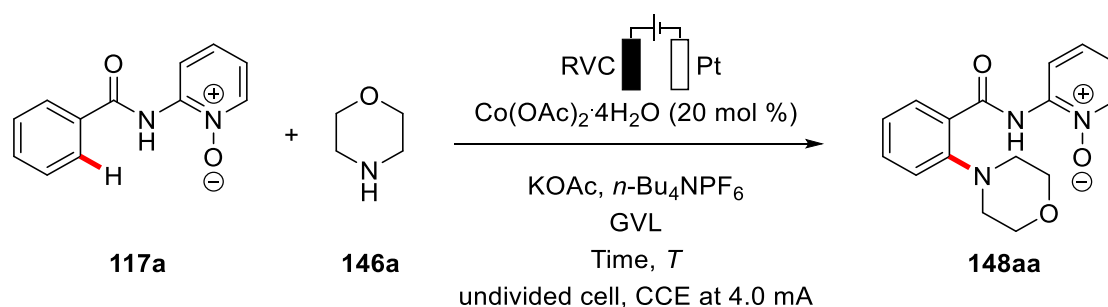
^[a] Reaction conditions: **117a** (0.50 mmol), Co(OAc)₂·4H₂O (20 mol %), additive (1.50 mmol), *n*-Bu₄NPF₆ (0.50 mmol) and **146a** (1.00 mmol) in GVL (2.0 mL), constant current of 4.0 mA, 16 h.

In the screening of basic additives, sodium pivalate resulted in good, although lower yields than sodium acetate (entries 1 and 2), while sodium carbonate was clearly less active. Potassium acetate (entry 4) resulted in the highest catalytic efficacy, while other

potassium-based additives (entries 5 and 6) did not result in high yields. A control experiment confirmed the essential nature of the basic additive (entry 7).

Finally, further reaction parameters, such as time and temperature were optimized to find the ideal conditions for this transformation (Table 3.31).

Table 3.31 Optimization of further reaction parameters^a



Entry	T [°C]	t [h]	Yield [%]
1	60	16	68
2	40	24	77 ^b
3	20	24	23 ^b
4	40	24	19 ^c
5	40	24	77^{b, d}
6	40	24	--- ^{b, d, e}

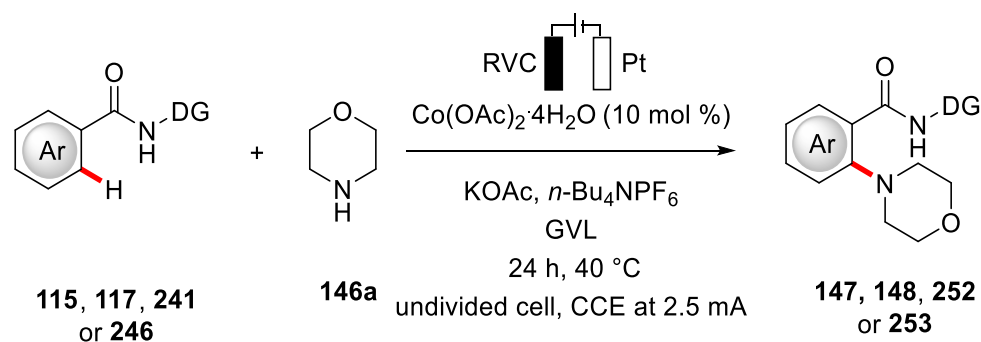
^a Reaction conditions: **117a** (0.50 mmol), $\text{Co(OAc)}_2 \cdot 4\text{H}_2\text{O}$ (20 mol %), additive (1.50 mmol) $n\text{-Bu}_4\text{NPF}_6$ (0.50 mmol) and **146a** (1.00 mmol) in GVL (2.0 mL), constant current of 4.0 mA, 16 h. ^b $\text{Co(OAc)}_2 \cdot 4\text{H}_2\text{O}$ (10 mol %), constant current of 2.5 mA. ^c $\text{Co(OAc)}_2 \cdot 4\text{H}_2\text{O}$ (5.0 mol %). ^d under air. ^e no current.

A longer reaction time at lower temperature of 40 °C was beneficial (entry 2), even at reduced catalyst loading of 10 mol % and lower current of 2.5 mA. A further reduction in temperature resulted in a significant loss of activity (entry 3), as did a further reduction in catalyst loading (entry 4). A nitrogen atmosphere was not necessary (entry 5), as air does not promote background reactivity, which was confirmed by a control experiment without electric current (entry 6). Based on these results, the optimized conditions consisted of cobalt(II)acetate tetrahydrate as the catalyst, potassium acetate as the base in GVL with a supporting electrolyte at 40 °C, with a current of 2.5 mA maintained for 24 h.

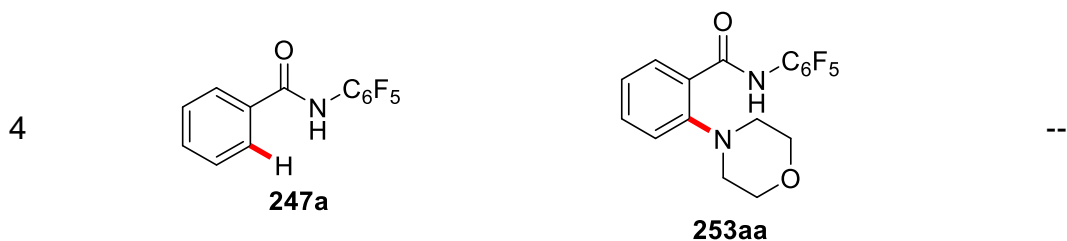
3.5.2 Scope of the Electrochemical Cobalt-Catalyzed C–H Amination

With the optimized catalytic system being identified, an initial study was conducted to confirm that indeed, pyridine-*N*-oxide was the *N*-substituent of choice (Table 3.32).

Table 3.32 *N*-directing groups for the electrochemical cobalt-catalyzed C–H oxygenation.^a



Entry	Benzamide	Product	Yield [%]
1			77
2			---
3			---

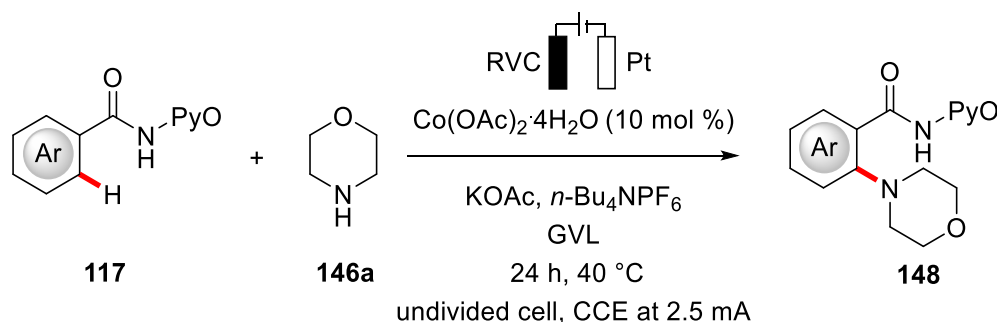


^a Reaction conditions: benzamide (0.50 mmol), $\text{Co}(\text{OAc})_2 \cdot 4\text{H}_2\text{O}$ (10 mol %), KOAc (1.50 mmol) $n\text{-Bu}_4\text{NPF}_6$ (0.50 mmol) and **146** (1.00 mmol) in GVL (2.0 mL), 40 °C, constant current of 2.5 mA, 24 h, under air.

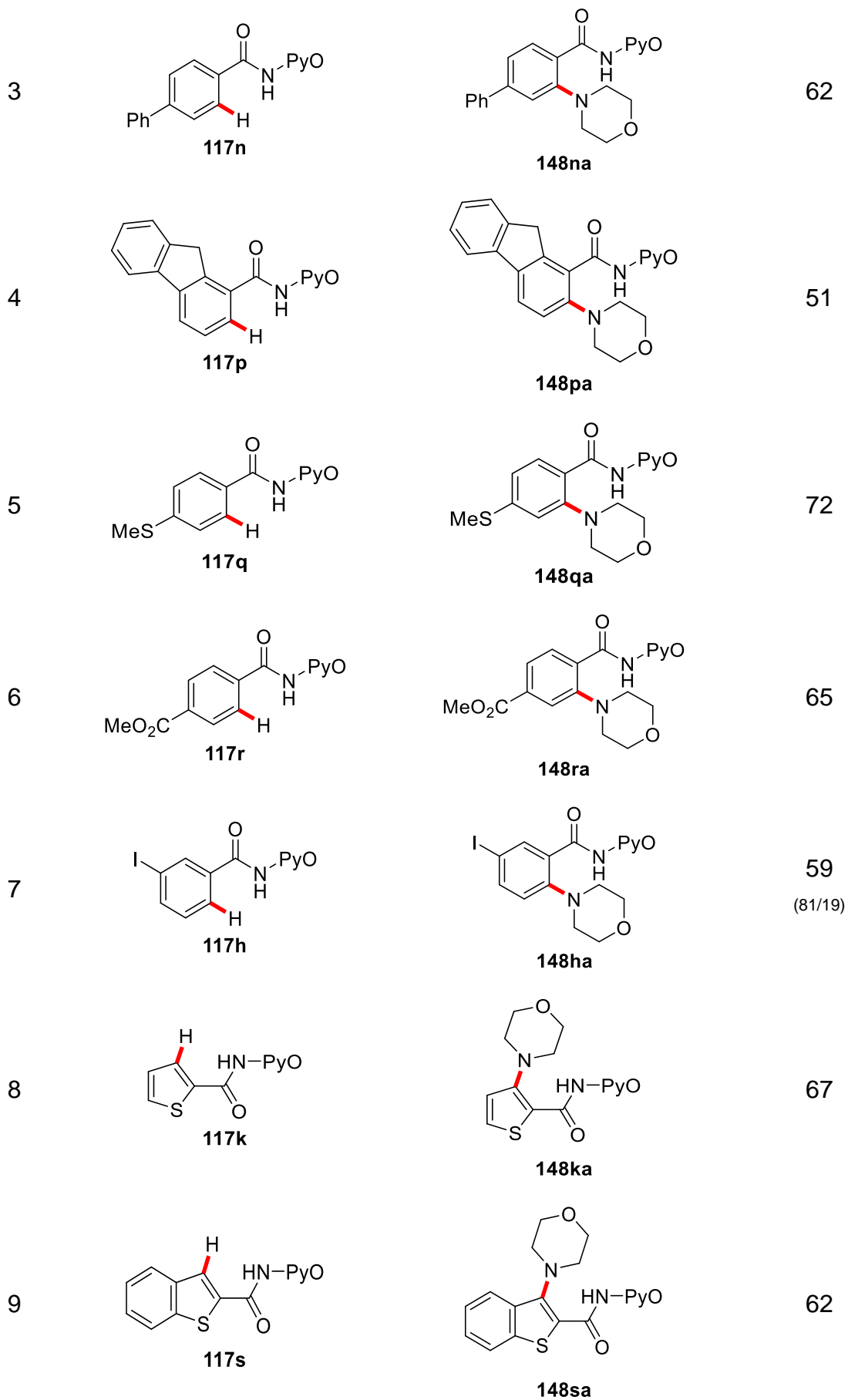
Surprisingly, not only was pyridine-*N*-oxide the best directing group, but the only one that enabled the reaction under the optimized conditions.

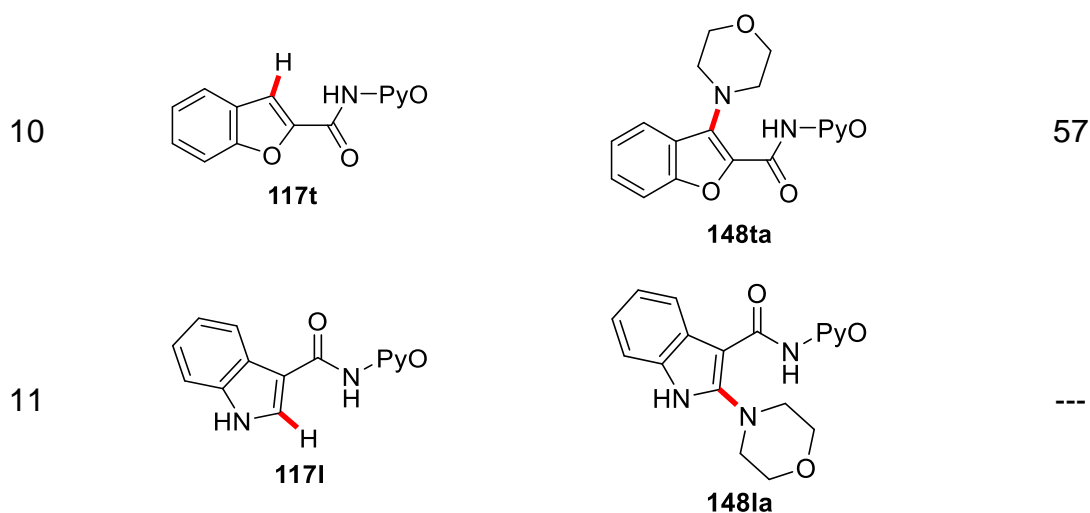
With the optimal *N*-substituent identified, the scope of benzamides **117** was established regarding the functional group tolerance of different substituents on the benzamide motif (Table 3.33).

Table 3.33 Scope of the electrochemical cobalt-catalyzed amination of benzamides **117**.^a



Entry	Benzamide	Product	Yield [%]
1			77
2			83

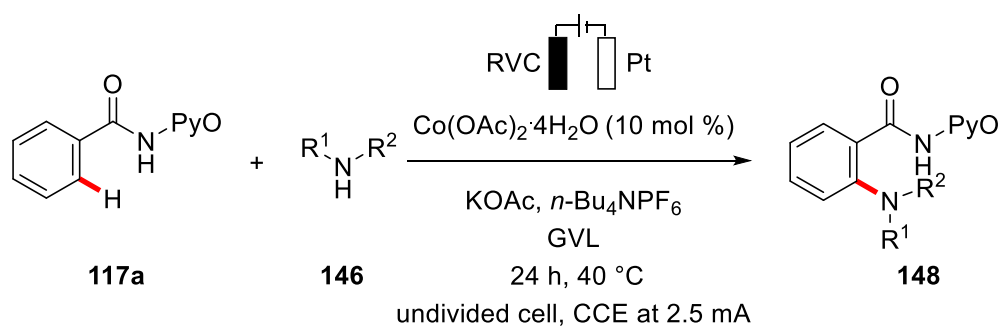




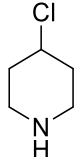
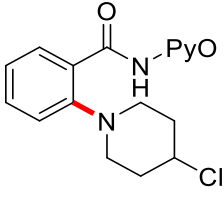
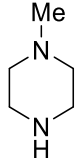
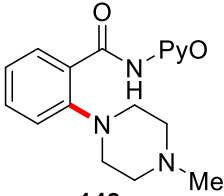
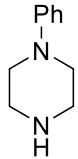
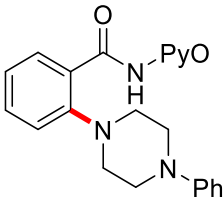
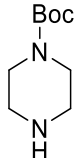
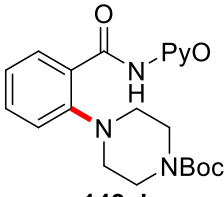
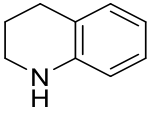
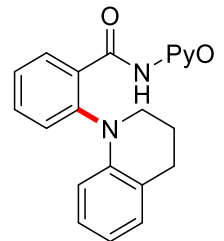
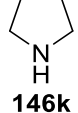
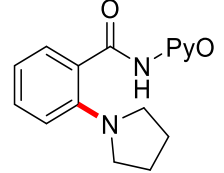
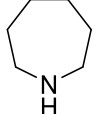
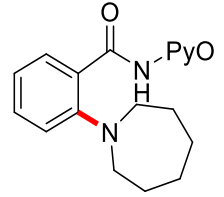
^a Reaction conditions: **117** (0.50 mmol), Co(OAc)₂·4H₂O (10 mol %), KOAc (1.50 mmol) *n*-Bu₄NPF₆ (0.50 mmol) and **246a** (1.00 mmol) in GVL (2.0 mL), 40 °C, constant current of 2.5 mA, 24 h, under air. (site-selectivities in parentheses).

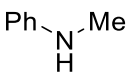
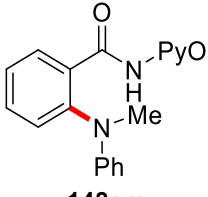
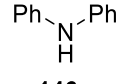
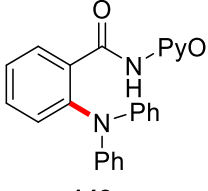
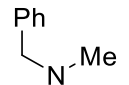
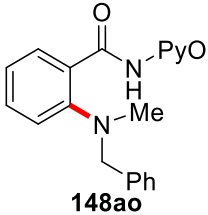
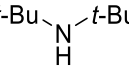
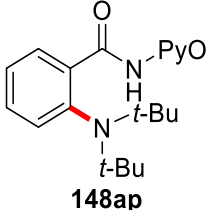
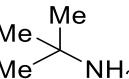
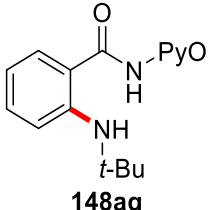
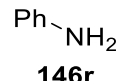
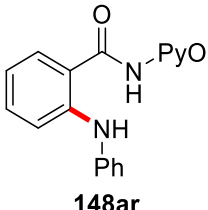
Besides the unsubstituted benzamide **117a**, which was converted smoothly, various alkyl and aryl substituents were well tolerated (entries 2-4). Contrary to the electrochemical cobalt-catalyzed C–H oxygenation, the use of *ortho*-substituted benzamide **117p** was possible, although only moderate yield was achieved (entry 4). Additionally, sensitive but also valuable functional groups, such as thioether and ester, were well tolerated (entries 5 and 6). An iodo substituent in the *meta* position was tolerated, but a mixture of regio-isomers was isolated (entry 7). Finally, electron-rich heterocycles were evaluated as substrates. Thiophene **117k** was efficiently converted (entry 8), which holds also true for the annulated substrates **117s** and **117t** (entries 9 and 10). Finally, the indole derived substrate **117l** did not show any activity under the optimized conditions (entry 11) and was reisolated quantitatively. With a viable scope containing valuable functional groups in hand for benzamides **117**, the amine coupling partner **146** was evaluated next (Table 3.34).

Table 3.34 Electrochemical cobalt-catalyzed C–H amination using amines **146**.^a



Entry	Amine	Product	Yield [%]
1	 146a	 148aa	77
2	 146b	 148ab	61
3	 146c	 148ac	74
4	 146d	 148ad	71
5	 146e	 148ae	69

6	 <p>146f</p>	 <p>148af</p>	54
7	 <p>146g</p>	 <p>148ag</p>	55
8	 <p>146h</p>	 <p>148ah</p>	trace
9	 <p>146i</p>	 <p>148ai</p>	---
10	 <p>146j</p>	 <p>148aj</p>	---
11	 <p>146k</p>	 <p>148ak</p>	---
12	 <p>146l</p>	 <p>148al</p>	---

13	 <p>146m</p>	 <p>148am</p>	trace
14	 <p>146n</p>	 <p>148an</p>	---
15	 <p>146o</p>	 <p>148ao</p>	trace
16	 <p>146p</p>	 <p>148ap</p>	---
17	 <p>146q</p>	 <p>148aq</p>	---
18	 <p>146r</p>	 <p>148ar</p>	---

^a Reaction conditions: **117a** (0.50 mmol), Co(OAc)₂·4H₂O (10 mol %), KOAc (1.50 mmol) *n*-Bu₄NPF₆ (0.50 mmol) and **146** (1.00 mmol) in GVL (2.0 mL), 40 °C, constant current of 2.5 mA, 24 h, under air.

The use of morpholine (**146a**) resulted in formation of the desired product **148aa** in good yield (entry 1), while the thio analogue **146b** (entry 2) showed slightly reduced efficacy. Unsubstituted piperidine (**146c**), as well as 4-methyl- and 4-phenylpiperidine **146d** and **146e** were converted with good yields to the desired products (entries 3-5). Remarkable is the smooth conversion of 4-chloropiperidine (**146f**) with moderate yield,

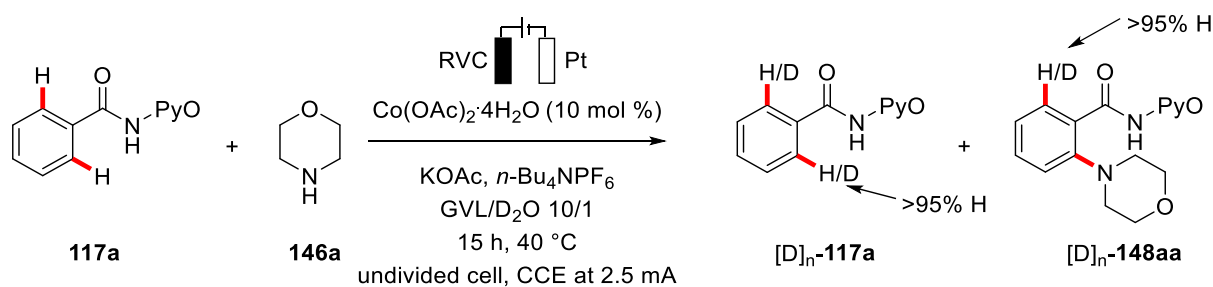
which offers a potential handle for subsequent functionalization of the products (entry 6). *N*-methylpiperazine (**146g**) was a competent substrate (entry 7), while the *N*-phenyl and *N*-Boc substituted analogues **146h** and **146i** showed only traces of the product or no conversion, respectively (entries 8 and 9). Tetrahydroisoquinoline (**146j**) as well as cyclic secondary amines **146k** and **146l** with different ring sizes (entries 10-12) did not lead to any observed product formation. Acyclic amines were generally not successful in this reaction. While trace amounts of the product could be observed in two cases (entries 13 and 15), all other experiments were not successful. The low reactivity of substrates **146p** and **146o** was initially attributed to a possible elimination of the α -hydrogens or an oxidation to the iminium ion. However, amines without α -hydrogens (entries 14 and 16) showed even worse results, although especially in the case of bis-*t*-butyl amine **146p** sterics could also play a role. Finally, primary amines **146q** and **146r** were evaluated and found to be not suitable for the amination under these optimized conditions (entries 17 and 18).

3.5.3 Mechanistic Studies and Proposed Mechanism

After evaluating the robustness of the electrochemical cobalt-catalyzed C–H amination in terms of functional group tolerance on both coupling partners, detailed mechanistic studies were conducted. Initially, the calculation of the current efficiency based on the formation of product **148aa**, revealed a value of 34% (*vide infra*), which is slightly lower than the one determined for the cobalt-catalyzed C–H alkoxylation.

$$\text{Efficacy} = \frac{n * y * z * F}{t * I} = \frac{0.0005 \text{ mol} * 0.77 * 2 * 96485 \text{ C/mol}}{86400 \text{ s} * 0.0025 \text{ C/s}} = 0.344 \quad (3)$$

Additionally, an H/D-exchange experiment was conducted in the presence of D₂O as the deuterated cosolvent which showed incorporation of deuterium neither in the product **148aa** nor in the reisolated starting material **146a**, suggesting an irreversible C–H metalation event (Scheme 3.20).



Scheme 3.20 H/D-exchange experiment in the presence of D_2O .

To gain further insights into the catalyst's mode of action, an *in-situ* study using React-IR technology was conducted, using acetonitrile as the solvent due to the strong IR bands of GVL overlaying the product signals. Initially a kinetic profile of the reaction was recorded over the complete reaction time. From the obtained surface plot, suitable peaks were identified, and the obtained values plotted against the reaction time to generate the kinetic profile (Figure 3.10).

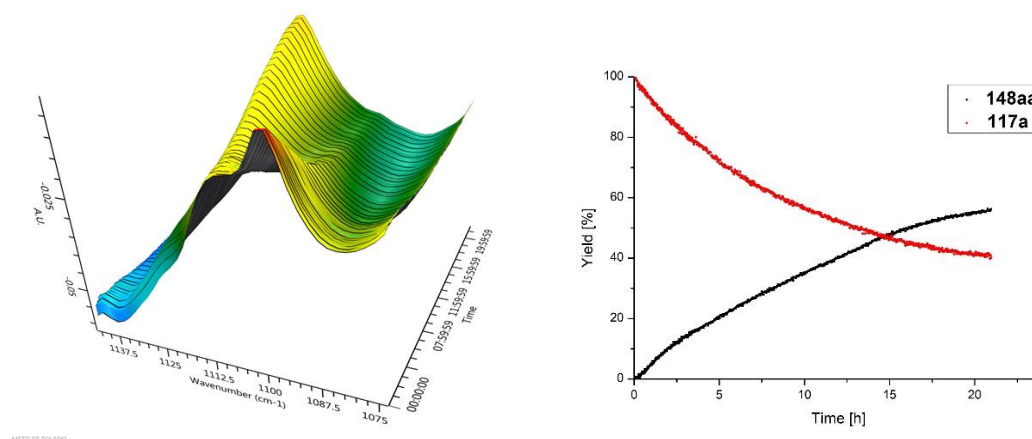
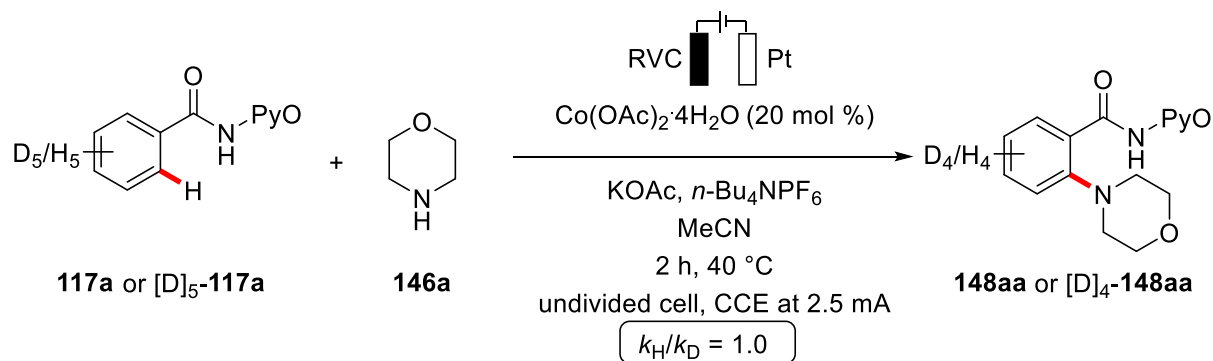


Figure 3.10 3D surface plot and kinetic profile of the electrochemical amination at 1115 cm^{-1} (red) and 1096 cm^{-1} (black).

The thus obtained data clearly showed, that an initiation period is not required, or extremely short, as the React-IR collected a measurement every minute and no initiation was observable for the cobalt catalyst. Moreover, a kinetic isotope effect (KIE) was measured using the same technique in two independent reactions for the standard substrate **117a** and the penta-deuterated substrate $[\text{D}]_5\text{-117a}$ (Scheme 3.21).



Scheme 3.21 KIE studies by react-IR technology.

From the data, no KIE ($k_{\text{H}}/k_{\text{D}} = 1.0$) was observed, which indicated that the C–H cleavage is facile and not involved in the rate, limiting step, which is in good agreement with our previous findings (Figure 3.11).

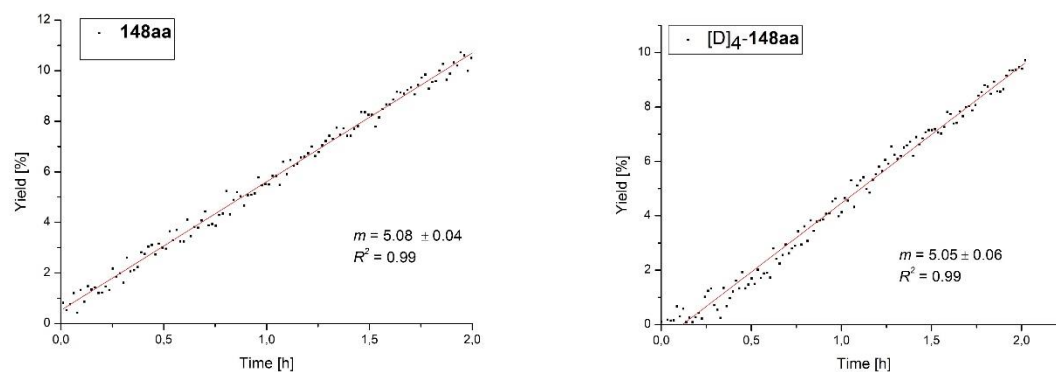
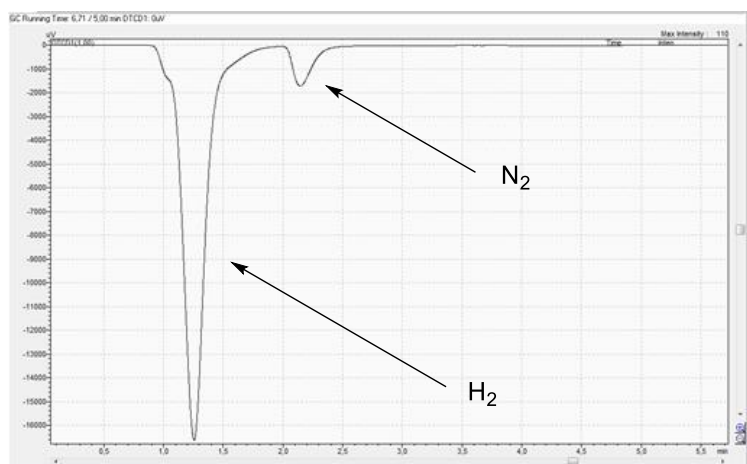
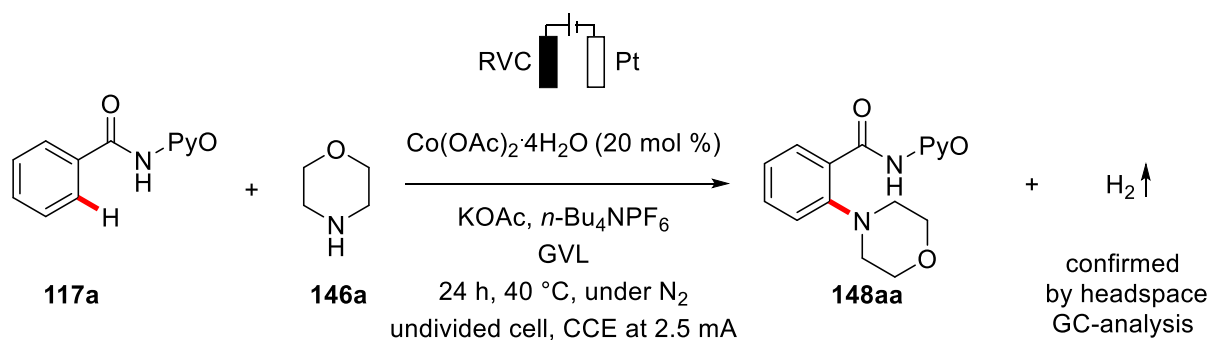


Figure 3.11 Initial rates of the electrochemical cobalt-catalyzed C–H amination.

Finally, the oxidative, cross-dehydrogenative protocol was suggestive of the formation of H_2 as the stoichiometric byproduct. Therefore, the gas phase over the reaction medium was analyzed by headspace GC technology to explore the formation of H_2 . The analysis qualitatively confirmed the formation of H_2 , which can be seen in the obtained chromatogram (Scheme 3.22).



Scheme 3.22 GC headspace analysis of the reaction mixture.

In addition to these studies, the reaction was also analyzed by CV studies of the reaction mixture in MeCN (Figure 3.12). While the oxidation of Co(OAc)_2 in the presence of KOAc was observed at a potential of $1.05 V_{\text{SCE}}$, the substrate **117a** was oxidized at a significantly higher potential of $1.58 V_{\text{SCE}}$. Interestingly a mixture of the cobalt salt, KOAc and **117a** was shifted to significantly lower potentials with a local maximum observable at $0.73 V_{\text{SCE}}$ and several new peaks were observed. Finally, upon addition of morpholine, no quenching could be observed, however oxidation of morpholine was overlaying with most of the CV curve. Nevertheless, the oxidation of morpholine occurs at a higher potential ($1.17 V_{\text{SCE}}$), and thus the data strongly supports a cobalt catalyzed, organometallic transformation over a radical addition pathway, which is known for electrochemical, metal-free aminations of activated oxazole heterocycles.^[210]

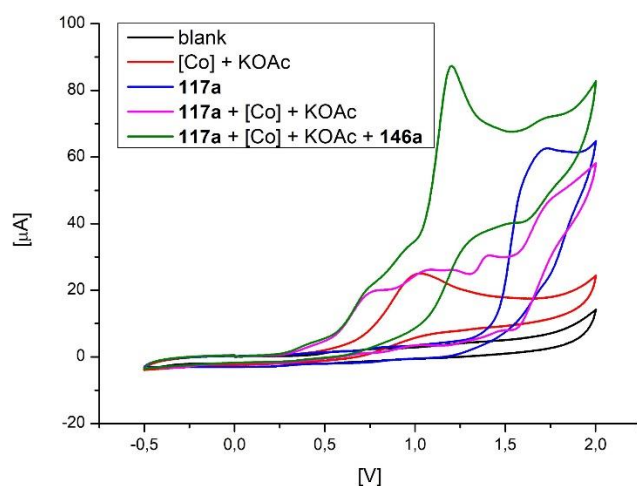
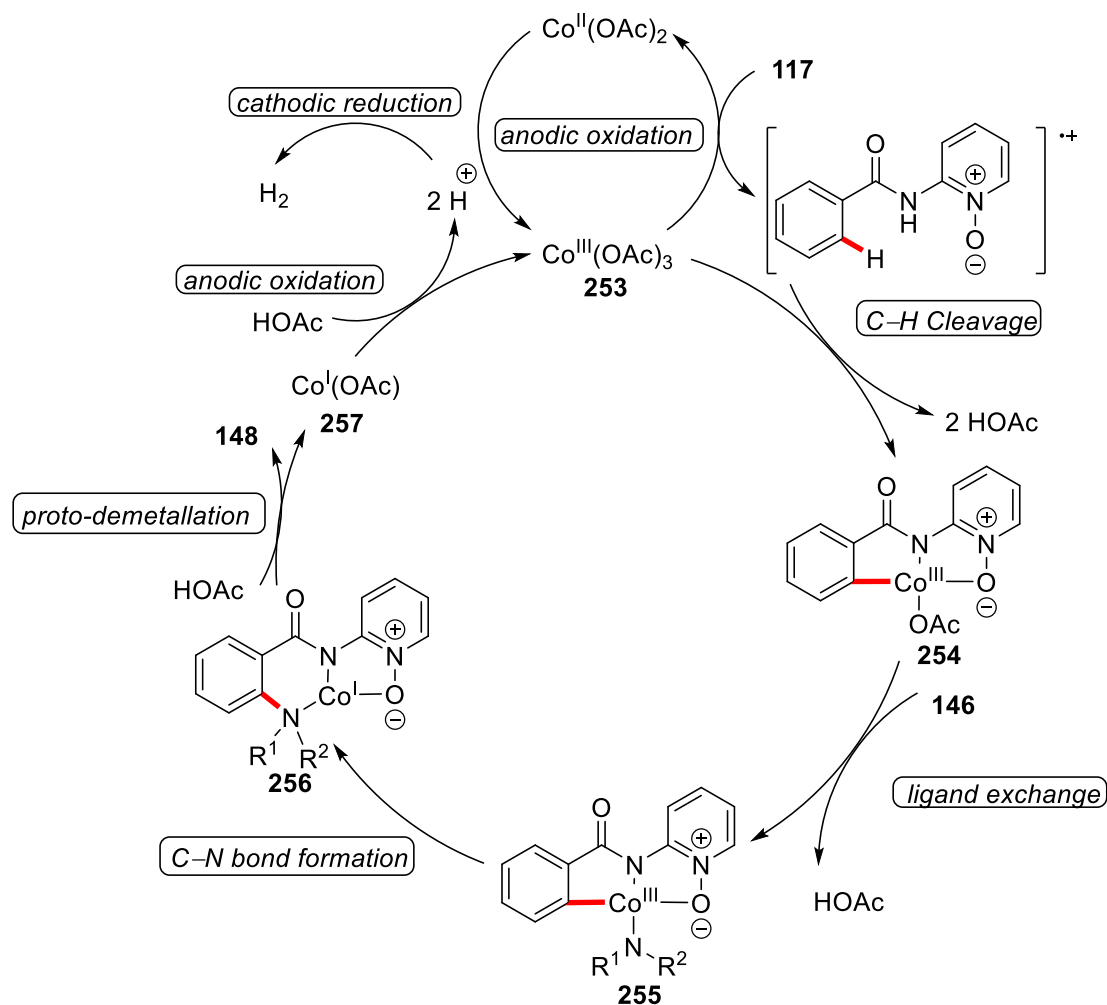


Figure 3.12 CV of the reaction mixture in MeCN.

Based on the sum of these mechanistic experiments, a plausible catalytic cycle is proposed. After generation of the active cobalt(III) catalyst **254**, the C–H activation occurs by BIES C–H cobaltation.^[29] The thus formed cyclometalated complex **255** can undergo a ligand exchange of substrate **146a** against the acetate to generate intermediate **256**. Formation of the C–N bond followed by proto-demetalation generates the desired product **148** and cobalt(I) species **257**, which is oxidized at the anode to regenerate the active catalyst **254** (Scheme 3.23).



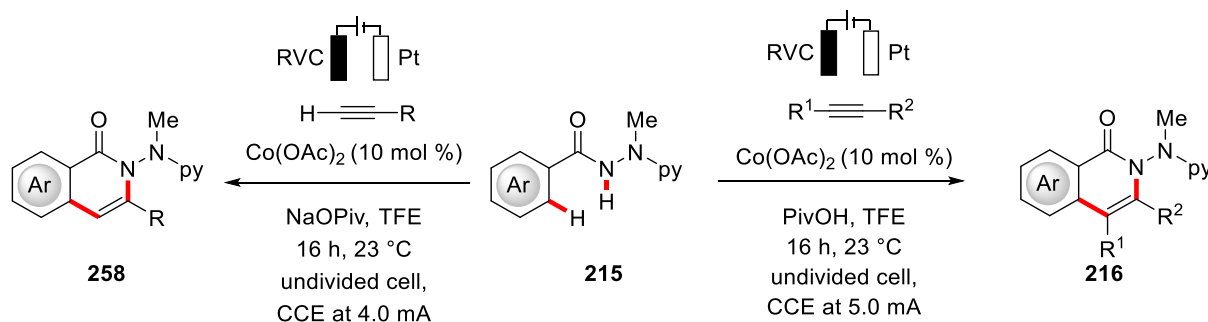
Scheme 3.23 Plausible catalytic cycle.

3.6 Mechanistic Studies on Transition Metal-Catalyzed Electrochemical C–H Activation.

During the studies on the cobalt-catalyzed C–H amination under electrochemical conditions, further electrochemical transition metal-catalyzed C–H functionalizations were developed. The optimization and scope of these reactions was investigated by Dr. R. Mei (cobalt)^[211] and Dr. Y. Qiu, Dr. W.-J. Kong, J. Struwe and A. Scheremetjew (rhodium)^[212] respectively, with theoretical considerations conducted by Dr. J. C. A. Oliveira and T. Rogge. Therefore, only a short overview over the general reaction will be given in the following chapter, with a detailed description of the mechanistic studies conducted in the range of this thesis.

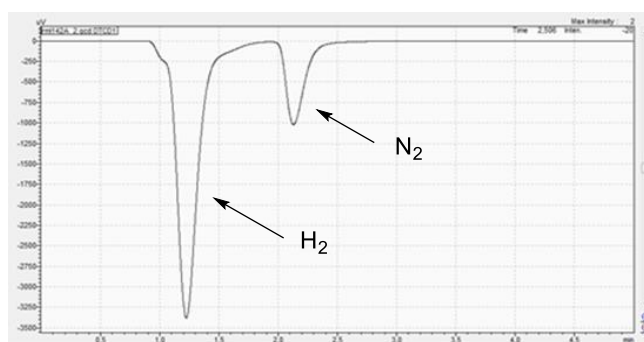
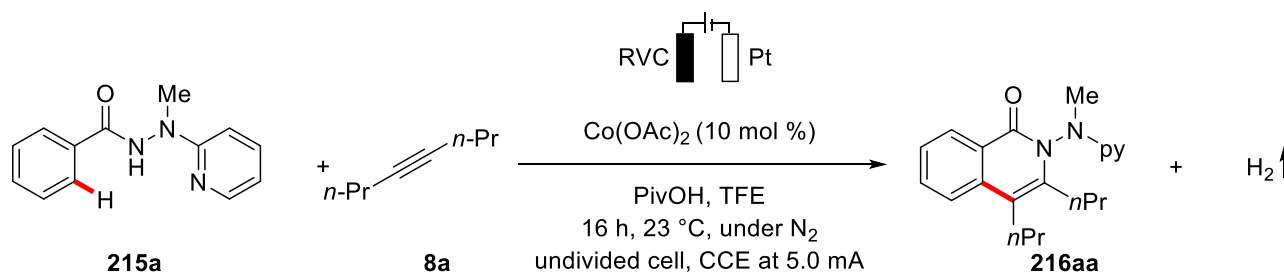
3.6.1 Cobalt-Catalyzed Electrochemical Annulation of Terminal and Internal Alkynes using an Electrocleavable Directing Group

During his studies, R. Mei identified *N*-methyl-*N*-pyridyl benzhydrazides **215** as viable substrates for the cobalt-catalyzed electrochemical C–H/N–H annulation using terminal as well as internal alkynes **8**.^[210] This is noteworthy, as previous protocols for C–H/N–H annulation by electrochemical cobalt-catalysis were limited to terminal alkynes **8**.^[168–169] The transformations of internal and terminal alkynes **8** were enabled under slightly different conditions, as shown below (Scheme 3.24).^[211]



Scheme 3.24 Electrochemical cobalt-catalyzed C–H/N–H annulation of alkynes **8**.

For this reaction, also the formation of hydrogen as a byproduct seems plausible. This was confirmed for the reaction of the internal alkyne **8a** by headspace GC analysis (Scheme 3.25).



Scheme 3.25 GC headspace analysis.

Additionally, a measurement of the kinetic profile by time-resolved UV/Vis spectroscopy was attempted. While the time-resolved spectra nicely showed several shifts in the UV/Vis region, no separated peaks could be obtained. A kinetic profile could be obtained by plotting peak intensities against time, however due to missing peak separation, this can only be a qualitative analysis not suited to calculate rate constants for the initial rates analysis (Figure 3.13).

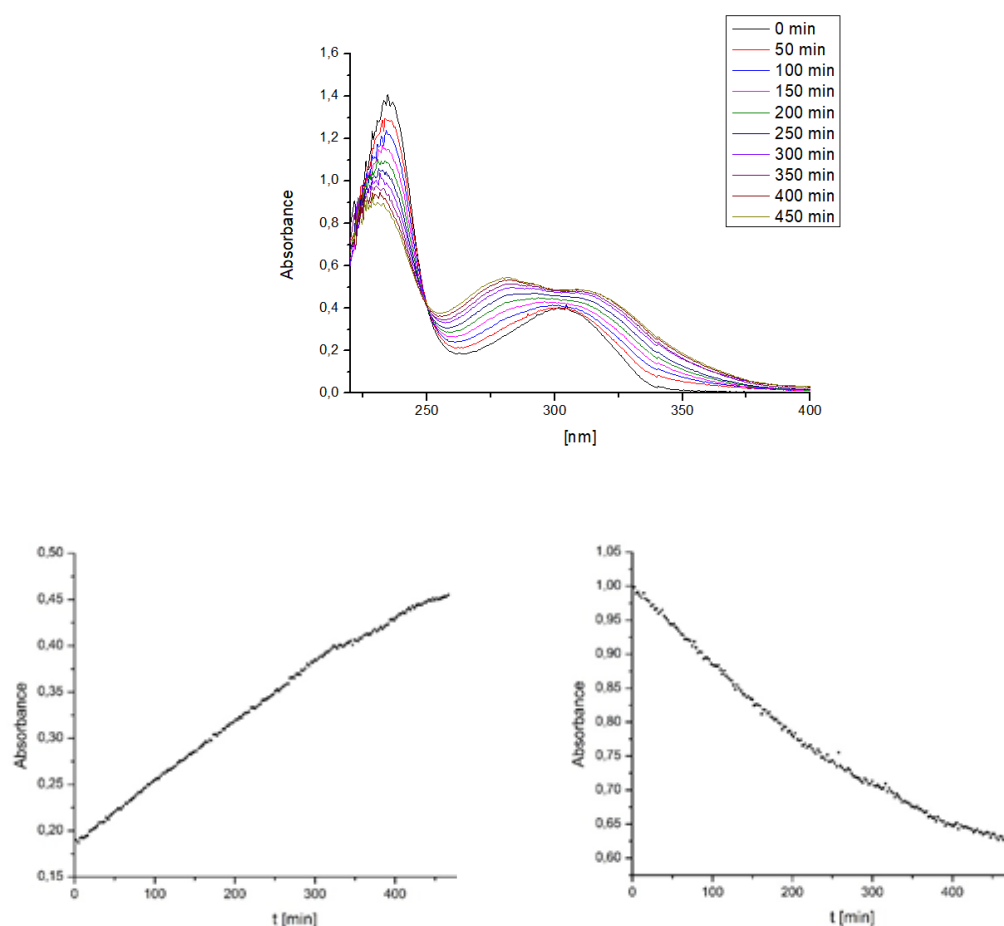
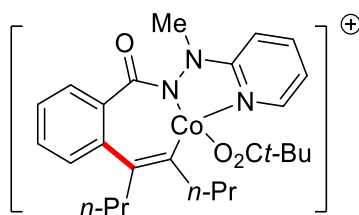


Figure 3.13 Time resolved UV/Vis spectra and kinetic profiles at 242 nm (left) and 266 nm (right).

To get further insight into possible intermediates of the reaction, the crude reaction mixture was subjected to ESI mass spectrometry. Besides several aggregates of the starting materials and products, a mass was observed, which was identified as the seven-membered cyclometalated intermediate **259** (Figure 3.14).



Molecular Formula: $C_{26}H_{34}CoN_3O_3$

Exact Mass: 495.1927

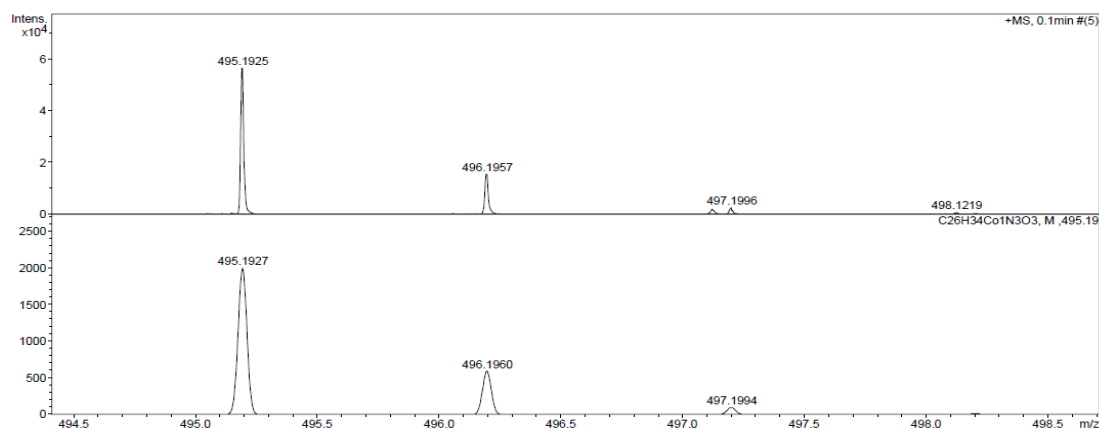


Figure 3.14 ESI-MS of the proposed intermediate **253**.

Since a five-membered cyclometalated cobalt complex coordinating the alkyne (**260**, Figure 3.15) should have the same exact mass, this ion was isolated and analyzed by MS/MS technology. In the resulting spectra, only the loss of pivalic acid was observed, while a π -coordinated alkyne should be removed first due to its weaker coordination (Figure 3.16). Furthermore, the mass for the five membered cobaltacycle fragment **261** ($m/z = 284$), which would be expected in this case was not observed, supporting the proposal that the mass does indeed belong to the seven-membered species **259**. Also, a complex of the product **216aa** coordinated to a Co(I)-species after reductive elimination seemed unlikely, as in this case the mass of **216aa** should be observable after fragmentation, which was not the case here. The same experiment was conducted using deuterated $[D]_5$ -**215a**, and indeed, the loss of one deuterium confirms the structure of intermediate **259**.

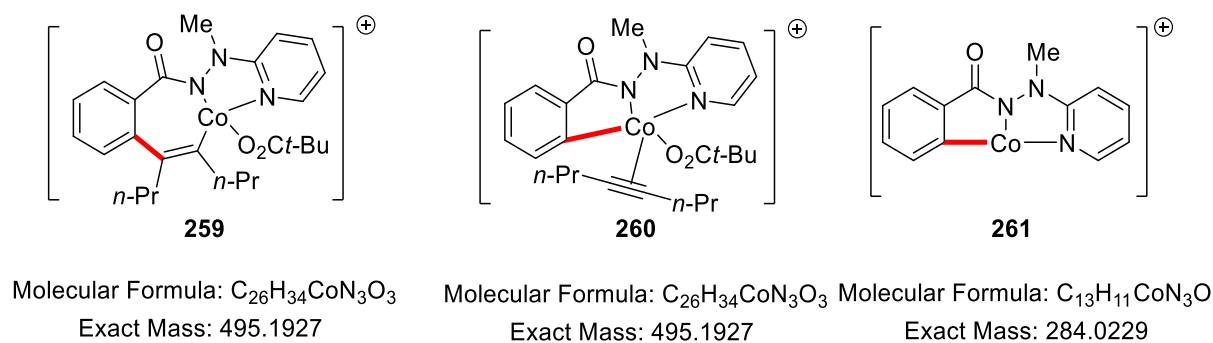


Figure 3.15. Possible Intermediates and Fragments.

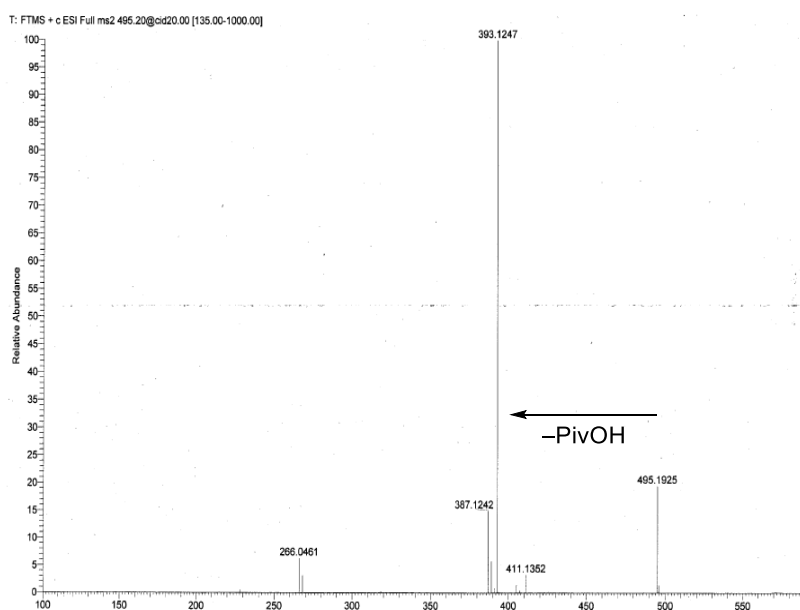


Figure 3.16 MS/MS spectra of the ion with m/z 495.1925.

In addition to the previous experiments, CV studies were conducted on this reaction system. Initially, the reaction of internal alkyne **8a** was studied, however the obtained spectra were inconclusive, as overlaying of the peaks occurred (Figure 3.17). In contrast, for terminal alkyne **8b** also the use of methanol as the solvent was possible, therefore a second measurement using this system was performed, resulting in better data. While the alkyne **8b** itself is not oxidized, the hydrazide **215a** is easily oxidized, even at lower potential than the cobalt catalyst, which is oxidized at 1.31 V_{SCE}. However, the complete reaction mixture is shifted to lower potential than the starting material **215a**, supporting the oxidation of cobalt(II) to cobalt(III) in the presence of the starting material at much lower potential of 0.99 V_{SCE}.

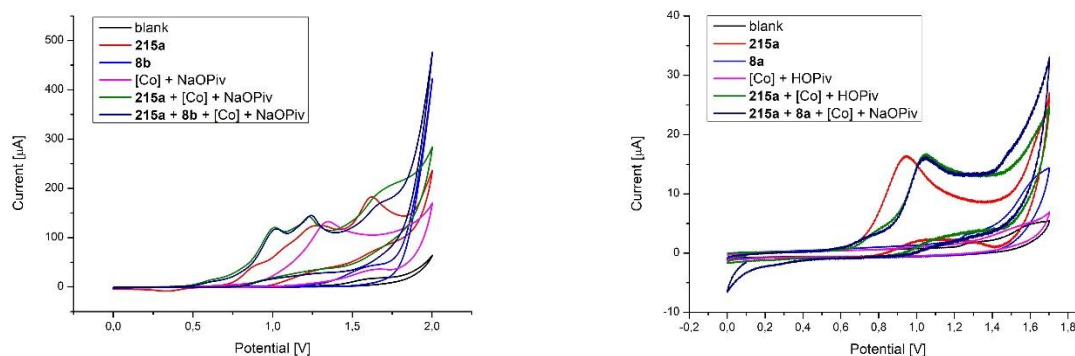
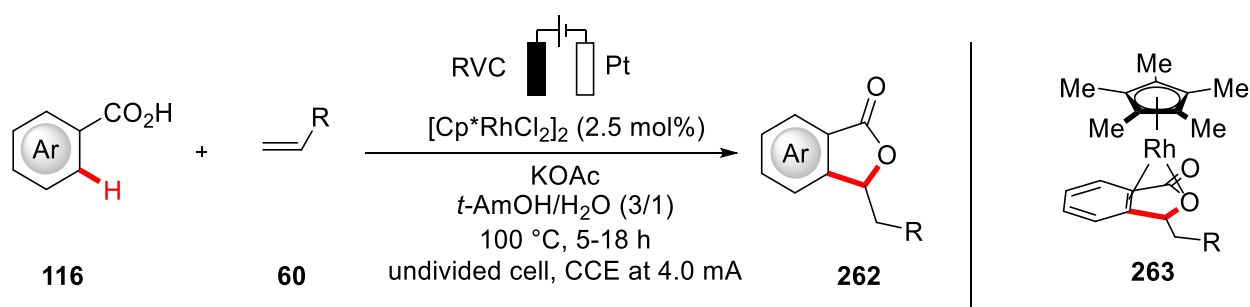


Figure 3.17 CV spectra of the reaction mixtures in MeOH (left) and TFE (right).

3.6.2 Rhodium-Catalyzed C–H/O–H Annulation of Benzoic Acids

Rhodium is one of the most powerful metals for transition metal-catalyzed C–H activation,^[31c, 31d] and while tremendous progress has been achieved, especially oxidative rhodium catalyzed reactions remain limited by the need for expensive stoichiometric oxidants^[31a, 31b, 32a, 213] with few exceptions utilizing hazardous O₂^[214] as the terminal oxidant.^[215] In this regard, Dr. Y. Qiu and Dr. W.J. Kong developed a rhodium-catalyzed C–H/O–H annulation of benzoic acids with acrylates under electrochemical conditions to avoid the need for costly chemical oxidants.^[210] The overall reaction equation is shown in scheme 3.26. As the optimization, scope and mechanistic studies were performed by my colleagues, only the CV studies shall be discussed here.



Scheme 3.26 Rhodium-catalyzed C–H/O–H annulation.

In this transformation the formation of rhodium(I) sandwich complex **263** is proposed as an intermediate. Experiments to synthesize a related complex by a known method proved to be unsuccessful.^[216] Therefore, this step was studied in its microscopic

reverse, e. g. a CV of the reductive region of $[\text{Cp}^*\text{RhCl}_2]_2$ in the absence and presence of the product **262** (Figure 3.18).

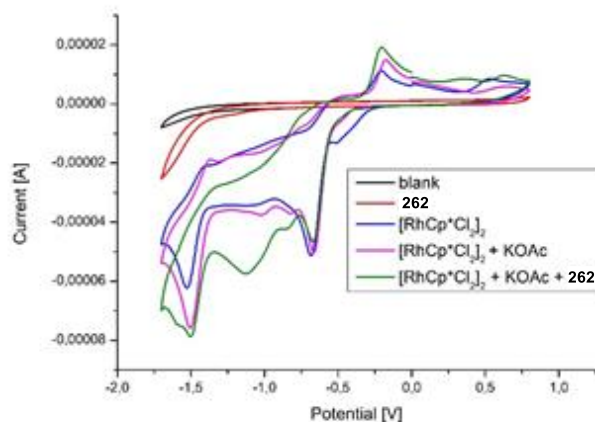


Figure 3.18 CV of $[\text{Cp}^*\text{RhCl}_2]_2$ under various conditions.

While the product **262** itself is not reduced under these conditions, $[\text{Cp}^*\text{RhCl}_2]_2$ shows clear reduction peaks, although the spectra are highly complex, and no assignment of the peaks is possible. Remarkably, no new signals upon addition of KOAc are observed, indicating that formation of the acetate complex may not occur under these conditions. Upon addition of the product however, a new peak at $-1.09 \text{ V}_{\text{SCE}}$ is observed.

As the generation of the acetate complex would be highly important, another measurement was conducted using HOAc as the additive instead of KOAc (Figure 3.19).

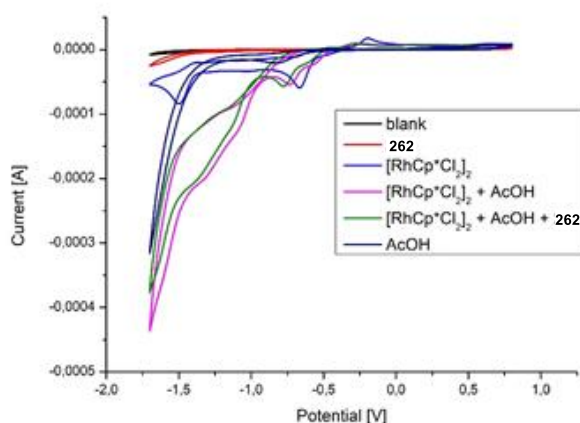


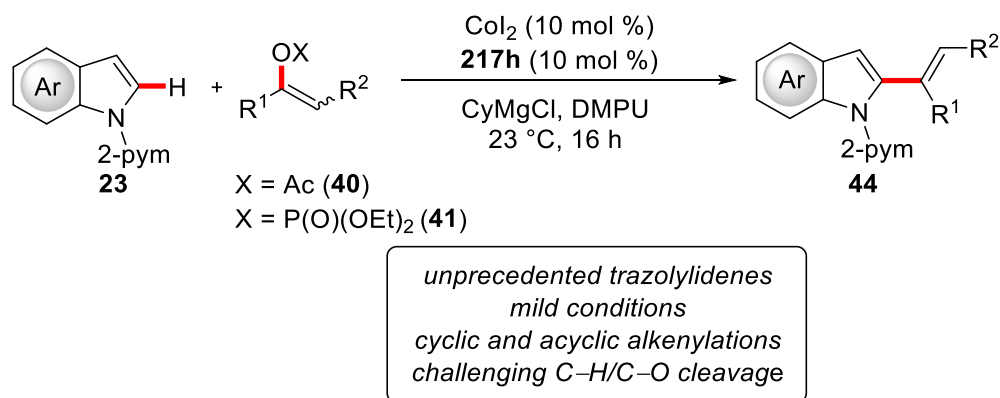
Figure 3.19 CV spectra in the presence of HOAc.

As can be seen in figure 3.16, there is a massive shift from the chloride dimer to a new CV curve after addition of HOAc, indicating the formation of the acetate complex, as a control experiment showed no reduction of HOAc in this area. Unfortunately, this curve undergoes no significant change upon addition of the product, so that no prediction about the proposed intermediate is possible from these CV studies.

4 Summary and Outlook

The sustainable and cost-efficient synthesis of key structural motifs for material sciences, medicinal chemistry and crop protection remains one of the biggest challenges in terms of declining resources and a heightened awareness of the ecological costs associated with many processes.^[3] Therefore, C–H activation greatly improves the tools for synthetic chemists to achieve these goals.^[1a, 25a, 25c, 31d, 32c, 33c, 33d, 212c]

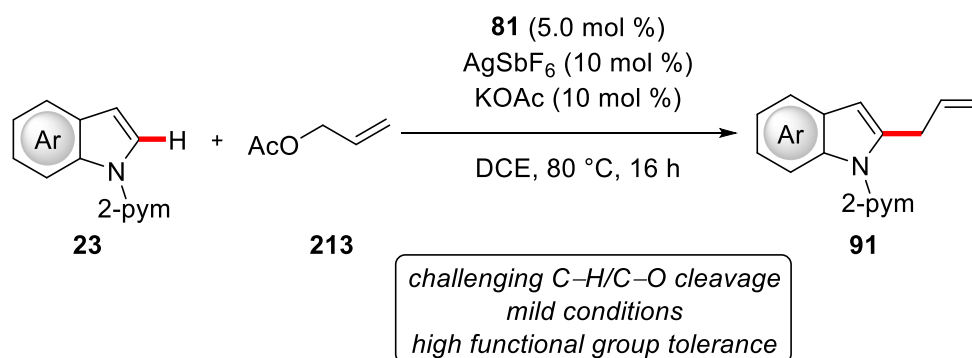
In the first project, the unprecedented use of triazolium salts **212** as preligands in cobalt-catalyzed C–H activation, was examined based on a previously described reaction.^[56] The reaction proceeded by facile C–H/C–O cleavage using easily accessible alkenyl acetates **40** and phosphates **41** (Scheme 4.1).^[217]



Scheme 4.1 Cobalt-catalyzed alkenylation by C–H/O–H cleavage.

Compared to the known hydroarylation protocols,^[57–61] this approach allows for the use of cyclic alkenes, a structural motif that is usually not achieved using alkynes **8** due to the high ring strain.^[176] The yields achieved using triazolylidene **212h** are good,^[217] with excellent levels of selectivity for the (*E*)-configured product. Although the formed products **44** do not contain a stereocenter, several chiral triazolylidenes are known and could prove applicable to future enantioselective processes.

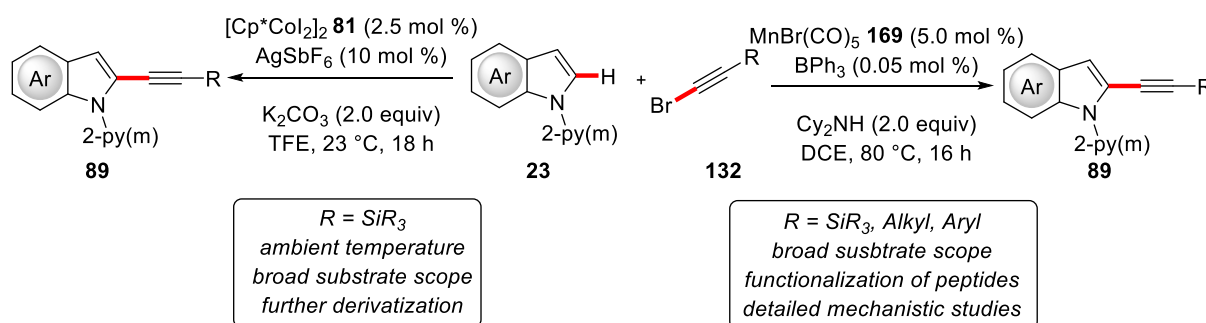
In a second project, Cp*Co(III) proved to be key to success for the efficient C–H allylation of indoles **23** and pyrroles **217** (Scheme 4.2).^[79a]



Scheme 4.2 Cobalt-catalyzed C–H allylation by C–H/C–O cleavage.

Due to the high robustness of the Cp*Co(III)-catalyst, a good functional group tolerance could be established, especially in contrast to low-valent cobalt catalysis.^[48a] Valuable functional groups,^[79a] such as amide, nitro and halides, were well tolerated and highlighted the chemoselectivity of the Cp*Co(III)-catalyst.

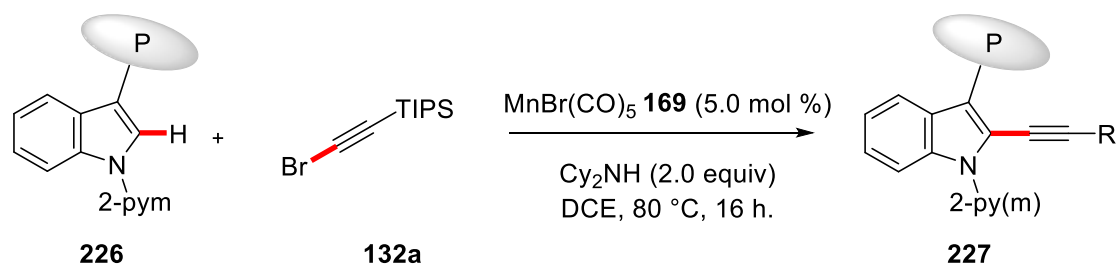
Cobalt(III)-catalysis was also used in the base metal-catalyzed C–H alkylation of heteroarenes **23** and **217** (Scheme 4.3).^[194]



Scheme 4.3 Base metal-catalyzed C–H alkylation of heteroarenes.

Initially, the C–H alkylation of indoles **23** and pyrroles **217** was realized using Cp*Co(III)-catalysis. The cobalt-catalyzed reaction proceeded under very mild conditions, that is at ambient temperature and a broad range of indoles and pyrroles could be functionalized. However, the reaction was limited to silyl substituted alkynes, as aryl or alkyl substituents did not provide any product. Finally, the usefulness the devised C–H alkylation could be highlighted by the derivatization of the synthesized products **89**. Complementary to the cobalt-catalyzed C–H alkylation, a manganese(I)-catalyzed C–H alkylation with the same substrates was developed.^[201] After extensive optimization, the transformation could be improved to include also alkyl and aryl alkynes **132**, which were previously not suitable.^[194]

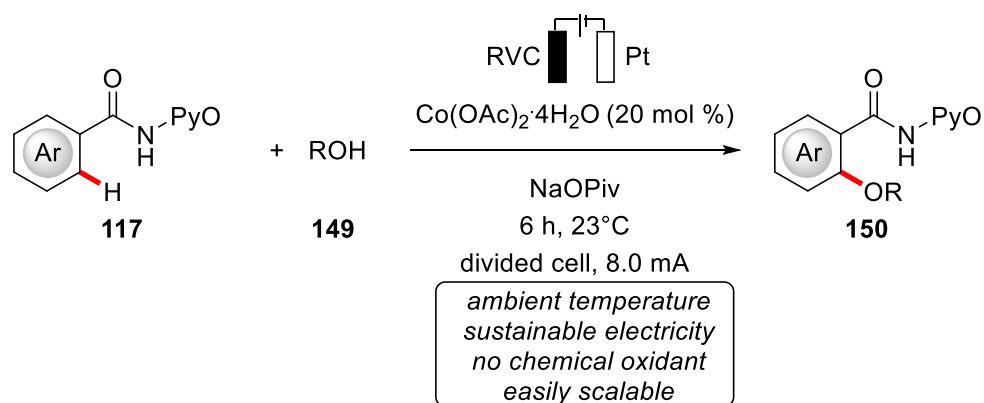
Furthermore, a broad substrate scope was established,^[201] including the functionalization of amino acids and peptides **226** without racemization (Scheme 4.4).



Scheme 4.4 Base metal-catalyzed C–H alkylation of peptides

Finally, detailed mechanistic studies were conducted. The reaction order for the substrates and the manganese catalyst were determined and offered support for the C–H activation not being rate-determining. In addition, cyclometalated manganese complex **238** was isolated and identified as a competent catalyst for the reaction as well as suitable to form the product in stoichiometric reactions suggesting that it is an on cycle intermediate.

In a fourth project, a cobalt-catalyzed C–H oxygenation under electrochemical conditions was realized.^[206] While electrochemical C–H activation using precious palladium catalysts is known,^[204, 218] this represents the first electrochemical cobalt-catalyzed C–H activation (Scheme 4.4).^[206]

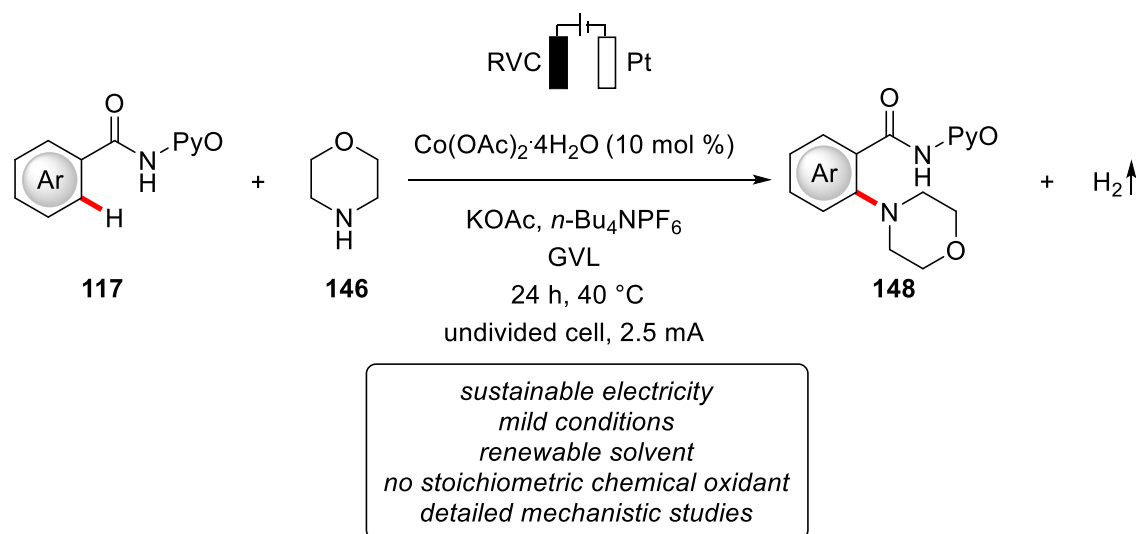


Scheme 4.4 Electrochemical cobalt-catalyzed C–H oxygenation.

The desired transformation could be realized under mild conditions, that is ambient temperature and using a mild base. The oxidative protocol was established using sustainable and cost-efficient electricity compared to previously employed stoichiometric amounts of silver(I)-salts as the terminal oxidant. The reaction was shown to tolerate various valuable functional groups,^[206] including oxidatively labile

moieties. Additionally, several alcohols were found to be competent coupling partners. An enantiomerically pure alcohol was used and found to be stereochemically stable under the reaction conditions. Additionally, detailed mechanistic studies, including H/D-exchange experiments, KIE studies and competition experiments were conducted. Finally, the reaction was analyzed by CV and a plausible mechanism proposed. The synthetic significance was highlighted by the easy scaleup of the reaction and the user-friendly handling of this technique. While primary alcohols were transformed very efficiently, secondary alcohols only resulted in trace amounts of product, a venue that should allow for future optimization to realize more sophisticated substitution patterns. Moreover, the use of the alcohol as the reaction medium greatly reduces the efficacy and is also prohibitive for the use of solid alcohols, therefore the identification of a suitable inert reaction medium would be highly desirable.

Based on the C–H/N–H annulation reported in the meantime,^[168] which involves an intramolecular C–N bond formation, an intermolecular C–N bond formation was devised (Scheme 4.5).^[219]



Scheme 4.5 Electrochemical cobalt-catalyzed C–H amination.

After considerable optimization, biomass-derived GVL^[19, 209] was identified as the best solvent. The reaction therefore was identified as the first electrochemical C–H activation in a renewable solvent, highlighting the potential to further increase the sustainability of this approach. Again, mild conditions could be achieved for the reaction,^[219] including a reaction temperature of 40 °C. Several substrates were smoothly converted, including important heterocyclic arenes. *In operando* studies by React IR were applied to electrocatalysis and showed the absence of a meaningful

initiation period. Furthermore, a KIE measurement was performed by the same technique, in addition to standard mechanistic experiments, such as H/D exchange. Moreover, the formation of H₂ as the sole byproduct was confirmed by headspace GC analysis of the gas phase over the reaction mixture.

Finally, two projects from colleagues were supported with detailed CV studies under different conditions,^[210] as well as headspace analysis and extensive studies on potential intermediates by ESI-MS,^[211] and evidence for the key seven-membered intermediate **259** could be obtained. Furthermore, it could be shown that besides *in situ* IR technology also *in situ* UV/Vis was a viable method to record kinetic profiles for cobalt-catalyzed electrochemical C–H activation, with future potential when suitable reactions are identified.

5 Experimental Part

5.1 General Remarks

All reactions involving air- and/or moisture-sensitive compounds were conducted under a nitrogen atmosphere using pre-dried glassware and standard Schlenk techniques. If not otherwise noted, yields refer to isolated compounds which were estimated to be >95% pure based on ¹H-NMR and/or GC analysis.

5.1.1 Vacuum

A Vacuubrand RZ 6 vacuum pump was used throughout the course of this thesis. The pressure was measured to be 0.7 mbar (uncorrected value).

5.1.2 Chromatography

Thin Layer Chromatography (TLC) was performed using silica gel 60 F₂₅₄ on aluminum sheets from Merck and either visualized under a UV-Lamp or developed using basic KMnO₄ solution or a vanillin stain upon careful heating. Purification of the compounds was carried out by column chromatography using Merck Geduran silica gel, grade 60 (40-63 μm, 70-230 mesh).

5.1.3 Gas Chromatography

Monitoring of the reaction progress or kinetic analysis was conducted using a 7890 GC-system with or without mass detector 5975C (triple-axis-detector) or a 7890B GC-system and a 5977A mass detector, both from Agilent Technologies.

Headspace analysis by GC was performed on a Shimadzu S2014 GC system using a thermal conductivity detector and a 5Å MS column.

5.1.4 Nuclear Magnetic Resonance

Spectra were recorded on a Varian Unity 300, Mercury 300, Inova 500 or Bruker Avance III 300, Bruker Avance III HD 400 and Bruker Avance III HD 500 in the solvent indicated; chemical shifts (δ) are given in ppm relative to the residual solvent peak.

	$^1\text{H-NMR}$	$^{13}\text{C-NMR}$
CDCl_3	7.26	77.16
DMSO-d_6	2.50	39.52

Analysis of the obtained spectra was conducted using MestreNova 10 software.

5.1.5 Mass Spectrometry

EI-MS-spectra were recorded on an AccuTOF from JEOL, ESI-MS- and HRMS-spectra were recorded on a microTOF or maXis from Bruker Daltonic. The ratio of mass to charge (m/z) are indicated and the intensities relative to the highest peak ($I = 100$) are given in parentheses.

5.1.6 Melting Points

Melting points were measured on a Stuart melting point apparatus SMP3, Barloworld Scientific, values are uncorrected.

5.1.7 Infrared Spectroscopy

IR spectra were recorded on a Bruker FT-IR Alpha device. Liquid samples were measured as a film and solid samples neat, spectra were recorded in the range of $4000\text{-}400\text{cm}^{-1}$, absorption is given in wavenumbers (cm^{-1}).

In-situ IR measurements were carried out using the React-IR15 from Mettler Toledo equipped with a diamond probe.

5.1.8 Electrochemistry

Platinum electrodes (10 mm×15 mm× 0.25 mm, 99.9%; obtained from ChemPur® Karlsruhe, Germany) and RVC electrodes (10 mm×15 mm×6 mm, SIGRACELL®GFA 6 EA, obtained from SGL Carbon, Wiesbaden, Germany) were connected using stainless steel adapters. Electrolysis was conducted using an AXIOMET AX-3003P potentiostat in constant current mode, CV studies were performed using a Metrohm Autolab PGSTAT204 workstation and Nova 2.0 software. Divided cells separated by a P4-glassfrit were obtained from Glasgerätebau Ochs Laborfachhandel e. K. (Bovenden, Germany).

5.1.9 Solvents

Solvents for column chromatography or reactions not sensitive to air and moisture were distilled under reduced pressure prior to use. All solvents for reactions involving air- or moisture sensitive compounds were dried, distilled and stored under inert atmosphere according to the following procedures:

Purified by solvent purification system (SPS-800, M. Braun): CH₂Cl₂, toluene, tetrahydrofuran, dimethylformamide, diethylether.

Dried and distilled over sodium/benzophenone: *tert*-Amyl alcohol, methanol, 1,4-dioxane.

Dried and distilled over CaH₂: 1,3-Dimethyltetrahydropyrimidin-2(1*H*)-one, 1,2-Dichlorethan.

Degassed and stored over activated molecular sieves: γ -Valerolactone, acetonitrile.

5.1.10 Chemicals

Chemicals obtained from commercial sources with a purity >95% were used as received without further purification. The following compounds were known from the literature and synthesized according to previously known methods:

(pyrimidine-2-yl)-indoles **23** and pyrroles **217**,^[200] alkenyl acetates **40**,^[55a] alkenyl phosphates **41**,^[55b] alkenyl carbonate **42b**,^[55c] alkenyl carbamate **43b**,^[55d] triazolium

salt **212a**,^[177] Cp*CoI₂(CO) (**81**),^[87] [Cp*Co(C₆H₆)]PF₆]₂ (**73**),^[67] [Cp*CoI₂]₂ (**82**),^[218] bromoalkynes **132**,^[221] benzamides **117**^[99] and alcohol **149g**.^[222]

The following compounds were kindly synthesized and provided by the persons listed below:

Joachim Loup: triazolium salt **212d**.

Marc Moselage: alkenyl acetates **40b**, **40j** and **40k**.

Tjark H. Meyer: amides **117a**, **117o**, **117q** and **117k**.

Ruhuai Mei: hydrazide **215a**.

Berkessel group: triazolium salts **212b**, **c**, **e-h**.

Sier Sang: amides **117a**, **117c**, **117e** and **117j**.

Elisabetta Manoni: indoles **23k**, **23o** and alkyne **132d**.

5.2 General Procedures

General Procedure A for the Cobalt-Catalyzed C–H/C–O Alkenylation: To a solution of **23** (0.25 mmol, 1.00 equiv), the enol derivative **40** or **41** (0.38 mmol, 1.50 equiv), CoI₂ (7.8 mg, 25.0 μmol, 10 mol %) and triazolium salt **212h** (13.1 mg, 25.0 μmol, 10 mol %) in DMPU (1.5 mL), CyMgCl (1.7 M in THF, 0.3 mL, 0.50 mmol, 2.00 equiv) was added dropwise. The mixture was stirred for 16 h at 23 °C. After completion of the reaction, saturated aq. NH₄Cl solution (10 mL) was added and the mixture was extracted with CH₂Cl₂ (3 × 5 mL). Drying over Na₂SO₄, evaporation of the solvents and purification by column chromatography on silica gel yielded the product **44**.

General Procedure B for the Cobalt-Catalyzed Allylation: To a solution of **23** (0.50 mmol, 1.00 equiv), [Cp*Co(CO)I₂] (**81**) (25.0 μmol, 5.0 mol %), AgSbF₆ (0.05 mmol, 10 mol %) and KOAc (0.05 mmol, 10 mol %) in DCE (1.5 mL) allyl acetate **213** (1.00 mmol, 2.00 equiv) was added. The mixture was stirred for 16 h at 80 °C. After completion of the reaction, saturated aq. NH₄Cl solution (5 mL) was added at ambient temperature and the mixture was extracted with MTBE (4 × 5 mL). Drying over

Na₂SO₄, evaporation of the solvents and purification by column chromatography on silica gel or further preparative HPLC using *n*-hexane/EtOAc yielded the product **91**.

General Procedure C for the Cobalt-Catalyzed C–H Alkynylation: To a solution of **23** (0.25 mmol, 1.00 equiv), [Cp*CoI₂]₂ (**82**) (6.25 μmol, 2.5 mol %), AgSbF₆ (25.0 μmol, 10 mol %) and K₂CO₃ (0.50 mmol, 2.00 equiv) in TFE (1.5 mL) **132** (0.30 mmol, 1.20 equiv) was added. The mixture was stirred for 18 h at 25 °C. After completion of the reaction saturated aq. NH₄Cl solution (5 mL) was added and the mixture was extracted with CH₂Cl₂ (4 × 5 mL). Drying over Na₂SO₄, evaporation of the solvents and purification by column chromatography on silica gel using *n*-pentane/EtOAc yielded the product **89**.

General Procedure D for the Manganese-Catalyzed C–H Alkynylation using Silylalkynes: To a solution of substrates **23** (0.50 mmol, 1.00 equiv), MnBr(CO)₅ (**169**) (6.9 mg, 5.0 mol %) and Cy₂NH (181 mg, 1.00 mmol, 2.00 equiv) in DCE (1.0 mL), silyl bromoalkynes **132** (0.60 mmol, 1.20 equiv) was added. The mixture was stirred at 80 °C for 16 h. After completion of the reaction, CH₂Cl₂ (3.0 mL) was added at ambient temperature and the volatiles were removed in *vacuo*. Purification by chromatography on silica gel afforded the desired product **89**.

General Procedure E for the Manganese-Catalyzed C–H Alkynylation: To a solution of substrates **23** (0.50 mmol, 1.00 equiv), MnBr(CO)₅ (**169**) (6.9 mg, 5.0 mol %), Cy₂NH (181 mg, 1.00 mmol, 2.00 equiv) and BPh₃ (25 μL, 0.05 mol %, 0.01 M stock solution in DCE) in DCE (1 mL), aryl or alkyl bromoalkynes **132** (0.60 mmol, 1.20 equiv) was added. The mixture was stirred at 80 °C for 16 h. After completion of the reaction, CH₂Cl₂ (3 mL) was added at ambient temperature and the volatiles were removed in *vacuo*. Purification by chromatography on silica gel afforded the desired product **89**.

General Procedure F for Electrochemical C–H Alkoxylation: The electrolysis was carried out in an H-type divided cell (P4 sintered glass membrane), with a RVC anode (10 mm × 15 mm × 6 mm) and a platinum cathode (10 mm × 15 mm × 0.25 mm). NaOPiv (122 mg, 1.00 mmol, 2.00 equiv) was added in the cathodic chamber and dissolved in alcohol **149** (7.0 mL). The anodic chamber was charged with Co(OAc)₂·4H₂O (25.7 mg, 0.10 mmol, 20 mol %), NaOPiv (122 mg, 1.00 mmol, 2.00 equiv) and benzamide **117** (0.50 mmol, 1.00 equiv) and dissolved in alcohol **149** (7.0 mL). Electrolysis was started at ambient temperature with a constant current of

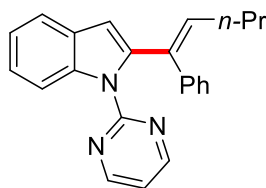
8.0 mA maintained for 6 h. Evaporation of the solvent and subsequent column chromatography on silica gel (CH₂Cl₂/acetone) yielded the desired product **150**.

General Procedure G for Electrochemical C–H Alkoxylation: The electrolysis was carried out in an undivided cell, with a RVC anode (10 mm × 15 mm × 6 mm) and a platinum cathode (10 mm × 15 mm × 0.25 mm). A mixture of NaOPiv (63.9 mg, 0.50 mmol, 2.00 equiv), Co(OAc)₂·4H₂O (12.7 mg, 0.05 mmol, 20 mol %), benzamide **117** (0.25 mmol, 1.00 equiv), *n*-Bu₄NPF₆ (387 mg, 1.00 mmol, 4.00 equiv.) and alcohol **149** (2.3 mL) in MeCN (0.9 mL) was added to the electrochemical cell. Electrolysis was started at ambient temperature with a constant current of 2.0 mA maintained for 12 h. Evaporation of the solvent and subsequent column chromatography on silica gel (CH₂Cl₂/acetone) yielded the desired product **150**.

General Procedure H for the Electrochemical C–H Amination: The electrolysis was carried out in an undivided cell, with a RVC anode (10 mm × 15 mm × 6 mm) and a platinum cathode (10 mm × 15 mm × 0.25 mm). Co(OAc)₂·4H₂O (12.7 mg, 0.05 mmol, 10 mol %), KOAc (149 mg, 1.50 mmol, 3.00 equiv) and benzamide **117** (0.50 mmol, 1.00 equiv) were dissolved in GVL (2.0 mL) and then the amine **146** (1.00 mmol, 2.00 equiv) was added. After heating to 40 °C, electrolysis was started with a constant current of 2.5 mA which was then maintained for 24 h. After 24 h, the mixture was transferred to a flask and the electrodes were rinsed with acetone (3 × 5.0 mL). Then the combined solvent was removed under reduced pressure, the residue diluted with EtOAc (10 mL) and washed with NaOH_(aq) (2 M, 10 mL) and H₂O (2 × 10 mL). Drying over Na₂SO₄ and evaporation of the solvent and subsequent column chromatography on silica gel (CH₂Cl₂/acetone) yielded the desired product **148**.

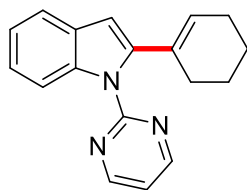
5.3 Cobalt-Catalyzed C–H Alkenylation under Triazole Assistance

5.3.1 Analytical Data and Experimental Procedures



(*E*)-2-(1-Phenylpent-1-en-1-yl)-1-(pyrimidin-2-yl)-1*H*-indole (**44aa**)

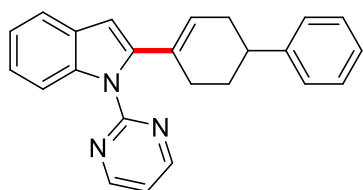
The general procedure **A** was followed using indole **23a** (49.7 mg, 0.25 mmol, 1.00 equiv) and enol acetate **40a** (78.5 mg, 0.38 mmol, 1.50 equiv, *E/Z* = 24/76). Purification by column chromatography on silica gel (*n*-pentane/EtOAc 25:1) yielded **44aa** (44.7 mg, 129 μ mol, 52%) as a yellow oil. $^1\text{H-NMR}$ (300 MHz, CDCl_3): δ = 8.55 (d, J = 5.0 Hz, 2H), 8.03–7.99 (m, 1H), 7.61–7.57 (m, 1H), 7.23–7.18 (m, 2H), 7.11–7.01 (m, 5H), 6.88 (t, J = 5.0 Hz, 1H), 6.72 (s, 1H), 6.15 (t, J = 7.0 Hz, 1H), 2.29 (dt, J = 7.0, 5.5 Hz, 2H), 1.49 (tq, J = 6.2, 5.5 Hz, 2H), 0.90 (t, J = 6.2 Hz, 3H). $^{13}\text{C-NMR}$ (125 MHz, CDCl_3): δ = 157.9 (CH), 157.6 (C_q), 142.8 (C_q), 138.8 (C_q), 137.7 (C_q), 134.5 (C_q), 132.3 (CH), 129.8 (CH), 129.0 (C_q), 127.4 (CH), 126.6 (CH), 123.3 (CH), 121.9 (CH), 120.4 (CH), 117.0 (CH), 113.0 (CH), 108.8 (CH), 31.5 (CH_2), 23.4 (CH_2), 14.1 (CH_3). IR (ATR): 2949, 2870, 1570, 1423, 1319, 1258, 1073, 852, 734 cm^{-1} . MS (ESI) m/z (relative intensity): 362 (27) $[\text{M}+\text{Na}]^+$, 340 (100) $[\text{M}+\text{H}]^+$, 297 (30), 257 (7), 117 (42). HR-MS (ESI) m/z calcd for $\text{C}_{23}\text{H}_{21}\text{N}_3$ $[\text{M}+\text{H}]^+$: 340.1808, found: 340.1818. The analytical data correspond with those reported in literature.^[56]



2-(Cyclohex-1-en-1-yl)-1-(pyrimidin-2-yl)-1*H*-indole (**44ab**)

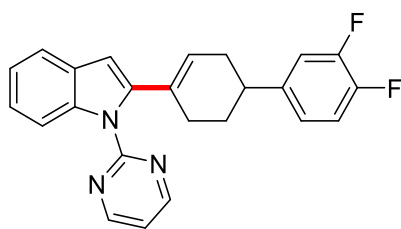
The general procedure **A** was followed using indole **23a** (49.5 mg, 0.25 mmol, 1.00 equiv) and enol acetate **40b** (62.1 mg, 0.38 mmol, 1.50 equiv). Purification by column chromatography on silica gel (*n*-pentane/EtOAc 20:1) yielded **44ab** (56.3 mg, 204 μ mol, 80%) as a yellow oil. Alternative preparations under otherwise identical conditions using enol phosphate **41b** (88.7 mg, 0.38 mmol, 1.50 equiv) yielded **44ab** (58.1 mg, 211 μ mol, 84%), using enol carbonate **42b** (64.7 mg, 0.38 mmol, 1.50 equiv)

yielded **44ab** (36.7 mg, 129 μmol , 52%), using enol carbamate **43b** (64.4 mg, 0.38 mmol, 1.50 equiv) yielded **44ab** (52.0 mg, 188 μmol , 75%). $^1\text{H-NMR}$ (300 MHz, CDCl_3): δ = 8.68 (d, J = 4.1 Hz, 2H), 8.18–8.15 (m, 1H), 7.59–7.56 (m, 1H), 7.27–7.18 (m, 2H), 7.11 (t, J = 4.1 Hz, 1H), 6.55 (s, 1H), 5.88 (m, 1H), 2.20–2.17 (m, 2H), 2.09–2.05 (m, 2H), 1.68–1.64 (m, 4H). $^{13}\text{C-NMR}$ (125 MHz, CDCl_3): δ = 158.4 (C_q), 158.2 (CH), 143.0 (C_q), 137.3 (C_q), 132.0 (C_q), 129.1 (C_q), 126.9 (CH), 122.7 (CH), 121.8 (CH), 120.0 (CH), 117.5 (CH), 112.8 (CH), 106.0 (CH), 28.8 (CH_2), 25.4 (CH_2), 22.7 (CH_2), 22.3 (CH_2). IR (ATR): 2931, 1555, 1450, 1344, 1322, 794, 739, 718, 619 cm^{-1} . MS (ESI) m/z (relative intensity): 298 (40) $[\text{M}+\text{Na}]^+$, 276 (100) $[\text{M}+\text{H}]^+$, 247 (22), 219 (8). HR-MS (ESI) m/z calcd for $\text{C}_{18}\text{H}_{17}\text{N}_3$ $[\text{M}+\text{H}]^+$: 276.1501, found: 276.1497. The analytical data correspond with those reported in literature.^[56]



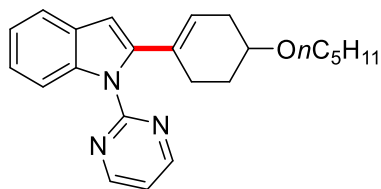
1-(Pyrimidin-2-yl)-2-(1,2,3,6-tetrahydro-[1,1'-biphenyl]-4-yl)-1H-indole (**44ac**)

The general procedure **A** was followed using indole **23a** (49.5 mg, 0.25 mmol, 1.00 equiv) and enol phosphate **41c** (106 mg, 0.38 mmol, 1.50 equiv). Purification by column chromatography on silica gel (*n*-pentane/EtOAc 13:1) yielded **44ac** (71.3 mg, 202 μmol , 81%) as a yellow solid. An alternative procedure using enol acetate **40c** (82.1 mg, 0.38 mmol, 1.50 equiv) yielded **44ac** (68.9 mg, 194 μmol , 78%) as a yellow oil. M. p. = 140–143 $^{\circ}\text{C}$. $^1\text{H-NMR}$ (300 MHz, CDCl_3): δ = 8.78 (d, J = 4.8 Hz, 2H), 8.17 (m, 1H), 7.60 (m, 1H), 7.34–7.20 (m, 6H), 7.13 (t, J = 4.8 Hz, 1H), 6.62 (s, 1H), 5.97–5.96 (m, 1H), 2.97–2.89 (m, 1H), 2.50–2.42 (m, 1H), 2.37–2.27 (m, 2H), 2.20–2.15 (m, 1H), 2.00–1.78 (m, 2H). $^{13}\text{C-NMR}$ (125 MHz, CDCl_3): δ = 158.3 (C_q), 158.1 (CH), 146.7 (C_q), 142.7 (C_q), 137.4 (C_q), 131.7 (C_q), 129.2 (C_q), 128.3 (CH), 126.8 (CH), 126.4 (CH), 126.0 (CH), 123.0 (CH), 121.9 (CH), 120.2 (CH), 117.2 (CH), 113.1 (CH), 106.4 (CH), 39.8 (CH), 33.8 (CH_2), 29.9 (CH_2), 29.4 (CH_2). IR (ATR): 2918, 2845, 2005, 1563, 1424, 1350, 1070 cm^{-1} . MS (ESI) m/z (relative intensity): 374 (40) $[\text{M}+\text{Na}]^+$, 352 (100) $[\text{M}+\text{H}]^+$, 323 (8), 309 (73), 269 (5), 231 (9). HR-MS (ESI) m/z calcd for $\text{C}_{24}\text{H}_{21}\text{N}_3$ $[\text{M}+\text{H}]^+$: 352.1808, found: 352.1805. The analytical data correspond with those reported in literature.^[56]



2-(3',4'-Difluoro-1,2,3,6-tetrahydro-[1,1'-biphenyl]-4-yl)-1-(pyrimidin-2-yl)-1H-indole (44ad)

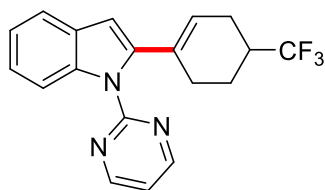
The general procedure **A** was followed using indole **23a** (49.7 mg, 0.25 mmol, 1.00 equiv) and enol phosphate **41d** (131 mg, 0.38 mmol, 1.50 equiv). Purification by column chromatography on silica gel (*n*-pentane/EtOAc 14:1) yielded **44ad** (67.2 mg, 171 μ mol, 69%) as a yellow oil. $^1\text{H-NMR}$ (300 MHz, CDCl_3): δ = 8.80 (d, J = 5.0 Hz, 2H), 8.21 (d, J = 8.1 Hz, 1H), 7.56 (d, J = 8.1 Hz, 1H), 7.27–7.20 (m, 2H), 4.12 (t, J = 5.0 Hz, 1H), 7.12–7.08 (m, 2H), 6.97–6.94 (m, 1H), 6.60 (s, 1H), 5.94–5.92 (m, 1H), 2.89–2.84 (m, 1H), 2.50–2.46 (m, 1H), 2.30–2.14 (m, 3H), 1.97–1.92 (m, 1H), 1.82–1.77 (m, 1H). $^{13}\text{C-NMR}$ (101 MHz, CDCl_3): δ = 158.3 (C_q), 158.2 (CH), 150.2 (dd, $^1J_{\text{C-F}}$ = 194 Hz, $^2J_{\text{C-F}}$ = 21.9 Hz, C_q), 148.4 (dd, $^1J_{\text{C-F}}$ = 194 Hz, $^2J_{\text{C-F}}$ = 21.9 Hz, C_q), 143.9 (dd, $^3J_{\text{C-F}}$ = 6.2 Hz, $^4J_{\text{C-F}}$ = 3.8 Hz, CH), 142.4 (C_q), 137.6 (C_q), 132.0 (C_q), 129.2 (C_q), 125.7 (CH), 123.2 (CH), 122.7 (dd, $^3J_{\text{C-F}}$ = 7.1 Hz, $^4J_{\text{C-F}}$ = 3.9 Hz, C_q), 121.8 (CH), 120.2 (CH), 117.4 (CH), 117.0 (d, $^2J_{\text{C-F}}$ = 21.0 Hz, CH), 115.7 (d, $^2J_{\text{C-F}}$ = 20.8 Hz, CH), 113.2 (CH), 106.6 (CH), 38.7 (CH), 33.5 (CH_2), 29.8 (CH_2), 28.9 (CH_2). $^{19}\text{F-NMR}$ (282 MHz, CDCl_3): δ -138.7, -142.5. IR (ATR): 2958, 1685, 1423, 1273, 1162, 965, 785 cm^{-1} . MS (ESI) m/z (relative intensity): 410 (8) $[\text{M}+\text{Na}]^+$, 388 (61) $[\text{M}+\text{H}]^+$, 345 (15), 185 (5). HR-MS (ESI) m/z calcd for $\text{C}_{24}\text{H}_{19}\text{F}_2\text{N}_3$ $[\text{M}+\text{Na}]^+$: 410.1439, found: 410.1449. The analytical data correspond with those reported in literature.^[56]



2-[4-(*n*-Pentyloxy)cyclohex-1-en-1-yl]-1-(pyrimidin-2-yl)-1H-indole (44ae)

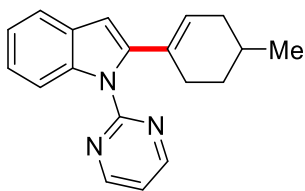
The general procedure **A** was followed using indole **23a** (49.9 mg, 0.25 mmol, 1.00 equiv) and enol phosphate **41e** (93.2 mg, 0.38 mmol, 1.50 equiv). Purification by column chromatography on silica gel (*n*-pentane/EtOAc 10:1) yielded **44ae** (73.9 mg, 201 μ mol, 80%) as a yellow oil. An alternative procedure using enol acetate **40e**

(87.1 mg, 0.38 mmol, 1.50 equiv) yielded **44ae** (69.3 mg, 189 μ mol, 75%) as a yellow oil. $^1\text{H-NMR}$ (300 MHz, CDCl_3): δ = 8.75 (d, J = 5.3 Hz, 2H), 8.20 (m, 1H), 7.56 (m, 1H), 7.22–7.19 (m, 2H), 7.13 (t, J = 5.3 Hz, 1H), 6.56 (s, 1H), 5.78–5.76 (m, 1H), 3.60–3.57 (m, 1H), 3.51–3.47 (m, 2H), 2.57–2.52 (m, 1H), 2.23–2.09 (m, 3H), 1.98–1.93 (m, 1H), 1.74–1.67 (m, 1H), 1.58–1.55 (m, 2H), 1.30–1.28 (m, 4H), 0.88 (t, J = 6.6 Hz, 3H). $^{13}\text{C-NMR}$ (125 MHz, CDCl_3): δ = 158.2 (C_q), 158.0 (CH), 142.3 (C_q), 137.3 (C_q), 131.7 (C_q), 129.2 (C_q), 124.3 (CH), 123.1 (CH), 121.9 (CH), 120.2 (CH), 117.8 (CH), 113.2 (CH), 106.5 (CH), 73.9 (CH), 68.3 (CH_2), 32.4 (CH_2), 29.9 (CH_2), 28.5 (CH_2), 28.4 (CH_2), 28.0 (CH_2), 22.6 (CH_2), 14.1 (CH_3). IR (ATR): 2934, 2852, 1558, 1449, 1340, 822, 746 cm^{-1} . MS (ESI) m/z (relative intensity): 384 (62) $[\text{M}+\text{Na}]^+$, 362 (100) $[\text{M}+\text{H}]^+$, 274 (13). HR-MS (ESI) m/z calcd for $\text{C}_{23}\text{H}_{27}\text{N}_3\text{O}$ $[\text{M}+\text{H}]^+$: 362.2227, found: 362.2226. The analytical data correspond with those reported in literature.^[56]



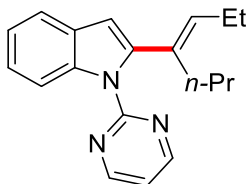
1-(Pyrimidin-2-yl)-2-[4-(trifluoromethyl)cyclohex-1-en-1-yl]-1H-indole (**44af**)

The general procedure **A** was followed using indole **23a** (49.8 mg, 0.25 mmol, 1.00 equiv) and enol phosphate **41f** (83.7 mg, 0.38 mmol, 1.50 equiv). Purification by column chromatography on silica gel (*n*-pentane/EtOAc 15:1) yielded **44af** (63.1 mg, 185 μ mol, 74%) as a colorless oil. $^1\text{H-NMR}$ (300 MHz, CDCl_3) δ = 8.78 (d, J = 4.8 Hz, 2H), 8.20 (dd, J = 7.9, 1.2 Hz, 1H), 7.54 (dd, J = 7.9, 1.2 Hz, 1H), 7.31–7.22 (m, 2H), 7.18 (td, J = 7.2, 1.5 Hz, 1H), 7.15 (t, J = 4.8 Hz, 1H), 6.58 (s, 1H), 5.82–5.81 (m, 1H), 2.44–2.33 (m, 2H), 2.29–2.20 (m, 3H), 2.07–2.03 (m, 1H), 1.67–1.60 (m, 1H). $^{13}\text{C-NMR}$ (125 MHz, CDCl_3): δ = 158.3 (C_q), 158.2 (CH), 141.8 (C_q), 137.3 (C_q), 132.1 (C_q), 129.4 (C_q), 129.1 (q, $^1J_{\text{C-F}}$ = 278 Hz, C_q), 123.1 (CH), 123.4 (CH), 122.0 (CH), 120.3 (CH), 117.2 (CH), 113.4 (CH), 106.9 (CH), 38.3 (q, $^2J_{\text{C-F}}$ = 30.5 Hz, CH), 28.3 (CH_2), 24.6 (q, $^3J_{\text{C-F}}$ = 2.6 Hz, CH_2), 21.8 (q, $^3J_{\text{C-F}}$ = 2.6 Hz, CH_2). $^{19}\text{F-NMR}$ (282 MHz, CDCl_3): δ = –74.07. IR (ATR): 2931, 1565, 1418, 1353, 1269, 1162, 824, 741 cm^{-1} . MS (ESI) m/z (relative intensity): 344 (52) $[\text{M}+\text{H}]^+$, 321 (100), 258 (23), 155 (19). HR-MS (ESI) m/z calcd for $\text{C}_{19}\text{H}_{16}\text{F}_3\text{N}_3$ $[\text{M}+\text{H}]^+$: 344.1369, found: 344.1367. The analytical data correspond with those reported in literature.^[56]



2-(4-Methylcyclohex-1-en-1-yl)-1-(pyrimidin-2-yl)-1H-indole (44ag)

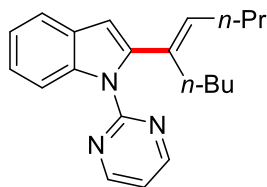
The general procedure **A** was followed using indole **23a** (49.7 mg, 0.25 mmol, 1.00 equiv) and enol phosphate **41g** (85.7 mg, 0.38 mmol, 1.50 equiv). Purification by column chromatography on silica gel (*n*-pentane/EtOAc 20:1) yielded **44ag** (52.1 mg, 177 μ mol, 71%) as a colorless oil. $^1\text{H-NMR}$ (300 MHz, CDCl_3) δ = 8.78 (d, J = 4.7 Hz, 2H), 8.13 (dd, J = 7.4, 1.2 Hz, 1H), 7.56 (dd, J = 7.4, 1.2 Hz, 1H), 7.22–7.08 (m, 3H), 6.53 (s, 1H), 5.83–5.81 (m, 1H), 2.29–2.06 (m, 3H), 1.83–1.64 (m, 3H), 1.36–1.29 (m, 1H), 0.99 (d, J = 8.1 Hz, 3H). $^{13}\text{C-NMR}$ (125 MHz, CDCl_3): δ = 158.3 (C_q), 158.0 (CH), 141.8 (C_q), 137.3 (C_q), 131.3 (C_q), 129.2 (C_q), 126.5 (CH), 122.9 (CH), 121.8 (CH), 120.1 (CH), 117.8 (CH), 112.9 (CH), 106.0 (CH), 34.2 (CH_2), 30.4 (CH_2), 28.8 (CH_2), 28.0 (CH), 21.8 (CH_3). IR (ATR): 2929, 1568, 1443, 1352, 1158, 822, 806, 738 cm^{-1} . MS (ESI) m/z (relative intensity): 312 (25) $[\text{M}+\text{Na}]^+$, 290 (100) $[\text{M}+\text{H}]^+$, 270 (18), 198 (15), 129 (19). HR-MS (ESI) m/z calcd for $\text{C}_{19}\text{H}_{19}\text{N}_3$ $[\text{M}+\text{H}]^+$: 290.1652, found: 290.1648.



(E)-2-(Hept-3-en-4-yl)-1-(pyrimidin-2-yl)-1H-indole (44ah)

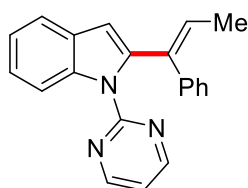
The general procedure **A** was followed using indole **23a** (49.2 mg, 0.25 mmol, 1.00 equiv) and enol phosphate **41h** (98.1 mg, 0.38 mmol, 1.50 equiv, E/Z = 30/70). Purification by column chromatography on silica gel (*n*-pentane/EtOAc 25:1) yielded **44ah** (54.4 mg, 183 μ mol, 73%) as a colorless oil. $^1\text{H-NMR}$ (300 MHz, CDCl_3): δ = 8.78 (d, J = 5.8 Hz, 2H), 8.12 (d, J = 8.0 Hz, 1H), 7.60 (m, 1H), 7.21–7.17 (m, 2H), 7.13 (t, J = 5.8 Hz, 1H), 6.58 (s, 1H), 5.58 (t, J = 6.9 Hz, 1H), 2.19–2.13 (m, 4H), 1.38 (dq, J = 6.9, 6.8 Hz, 2H), 0.96 (t, J = 6.9 Hz, 3H), 0.87 (t, J = 6.8 Hz, 3H). $^{13}\text{C-NMR}$ (101 MHz, CDCl_3): δ = 158.4 (C_q), 158.1 (CH), 143.3 (C_q), 137.4 (C_q), 133.1 (C_q), 132.6 (CH), 129.3 (C_q), 122.8 (CH), 121.7 (CH), 120.0 (CH), 117.2 (CH), 113.0 (CH), 106.9 (CH), 33.0 (CH_2), 21.8 (CH_2), 21.5 (CH_2), 14.1 (CH_3), 14.0 (CH_3). IR (ATR): 2950, 1558,

1453, 1419, 1247, 822, 745 cm^{-1} . MS (ESI) m/z (relative intensity): 314 (27) $[\text{M}+\text{Na}]^+$, 292 (100) $[\text{M}+\text{H}]^+$, 117 (8). HR-MS (ESI) m/z calcd for $\text{C}_{19}\text{H}_{21}\text{N}_3$ $[\text{M}+\text{H}]^+$: 292.1808, found: 292.1816. The analytical data correspond with those reported in literature.^[56]



(E)-2-(Non-4-en-5-yl)-1-(pyrimidin-2-yl)-1H-indole (44ai)

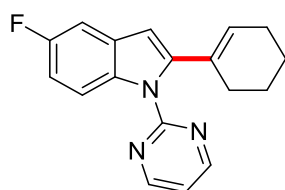
The general procedure **A** was followed using indole **23a** (49.8 mg, 0.25 mmol, 1.00 equiv) and enol phosphate **41i** (103 mg, 0.38 mmol, 1.50 equiv, $E/Z = 30/70$). Purification by column chromatography on silica gel (n -pentane/EtOAc 20:1) yielded **44a** (55.6 mg, 172 μmol , 69%) as a colorless oil. $^1\text{H-NMR}$ (300 MHz, CDCl_3): $\delta = 8.74$ (d, $J = 4.5$ Hz, 2H), 8.13 (m, 1H), 7.58 (m, 1H), 7.23–7.18 (m, 2H), 7.10 (t, $J = 4.5$ Hz, 1H), 6.55 (s, 1H), 5.59 (t, $J = 7.7$ Hz, 1H), 2.20–2.12 (m, 4H), 1.46–1.31 (m, 2H), 1.28–1.17 (m, 4H), 0.89 (t, $J = 7.9$ Hz, 3H), 0.80 (t, $J = 7.4$ Hz, 3H). $^{13}\text{C-NMR}$ (101 MHz, CDCl_3): $\delta = 158.4$ (C_q), 158.1 (CH), 143.3 (C_q), 137.4 (C_q), 134.4 (C_q), 130.7 (CH), 129.3 (C_q), 122.9 (CH), 121.8 (CH), 120.1 (CH), 117.2 (CH), 113.0 (CH), 106.9 (CH), 30.9 (CH_2), 30.8 (CH_2), 30.2 (CH_2), 22.7 (CH_2), 22.6 (CH_2), 13.9 (CH_3), 13.8 (CH_3). IR (ATR): 2927, 1558, 1451, 1342, 1317, 1251, 1161, 797, 732 cm^{-1} . MS (ESI) m/z (relative intensity): 342 (12) $[\text{M}+\text{Na}]^+$, 320 (100) $[\text{M}+\text{H}]^+$, 290 (10) 149 (9), 117 (60). HR-MS (ESI) m/z calcd for $\text{C}_{21}\text{H}_{25}\text{N}_3$ $[\text{M}+\text{H}]^+$: 320.2121, found: 320.2129. The analytical data corresponds with those reported in literature.^[56]



(E)-2-(1-Phenylprop-1-en-1-yl)-1-(pyrimidin-2-yl)-1H-indole (44aj)

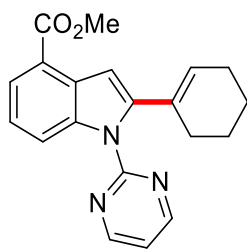
The general procedure **A** was followed using indole **23a** (49.8 mg, 0.25 mmol, 1.00 equiv) and enol phosphate **41j** (94.2 mg, 0.38 mmol, 1.50 equiv, $E/Z = 25/75$). Purification by column chromatography on silica gel (n -pentane/EtOAc 20:1) yielded **44aj** (44.6 mg, 139 μmol , 55%) as a yellow oil. $^1\text{H-NMR}$ (300 MHz, CDCl_3): $\delta = 8.53$ (d, $J = 4.7$ Hz, 2H), 8.02 (d, $J = 8.0$ Hz, 1H), 7.65 (d, $J = 8.0$ Hz, 1H), 7.27–7.21 (m,

2H), 7.10–7.05 (m, 4H), 6.99–6.96 (m, 1H), 6.84 (t, $J = 4.7$ Hz, 1H), 6.72 (s, 1H), 6.33 (q, $J = 10.4$ Hz, 1H), 1.98 (d, $J = 10.4$ Hz, 3H). ^{13}C -NMR (101 MHz, CDCl_3): $\delta = 157.8$ (CH), 157.4 (C_q), 142.6 (C_q), 138.3 (C_q), 137.3 (C_q), 135.5 (C_q), 129.8 (CH), 128.9 (C_q), 127.3 (CH), 126.5 (CH), 126.1 (CH), 123.3 (CH), 121.8 (CH), 120.4 (CH), 116.8 (CH), 112.9 (CH), 108.8 (CH), 15.4 (CH_3). IR (ATR): 2937, 2035, 1568, 1447, 1252, 1082, 824, 793 cm^{-1} . MS (ESI) m/z (relative intensity): 334 (24) $[\text{M}+\text{Na}]^+$, 312 (100) $[\text{M}+\text{H}]^+$, 299 (13). HR-MS (ESI) m/z calcd for $\text{C}_{21}\text{H}_{17}\text{N}_3$ $[\text{M}+\text{H}]^+$: 312.1495, found: 312.1491. The analytical data corresponds with those reported in literature.^[56]



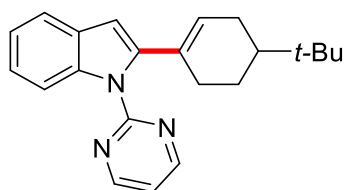
2-(Cyclohex-1-en-1-yl)-5-fluoro-1-(pyrimidin-2-yl)-1H-indole (44bb)

The general procedure **A** was followed using indole **23b** (53.2 mg, 0.25 mmol, 1.00 equiv) and enol phosphate **41b** (89 mg, 0.38 mmol, 1.50 equiv). Purification by column chromatography on silica gel (*n*-pentane/EtOAc 15:1) yielded **44bb** (45.2 mg, 153 μmol , 61%) as a pale yellow solid. An alternative procedure using enol acetate **40b** (62.1 mg, 0.38 mmol, 1.5 equiv) yielded **44bb** (51.8 mg, 175 μmol , 70%) as a yellow solid. M. p. = 140–142 $^\circ\text{C}$. ^1H -NMR (300 MHz, CDCl_3) $\delta = 8.72$ (d, $J = 4.8$ Hz, 2H), 8.10 (dd, $J = 8.7, 4.2$ Hz, 1H), 7.17 (dd, $J = 8.7, 2.8$ Hz, 1H), 7.15 (t, $J = 4.8$ Hz, 1H), 6.91 (td, $J = 8.7, 2.8$ Hz, 1H), 6.50 (s, 1H), 5.86–5.83 (m, 1H), 2.17–2.14 (m, 2H), 2.08–2.05 (m, 2H), 1.67–1.62 (m, 4H). ^{13}C -NMR (101 MHz, CDCl_3): $\delta = 159.0$ (d, $^1J_{\text{CF}} = 244$ Hz, C_q), 158.2 (CH), 145.0 (C_q), 133.8 (C_q), 131.8 (C_q), 131.1 (C_q), 130.9 (d, $^3J_{\text{CF}} = 10.8$ Hz, C_q), 127.5 (CH), 117.4 (CH), 114.0 (d, $^3J_{\text{CF}} = 9.9$ Hz, CH), 110.7 (d, $^2J_{\text{CF}} = 27.0$ Hz, CH), 106.1 (CH), 105.4 (d, $^2J_{\text{CF}} = 23.8$ Hz, CH), 29.0 (CH_2), 25.8 (CH_2), 23.6 (CH_2), 22.0 (CH_2). ^{19}F -NMR (282 MHz, CDCl_3): $\delta = -122.52$. IR (ATR): 2931, 1568, 1420, 1270, 1214, 806, 771 cm^{-1} . MS (ESI) m/z (relative intensity): 316 (22) $[\text{M}+\text{Na}]^+$, 294 (100) $[\text{M}+\text{H}]^+$, 261 (34), 221 (8), 125 (5). HR-MS (ESI) m/z calcd for $\text{C}_{18}\text{H}_{16}\text{FN}_3$ $[\text{M}+\text{H}]^+$: 294.1401, found: 294.1404. The analytical data correspond with those reported in literature.^[56]



Methyl-2-(cyclohex-1-en-1-yl)-1-(pyrimidin-2-yl)-1H-indole-4-carboxylate (**44cb**)

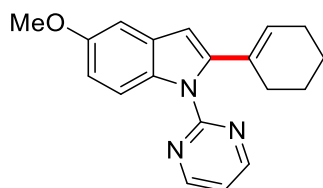
The general procedure **A** was followed using indole **23c** (66.1 mg, 0.24 mmol, 1.00 equiv) and enol phosphate **41b** (91.2 mg, 0.38 mmol, 1.50 equiv). Purification by column chromatography on silica gel (*n*-pentane/EtOAc 7:1) yielded **44cb** (55.1 mg, 163 μ mol, 65%) as a pale yellow oil. An alternative procedure using enol acetate **40b** (62.3 mg, 0.38 mmol, 1.5 equiv) yielded **44cb** (51.9 mg, 153 μ mol, 61%) as a yellow oil. $^1\text{H-NMR}$ (300 MHz, CDCl_3) δ = 8.83 (d, J = 5.4 Hz, 2H), 8.23 (d, J = 8.3 Hz, 1H), 7.89 (d, J = 8.3 Hz, 1H), 7.27–7.16 (m, 3H), 5.92–5.88 (m, 1H), 3.98 (s, 3H), 2.14–2.12 (m, 2H), 2.05–2.04 (m, 2H), 1.64–1.61 (m, 4H). $^{13}\text{C-NMR}$ (125 MHz CDCl_3): δ = 167.9 (C_q), 158.3 (C_q), 158.1 (CH), 145.4 (C_q), 138.1 (C_q), 131.6 (C_q), 129.2 (C_q), 128.2 (CH), 124.9 (CH), 122.2 (CH), 121.2 (C_q), 117.8 (CH), 117.5 (CH), 106.7 (CH), 51.8 (CH_3), 28.9 (CH_2), 25.7 (CH_2), 22.8 (CH_2), 21.9 (CH_2). IR (ATR): 2931, 1714, 1444, 1341, 1304, 1153, 821, 727 cm^{-1} . MS (ESI) m/z (relative intensity) 356 (67) $[\text{M}+\text{Na}]^+$, 334 (100) $[\text{M}+\text{H}]^+$, 316 (11), 302 (14). HR-MS (ESI) m/z calcd for $\text{C}_{20}\text{H}_{19}\text{N}_3\text{O}_2$ $[\text{M}+\text{H}]^+$: 334.1550, found: 334,1551.



2-[4-(*tert*-Butyl)cyclohex-1-en-1-yl]-1-(pyrimidin-2-yl)-1H-indole (**44ak**):

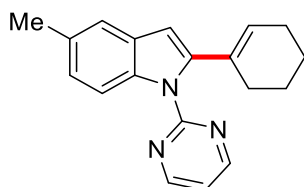
The general procedure **A** was followed using indole **23a** (49.5 mg, 0.25 mmol, 1.00 equiv) and enol acetate **40k** (77.1 mg, 0.38 mmol, 1.50 equiv). Purification by column chromatography on silica gel (*n*-pentane/EtOAc 12:1) yielded **44ak** (57.1 mg, 176 μ mol, 71%) as a colorless oil. $^1\text{H-NMR}$ (300 MHz, CDCl_3) δ = 8.76 (d, J = 5.1 Hz, 2H), 8.15 (dd, J = 8.2, 1.2 Hz, 1H), 7.57 (d, J = 8.2 Hz, 1H), 7.26–7.14 (m, 2H), 7.15 (t, J = 5.1 Hz, 1H), 6.55 (s, 1H), 5.90–5.86 (m, 1H), 2.21–2.09 (m, 3H), 2.00–1.88 (m, 1H), 1.83–1.75 (m, 1H), 1.37 (m, 1H), 1.24 (m, 1H), 0.86 (s, 9H). $^{13}\text{C-NMR}$ (101 MHz,

CDCl₃): δ = 157.4 (C_q), 157.2 (CH), 142.0 (C_q), 136.6 (C_q), 130.5 (C_q), 128.3 (C_q), 126.3 (CH), 121.9 (CH), 120.8 (CH), 119.2 (CH), 116.3 (CH), 111.8 (CH), 105.3 (CH), 42.7 (CH), 31.2 (CH₂), 29.7 (CH₂), 26.4 (CH₂), 26.1 (CH₃), 24.1 (C_q). IR (ATR): 2958, 1561, 1454, 1340, 1262, 1116, 798, 675, 627 cm⁻¹. MS (ESI) *m/z* (relative intensity): 354 (22) [M+Na]⁺, 332 (100) [M+H]⁺, 177 (8), 149 (11). HR-MS (ESI) *m/z* calcd for C₂₂H₂₅N₃ [M+H]⁺: 332.2121, found: 332.2126. The analytical data correspond with those reported in literature.^[56]



2-(Cyclohex-1-en-1-yl)-1-(pyrimidin-2-yl)-5-methoxy-1H-indole (44db)

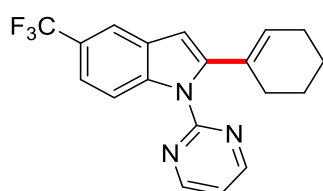
The general procedure **A** was followed using indole **23d** (58.7 mg, 0.25 mmol, 1.00 equiv) and enol acetate **40b** (61.7 mg, 0.38 mmol, 1.50 equiv). Purification by column chromatography on silica gel (*n*-pentane/EtOAc 8:1) yielded **44db** (54.6 mg, 179 μ mol, 72%) as a pale yellow oil. ¹H-NMR (300 MHz, CDCl₃) δ = 8.75 (d, *J* = 4.7 Hz, 2H), 8.09 (d, *J* = 7.9 Hz, 1H), 7.10 (t, *J* = 4.7 Hz, 1H), 7.02 (d, *J* = 1.0 Hz, 1H), 6.84 (dd, *J* = 7.9, 1.0 Hz, 1H), 6.43 (s, 1H), 5.87–5.84 (m, 1H), 3.84 (s, 3H), 2.18–2.13 (m, 2H), 2.07–2.02 (m, 2H), 1.66–1.61 (m, 4H). ¹³C-NMR (125 MHz, CDCl₃): δ = 158.3 (CH), 158.1 (C_q), 155.5 (C_q), 144.1 (C_q), 132.4 (C_q), 132.2 (C_q), 130.1 (C_q), 126.2 (CH), 116.9 (CH), 114.2 (CH), 111.9 (CH), 106.2 (CH), 102.5 (CH), 55.1 (CH₃), 29.1 (CH₂), 25.6 (CH₂), 22.7 (CH₂), 22.1 (CH₂). IR (ATR): 2934, 1557, 1441, 1317, 1157, 1027, 807, 723 cm⁻¹. MS (ESI) *m/z* (relative intensity): 306 (100) [M+H]⁺, 282 (33), 261 (40), 219 (85). HR-MS (ESI) *m/z* calcd for C₁₉H₁₈N₃O [M+H]⁺: 306.1601, found: 306.1601.



2-(Cyclohex-1-en-1-yl)-1-(pyrimidin-2-yl)-5-methyl-1H-indole (44eb)

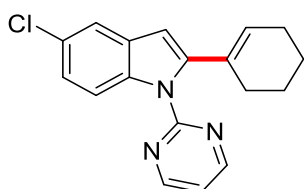
The general procedure **A** was followed using indole **23e** (52.7 mg, 0.25 mmol, 1.00 equiv) and enol acetate **40b** (61.7 mg, 0.38 mmol, 1.50 equiv). Purification by column chromatography on silica gel (*n*-pentane/EtOAc 14:1) yielded **44eb** (58.6 mg,

202 μmol , 80%) as a pale yellow oil. $^1\text{H-NMR}$ (300 MHz, CDCl_3) δ = 8.69 (d, J = 4.7 Hz, 2H), 7.89 (d, J = 7.9 Hz, 1H), 7.32 (d, J = 0.7 Hz, 1H), 7.05 (t, J = 4.7 Hz, 1H), 6.98 (dd, J = 7.9, 0.7 Hz, 1H) 6.43 (s, 1H), 5.83–5.81 (m, 1H), 2.37 (s, 3H), 2.14–2.08 (m, 2H), 2.02–1.95 (m, 2H), 1.66–1.61 (m, 4H). $^{13}\text{C-NMR}$ (101 MHz, CDCl_3): δ = 158.4 (CH), 158.1 (C_q), 143.4 (C_q), 135.8 (C_q), 132.2 (C_q), 131.2 (C_q), 129.7 (C_q), 126.5 (CH), 124.5 (CH), 120.2 (CH), 116.9 (CH), 112.9 (CH), 106.2 (CH), 28.9 (CH_3), 25.6 (CH_2), 22.7 (CH_2), 22.1 (CH_2), 21.2 (CH_2). IR (ATR): 2934, 1552, 1371, 1312, 1256, 1127, 824 cm^{-1} . MS (ESI) m/z (relative intensity): 312 (21) $[\text{M}+\text{Na}]^+$, 290 (100) $[\text{M}+\text{H}]^+$, 263 (5). HR-MS (ESI) m/z calcd for $\text{C}_{19}\text{H}_{19}\text{N}_3$ $[\text{M}+\text{H}]^+$: 290.1652, found: 290.1653.



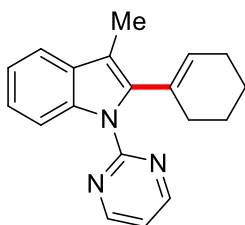
2-(Cyclohex-1-en-1-yl)-1-(pyrimidin-2-yl)-5-(trifluoromethyl)-1H-indole (44fb)

The general procedure **A** was followed using indole **23f** (68.7 mg, 0.25 mmol, 1.00 equiv) and enol acetate **40b** (63.4 mg, 0.38 mmol, 1.50 equiv). Purification by column chromatography on silica gel (*n*-pentane/EtOAc 15:1) yielded **44fb** (64.9 mg, 184 μmol , 74%) as a pale yellow oil. $^1\text{H-NMR}$ (300 MHz, CDCl_3) δ = 8.80 (d, J = 4.7 Hz, 2H), 8.15 (dd, J = 7.3, 0.9 Hz, 1H), 7.85–7.82 (m, 1H), 7.45 (dd, J = 7.3, 1.9 Hz, 1H), 7.21 (t, J = 4.7 Hz, 1H), 6.61 (s, 1H), 5.86–5.84 (m, 1H), 2.17–2.15 (m, 2H), 2.06–2.02 (m, 2H), 1.67–1.61 (m, 4H). $^{13}\text{C-NMR}$ (101 MHz, CDCl_3): δ = 158.4 (CH), 158.0 (C_q), 145.0 (C_q), 138.7 (C_q), 131.3 (C_q), 128.8 (C_q), 128.2 (CH), 125.1 (q, $^1J_{\text{C-F}}$ = 269.1 Hz, C_q), 124.1 (q, $^2J_{\text{C-F}}$ = 31.5 Hz, C_q), 119.7 (q, $^3J_{\text{C-F}}$ = 3.9 Hz, CH) 118.0 (CH), 117.6 (q, $^3J_{\text{C-F}}$ = 3.3 Hz, CH) 113.2 (CH), 105.9 (CH), 29.2 (CH_2), 25.8 (CH_2), 22.7 (CH_2), 21.5 (CH_2). $^{19}\text{F-NMR}$ (282 MHz, CDCl_3): δ = -60.74. IR (ATR): 2933, 1557, 1441, 1333, 1271, 1051, 796 cm^{-1} . MS (ESI) m/z (relative intensity): 344 (100) $[\text{M}+\text{H}]^+$, 321 (11), 306 (15), 261 (10), 219 (13). HR-MS (ESI) m/z calcd for $\text{C}_{19}\text{H}_{16}\text{F}_3\text{N}_3$ $[\text{M}+\text{H}]^+$: 344.1369 found: 344.1366. The analytical data correspond with those reported in literature.^[56]



2-(Cyclohex-1-en-1-yl)-1-(pyrimidin-2-yl)-5-chloro-1H-indole (**44gb**)

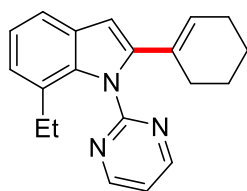
The general procedure **A** was followed using indole **23g** (59.7 mg, 0.25 mmol, 1.00 equiv) and enol acetate **40b** (62.2 mg, 0.38 mmol, 1.50 equiv). Purification by column chromatography on silica gel (*n*-pentane/EtOAc 20:1) yielded **44gb** (45.6 mg, 147 μ mol, 59%) as a pale yellow oil. $^1\text{H-NMR}$ (300 MHz, CDCl_3) δ = 8.76 (d, J = 4.7 Hz, 2H), 8.05 (d, J = 7.7 Hz, 1H), 7.49 (d, J = 0.8 Hz, 1H), 7.17–7.13 (m, 2H), 6.58 (s, 1H), 5.83–5.81 (m, 1H), 2.14–2.08 (m, 2H), 2.08–2.02 (m, 2H), 1.62–1.57 (m, 4H). $^{13}\text{C-NMR}$ (101 MHz, CDCl_3): δ = 158.2 (CH), 158.0 (C_q), 144.7 (C_q), 135.8 (C_q), 131.5 (C_q), 130.5 (C_q), 127.6 (CH), 127.1 (C_q), 123.0 (CH), 119.6 (CH), 117.6 (CH), 114.2 (CH), 106.4 (CH), 28.9 (CH_2), 25.6 (CH_2), 22.8 (CH_2), 21.8 (CH_2). IR (ATR): 2934, 1572, 1423, 1325, 1212, 1047, 802, 736 cm^{-1} . MS (ESI) m/z (relative intensity): 312 (24) $[\text{M}+\text{H}]^+$ (^{37}Cl), 310 (90) $[\text{M}+\text{H}]^+$ (^{35}Cl), 280 (100), 254 (14), 229 (11). HR-MS (ESI) m/z calcd for $\text{C}_{18}\text{H}_{15}\text{N}_3^{37}\text{Cl} [\text{M}]^+$: 309.1027, found: 309.1019.



2-(Cyclohex-1-en-1-yl)-3-methyl-1-(pyrimidin-2-yl)-1H-indole (**44jb**)

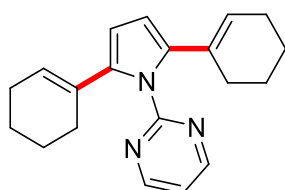
The general procedure **A** was followed using indole **23j** (53.4 mg, 0.25 mmol, 1.00 equiv) and enol acetate **40b** (62.7 mg, 0.38 mmol, 1.50 equiv). Purification by column chromatography on silica gel (*n*-pentane/EtOAc 18:1) yielded **44jb** as a pale yellow solid (62.2 mg, 214 μ mol, 85%). M. p. = 168–170 $^\circ\text{C}$. $^1\text{H-NMR}$ (300 MHz, CDCl_3): δ = 8.74 (d, J = 4.4 Hz, 2H), 8.30 (m, 1H), 7.58–7.52 (m, 1H), 7.24–7.19 (m, 2H), 7.085 (t, J = 4.4 Hz, 1H), 5.80–5.77 (m, 1H), 2.25 (s, 3H), 2.24–2.20 (m, 2H), 2.04–1.99 (m, 2H), 1.69–1.67 (m, 4H). $^{13}\text{C-NMR}$ (125 MHz, CDCl_3): δ = 158.1 (C_q), 157.8 (CH), 138.7 (C_q), 136.6 (C_q), 131.5 (C_q), 130.5 (C_q), 128.5 (CH), 123.2 (CH), 123.1 (CH), 121.6 (CH), 118.2 (CH), 116.2 (CH), 113.3 (C_q), 29.8 (CH_2), 25.6 (CH_2), 23.3 (CH_2), 22.0 (CH_2), 9.6 (CH_3). IR (ATR): 2915, 1561, 1427, 1355, 1271, 1138, 824,

792. cm^{-1} . MS (ESI) m/z (relative intensity): 312 (41) $[\text{M}+\text{Na}]^+$, 290 (100) $[\text{M}+\text{H}]^+$, 263 (9), 247 (19), 159 (11). HR-MS (ESI) m/z calcd for $\text{C}_{19}\text{H}_{19}\text{N}_3$ $[\text{M}+\text{H}]^+$: 290.1652, found: 290.1652. The analytical data correspond with those reported in literature.^[56]



2-(Cyclohex-1-en-1-yl)-7-ethyl-1-(pyrimidin-2-yl)-1H-indole (44kb)

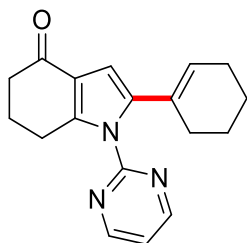
The general procedure **A** was followed using indole **23k** (59.9 mg, 0.25 mmol, 1.00 equiv) and enol acetate **40b** (61.8 mg, 0.38 mmol, 1.50 equiv). Purification by column chromatography on silica gel (*n*-pentane/EtOAc 20:1) yielded **44kb** (56.6 mg, 185 μmol , 74%) as a pale yellow oil. $^1\text{H-NMR}$ (300 MHz, CDCl_3) δ = 8.82 (d, J = 5.1 Hz, 2H), 7.42 (d, J = 7.5 Hz, 1H), 7.29 (dd, J = 7.5, 7.2 Hz, 1H), 7.07 (t, J = 5.1 Hz, 1H), 6.98 (d, J = 7.2 Hz, 1H), 6.53 (s, 1H), 5.63–5.61 (m, 1H), 2.29 (q, J = 6.8 Hz, 2H), 2.14–2.03 (m, 2H), 1.98–1.91 (m, 2H), 1.62–1.46 (m, 4H), 0.89 (t, J = 6.8 Hz, 3H). $^{13}\text{C-NMR}$ (125 MHz, CDCl_3): δ = 160.5 (C_q), 158.0 (CH), 144.2 (C_q), 136.3 (C_q), 129.9 (C_q), 129.5 (C_q), 128.9 (CH), 127.9 (C_q), 123.0 (CH), 121.2 (CH), 119.6 (CH), 118.2 (CH), 103.4 (CH), 28.9 (CH_2), 25.7 (CH_2), 25.2 (CH_2), 22.7 (CH_2), 21.8 (CH_2), 14.4 (CH_3). IR (ATR): 2937, 1558, 1371, 1227, 1162. 1039, 822, 744 cm^{-1} . MS (ESI) m/z (relative intensity): 304 (100) $[\text{M}+\text{H}]^+$, 279 (18), 219 (14), 179 (11). HR-MS (ESI) m/z calcd for $\text{C}_{20}\text{H}_{21}\text{N}_3$ $[\text{M}]^+$: 303.1808, found: 303.1796.



2-[2,5-Bis(cyclohex-1-en-1-yl)-1H-pyrrol-1-yl]pyrimidine (218ab)

The general procedure **A** was followed using pyrrole **217a** (39.3 mg, 0.25 mmol, 1.00 equiv) and enol acetate **40b** (106 mg, 0.75 mmol, 1.50 equiv). Purification by column chromatography on silica gel (*n*-pentane/EtOAc 18:1) yielded **218ab** as a colorless oil (58.0 mg, 186 μmol , 74%). $^1\text{H-NMR}$ (300 MHz, CDCl_3): δ = 8.77 (d, J = 4.6 Hz, 2H), 7.21 (t, 4.6 Hz, 1H), 6.07 (s, 2H), 5.35–5.32 (m, 2H), 1.97–1.90 (m, 8H), 1.55–1.44 (m, 8H). $^{13}\text{C-NMR}$ (125 MHz, CDCl_3): δ = 159.4 (C_q), 158.1 (CH), 137.6

(C_q), 130.6 (C_q), 125.9 (CH), 120.2 (CH), 108.8 (CH), 28.6 (CH₂), 25.5 (CH₂), 22.8 (CH₂), 22.1 (CH₂). IR (ATR): 2927, 1578, 1512, 1327, 1024, 824 cm⁻¹. MS (ESI) *m/z* (relative intensity): 328 (25) [M+Na]⁺ 306 (100) [M+H]⁺, 219 (5), 117 (10). HR-MS (ESI) *m/z* calcd for C₂₀H₂₃N₃ [M+H]⁺: 306.1965, found: 306.1976.

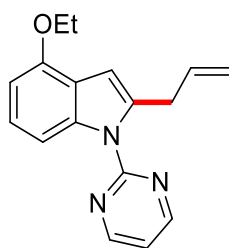


2-(Cyclohex-1-en-1-yl)-1-(pyrimidin-2-yl)-1,5,6,7-tetrahydro-4H-indol-4-one (218cb)

The general procedure **A** was followed using 1-(pyrimidin-2-yl)-1,5,6,7-tetrahydro-4H-indol-4-one (**217c**) (80.3 mg, 0.50 mmol, 1.00 equiv) and enol acetate **40b** (62.9 mg, 0.38 mmol, 1.50 equiv). Purification by column chromatography on silica gel (*n*-pentane/EtOAc 1:2) yielded **218cb** (39.3 mg, 134 μmol, 53%) as a white solid. M. p. = 112-116 °C. ¹H-NMR (300 MHz, CDCl₃): δ = 8.80 (d, *J* = 4.6 Hz, 2H), 7.31 (t, *J* = 4.6 Hz, 1H), 6.49 (s, 1H), 5.48-5.44 (m, 1H), 2.83 (t, *J* = 6.1 Hz, 2H), 2.47 (dd, *J* = 7.2, 5.5 Hz, 2H), 2.11 (tt, *J* = 7.2, 5.5 Hz, 2H), 2.02–1.91 (m, 2H), 1.89–1.81 (m, 2H), 1.59–1.52 (m, 4H). ¹³C-NMR (125 MHz, CDCl₃): δ = 194.3 (C_q), 158.4 (CH), 157.4 (C_q), 145.2 (C_q), 138.3 (C_q), 129.6 (C_q), 126.9 (CH), 121.4 (C_q), 119.3 (CH), 105.3 (CH), 37.9 (CH₂), 28.7 (CH₂), 25.6 (CH₂), 23.8 (CH₂), 23.7 (CH₂), 22.7 (CH₂), 21.9 (CH₂). IR (ATR): 2930, 1658, 1573, 1410, 1218, 1178, 1017, 834, 635 cm⁻¹. MS (ESI) *m/z* (relative intensity): 332 (80) [M+K]⁺, 316 (28) [M+Na]⁺, 294 (100) [M+H]⁺. HR-MS (ESI) *m/z* calcd for C₁₈H₁₉N₃O [M+H]⁺: 294.1606, found: 294.1602. The analytical data correspond with those reported in literature.^[56]

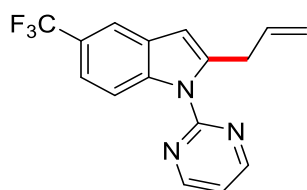
5.4 Cobalt-Catalyzed Allylation of Indoles

5.4.1 Analytical Data and Experimental Procedures



2-Allyl-4-ethoxy-1-(pyrimidin-2-yl)-1H-indole (**91m**)

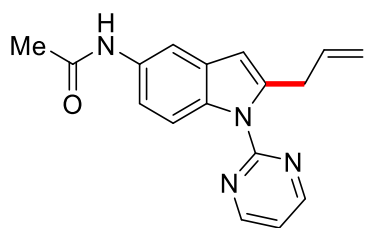
The general procedure **B** was followed using indole **23m** (118 mg, 0.50 mmol, 1.00 equiv) and allyl acetate **213** (106 mg, 1.00 mmol, 2.00 equiv). Purification by column chromatography on silica gel (*n*-hexane/EtOAc 12:1) yielded **91m** (125 mg, 452 μ mol, 89%) as a colourless solid. M. p. = 125–126 °C. $^1\text{H-NMR}$ (300 MHz, CDCl_3) δ = 8.75 (d, J = 4.8 Hz, 2H), 7.82 (d, J = 7.8 Hz, 1H), 7.13–7.09 (m, 2H), 6.62–6.60 (m, 2H), 5.98 (ddt, J = 17.0, 10.3, 6.5 Hz, 1H), 5.01 (ddt, J = 17.0, 1.7 Hz, 1H), 5.00 (ddt, J = 10.3, 1.7 Hz, 1H), 4.16 (q, J = 6.9 Hz, 2H) 3.92 (dd, J = 6.5, 1.2 Hz, 2H), 1.48 (t, J = 6.9 Hz, 3H). $^{13}\text{C-NMR}$ (125 MHz, CDCl_3): δ = 158.3 (C_q), 158.0 (CH), 151.7 (C_q) 138.4 (C_q), 138.0 (C_q) 135.7 (CH), 123.4 (CH), 119.8 (C_q), 117.1 (CH), 116.3 (CH_2), 107.0 (CH), 103.5 (CH), 103.2 (CH), 63.6 (CH_2), 34.0 (CH_2), 15.0 (CH_3). IR (ATR): ν (cm^{-1}) = 2973, 1642, 1425, 1302, 736, 727, 654 cm^{-1} . EI-MS: m/z (relative intensity): 279 (91) $[\text{M}]^+$, 264 (100), 250 (59), 236 (22), 222 (28) 79 (13), 43, (11). HR-MS (ESI): m/z calcd for $\text{C}_{17}\text{H}_{17}\text{N}_3\text{O}$ $[\text{M}]^+$: 279.1372, found: 279.1376.



2-Allyl-5-(trifluoromethyl)-1-(pyrimidin-2-yl)-1H-indole (**91f**)

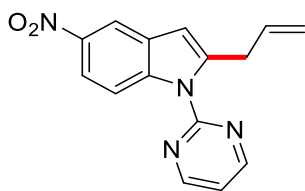
The general procedure **B** was followed using indole **23f** (132 mg, 0.50 mmol, 1.00 equiv) and allyl acetate **213** (107 mg, 1.00 mmol, 2.00 equiv). Purification by HPLC (*n*-hexane/EtOAc 80:20) yielded **91f** (128 mg, 421 μ mol, 84%) as a yellow oil. $^1\text{H-NMR}$ (300 MHz, CDCl_3) δ = 8.80 (d, J = 4.8 Hz, 2H), 8.29 (d, J = 7.9 Hz, 1H), 7.79 (s, 1H), 7.43 (d, J = 7.9, 1H), 7.19 (t, J = 4.8 Hz, 1H), 6.54 (s, 1H), 5.94 (ddt, J = 16.8, 10.2, 6.3 Hz, 1H), 5.04 (ddt, J = 16.8, 1.7, 1.3 Hz, 1H), 5.00 (ddt, J = 10.2, 1.7 Hz,

1H), 3.95 (d, $J = 6.3$ Hz, 2H). $^{13}\text{C-NMR}$ (125 MHz, CDCl_3): $\delta = 158.2$ (CH), 157.8 (C_q), 141.7 (C_q) 138.5 (C_q), 135.0 (CH) 138.7 (C_q), 125.1 (q, $^1J_{\text{CF}} = 271$ Hz, C_q), 124.0 (q, $^2J_{\text{CF}} = 32.2$ Hz, C_q), 119.3 (q, $^3J_{\text{CF}} = 3.8$ Hz, CH), 117.7 (CH), 117.2 (q, $^3J_{\text{CF}} = 3.8$ Hz, CH), 116.8 (CH_2), 114.0 (CH), 106.5 (CH), 33.9 (CH_2). $^{19}\text{F-NMR}$ (282 MHz, CDCl_3): $d = -61.17$. IR (ATR): ν (cm^{-1}) = 2977, 1561, 1426, 1324, 1112, 1058, 805 cm^{-1} . EI-MS: m/z (relative intensity): 303 (26) $[\text{M}]^+$, 288 (100), 275 (9), 219 (11), 154 (8), 79, (6). HR-MS (ESI): m/z calcd for $\text{C}_{16}\text{H}_{12}\text{N}_3\text{F}_3$ $[\text{M}+\text{H}]^+$: 304.1062, found: 304.1056.



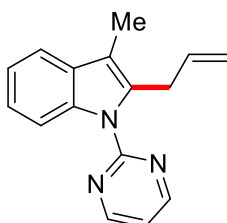
***N*-(2-Allyl-1-(pyrimidin-2-yl)-1*H*-indol-5-yl)acetamide (91i)**

The general procedure **B** was followed using indole **23i** (42.3 mg, 0.17 mmol, 1.00 equiv) and allyl acetate **213** (34.0 mg, 0.34 mmol, 2.00 equiv). Purification by column chromatography on silica gel (*n*-hexane/EtOAc 12:1) yielded **91i** (38.7 mg, 132 μmol , 78%) as a yellow oil. $^1\text{H-NMR}$ (300 MHz, CDCl_3) $\delta = 8.73$ (d, $J = 5.7$ Hz, 2H), 8.19 (d, $J = 7.2$ Hz, 1H), 7.79 (d, $J = 1.3$ Hz, 1H), 7.39 (s, 1H), 7.15 (dd, $J = 8.9$, 2.2 Hz, 1H), 7.09 (t, $J = 5.7$ Hz, 1H), 6.44 (s, 1H), 5.95 (ddt, $J = 17.9$, 10.4, 5.5 Hz, 1H), 5.03 (ddt, $J = 17.9$, 1.4 Hz, 1H), 5.00 (ddt, $J = 10.4$, 1.4 Hz, 1H), 3.93 (d, $J = 5.5$ Hz, 2H) 2.15 (s, 3H). $^{13}\text{C-NMR}$ (125 MHz, CDCl_3): $\delta = 168.2$ (C_q), 158.1 (C_q), 158.0 (CH), 140.7 (C_q) 135.4 (CH), 134.1 (C_q) 132.3 (C_q), 129.5 (C_q), 116.9 (CH), 116.4 (CH_2), 115.8 (CH), 114.3 (CH), 111.4 (CH), 106.7 (CH), 34.2 (CH_2), 24.5 (CH_3). IR (ATR): ν (cm^{-1}) = 2981, 1681, 1429, 1302, 1251, 730, 651 cm^{-1} . EI-MS: m/z (relative intensity): 292 (43) $[\text{M}]^+$, 277 (100), 249 (17), 235 (33), 79 (8), 43 (24). HR-MS (ESI): m/z calcd for $\text{C}_{17}\text{H}_{17}\text{N}_4\text{O}$ $[\text{M}+\text{H}]^+$: 293.1402, found: 293.1398.



2-Allyl-5-nitro-1-(pyrimidin-2-yl)-1H-indole (91n)

The general procedure **B** was followed using indole **23n** (119 mg, 0.50 mmol, 1.00 equiv) and allyl acetate **213** (104 mg, 1.00 mmol, 2.00 equiv). Purification by column chromatography on silica gel (*n*-hexane/EtOAc 12:1) yielded **91n** (127 mg, 455 μ mol, 91%) as a yellow solid. M. p. = 106–108 °C. $^1\text{H-NMR}$ (300 MHz, CDCl_3) δ = 8.83 (d, J = 4.7 Hz, 2H), 8.43 (d, J = 2.3 Hz, 1H), 8.22 (d, J = 8.7 Hz, 1H), 8.09 (dd, J = 8.7, 2.3 Hz, 1H), 7.25 (t, J = 4.7 Hz, 1H), 6.60 (s, 1H), 5.93 (ddt, J = 16.9, 10.5, 6.5 Hz, 1H), 5.06 (ddt, J = 16.9, 1.3 Hz, 1H), 5.04 (ddt, J = 10.5, 1.3 Hz, 1H), 3.94 (dd, J = 6.5, 1.3 Hz, 2H). $^{13}\text{C-NMR}$ (125 MHz, CDCl_3): δ = 158.4 (CH), 157.5 (C_q), 143.3 (C_q), 143.0 (C_q), 140.0 (C_q), 134.5 (CH), 128.7 (C_q), 118.3 (CH), 118.0 (CH), 117.1 (CH_2), 116.3 (CH), 113.7 (CH), 107.0 (CH), 33.9 (CH_2). IR (ATR): ν (cm^{-1}) = 2977, 1610, 1570, 1421, 1071, 924, 745, 541 cm^{-1} . EI-MS: m/z (relative intensity): 280 (34) $[\text{M}]^+$, 265 (100), 219 (44), 207 (18). HR-MS (ESI): m/z calcd for $\text{C}_{15}\text{H}_{12}\text{N}_4\text{O}_2$ $[\text{M}]^+$: 280.0960, found: 280.0963.



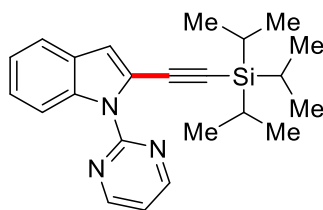
2-Allyl-3-methyl-1-(pyrimidin-2-yl)-1H-indole (91j)

The general procedure **B** was followed using indole **23j** (106 mg, 0.50 mmol, 1.00 equiv) and allyl acetate **213** (105 mg, 1.00 mmol, 2.00 equiv). Purification by column chromatography on silica gel (*n*-hexane/EtOAc 15:1) yielded **91j** (116 mg, 467 μ mol, 93%) as a colourless solid. M. p. = 79–81 °C. $^1\text{H-NMR}$ (300 MHz, CDCl_3) δ = 8.75 (d, J = 5.2 Hz, 2H), 8.23–8.21 (m, 1H), 7.52–7.50 (m, 1H), 7.22–7.19 (m, 2H), 7.06 (t, J = 5.2 Hz, 1H), 5.90 (ddt, J = 16.7, 9.9, 5.9 Hz, 1H), 4.87 (ddt, J = 16.7, 1.9 Hz, 1H), 4.84 (ddt, J = 9.9, 1.9 Hz, 1H), 3.97 (dd, J = 5.9, 1.8 Hz, 2H), 2.29 (s, 3H). $^{13}\text{C-NMR}$ (125 MHz, CDCl_3): δ = 158.2 (C_q), 158.0 (CH), 136.2 (C_q), 135.9 (CH), 134.1 (C_q), 130.4 (C_q), 122.9 (CH), 121.4 (CH), 118.0 (CH), 116.7 (CH), 115.0 (CH_2), 113.8

(C_q), 113.5 (CH), 30.4 (CH₂), 8.8 (CH₃). IR (ATR): ν (cm⁻¹) = 2912, 1656, 1416, 1197, 809, 734, 603, 440 cm⁻¹. EI-MS: m/z (relative intensity): 249 (32) [M]⁺, 234 (100), 220 (20), 154 (11), 43, (18). HR-MS (ESI): m/z calcd for C₁₆H₁₅N₃ [M]⁺: 249.1266, found: 249.1264. The analytical data correspond with those reported in literature.^[79b]

5.5 Base-Metal Catalyzed C–H Alkynylation

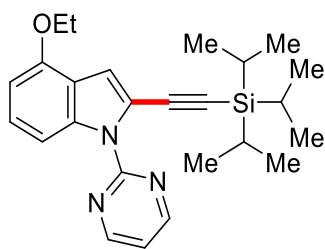
5.5.1 Analytical Data and Experimental Procedures



1-(Pyrimidin-2-yl)-2-[(triisopropylsilyl)ethynyl]-1H-indole (89aa)

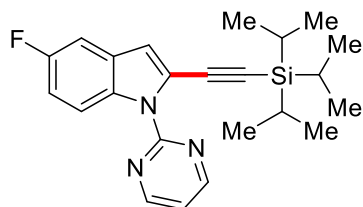
The general procedure **C** was followed using indole **23a** (48.9 mg, 0.25 mmol, 1.00 equiv) and **132a** (79.1 mg, 0.30 mmol, 1.20 equiv). Purification by column chromatography on silica gel (*n*-pentane/EtOAc 8:1) yielded **89aa** (90.3 mg, 241 μ mol, 96%) as a yellow oil.

The general procedure **D** was followed using indole **23a** (98 mg, 0.50 mmol, 1.00 equiv) and **132a** (157 mg, 0.60 mmol, 1.20 equiv). Isolation by column chromatography (*n*-hexane/EtOAc: 9/1) yielded **89aa** (186 mg, 99%) as a colorless liquid. ¹H-NMR (500 MHz, CDCl₃) δ = 8.79 (d, J = 4.8 Hz, 2H), 8.28 (ddd, J = 8.1, 1.0, 0.6 Hz 1H), 7.57 (ddd, J = 8.1, 1.0, 0.6 Hz 1H), 7.33 (ddd, J = 8.5, 2.0, 1.3 Hz, 1H), 7.23 (ddd, J = 8.5, 2.0, 1.3 Hz, 1H), 7.18 (t, J = 4.8 Hz, 1H), 7.07 (d, J = 0.6 Hz, 1H), 1.13–1.11 (m, 21H). ¹³C-NMR (125 MHz, CDCl₃): δ = 158.1 (CH), 157.4 (C_q), 136.2 (C_q), 128.5 (C_q), 124.8 (CH), 122.3 (CH), 120.9 (C_q), 120.7 (CH), 117.5 (CH), 115.7 (CH), 114.0 (CH), 98.7 (C_q), 97.8 (C_q), 18.7 (CH₃), 11.4 (CH). IR (ATR): 2940, 2862, 2149, 1561, 1422, 1253, 715 cm⁻¹. MS (EI) m/z (relative intensity): 375 (32), 332 (100), 304 (16), 290 (32), 262 (18), 222 (24), 138 (9), 69 (14). HR-MS (ESI) m/z calcd for C₂₃H₂₉N₃Si [M]⁺: 375.2131, found: 375.2132. The analytical data are in accordance with those previously reported in the literature.^[78]



4-Ethoxy-1-(pyrimidin-2-yl)-2-[(triisopropylsilyl)ethynyl]-1H-indole (**89ma**)

The general procedure **C** was followed using indole **23m** (60.1 mg, 0.25 mmol, 1.00 equiv), and **132a** (78.9 mg, 0.30 mmol, 1.20 equiv). Purification by column chromatography on silica gel (*n*-pentane/EtOAc 6:1) yielded **89ma** (63.8 mg, 164 μ mol, 91%) as a white solid. M. p. = 112–114 °C. $^1\text{H-NMR}$ (500 MHz, CDCl_3) δ = 8.76 (d, J = 5.0 Hz, 2H), 7.82 (ddd, J = 8.1, 1.6, 0.7 Hz, 1H), 7.22–7.17 (m, 2H), 7.14 (t, J = 5.0 Hz, 1H), 6.59 (dd, J = 8.1, 0.7 Hz, 1H), 4.16 (q, J = 6.7 Hz, 2H), 1.48 (t, J = 6.7 Hz, 3H), 1.11–1.09 (m, 21H). $^{13}\text{C-NMR}$ (125 MHz, CDCl_3): δ = 158.0 (CH), 157.5 (C_q), 152.1 (C_q), 137.4 (C_q), 125.7 (CH), 119.5 (C_q), 119.4 (C_q), 117.5 (CH), 113.2 (CH), 107.0 (CH), 103.1 (CH), 99.0 (C_q), 97.0 (C_q), 63.6 (CH_2), 18.7 (CH_3), 14.9 (CH_3), 11.4 (CH). IR (ATR): 2941, 2863, 2142, 1571, 1417, 1246, 740, 727 cm^{-1} . MS (EI) m/z (relative intensity): 419 (65), 376 (100), 348 (18), 334 (23), 304 (16). HR-MS (ESI) m/z calcd for $\text{C}_{25}\text{H}_{33}\text{N}_3\text{OSi}$ $[\text{M}]^+$: 419.2393, found: 419.2395.

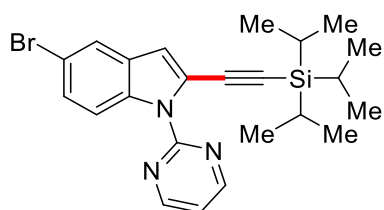


5-Fluoro-1-(pyrimidin-2-yl)-2-[(triisopropylsilyl)ethynyl]-1H-indole (**89oa**)

The general procedure **C** was followed using indole **23o** (53.4 mg, 0.25 mmol, 1.00 equiv) and **132a** (78.8 mg, 0.30 mmol, 1.20 equiv) at 80 °C. Purification by column chromatography on silica gel (*n*-pentane/EtOAc 8:1) yielded **89oa** (80.9 mg, 206 μ mol, 82%) as a white solid.

The general procedure **D** was followed using indole **23o** (108 mg, 0.50 mmol, 1.00 equiv) and **132a** (155 mg, 0.60 mmol, 1.20 equiv). Isolation by column chromatography (*n*-pentane/EtOAc: 8/1) yielded **89oa** (174 mg, 88%) as a yellow solid. M. p. = 91–93 °C. $^1\text{H-NMR}$ (500 MHz, CDCl_3) δ = 8.77 (d, J = 4.7 Hz, 2H), 8.26 (dd, J = 9.1, 4.7 Hz 1H), 7.23–7.17 (m, 2H), 7.05 (ddd, J = 9.1, 3.0, 1.5 Hz, 1H), 7.01 (s,

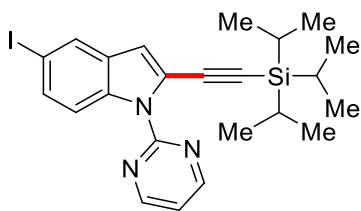
1H), 1.13–1.11 (m, 21H). ¹³C-NMR (125 MHz, CDCl₃): δ = 159.2 (d, ¹J_{CF} = 238 Hz, C_q), 158.1 (CH), 157.2 (C_q), 132.5 (C_q), 129.2 (d, ³J_{CF} = 10 Hz, C_q), 122.4 (C_q), 117.7 (CH), 115.3 (d, ³J_{CF} = 12 Hz, CH), 115.2 (CH), 112.8 (d, ²J_{CF} = 25 Hz, CH), 105.5 (d, ²J_{CF} = 23 Hz, CH), 98.6 (C_q), 98.3 (C_q), 18.6 (CH₃), 11.4 (CH). ¹⁹F-NMR (282 MHz, CDCl₃): -121.9. IR (ATR): 2940, 2862, 2143, 1573, 1556, 1419, 1253, 1211, 723 cm⁻¹. MS (EI) *m/z* (relative intensity): 393 (22), 350 (100), 322 (19), 308 (30), 280 (22), 240 (28), 147 (12). HR-MS (ESI) *m/z* calcd for C₂₃H₂₈N₃FSi [M]⁺: 393.2037, found: 393.2020. The analytical data are in accordance with those previously reported in the literature.^[78]



5-Bromo-1-(pyrimidin-2-yl)-2-[(triisopropylsilyl)ethynyl]-1H-indole (89ha)

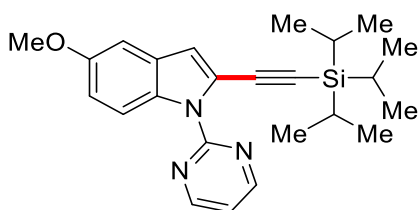
The general procedure **C** was followed using indole **23h** (68.1 mg, 0.25 mmol, 1.00 equiv) and **132a** (78.4 mg, 0.30 mmol, 1.20 equiv) at 80 °C. Purification by column chromatography on silica gel (*n*-pentane/EtOAc 8:1) yielded **89ha** (104.4 mg, 231 μmol, 92%) as a white solid.

The general procedure **D** was followed using indole **23h** (137 mg, 0.50 mmol, 1.00 equiv) and **132a** (159 mg, 0.60 mmol, 1.20 equiv). Isolation by column chromatography (*n*-pentane/EtOAc: 8/1) yielded **89ha** (204 mg, 91%) as a yellow solid. M. p. = 94–96 °C. ¹H-NMR (500 MHz, CDCl₃) δ = 8.76 (d, *J* = 5.4 Hz, 2H), 8.04 (ddd, *J* = 9.0, 1.5, 0.5 Hz 1H), 7.90 (dd, *J* = 1.5, 0.5 Hz, 1H), 7.53 (dd, *J* = 8.7, 1.9 Hz, 1H), 7.18 (t, *J* = 5.4 Hz, 1H), 6.94 (d, *J* = 0.3 Hz, 1H), 1.11–1.08 (m, 21H). ¹³C-NMR (125 MHz, CDCl₃): δ = 158.1 (CH), 157.1 (C_q), 135.3 (C_q), 133.0 (CH), 130.9 (C_q), 129.3 (CH), 121.7 (C_q), 117.9 (CH), 116.2 (CH), 114.3 (CH), 98.8 (C_q), 98.1 (C_q), 86.2 (C_q), 18.6 (CH₃), 11.4 (CH). IR (ATR): 2960, 2861, 2140, 1572, 1420, 1256, 1014, 792, 657 cm⁻¹. MS (EI) *m/z* (relative intensity): 455 (21), 412 (100), 368 (33), 302 (24), 178 (14). HR-MS (ESI) *m/z* calcd for C₂₃H₂₈N₃BrSi [M]⁺: 453.1236, found: 453.1229. The analytical data are in accordance with those previously reported in the literature.^[78]



5-Iodo-1-(pyrimidin-2-yl)-2-[(triisopropylsilyl)ethynyl]-1H-indole (**89pa**)

The general procedure **C** was followed using indole **23p** (80.1 mg, 0.25 mmol, 1.00 equiv) and **132a** (78.9 mg, 0.30 mmol, 1.20 equiv) at 80 °C. Purification by column chromatography on silica gel (*n*-pentane/EtOAc 8:1) yielded **89pa** (109.4 mg, 217 μmol, 87%) as a white solid. M. p. = 68–69 °C. ¹H-NMR (500 MHz, CDCl₃) δ = 8.77 (d, *J* = 4.9 Hz, 2H), 8.16 (ddd, *J* = 8.8, 1.4, 0.6 Hz 1H), 7.67 (dd, *J* = 2.0, 0.6 Hz, 1H), 7.36 (dd, *J* = 8.8, 2.0 Hz, 1H), 7.19 (t, *J* = 4.9 Hz, 1H), 6.98 (d, *J* = 0.5 Hz, 1H), 1.11–1.09 (m, 21H). ¹³C-NMR (125 MHz, CDCl₃): δ = 158.1 (CH), 157.1 (C_q), 134.7 (C_q), 130.2 (C_q), 127.5 (CH), 123.0 (CH), 122.1 (C_q), 117.9 (CH), 115.7 (CH), 115.5 (C_q), 114.6 (CH), 98.9 (C_q), 98.1 (C_q), 18.6 (CH₃), 11.4 (CH). IR (ATR): 2939, 2860, 2149, 1562, 1422, 1180, 782, 662 cm⁻¹. MS (EI) *m/z* (relative intensity): 501 (32), 458 (100), 430 (16), 416 (28), 388 (15), 348 (12), 201 (11). HR-MS (ESI) *m/z* calcd for C₂₃H₂₈N₃ISi [M]⁺: 501.1097, found: 501.1104.

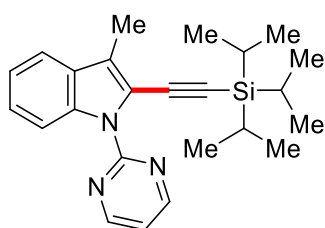


5-Methoxy-1-(pyrimidin-2-yl)-2-[(triisopropylsilyl)ethynyl]-1H-indole (**89da**)

The general procedure **C** was followed using indole **23d** (56.4 mg, 0.25 mmol, 1.00 equiv) and **132a** (78.7 mg, 0.30 mmol, 1.20 equiv). Purification by column chromatography on silica gel (*n*-pentane/EtOAc 5:1) yielded **89da** (94.9 mg, 234 μmol, 94%) as a white solid.

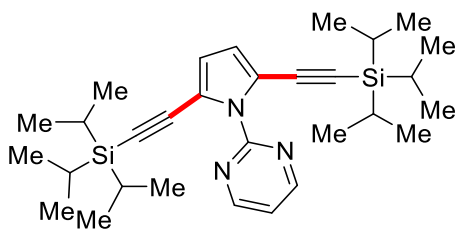
The general procedure **D** was followed using indole **23** (113 mg, 0.50 mmol, 1.00 equiv) and **132a** (157 mg, 0.60 mmol, 1.20 equiv). Isolation by column chromatography (*n*-pentane/EtOAc: 9/1) yielded **89da** (158 mg, 78%) as a white solid. M. p. = 116–118 °C. ¹H-NMR (500 MHz, CDCl₃) δ = 8.74 (d, *J* = 4.8 Hz, 2H), 8.21 (m, *J* = 9.0, 1.1, 0.6 Hz 1H), 7.23 (ddd, *J* = 8.5, 2.0, 1.3 Hz, 1H), 7.15 (t, *J* = 4.8 Hz, 1H),

7.01–6.99 (m, 1H), 6.98 (d, $J = 0.4$ Hz, 1H), 3.86 (s, 3H), 1.13–1.11 (m, 21H). ^{13}C -NMR (125 MHz, CDCl_3): $\delta = 158.0$ (CH), 157.3 (C_q), 155.7 (C_q), 131.1 (C_q), 129.3 (C_q), 121.3 (C_q), 117.3 (CH), 115.6 (CH), 115.3 (CH), 114.4 (CH), 102.2 (CH), 98.9 (C_q), 97.8 (C_q), 55.6 (CH_3) 18.7 (CH_3), 11.4 (CH). IR (ATR): 2940, 2864, 2143, 1562, 1417, 1335, 1207, 840, 741 cm^{-1} . MS (EI) m/z (relative intensity): 405 (46), 362 (100), 320 (29), 292 (11), 252 (13), 153 (10). HR-MS (ESI) m/z calcd for $\text{C}_{24}\text{H}_{32}\text{N}_3\text{OSi}$ $[\text{M}+\text{H}]^+$: 406.2315, found: 406.2318. The analytical data are in accordance with those previously reported in the literature.^[78]



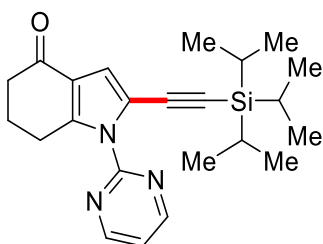
3-Methyl-1-(pyrimidin-2-yl)-2-[(triisopropylsilyl)ethynyl]-1H-indole (**89ja**)

The general procedure **C** was followed using indole **23j** (53.4 mg, 0.25 mmol, 1.00 equiv) and **132a** (79.1 mg, 0.30 mmol, 1.20 equiv) at 80 °C. Purification by column chromatography on silica gel (*n*-pentane/EtOAc 20:1) yielded **89ja** (63.8 mg, 164 μmol , 66%) as a yellow oil. ^1H -NMR (500 MHz, CDCl_3) $\delta = 8.73$ (d, $J = 4.6$ Hz, 2H), 8.32 (ddd, $J = 8.5, 1.2$ Hz, 1H), 7.53 (ddd, $J = 8.5, 1.2, 0.8$ Hz, 1H), 7.31 (ddd, $J = 7.4, 4.2, 2.0$ Hz, 1H), 7.21 (ddd, $J = 7.4, 4.2, 2.0$ Hz, 1H), 7.10 (t, $J = 4.6$ Hz, 1H), 2.45 (s, 3H), 1.11–1.09 (m, 21H). ^{13}C -NMR (125 MHz, CDCl_3): $\delta = 158.1$ (C_q), 157.9 (CH), 157.5 (C_q), 135.8 (C_q), 129.4 (C_q), 125.1 (C_q), 125.0 (CH), 122.0 (CH), 119.0 (CH), 116.7 (CH), 114.2 (CH), 100.7 (C_q), 98.4 (C_q), 18.7 (CH_3), 11.4 (CH) 9.9 (CH_3). IR (ATR): 2940, 2862, 2143, 1561, 1426, 727 cm^{-1} . MS (EI) m/z (relative intensity): 389 (57), 346 (100), 330 (40), 304 (24), 236 (14). HR-MS (ESI) m/z calcd for $\text{C}_{23}\text{H}_{32}\text{N}_3\text{OSi}$ $[\text{M}+\text{H}]^+$: 389.2287, found: 389.2300.



2-(2,5-Bis[(triisopropylsilyl)ethynyl]-1H-pyrrol-1-yl)pyrimidine (**223aa**)

The general procedure **C** was followed using pyrrole **217a** (35.8 mg, 0.25 mmol, 1.00 equiv) and **132a** (79.0 mg, 0.30 mmol, 1.20 equiv). Purification by column chromatography on silica gel (*n*-pentane/EtOAc 5:1) yielded **218aa** (114.5 mg, 226 μ mol, 91%) as a white solid. M. p. = 74–76 °C. $^1\text{H-NMR}$ (500 MHz, CDCl_3) δ = 8.76 (d, J = 4.3 Hz, 2H), 7.26 (t, J = 4.3 Hz, 1H), 6.51 (s, 2H), 1.00–0.97 (m, 42H). $^{13}\text{C-NMR}$ (125 MHz, CDCl_3): δ = 158.3 (CH), 156.5 (C_q), 119.4 (CH), 117.6 (CH), 117.3 (C_q), 97.7 (C_q), 95.2 (C_q), 18.5 (CH_3), 11.2 (CH). IR (ATR): 2940, 2863, 2146, 1563, 1421, 918, 767, 626 cm^{-1} . MS (EI) m/z (relative intensity): 505 (42), 462 (100), 420 (21). HR-MS (ESI) m/z calcd for $\text{C}_{30}\text{H}_{47}\text{N}_3\text{Si}_2$ $[\text{M}]^+$: 505.3309, found 505.3300.

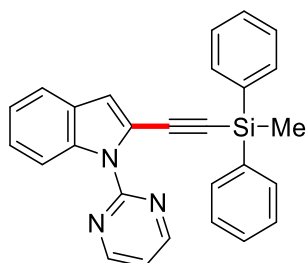


1-(Pyrimidin-2-yl)-2-[(triisopropylsilyl)ethynyl]-5,6,7,7a-tetrahydro-1H-indol-4(3aH)-one (**218ca**)

The general procedure **C** was followed using pyrrole **217c** (53.2 mg, 0.25 mmol, 1.00 equiv) and **132a** (78.6 mg, 0.30 mmol, 1.20 equiv). Purification by column chromatography on silica gel (*n*-pentane/EtOAc 5:1) yielded **218ca** (79.3 mg, 202 μ mol, 80%) as a white solid.

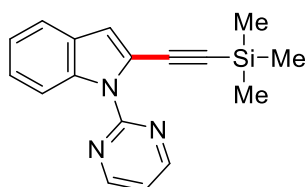
The general procedure **D** was followed using pyrrole **217c** (107 mg, 0.50 mmol, 1.00 equiv) and **132a** (157 mg, 0.60 mmol, 1.20 equiv). Isolation by column chromatography (*n*-pentane/EtOAc: 4/1) yielded **218ca** (187 mg, 96%) as a white solid. M. p. = 144–146 °C. $^1\text{H-NMR}$ (500 MHz, CDCl_3) δ = 8.78 (d, J = 4.9 Hz, 2H), 7.30 (t, J = 4.9 Hz, 1H), 6.96 (s, 1H), 2.96 (dd, J = 6.4, 5.2 Hz, 2H), 2.49 (dd, J = 9.2, 5.8 Hz, 2H), 2.10 (dddd, J = 9.2, 6.4, 5.8, 5.2 Hz, 2H), 1.11–1.08 (m, 21H). $^{13}\text{C-NMR}$

(125 MHz, CDCl₃): δ = 194.1 (C_q), 158.4 (CH), 156.1 (C_q), 145.4 (C_q), 121.6 (C_q), 119.5 (CH), 117.3 (C_q), 115.1 (CH), 97.2 (C_q), 96.0 (C_q), 37.8 (CH₂), 24.2 (CH₂), 23.6 (CH₂), 18.5 (CH₃), 11.2 (CH). IR (ATR): 2940, 2862, 2148, 1660, 1573, 1415, 1135, 808, 720 cm⁻¹. MS (EI) *m/z* (relative intensity): 393 (35), 350 (100), 322 (18), 308 (22), 280 (10), 240 (10). HR-MS (ESI) *m/z* calcd for C₂₃H₃₂N₃OSi [M+H]⁺: 394.2315, found: 394.2309.



2-[(Methyldiphenylsilyl)ethynyl]-1-(pyrimidin-2-yl)-1H-indole (89ab)

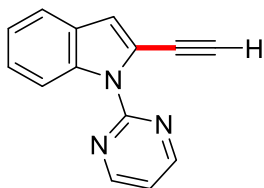
The general procedure **C** was followed using indole **23a** (49.8 mg, 0.25 mmol, 1.00 equiv) and **132b** (53.1 mg, 0.30 mmol, 1.20 equiv). Purification by column chromatography on silica gel (*n*-pentane/EtOAc 20:1) yielded **89ab** (64.6 mg, 156 μ mol, 62%) as a yellow oil. ¹H-NMR (500 MHz, CDCl₃) δ = 8.66 (d, *J* = 4.8 Hz, 2H), 8.32 (ddd, *J* = 8.4, 2.5, 0.8 Hz, 1H), 7.72–7.69 (m, 4H), 7.59 (ddd, *J* = 7.9, 1.9, 1.0 Hz, 1H), 7.42–7.34 (m, 7H), 7.23 (ddd, *J* = 7.9, 1.9, 1.0 Hz, 1H), 7.15 (s, 1H), 7.10 (t, *J* = 4.8 Hz, 1H), 0.76 (s, 3H). ¹³C-NMR (125 MHz, CDCl₃): δ = 158.0 (CH), 157.2 (C_q), 136.3 (C_q), 135.3 (C_q), 134.6 (CH), 133.9 (C_q), 129.6 (CH), 128.4 (C_q), 127.9 (CH), 125.2 (CH), 122.5 (CH), 121.0 (CH), 120.3 (C_q), 117.6 (CH), 116.3 (CH), 114.3 (CH), 100.4 (C_q), 97.2 (C_q), -2.2 (CH₃). IR (ATR): 3046, 2959, 2152, 1562, 1425, 1115, 868, 792 cm⁻¹. MS (EI) *m/z* (relative intensity): 414 (100), 400 (20), 338 (14), 294 (11), 108 (8). HR-MS (ESI) *m/z* calcd C₂₇H₂₀N₃Si [M-H]⁺: 414.1426, found: 414.1422.



1-(Pyrimidin-2-yl)-2-[(trimethylsilyl)ethynyl]-1H-indole (89ac)

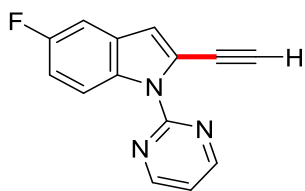
The general procedure **C** was followed using indole **23a** (49.7 mg, 0.25 mmol, 1.00 equiv) and **132c** (53.3 mg, 0.30 mmol, 1.20 equiv). Purification by column chromatography on silica gel (*n*-pentane/EtOAc 80:1) yielded **89ac** (52.9 mg, 183 μ mol, 73%) as a yellow oil. ¹H-NMR (500 MHz, CDCl₃) δ = 8.78 (d, *J* = 4.7 Hz,

2H), 8.28 (ddd, $J = 8.4, 2.1, 0.7$ Hz, 1H), 7.56 (ddd, $J = 7.7, 2.4, 0.9$ Hz, 1H), 7.31 (ddd, $J = 7.7, 2.4, 0.9$ Hz, 1H), 7.23–7.16 (m, 2H), 7.04 (s, 1H), 0.24 (s, 9H). $^{13}\text{C-NMR}$ (125 MHz, CDCl_3): $\delta = 158.0$ (CH), 157.2 (C_q), 136.2 (C_q), 128.4 (C_q), 124.9 (CH), 122.4 (CH), 120.9 (CH), 120.6 (C_q), 117.7 (CH), 115.4 (CH), 114.0 (CH), 101.1 (C_q), 97.1 (C_q), 0.2 (CH_3). IR (ATR): 2957, 2150, 1561, 1421, 1248, 839, 746 cm^{-1} . MS (EI) m/z (relative intensity): 290 (100), 276 (29), 250 (8), 223 (11). HR-MS (ESI) m/z calcd $\text{C}_{17}\text{H}_{16}\text{N}_3\text{Si}$ $[\text{M}-\text{H}]^+$: 290.1113, found: 290.1121.



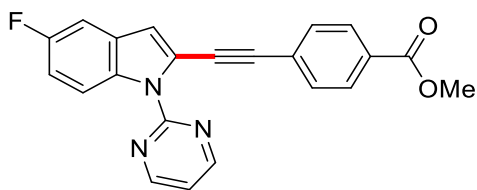
2-Ethynyl-1-(pyrimidin-2-yl)-1H-indole (233a)

To a solution of **89aa** (29.3 mg, 0.15 mmol, 1.00 equiv) in THF (1 mL), tetra-*n*-butylammoniumfluoride trihydrate (141 mg, 0.45 mmol, 3.00 equiv) in THF (1 mL) was added and stirred at 25 °C for 1 h. H_2O (5 mL) was added and the mixture was extracted with CH_2Cl_2 (3 \times 5 mL). The combined organic phases were dried over Na_2SO_4 and the solvent removed at reduced pressure. Purification by column chromatography on silica gel (*n*-pentane/EtOAc 3:1) yielded **233a** (26.5 mg, 121 μmol , 81%) as a brown oil. $^1\text{H-NMR}$ (500 MHz, CDCl_3): $\delta = 8.82$ (d, $J = 5.5$ Hz, 2H), 8.29 (ddd, $J = 8.3, 2.3, 1.0$ Hz, 1H) 7.58 (ddd, $J = 7.9, 1.9, 0.9$ Hz, 1H), 7.34 (ddd, $J = 8.3, 2.3, 1.0$ Hz, 1H) 7.22 (ddd, $J = 7.9, 1.9, 0.9$ Hz, 1H), 7.19 (t, $J = 5.5$ Hz, 1H), 7.10 (s, 1H), 3.45 (s, 1H). $^{13}\text{C-NMR}$ (125 MHz CDCl_3): $\delta = 158.1$ (CH), 157.2 (C_q), 136.2 (C_q), 128.3 (C_q), 125.1 (CH), 122.5 (CH), 120.8 (CH), 119.5 (C_q), 117.7 (CH), 116.2 (CH), 114.2 (CH), 83.3 (CH), 76.4 (C_q). IR (ATR): 3285, 1626, 1563, 1423, 806, 747 cm^{-1} . MS (ESI) m/z (relative intensity): 219 (100), 192 (13), 169 (8), 85 (15). HR-MS (ESI) m/z calcd for $\text{C}_{14}\text{H}_9\text{N}_3$ $[\text{M}]^+$: 219.0796, found: 219.0788.



2-Ethynyl-5-fluoro-1-(pyrimidin-2-yl)-1H-indole (**233b**)

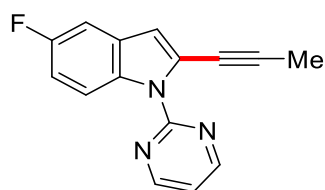
To a solution of **89oa** (32.0 mg, 0.15 mmol, 1.00 equiv) in THF (1 mL), tetra-*n*-butylammoniumfluoride trihydrate (141 mg, 0.45 mmol, 3.00 equiv) in THF (1 mL) was added and stirred at 25 °C for 1 h. H₂O (5 mL) was added (5 mL) and the mixture extracted with CH₂Cl₂ (3 × 5 mL). The combined organic phases were dried over Na₂SO₄ and the solvent removed at reduced pressure. Purification by column chromatography on silica gel (*n*-pentane/EtOAc 3:1) yielded **233b** (28.9 mg, 122 μmol, 81%) as a brown oil. ¹H-NMR (500 MHz, CDCl₃): δ = 8.81 (d, *J* = 5.2 Hz, 2H), 8.28 (dd, *J* = 9.4, 2.5 Hz, 1H) 7.23–7.19 (m, 2H), 7.06 (ddd, *J* = 8.6, 2.3, 1.0 Hz, 1H), 7.03 (s, 1H), 3.47 (s, 1H). ¹³C-NMR (125 MHz CDCl₃): δ = 159.0 (d, ¹*J*_{CF} = 235 Hz, C_q), 158.2 (CH), 157.0 (C_q), 132.6 (C_q), 128.9 (d, ³*J*_{CF} = 12 Hz, C_q), 121.0 (C_q), 117.9 (CH), 115.8 (d, ⁴*J*_{CF} = 5 Hz, CH), 115.4 (d, ³*J*_{CF} = 9 Hz, CH), 113.2 (d, ²*J*_{CF} = 27 Hz, CH), 105.7 (d, ²*J*_{CF} = 29 Hz, CH), 83.9 (CH), 76.0 (C_q). ¹⁹F-NMR (282 MHz, CDCl₃): -121.6. IR (ATR): 3278, 1631, 1562, 1425, 1103, 868, 791 cm⁻¹. MS (ESI) *m/z* (relative intensity): 237 (100), 210 (20), 187 (17), 157 (11). HR-MS (ESI) *m/z* calcd for C₁₄H₈N₃F [M]⁺: 237.0702, found: 237.0708.



Methyl-4-([5-fluoro-1-(pyrimidin-2-yl)-1H-indol-2-yl]ethynyl)benzoate (**234**)

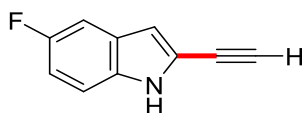
Following a published procedure,^[197] **233b** (32.2 mg, 0.15 mmol, 1.00 equiv), Pd(OAc)₂ (1.7 mg, 7.5 μmol, 5 mol %), CuI (1.4 mg, 7.5 μmol, 5 mol %), PPh₃ (3.9 mg, 15.0 μmol, 10 mol %) and methyl-4-iodobenzoate (39.8 mg, 0.15 mmol, 1.00 equiv) were suspended in a mixture of DMF (0.4 mL) and NEt₃ (1.2 mL) and stirred at 60 °C for 18 h. After completion of the reaction saturated aq. NH₄Cl solution (5 mL) was added and the mixture was extracted with EtOAc (4 × 5 mL). Drying over Na₂SO₄, evaporation of the solvents and purification by column chromatography on silica gel using *n*-pentane/EtOAc (10:1) yielded the product **234** (42.3 mg, 114 μmol, 76%) as

an orange solid. M. p. = 152–154 °C. ¹H-NMR (500 MHz, CDCl₃): δ = 8.84 (d, *J* = 5.4 Hz, 2H), 8.33 (dd, *J* = 9.1, 4.3 Hz, 1H), 8.02 (d, *J* = 8.2 Hz, 2H), 7.54 (d, *J* = 8.2 Hz, 2H), 7.30–7.25 (m, 2H), 7.11–7.05 (m, 2H), 3.92 (s, 3H). ¹³C-NMR (125 MHz CDCl₃): δ = 166.5 (C_q), 159.2 (d, ¹*J*_{CF} = 251 Hz, C_q), 158.2 (CH), 157.1 (C_q), 133.7 (d, ²*J*_{CF} = 24 Hz, CH), 132.9 (C_q), 131.1 (CH), 129.6 (C_q), 129.5 (CH), 129.3 (³*J*_{CF} = 9 Hz, C_q), 128.4 (³*J*_{CF} = 9 Hz, CH), 127.8 (C_q), 121.6 (C_q), 117.9 (CH), 115.6 (⁴*J*_{CF} = 6 Hz, CH), 115.0 (⁴*J*_{CF} = 5 Hz, CH), 113.2 (²*J*_{CF} = 26 Hz, CH) 105.7 (CH), 94.7 (C_q), 85.2 (C_q), 52.3 (CH₃). ¹⁹F-NMR (282 MHz CDCl₃): δ = -121.4. IR (ATR): 2959, 2202, 1720, 1562, 1424, 1224, 1155, 787, 539 cm⁻¹. MS (EI) *m/z* (relative intensity) 370 (100), 311 (33), 277 (15), 232 (10). HR-MS (ESI) *m/z* calcd for C₂₂H₁₃N₃FO₂ [M-H]⁺: 370.0992, found: 370.0997.



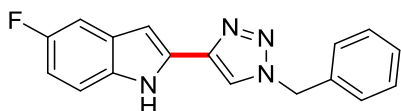
5-Fluoro-2-(prop-1-yn-1-yl)-1-(pyrimidin-2-yl)-1*H*-indole (**235**)

In a modification of a known procedure,^[196] to a solution of **233b** (32.2 mg, 0.15 mmol, 1.00 equiv) in THF (1.5 mL) lithiumbis(trimethylsilyl)amide in THF (0.9 M, 0.185 mL, 0.17 mmol, 1.10 equiv) was added at -40 °C and stirred for 30 min. Then methyl iodide (42.5 mg, 0.30 mmol, 2.00 equiv) was added and the mixture was slowly warmed to 25 °C and stirred for 12 h. H₂O (5 mL) was added and the mixture extracted with CH₂Cl₂ (3 × 5 mL). The combined organic phases were dried over Na₂SO₄ and the solvent removed at reduced pressure. Purification by column chromatography on silica gel (*n*-pentane/EtOAc 5:1) yielded **235** (18.6 mg, 137 μmol, 92%) as a brown oil. ¹H-NMR (500 MHz, CDCl₃): δ = 8.82 (d, *J* = 5.2 Hz, 2H), 8.15 (dd, *J* = 8.7, 5.2 Hz, 1H) 7.22–7.15 (m, 2H), 7.00 (ddd, *J* = 8.4, 2.5, 0.7 Hz, 1H), 6.86 (s, 1H), 2.10 (s, 3H). ¹³C-NMR (125 MHz CDCl₃): δ = 158.9 (d, ¹*J*_{CF} = 234 Hz, C_q), 158.1 (CH), 157.1 (C_q), 132.3 (C_q), 129.3 (d, ³*J*_{CF} = 13 Hz, C_q), 122.8 (C_q), 117.7 (CH), 114.9 (d, ⁴*J*_{CF} = 6 Hz, CH), 113.3 (d, ⁴*J*_{CF} = 4 Hz, CH), 112.2 (d, ²*J*_{CF} = 26 Hz, CH), 105.4 (d, ²*J*_{CF} = 27 Hz, CH), 92.6 (C_q), 72.1 (C_q), 5.1 (CH₃). ¹⁹F-NMR (282 MHz, CDCl₃): δ = -122.1. IR (ATR): 3023, 1562, 1422, 1193, 855, 800, 630 cm⁻¹. MS (ESI) *m/z* (relative intensity): 251 (100), 223 (22), 197 (17), 172 (10) 125 (8). HR-MS (ESI) *m/z* calcd for C₁₅H₁₁N₃F [M+H]⁺: 252.0937, found: 252.0932.



2-Ethynyl-5-fluoro-1H-indole (236)

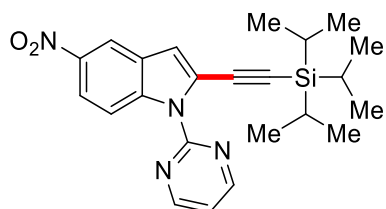
To a solution of **890a** (32.0 mg, 0.15 mmol, 1.00 equiv) in DMSO (1.5 mL) and CH₃OH (0.5 mL), sodium ethanolate (30.6 mg, 0.45 mmol, 3.00 equiv) was added and stirred at 60 °C for 3 h. H₂O (5 mL) was added and the mixture extracted with CH₂Cl₂ (3 × 5 mL). The combined organic phases were dried over Na₂SO₄ and the solvent removed at reduced pressure. Purification by column chromatography on silica gel (*n*-pentane/EtOAc 2:1) yielded **236** (18.6 mg, 116 μmol, 77%) as a brown oil. ¹H-NMR (500 MHz, CDCl₃): δ = 8.19 (s, 1H), 7.23–7.18 (m, 2H), 6.98 (ddd, *J* = 8.2, 3.2, 2.3 Hz, 1H), 6.75 (s, 1H), 3.31 (s, 1H). ¹³C-NMR (125 MHz CDCl₃): δ = 158.2 (d, ¹*J*_{CF} = 247 Hz, C_q), 132.3 (C_q), 127.6 (d, ³*J*_{CF} = 12 Hz, C_q), 119.2 (C_q), 112.4 (d, ²*J*_{CF} = 28 Hz, CH), 111.4 (d, ³*J*_{CF} = 10 Hz, CH), 109.5 (d, ⁴*J*_{CF} = 6 Hz, CH), 105.4 (d, ²*J*_{CF} = 26 Hz, CH), 81.1 (CH), 75.8 (C_q). ¹⁹F-NMR (282 MHz, CDCl₃): -124.0. IR (ATR): 3422, 2383, 1484, 1166, 854, 597 cm⁻¹. MS (ESI) *m/z* (relative intensity): 159 (100), 132 (32), 118 (17). HR-MS (ESI) *m/z* calcd for C₁₀H₆NF [M]⁺: 159.0484, found: 159.0485.



2-(1-Benzyl-1H-1,2,3-triazol-4-yl)-5-fluoro-1H-indole (237)

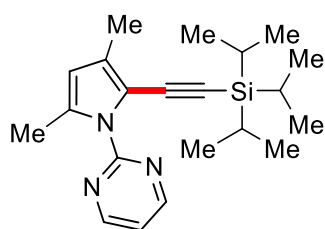
Following a previously published procedure,^[198] **237** (24.2 mg, 0.15 mmol, 1.00 equiv), CuI (2.9 mg, 15.0 μmol, 10 mol %) and benzyl azide (13.7 mg, 0.15 mmol, 1.00 equiv) were dissolved in DMF (1.5 mL) and stirred at 60 °C for 14 h. After completion of the reaction saturated aq. NH₄Cl solution (5 mL) was added and the mixture was extracted with CH₂Cl₂ (4 × 5 mL). Drying over Na₂SO₄, evaporation of the solvents and purification by column chromatography on silica gel using *n*-pentane/EtOAc (2:1) yielded the product **232** (31.1 mg, 107 μmol, 71%) as a white solid. Decomposed at 240 °C. ¹H-NMR (500 MHz, DMSO-*d*₆): δ = 11.70 (s, 1H), 8.53 (s, 1H), 7.44–7.36 (m, 6H), 7.28 (dd, *J* = 9.3, 2.5 Hz, 1H), 6.93 (dd, *J* = 7.3, 4.3 Hz, 1H), 6.76 (s, 1H), 5.67 (s, 2H). ¹³C-NMR (125 MHz CDCl₃): δ = 157.1 (d, ¹*J*_{CF} = 229 Hz, C_q), 140.6 (C_q), 135.8 (C_q), 133.1 (C_q), 131.0 (C_q), 128.8 (CH), 128.5 (CH), 128.4 (CH), 128.2 (C_q), 121.6 (CH), 112.3 (d, ³*J*_{CF} = 11 Hz, CH), 109.4 (d, ²*J*_{CF} = 25 Hz, CH), 104.5 (d, ²*J*_{CF} = 27 Hz,

CH), 98.6 (d, $^4J_{CF}$ = 6 Hz, CH) 53.0 (CH₂). ^{19}F -NMR (282 MHz, DMSO-*d*₆): δ = -125.2. IR (ATR): 3288, 1624, 1419, 1216, 1013, 790, 690, 411 cm⁻¹. MS (EI) *m/z* (relative intensity): 292 (48), 263 (100), 236 (35), 187 (22), 91 (51), 43 (44). HR-MS (ESI) *m/z* calcd for C₁₇H₁₃N₄F [M]⁺: 292.1124, found: 292.1120.



5-Nitro-1-(pyrimidin-2-yl)-2-[(triisopropylsilyl)ethynyl]-1*H*-indole (**89na**)

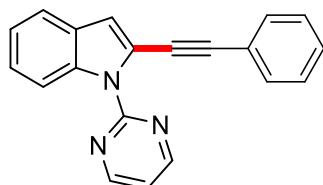
The general procedure **D** was followed using indole **23n** (121 mg, 0.50 mmol, 1.00 equiv) and **132a** (158 mg, 0.60 mmol, 1.20 equiv) at 100 °C. Isolation by column chromatography (*n*-pentane/EtOAc: 3/1) yielded **89na** (135 mg, 63%) as a yellow solid. M.p. = 127–129 °C. ^1H NMR (400 MHz, CDCl₃) δ = 8.83 (d, J = 5.9 Hz, 2H), 8.49 (d, J = 2.0 Hz, 1H), 8.29 (d, J = 9.5 Hz, 1H), 8.17 (dd, J = 9.5, 2.0 Hz, 1H), 7.28 (t, J = 5.9 Hz, 1H), 7.17 (s, 1H), 1.11–1.09 (m, 21H). ^{13}C NMR (125 MHz, CDCl₃) δ = 158.4 (CH), 156.7 (C_q), 143.5 (C_q), 138.8 (C_q), 128.0 (C_q), 124.2 (C_q), 119.7 (CH), 118.7 (CH), 117.2 (CH), 115.7 (CH), 114.2 (CH), 100.5 (C_q), 97.1 (C_q), 18.6 (CH₃), 11.3 (CH). IR (neat): 2940, 2863, 2163, 1568, 1414, 1209, 676, 659 cm⁻¹. MS (ESI) *m/z* (relative intensity) 443 (100) [M+Na⁺], 421 [M+H⁺] (75), 383 (22), 301 (11), 242 (27), 182 (58). HR-MS (ESI) *m/z* calcd for C₂₃H₂₉N₄O₂Si [M+H⁺] 421.2060, found 421.2060.



2-(3,5-Dimethyl-2-[(triisopropylsilyl)ethynyl]-1*H*-pyrrol-1-yl)pyrimidine (**223ba**)

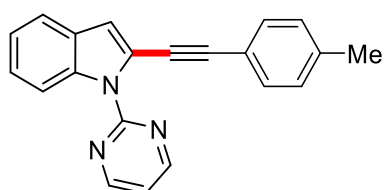
The general procedure **D** was followed using pyrrole **217b** (87 mg, 0.50 mmol, 1.00 equiv) and **132a** (154 mg, 0.60 mmol, 1.20 equiv). Isolation by column chromatography (*n*-pentane/EtOAc:10/1) yielded **223ba** (161 mg, 92%) as white solid. M.p. = 139–141 °C. ^1H NMR (400 MHz, CDCl₃) δ = 8.70 (d, J = 4.7 Hz, 2H), 7.15 (t, J = 4.7 Hz, 1H), 5.86 (s, 1H), 2.34 (s, 3H), 2.15 (s, 3H), 1.07–1.03 (m, 21H). ^{13}C NMR (125 MHz, CDCl₃) δ = 158.0 (CH), 157.2 (C_q), 131.8 (C_q), 129.4 (C_q), 118.2 (CH), 113.7

(C_q), 111.8 (CH), 98.7 (C_q), 96.1 (C_q), 18.3 (CH₃), 14.3 (CH₃), 11.9 (CH₃), 11.3 (CH). IR (neat): 2938, 2851, 2141, 1526, 1433, 1169, 1083, 740, 669 cm⁻¹. MS (ESI) *m/z* (relative intensity) 376 (100) [M+Na⁺], 353 [M+H⁺] (72), 312 (5). HR-MS (ESI) *m/z* calcd for C₂₁H₃₁N₃SiNa [M+Na⁺] 376.2179, found 376.2170.



2-(Phenylethynyl)-1-(pyrimidin-2-yl)-1H-indole (89ad)

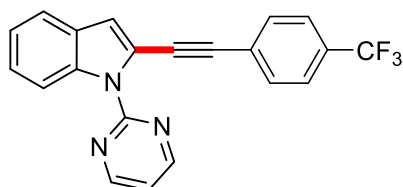
The general procedure **E** was followed using indole **23a** (98 mg, 0.50 mmol, 1.00 equiv) and **132d** (108 mg, 0.60 mmol, 1.20 equiv) for 1 h. Isolation by column chromatography (*n*-pentane/EtOAc: 5/1) yielded **89ad** (141 mg, 95%) as a colorless oil. ¹H NMR (500 MHz, CDCl₃) δ = 8.85 (d, *J* = 4.9 Hz, 2H), 8.31 (d, *J* = 8.4 Hz, 1H), 7.60 (d, *J* = 7.6 Hz, 1H), 7.52–7.48 (m, 2H), 7.35–7.31 (m, 4H), 7.25–7.21 (m, 1H), 7.21 (t, *J* = 4.9 Hz, 1H), 7.08 (s, 1H). ¹³C NMR (125 MHz, CDCl₃) δ = 158.1 (CH), 157.4 (C_q), 136.4 (C_q), 131.3 (CH), 128.8 (C_q), 128.4 (CH), 128.3 (CH), 124.8 (CH), 123.3 (C_q), 122.4 (CH), 120.9 (C_q), 120.8 (CH), 117.7 (CH), 114.6 (CH), 114.1 (CH), 95.0 (C_q), 82.5 (C_q). IR (neat): 3048, 2963, 2851, 1560, 1418, 1081, 741, 686, 521 cm⁻¹. MS (ESI) *m/z* (relative intensity) 296 (5) [M⁺], 214 (11), 196 (100), 173 (20), 149 (15). HR-MS (ESI) *m/z* calcd for C₂₀H₁₄N₃ [M+H⁺] 296.1182, found 296.1188.



1-(Pyrimidin-2-yl)-2-(*p*-tolylethynyl)-1H-indole (89af)

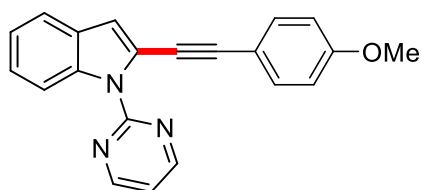
The general procedure **E** was followed using indole **23a** (98 mg, 0.50 mmol, 1.00 equiv) and **132f** (117 mg, 0.60 mmol, 1.20 equiv) for 1 h. Isolation by column chromatography (*n*-pentane/EtOAc: 9/1) yielded **89af** (153 mg, 99%) as a colorless solid. M.p. = 100–102 °C. ¹H NMR (500 MHz, CDCl₃) δ = 8.84 (d, *J* = 4.8 Hz, 2H), 8.30 (d, *J* = 8.4 Hz, 1H), 7.59 (d, *J* = 7.8 Hz, 1H), 7.39 (d, *J* = 8.0 Hz, 2H), 7.32 (ddd, *J* = 8.3, 6.9, 1.0 Hz, 1H), 7.24–7.21 (m, 1H), 7.19 (t, *J* = 4.8 Hz, 1H), 7.14 (d, *J* = 7.9 Hz, 2H), 7.06 (s, 1H), 2.35 (s, 3H). ¹³C NMR (125 MHz, CDCl₃) δ = 158.1 (CH), 157.4 (C_q), 138.5 (C_q), 136.3

(C_q), 131.2 (CH), 129.1 (CH), 128.8 (C_q), 124.6 (CH), 122.4 (CH), 121.0 (C_q), 120.7 (CH), 120.2 (C_q), 117.7 (CH), 114.3 (CH), 114.0 (CH), 95.1 (C_q), 81.8 (C_q), 21.5 (CH₃). IR (neat): 3046, 2920, 2851, 1557, 1422, 800, 739, 526 cm⁻¹. MS (EI) *m/z* (relative intensity) 309 (100) [M⁺], 294 (15). HR-MS (ESI) *m/z* calcd for C₂₁H₁₆N₃ [M+H⁺] 310.1344, found 310.1339.



2-[(4-Trifluoromethylphenyl)ethynyl]-1-(pyrimidin-2-yl)-1H-indole (89ag)

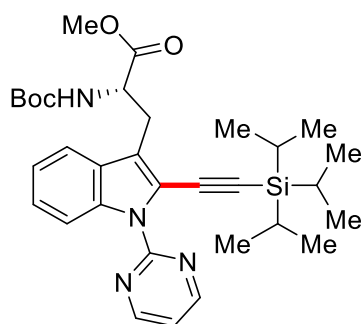
The general procedure **E** was followed using indole **23a** (98 mg, 0.50 mmol, 1.00 equiv) and **132g** (148 mg, 0.60 mmol, 1.20 equiv). Isolation by column chromatography (*n*-pentane/EtOAc: 7/1) yielded **89ag** (96 mg, 54%) as a colorless oil. ¹H NMR (500 MHz, CDCl₃) δ = 8.84 (d, *J* = 4.5 Hz, 2H), 8.35 (d, *J* = 8.2 Hz, 1H), 7.63–7.59 (m, 5H), 7.36 (dd, *J* = 8.2, 2.3 Hz, 1H), 7.24–7.20 (m, 2H), 7.13 (s, 1H). ¹³C NMR (125 MHz, CDCl₃) δ = 157.9 (CH), 157.2 (C_q), 156.5 (C_q), 131.3 (CH), 129.8 (q, ²*J*_{CF} = 32.0 Hz, C_q) 128.6 (C_q), 127.1 (C_q), 125.2 (q, ³*J*_{CF} = 12.0 Hz, CH), 125.1 (CH), 123.8 (q, ¹*J*_{CF} = 265.0 Hz, C_q), 122.6 (CH), 120.9 (CH), 120.0 (C_q), 117.7 (CH), 115.6 (CH), 114.3 (CH), 93.5 (C_q), 85.1 (C_q). ¹⁹F NMR (282 MHz, CDCl₃) δ = -62.8. IR (neat): 3041, 2960, 1562, 1449, 1424, 805, 747, 690 cm⁻¹. MS (EI) *m/z* (relative intensity) 363 [M⁺] (100), 344 [M-F⁺] (10), 293 (12), 214 (10), 147 (15), 43 (18). HR-MS (ESI) *m/z* calcd for C₂₁H₁₃N₃F₃ [M+H⁺] 364.1056, found 364.1059.



2-[(4-Methoxyphenyl)ethynyl]-1-(pyrimidin-2-yl)-1H-indole (89ah)

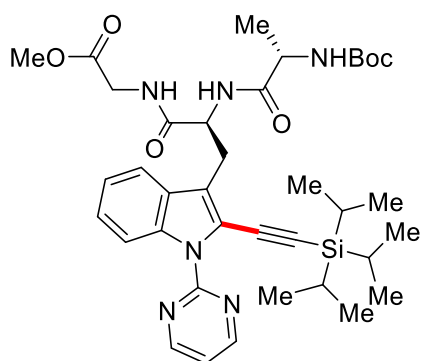
The general procedure **E** was followed using indole **23a** (98 mg, 0.50 mmol, 1.00 equiv), **132h** (128 mg, 0.60 mmol, 1.20 equiv) and MnBr(CO)₅ (3.4 mg, 2.5 mol %). Isolation by column chromatography (*n*-pentane/EtOAc: 4/1) yielded **89ah** (132 mg, 81%) as a colorless oil. ¹H NMR (500 MHz, CDCl₃) δ = 8.85 (d, *J* = 4.6 Hz, 2H), 8.29 (d, *J* = 7.6 Hz, 1H), 7.59 (d, *J* = 7.6 Hz, 1H), 7.43 (d, *J* = 9.4 Hz, 2H), 7.31 (dd, *J*

= 7.6, 1.8 Hz, 1H) 7.23–7.21 (m, 1H), 7.20 (t, $J = 4.6$ Hz, 1H), 7.03 (s, 1H), 6.86 (d, $J = 9.4$ Hz, 2H), 3.81 (s, 3H). ^{13}C NMR (125 MHz, CDCl_3) $\delta = 159.7$ (C_q), 158.1 (CH), 157.4 (C_q), 136.3 (C_q), 132.8 (CH), 128.8 (C_q), 124.6 (CH), 122.4 (CH), 121.2 (C_q), 120.7 (CH), 117.7 (CH), 115.4 (C_q), 114.1 (CH), 114.0 (CH), 113.9 (CH), 95.0 (C_q), 81.2 (C_q), 55.3 (CH_3). IR (neat): 3041, 2931, 2835 1604, 1561, 1420, 1204, 801, 746, 521 cm^{-1} . MS (ESI) m/z (relative intensity). 348 [$\text{M}+\text{Na}^+$] (95), 326 [$\text{M}+\text{H}^+$] (100), 288 (7), 198 (11), 149 (8). HR-MS (ESI) m/z calcd for $\text{C}_{21}\text{H}_{15}\text{N}_3\text{ONa}$ [$\text{M}+\text{Na}^+$] 348.1107, found 348.1117.



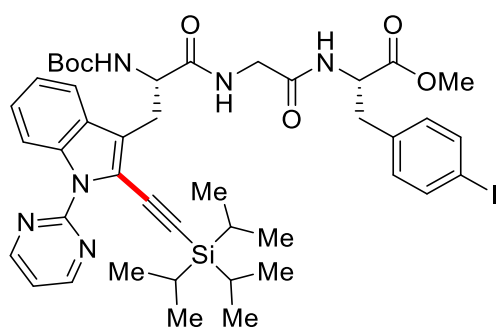
Methyl-(S)-2-[(*tert*-butoxycarbonyl)amino]-3-{1-(pyrimidin-2-yl)-2-[(triisopropylsilyl)ethynyl]-1*H*-indol-3-yl}propanoate (227aa**)**

The general procedure **D** was followed using substrate **226a** (198 mg, 0.50 mmol, 1.00 equiv) and **132a** (154 mg, 0.60 mmol, 1.20 equiv). Isolation by column chromatography (*n*-pentane/EtOAc: 2/1) yielded **227aa** (237 mg, 82%) as white solid. M.p. = 111–113 °C ^1H NMR (400 MHz, CDCl_3) $\delta = 8.75$ (d, $J = 5.0$ Hz, 2H), 8.32 (d, $J = 9.0$ Hz, 1H), 7.60 (d, $J = 7.3$ Hz, 1H), 7.32 (dd, $J = 7.3, 2.2$ Hz, 1H), 7.23 (dd, $J = 9.0, 2.2$ Hz, 1H), 7.14 (t, $J = 5.0$ Hz, 1H), 5.24 (d, $J = 7.6$ Hz, 1H), 4.55 (dd, $J = 8.2, 7.6$ Hz, 1H), 3.67 (s, 3H), 3.41–3.31 (m, 2H), 1.33 (s, 9H), 1.15–1.13 (m, 21H). ^{13}C NMR (125 MHz, CDCl_3) $\delta = 172.8$ (C_q), 158.0 (CH), 157.2 (C_q), 155.3 (C_q), 135.9 (C_q), 128.3 (C_q), 125.4 (CH), 123.2 (C_q), 122.4 (CH), 120.0 (C_q), 119.0 (CH), 117.4 (CH), 114.4 (CH), 101.6 (C_q), 97.8 (C_q), 79.6 (C_q), 54.3 (CH), 52.2 (CH_3), 28.2 (CH_3), 28.0 (CH_2), 18.7 (CH_3), 11.4 (CH). IR (neat): 2960, 2864, 2138, 1738, 1420, 1257, 996, 747, 675 cm^{-1} . MS (ESI) m/z (relative intensity): 1175 [$2\text{M}+\text{Na}^+$] (100), 599 [$\text{M}+\text{Na}^+$] (77), 577 [$\text{M}+\text{H}^+$] (23), 512 (11), 389 (13), 208 (5). HR-MS (ESI) m/z calcd for $\text{C}_{32}\text{H}_{44}\text{N}_4\text{O}_4\text{SiNa}$ [$\text{M}+\text{Na}^+$] 599.3024, found 599.3024. The enantiomeric excess was determined to be >98% by HPLC analysis of compound (*S*)-**227aa** and a racemic sample (\pm)-**227aa**.



Methyl-((S)-2-((S)-2-[(*tert*-butoxycarbonyl)amino]propanamido)-3-{1-(pyrimidin-2-yl)-2-[(triisopropylsilyl)ethynyl]-1*H*-indol-3-yl}propanoyl)glycinate (227ba**)**

The general procedure **D** was followed using substrate **226b** (132 mg, 0.25 mmol, 1.00 equiv) and **132a** (78 mg, 0.30 mmol, 1.20 equiv). Isolation by column chromatography (*n*-pentane/EtOAc: 1/2) yielded **227ba** (124 mg, 71%) as a yellow solid. M.p. = 64–66 °C ¹H NMR (400 MHz, CDCl₃) δ = 8.75 (d, *J* = 5.4 Hz, 2H), 8.30 (d, *J* = 8.8 Hz, 1H), 7.74 (d, *J* = 8.6 Hz, 1H), 7.33 (dd, *J* = 8.8, 2.7 Hz, 1H), 7.23 (dd, *J* = 8.6, 2.7 Hz, 1H), 7.15 (t, *J* = 5.4 Hz, 1H), 6.67 (d, *J* = 6.7 Hz, 1H), 6.50 (s, 1H), 4.93 (s, 1H), 4.80 (dd, *J* = 7.0, 4.5 Hz, 1H), 4.03 (dd, *J* = 6.8, 3.3 Hz, 1H), 3.97 (dd, *J* = 10.2, 5.6 Hz, 1H), 3.86 (dd, *J* = 10.2, 5.6 Hz, 1H), 3.60 (s, 3H), 3.47–3.41 (m, 2H), 1.33 (s, 9H), 1.22 (d, *J* = 7.0 Hz, 3H), 1.15–1.13 (m, 21H). ¹³C NMR (125 MHz, CDCl₃) δ = 172.5 (C_q), 170.8 (C_q), 169.4 (C_q), 158.0 (CH), 157.3 (C_q), 155.5 (C_q), 136.0 (C_q), 128.0 (C_q), 125.6 (CH), 123.2 (C_q), 122.7 (CH), 120.1 (C_q), 119.5 (CH), 117.5 (CH), 114.4 (CH), 101.6 (C_q), 97.8 (C_q), 80.2 (C_q), 53.0 (CH), 52.1 (CH₃), 50.9 (CH), 41.5 (CH₂), 28.2 (CH₃), 28.0 (CH₂), 18.7 (CH₃), 18.3 (CH₃), 11.4 (CH). IR (neat): 2926, 2861, 2144, 1747, 1657, 1423, 1205, 710 cm⁻¹. MS (ESI) *m/z* (relative intensity): 1431 [2M+Na⁺] (18), 727 [M+Na⁺] (100), 705 [M+H⁺] (9), 389 (11), 301 (7), 182 (14). HR-MS (ESI) *m/z* calcd for C₃₇H₅₃N₆O₆Si [M+H⁺] 705.3790, found 705.3789. The enantiomeric excess was determined to be >98% by HPLC analysis of compound **227ba** and a racemic control sample.

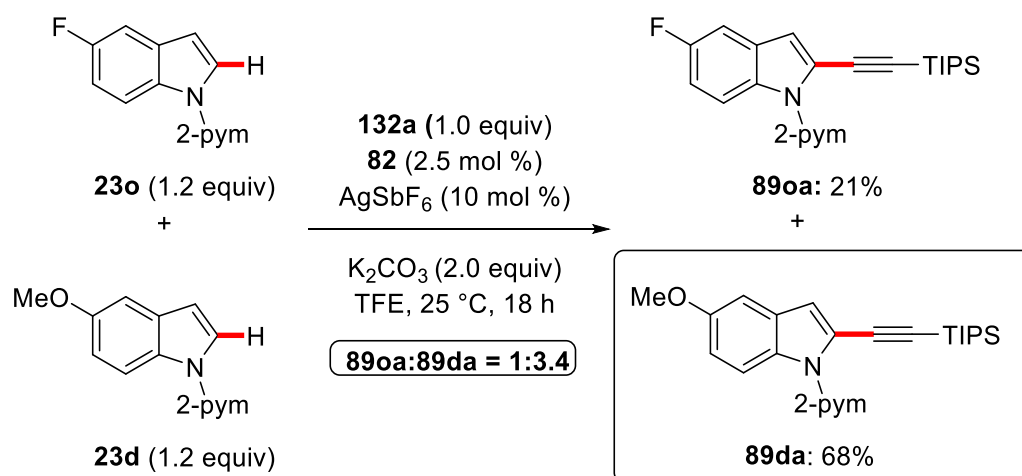


Methyl-(6*S*,12*S*)-12-(4-iodobenzyl)-2,2-dimethyl-4,7,10-trioxo-6-[[1-(pyrimidin-2-yl)-2-[(triisopropylsilyl)ethynyl]-1*H*-indol-3-yl]methyl]-3-oxa-5,8,11-triazatridecan-13-oate (227ca)

The general procedure **D** was followed using substrate **226c** (183 mg, 0.25 mmol, 1.00 equiv) and **132a** (78 mg, 0.30 mmol, 1.20 equiv). Isolation by column chromatography (*n*-pentane/EtOAc: 1/4) yielded **227ca** (154 mg, 69%) as a colorless oil. ¹H NMR (400 MHz, CDCl₃) δ = 8.76 (d, *J* = 4.6 Hz, 2H), 8.31 (d, *J* = 7.7 Hz, 1H), 7.61 (d, *J* = 8.5 Hz, 1H), 7.57 (d, *J* = 8.7 Hz, 2H), 7.31 (dd, *J* = 8.5, 1.7 Hz, 1H), 7.21 (dd, *J* = 7.7, 1.7 Hz, 1H), 7.16 (t, *J* = 4.6 Hz, 1H), 6.86 (d, *J* = 8.7 Hz, 2H), 6.46 (dd, *J* = 6.4, 6.4 Hz, 1H), 5.38 (s, 1H), 4.70 (dd, *J* = 6.2, 4.4 Hz, 1H), 4.38 (dd, *J* = 6.8, 3.9 Hz, 1H), 3.83–3.73 (m, 2H), 3.64 (s, 3H), 3.47–3.34 (m, 2H), 3.04 (dd, *J* = 11.0, 6.6 Hz, 1H), 2.93 (dd, *J* = 11.0, 6.6 Hz, 1H), 1.33 (s, 9H), 1.18–1.14 (m, 21H). ¹³C NMR (101 MHz, CDCl₃) δ = 172.1 (C_q), 171.2 (C_q), 168.4 (C_q), 158.0 (CH), 157.9 (C_q), 157.1 (C_q), 155.8 (C_q), 137.5 (CH), 135.8 (C_q), 131.2 (CH), 128.1 (C_q), 125.6 (CH), 123.2 (C_q), 122.6 (CH), 119.9 (C_q), 119.3 (CH), 117.6 (CH), 114.3 (CH), 102.1 (C_q), 97.7 (C_q), 92.5 (C_q), 80.5 (C_q), 58.8 (CH₂), 56.1 (CH), 53.3 (CH), 52.2 (CH₃), 43.1 (CH₂), 37.2 (CH₂), 28.2 (CH₃), 18.7 (CH₃), 11.3 (CH). IR (neat): 2941, 2863, 2142, 1733, 1656, 1436, 1339, 1163, 725 cm⁻¹. MS (ESI) *m/z* (relative intensity): 1836 [2M+Na⁺] (27), 929 [M+Na⁺] (100), 907 [M+H⁺] (9), 389 (12). HR-MS (ESI) *m/z* calcd for C₄₃H₅₅N₆O₆ISiNa [M+Na⁺] 705.3790, found 705.3789.

5.5.2 Mechanistic Experiments for the Cobalt Catalysis

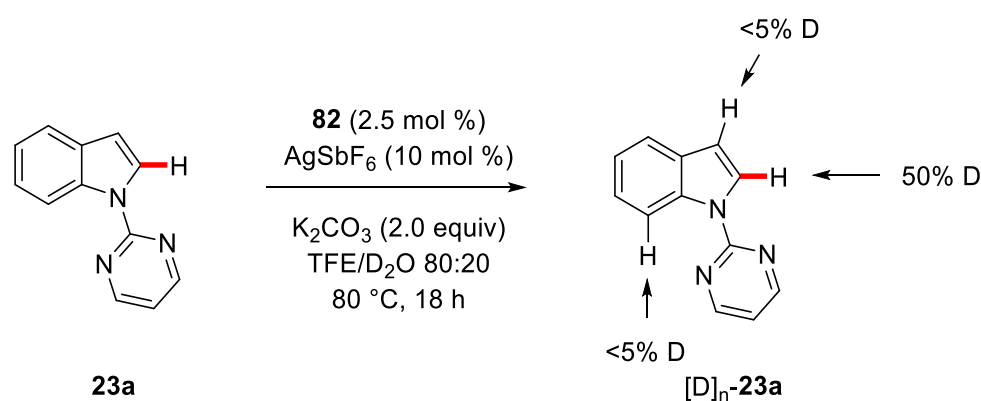
Competition Experiments:



Scheme 5.1. Intermolecular competition experiment between indoles **23o** and **23d**.

To a solution of 5-fluoro-1-(pyrimidin-2-yl)-1*H*-indole (**23o**) (63.8 mg, 0.30 mmol, 1.20 equiv), 5-methoxy-1-(pyrimidin-2-yl)-1*H*-indole (**23d**) (65.9 mg, 0.30 mmol, 1.20 equiv), [Cp*CoI₂]₂ (**82**) (5.6 mg, 6.25 μmol, 2.5 mol%), AgSbF₆ (8.8 mg, 25.0 μmol, 10 mol %) and K₂CO₃ (69.8 mg, 0.50 mmol, 2.00 equiv) in TFE (1.5 mL), **132a** (65.7 mg, 0.25 mmol, 1.0 equiv) was added. The mixture was stirred for 18 h at 25 °C. The crude mixture was analyzed by GC using tridecane as an internal standart.

H/D-Exchange Experiment



Scheme 5.2. H/D-Exchange experiment.

A solution of (pyrimidin-2-yl)-1*H*-indole (**23a**) (49.5 mg, 0.25 mmol, 1.00 equiv), [Cp*CoI₂]₂ (**82**) (5.6 mg, 6.25 μmol, 2.5 mol%), AgSbF₆ (8.8 mg, 25.0 μmol, 10 mol %) and KOAc (50.1 mg, 0.50 mmol, 2.00 equiv) in TFE (1.6 mL) and D₂O (0.4 mL) was stirred at 80 °C for 18 h. After completion of the reaction, the solvent was removed at reduced pressure and the mixture purified by column chromatography using *n*-pentane/EtOAc 5:1. The amount of deuterium incorporation was determined by ¹H-NMR.

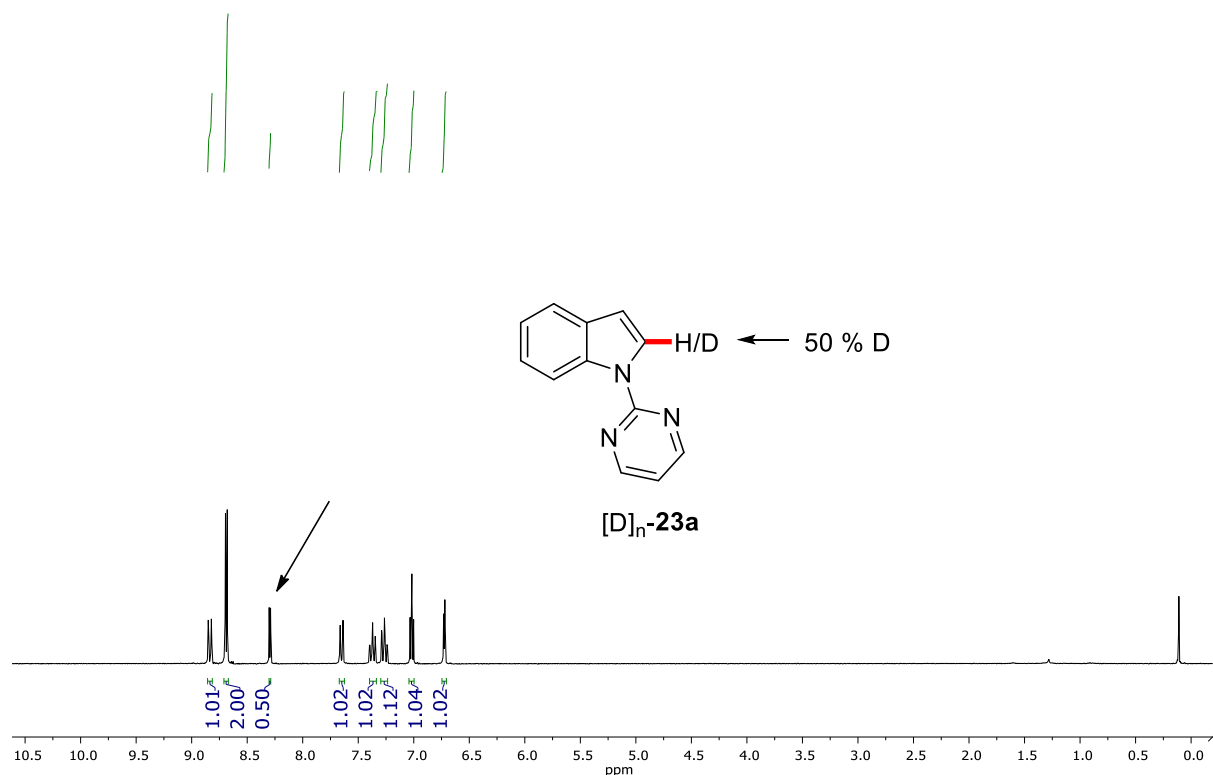


Figure 5.1. ^1H -NMR spectra of the H/D-exchange experiment.

5.5.3 Mechanistic Experiments for the Manganese Catalysis

Studies on a potential racemization of *L*- and *D*-peptides

In order to confirm that no racemization occurred within the peptides during the manganese-catalyzed C–H alkylation, we prepared the racemic substrates methyl *N*-(*tert*-butoxycarbonyl)-1-(pyrimidin-2-yl)tryptophanate (*rac*-**226a**) and methyl *N*-[(*tert*-butoxycarbonyl)alanyl]-1-(pyrimidin-2-yl)tryptophylglycinate (*rac*-**226b**). Alkylation reactions were carried out under the optimized reaction conditions. The manganese-catalyzed alkylation of *rac*-**226a** and *rac*-**226b** yielded racemic products *rac*-**227aa** and *rac*-**227ba**, respectively. Chiral HPLC analysis showed that no racemization after the manganese-catalyzed C–H alkylation process. HPLC chromatograms were recorded on an Agilent 1290 Infinity using the column CHIRALPAK® IC-3 and *n*-hexane/*i*PrOH (90:10, 1 mL/min, detection at 274 nm).

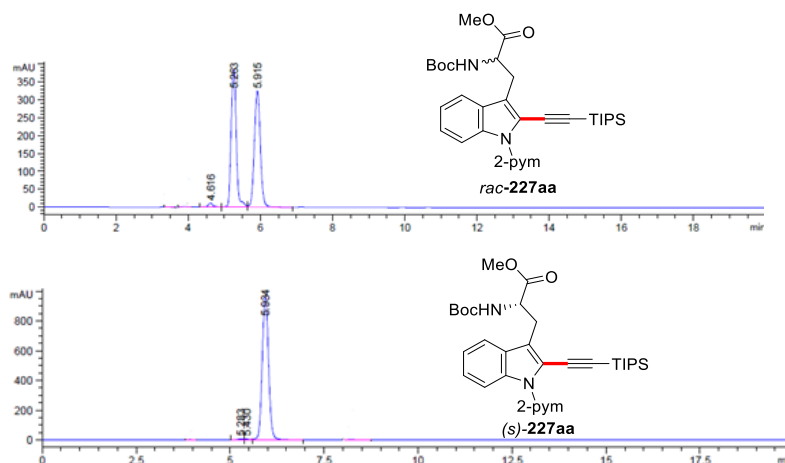


Figure 5.2. HPLC Chromatograms of *rac*-227aa and (*S*)-227aa.

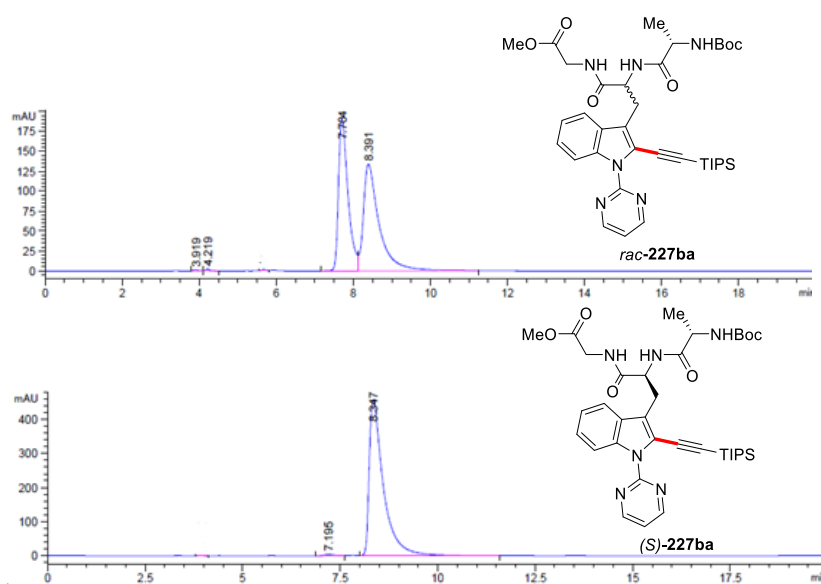
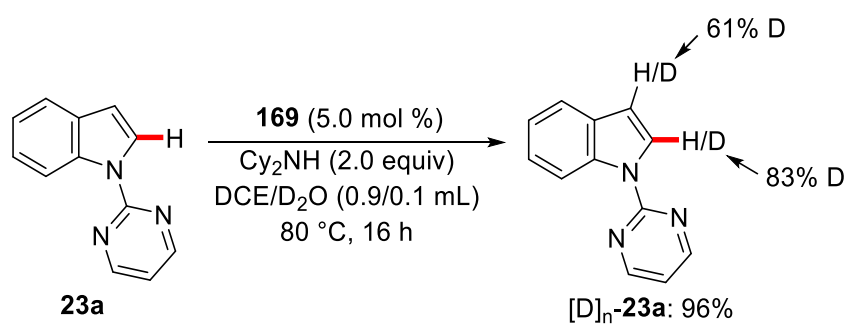


Figure 5.3. HPLC Chromatogram of *rac*-227ba and (*S*)-227ba.

Manganese-Catalyzed H/D Exchange Experiments



Scheme 5.3. H/D exchange in the absence of bromoalkyne **132a**.

1-(Pyrimidin-2-yl)-1*H*-indole (**23a**) (98.2 mg, 0.50 mmol, 1.00 equiv), MnBr(CO)₅ (**169**) (6.9 mg, 5.0 mol %), Cy₂NH (181 mg, 1.00 mmol, 2.00 equiv), DCE (0.9 mL) and D₂O (0.1 mL) were placed in a 25 mL Schlenk tube under N₂ and were then stirred at 80 °C for 16 h. At ambient temperature, the reaction mixture was diluted with H₂O (10 mL) and extracted with EtOAc (3 × 15 mL). The combined organic layer was dried with Na₂SO₄ and concentrated under reduced pressure. Purification by flash column chromatography on silica gel (*n*-hexane/EtOAc: 10/1) yielded [D]_n-**23a** (94.6 mg, 0.25 mmol, 96%). The D incorporation was determined by ¹H-NMR spectroscopy.

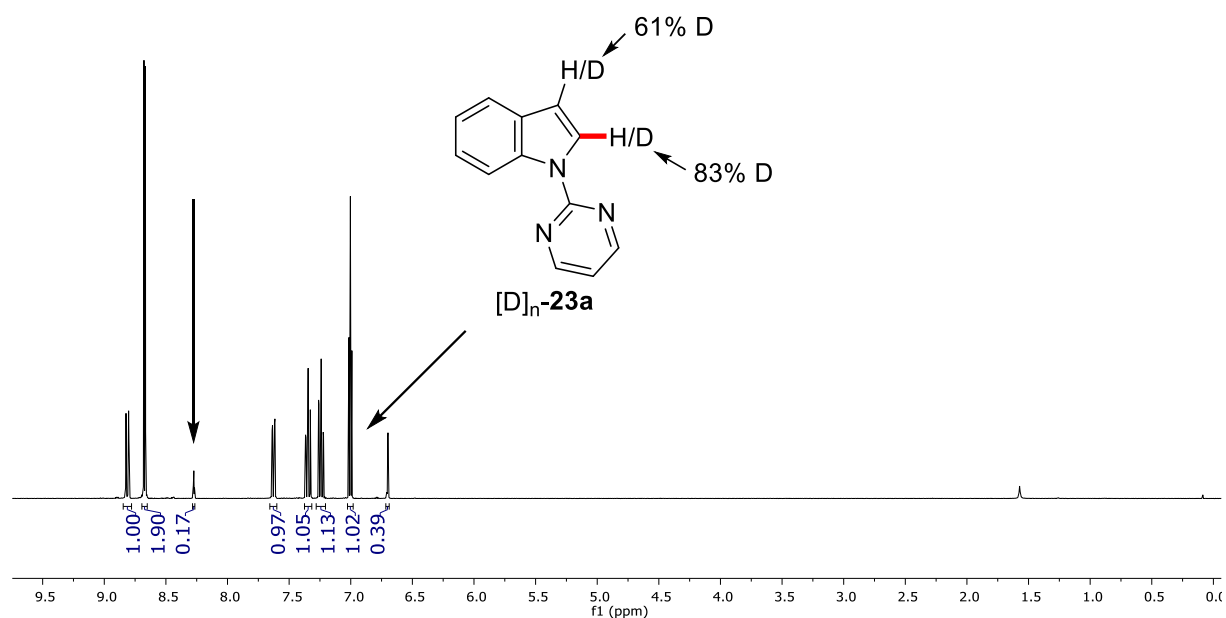
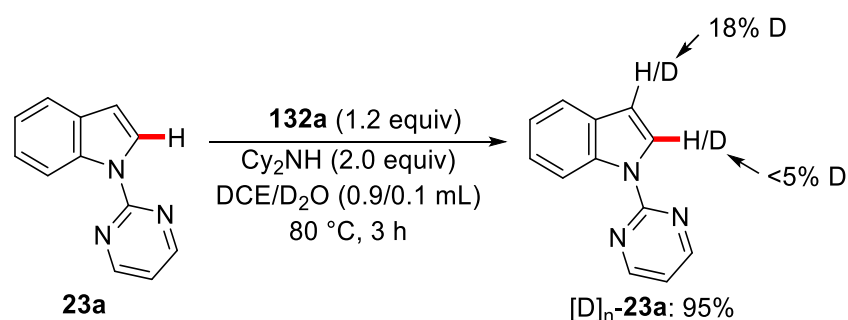


Figure 5.4. ¹H-NMR spectra of the H/D-exchange experiment in absence of bromoalkyne **132a**.

H/D Exchange Experiments in the Absence of MnBr(CO)₅



Scheme 5.4. H/D-exchange experiment in the absence of catalyst **169**.

1-(Pyrimidin-2-yl)-1*H*-indole (**23a**) (49.0 mg, 0.25 mmol, 1.00 equiv), bromoalkyne **132a** (77.5 mg, 0.30 mmol, 1.20 equiv), Cy_2NH (93.2 mg, 0.50 mmol, 2.00 equiv), DCE (0.9 mL) and D_2O (0.1 mL) were placed in a 25 mL Schlenk tube under N_2 and were then stirred at 80 °C for 3 h. At ambient temperature, the reaction mixture was diluted with H_2O (10 mL) and extracted with EtOAc (3 × 15 mL). The combined organic layer was dried with Na_2SO_4 and concentrated under reduced pressure. Purification by flash column chromatography on silica gel (*n*-hexane/EtOAc: 10/1) yielded $[\text{D}]_n\text{-23a}$ (47.3 mg, 0.24 mmol, 95%). The D incorporation was determined by $^1\text{H-NMR}$ spectroscopy.

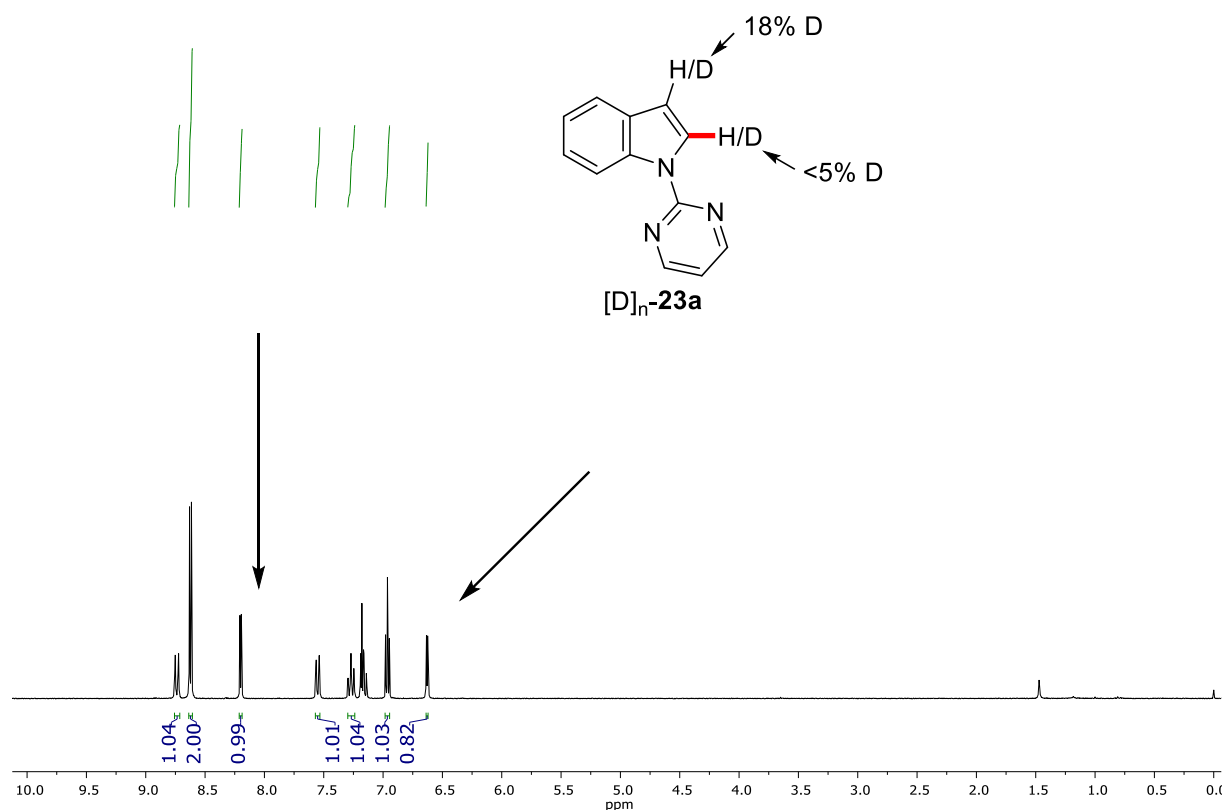
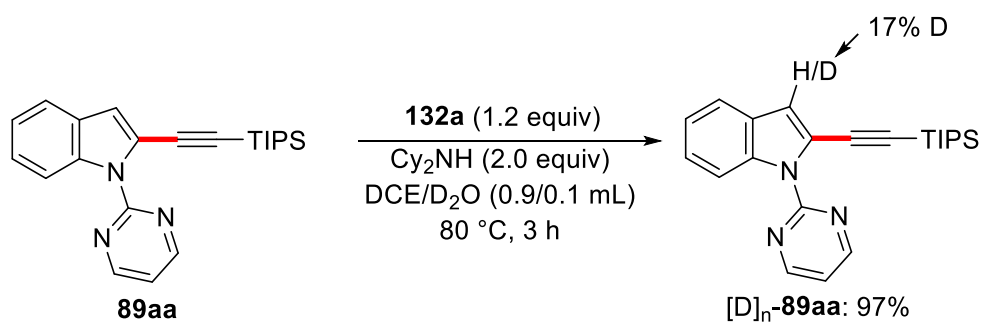


Figure 5.5. $^1\text{H-NMR}$ spectra of the H/D-exchange experiment in the absence of catalyst **169**.



Scheme 5.5. H/D-exchange experiment of product **89aa**.

1-(Pyrimidin-2-yl)-2-[(triisopropylsilyl)ethynyl]-1*H*-indole (**89aa**) (95.3 mg, 0.25 mmol, 1.00 equiv), bromoalkyne **132a** (75.2 mg, 0.30 mmol, 1.20 equiv), Cy_2NH (190 mg, 0.50 mmol), DCE (0.9 mL) and D_2O (0.1 mL) were placed in a 25 mL Schlenk tube under N_2 and were then stirred at 80 °C for 3 h. At ambient temperature, the reaction mixture was diluted with H_2O (10 mL) and extracted with EtOAc (3 × 15 mL). The combined organic layer was dried with Na_2SO_4 and concentrated under reduced pressure. Purification by flash column chromatography on silica gel (*n*-hexane/EtOAc: 10/1) yielded $[\text{D}]_n\text{-89aa}$ (91.2 mg, 0.25 mmol, 97%). The D incorporation was determined by $^1\text{H-NMR}$ spectroscopy.

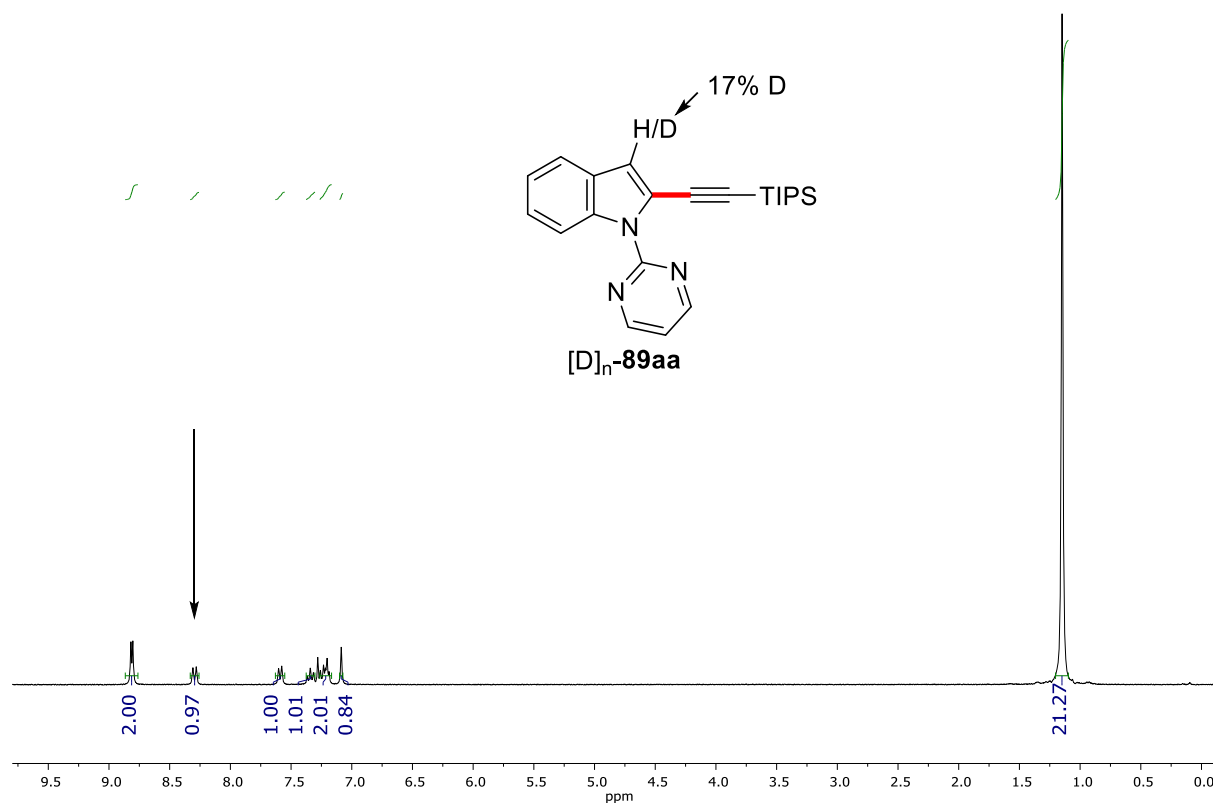
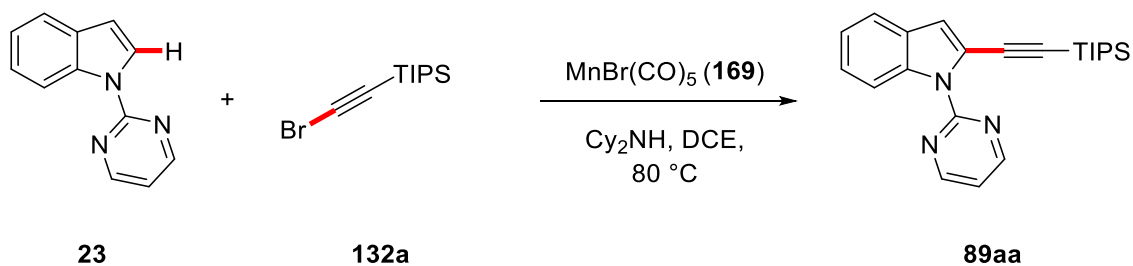


Figure 5.6. $^1\text{H-NMR}$ spectra of the H/D-exchange experiment of product **169**.

Kinetic Analysis



Scheme 5.6. Determination of the reaction order in indole **23a**.

The reaction order with respect to indole **23a** was examined using the initial rate method.^[223] A Schlenk-flask was charged with indole **23a** (0.80, 0.90, 1.00, 1.10 equiv.), **132a** (209 mg, 0.80 mmol), MnBr(CO)₅ (**169**) (11 mg, 5.0 mol %) and *n*-tridecane (80 μL). DCE (4.0 mL) was added and the mixture was divided into four pre-heated Schlenk-tubes and stirred at 80 °C. After one minute the first reaction was opened and a sample removed by syringe, diluted with EtOAc, filtered through a short plug of silica gel and Na₂SO₄ and analyzed by gas chromatography. This was repeated for all reactions with a time difference of one minute between each sample.

Equiv 23q	$\Delta[\mathbf{89aa}] \Delta t^{-1} / \text{mol L}^{-1} \text{ s}^{-1}$	$\log(c / \text{mol L}^{-1})$	$\log(\Delta[\mathbf{89aa}] \Delta t^{-1} / \text{mol L}^{-1} \text{ s}^{-1})$
0.8	2.188	-0.795	0.340
0.9	2.500	-0.745	0.398
1.0	2.858	-0.699	0.456
1.1	3.069	-0.658	0.487

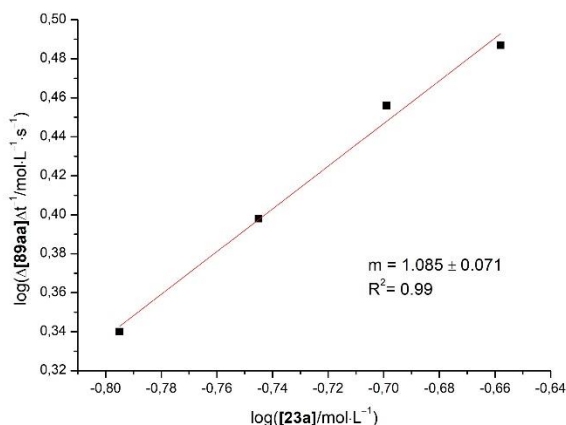
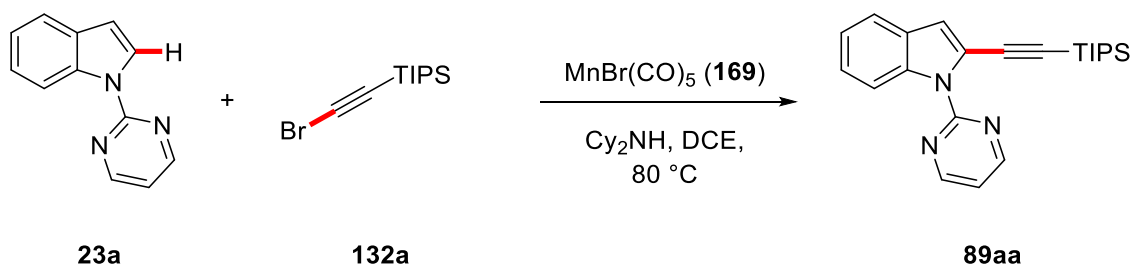


Figure 5.7. Reaction order in indole **23a**.



Scheme 5.7. Determination of the reaction order in bromoalkyne **132a**.

The reaction order with respect to alkyne **132a** was examined using the initial rate method.^[223] A Schlenk-flask was charged with indole **23a** (156 mg, 0.80 mmol, 1.00 equiv.), **132a** (0.80, 1.00, 1.20, 1.40 equiv), MnBr(CO)₅ (**169**) (11 mg, 5.0 mol %) and *n*-tridecane (80 μL). DCE (4.0 mL) was added and the mixture was divided into four pre-heated Schlenk-tubes and stirred at 80 °C. After one minute the first reaction was opened and a sample removed by syringe, diluted with EtOAc, filtered through a short plug of silica gel and Na₂SO₄ and analyzed by gas chromatography. This was repeated for all reactions with a time difference of one minute between each sample.

Equiv 132a	$\Delta[\mathbf{89aa}] \Delta t^{-1} / \text{mol L}^{-1} \text{s}^{-1}$	$\log(c / \text{mol L}^{-1})$	$\log(\Delta[\mathbf{89aa}] \Delta t^{-1} / \text{mol L}^{-1} \text{s}^{-1})$
0.8	2.187	-0.795	0.340
1.0	2.853	-0.699	0.455
1.2	3.250	-0.619	0.512
1.4	3.802	-0.553	0.580

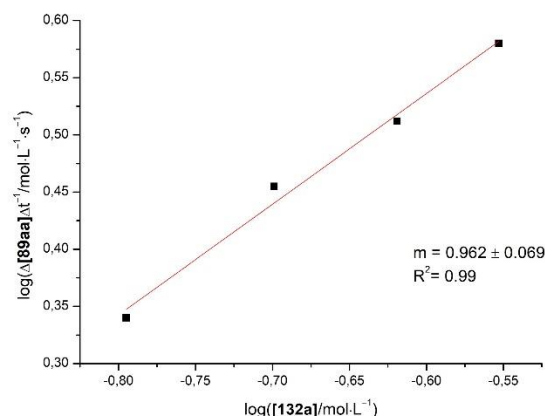
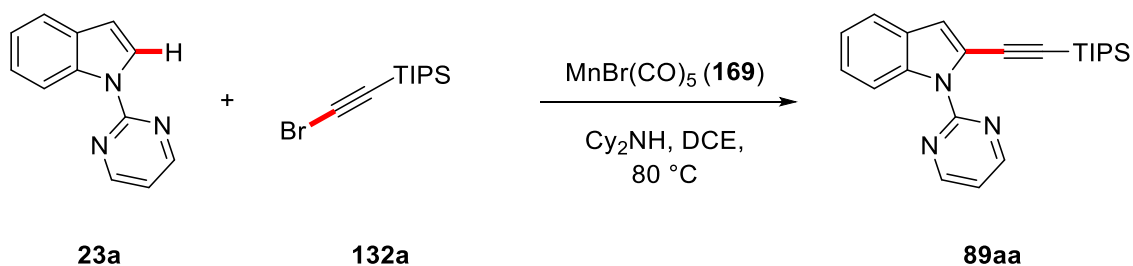


Figure 5.8. Reaction order in bromoalkyne **132a**.



Scheme 5.8. Determination of the reaction order in catalyst **169**.

The reaction order with respect to the catalyst **169** was examined using the initial rate method.^[223] A Schlenk-flask was charged with indole **23a** (117 mg, 0.60 mmol, 1.00 equiv.), **132a** (188 mg, 0.72 mmol, 1.20 equiv), MnBr(CO)_5 (2.5, 5.0, 7.5, 10 mol %) and *n*-tridecane (80 μL). DCE (4.0 mL) was added and the mixture was divided into four pre-heated Schlenk-tubes and stirred at 80 °C. After one minute the first reaction was opened and a sample removed by syringe, diluted with EtOAc, filtered through a short plug of silica gel and Na_2SO_4 and analyzed by gas chromatography. This was repeated for all reactions with a time difference of one minute between each sample.

Mol % catalyst	$\Delta[\mathbf{89aa}] \Delta t^{-1} / 10^{-8} \text{ mol L}^{-1} \text{ s}^{-1}$	$\log(c / \text{mol L}^{-1})$	$\log(\Delta[\mathbf{89aa}] \Delta t^{-1} / \text{mol L}^{-1} \text{ s}^{-1})$
3.5	0.889	-2.426	-0.051
5.0	1.528	-2.125	0.184
7.5	2.208	-1.948	0.344

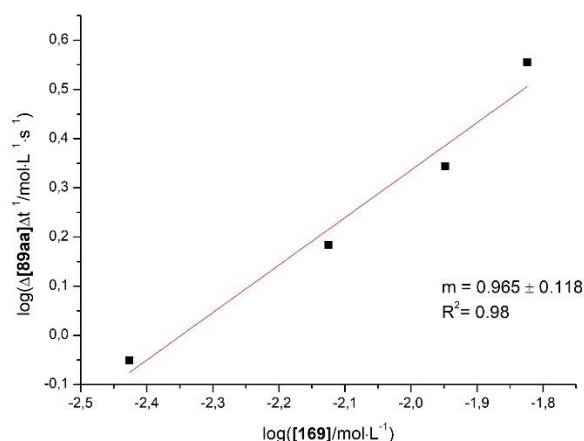
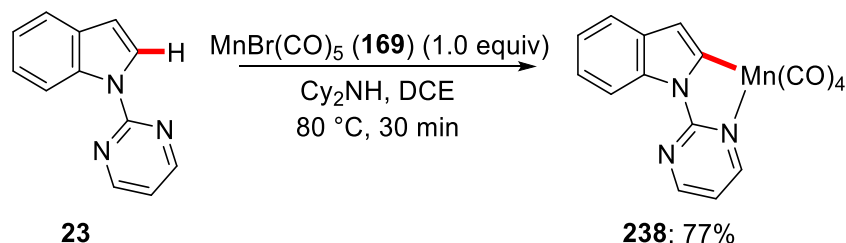


Figure 5.9. Reaction order in catalyst **169**.

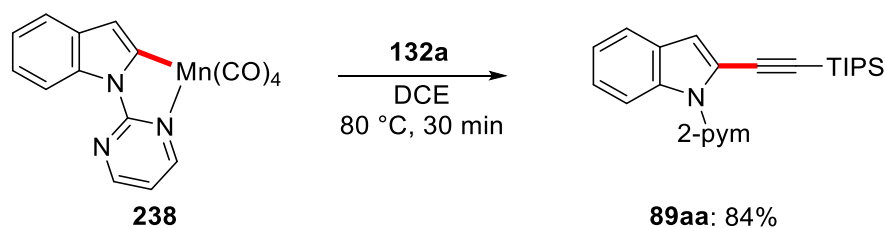
C–H Alkynylations with Cyclometalated Complex **238**



Scheme 5.10. Synthesis of manganacycle **238**.

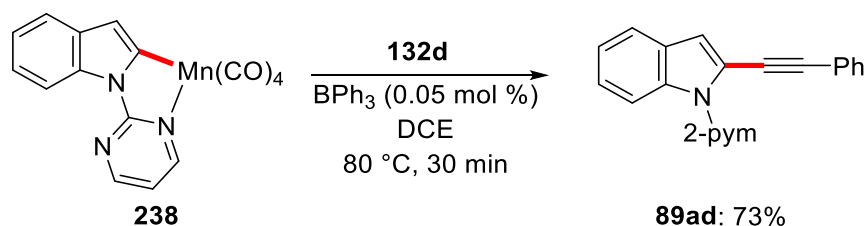
Following a modification of a reported procedure,^[129] 1-(pyrimidin-2-yl)-1*H*-indole (**23**) (195 mg, 1.00 mmol, 1.00 equiv), MnBr(CO)₅ (**169**) (274 mg, 1.00 mmol, 1.00 equiv), Cy₂NH (362 mg, 2.00 mmol, 2.00 equiv) and DCE (2.0 mL) were placed in a 25 mL Schlenk tube under N₂ and then stirred at 80 °C for 30 min. At ambient temperature, the mixture was diluted with EtOAc (20 ml) and filtered through a short pad of celite. The solvent was removed by rotary evaporation and the residue was purified by flash column chromatography on silica gel (*n*-hexane/EtOAc: 20/1) afforded **238** (279 mg, 0.77 mmol, 77%) as a yellow solid. An alternative preparation with catalytic amounts of BPh₃ (0.05 mol %, 0.01 M stock solution in DCE) under otherwise identical conditions afforded the same product (268 mg, 0.74 mmol, 74%). M.p. = 150–151 °C. ¹H NMR (300 MHz, CDCl₃) δ = 8.69 (dd, *J* = 4.8, 2.4 Hz, 1H), 8.57 (dd, *J* = 5.6, 2.4 Hz, 1H), 8.50 (d, *J* = 8.0 Hz, 1H), 7.44 (d, *J* = 7.5 Hz, 1H), 7.20 (dd, *J* = 7.5, 7.3 Hz, 1H),

7.12 (dd, $J = 7.5, 7.2$, 1H), 6.85 (t, $J = 5.2$ Hz, 1H), 6.79 (s, 1H). ^{13}C NMR (125 MHz, CDCl_3) $\delta = 218.4$ (C_q), 213.1 (C_q), 210.7 (C_q), 162.2 (CH), 161.3 (C_q), 160.9 (C_q), 160.1 (CH), 138.5 (C_q), 136.0 (C_q), 122.9 (CH), 120.7 (CH), 119.3 (CH), 117.5 (CH), 114.1 (CH), 113.6 (CH). IR (neat): 2078, 1974, 1937, 1920, 1575, 1491, 1380, 787, 639 cm^{-1} . MS (EI) m/z (relative intensity): 360 [M^+] (5), 249 (35), 195 (100). HR-MS (EI) m/z calcd for $\text{C}_{16}\text{H}_8\text{MnN}_3\text{O}_4$ [M^+] 360.9895, found 360.9880.



Scheme 5.11. Stoichiometric C–H alkylation using bromoalkyne **132a**.

Complex **238** (72.8 mg, 0.20 mmol, 1.00 equiv), bromoalkyne **132a** (62.3 mg, 0.24 mmol, 1.20 equiv), and DCE (0.5 mL) were placed in a 25 mL Schlenk tube under N_2 and were then stirred at 80 °C for 30 min. At ambient temperature, CH_2Cl_2 (2 mL) was added, and the reaction mixture was transferred into a round bottom flask with CH_2Cl_2 and concentrated under reduced pressure. Purification by flash column chromatography on silica gel (n -hexane/EtOAc: 10/1) afforded **89aa** (64.3 mg, 0.17 mmol, 84%).

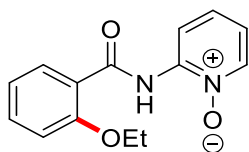


Scheme 5.12. Stoichiometric C–H alkylation **132d**.

Complex **238** (72 mg, 0.20 mmol, 1.00 equiv), bromoalkyne **132d** (43.4 mg, 0.24 mmol, 1.20 equiv), BPh_3 (10 μL , 0.05 mol %, 0.01 M stock solution in DCE) and DCE (0.5 mL) were placed in a 25 mL Schlenk tube under N_2 and were then stirred at 80 °C for 30 min. At ambient temperature, CH_2Cl_2 (2 mL) was added, and the reaction mixture was transferred into a round bottom flask with CH_2Cl_2 and concentrated under reduced pressure. Purification by flash column chromatography on silica gel (n -hexane/EtOAc: 8/1) afforded **89ad** (43.2 mg, 0.15 mmol, 73%).

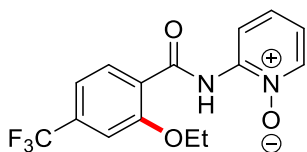
5.6 Electrochemical Cobalt-Catalyzed C–H Oxygenation

5.6.1 Analytical Data and Experimental Procedures



2-(2-Ethoxybenzamido)pyridine-1-oxide (**150aa**)

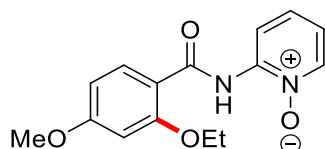
The general procedure **F** was followed using benzamide **117a** (107 mg, 0.50 mmol, 1.00 equiv) and ethanol (**149a**) (2 × 7.0 mL). Purification by column chromatography on silica gel (CH₂Cl₂/acetone 3:1) yielded **150aa** (97.5 mg, 376 μmol, 75%) as a white solid. M. p.: 141–143 °C. ¹H-NMR (500 MHz, CDCl₃): δ = 12.29 (s, 1H), 8.72 (dd, *J* = 8.6, 1.9 Hz, 1H), 8.30–8.23 (m, 2H), 7.50 (ddd, *J* = 8.4, 2.1, 0.7 Hz 1H), 7.32 (dd, *J* = 8.6, 1.9 Hz, 1H), 7.11–7.01 (m, 2H), 6.97 (dd, *J* = 8.4, 2.1 Hz, 1H), 4.29 (q, *J* = 6.7 Hz, 2H), 1.69 (t, *J* = 6.7 Hz, 3H). ¹³C-NMR (125 MHz, CDCl₃): δ = 163.8 (C_q), 157.3 (C_q), 145.3 (C_q), 137.2 (CH), 134.2 (CH), 132.5 (CH), 127.7 (CH), 121.0 (CH), 120.5 (C_q), 118.3 (CH), 115.7 (CH), 112.3 (CH), 65.3 (CH₂), 14.8 (CH₃). IR (ATR): 3178, 3060, 1658, 1507, 1278, 1241, 1029, 737 cm⁻¹. MS (EI) *m/z* (relative intensity): 258 (10) [M]⁺, 241 (12), 197 (34), 149 (55), 121 (100), 93 (22). HR-MS (EI) *m/z* calcd for C₁₄H₁₄N₂O₃ [M]⁺: 258.1004, found: 258.1009. The analytical data correspond with those reported in the literature.^[111b]



2-(2-Ethoxy-4-(trifluoromethyl)benzamido)pyridine-1-oxide (**150ba**)

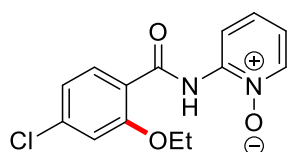
The general procedure **F** was followed using benzamide **117b** (141 mg, 0.50 mmol, 1.00 equiv) and ethanol (**149a**) (2 × 7.0 mL). Purification by column chromatography on silica gel (CH₂Cl₂/acetone 3:1) yielded **150ba** (85.3 mg, 262 μmol, 52%) as a white solid. M. p.: 186–189 °C. ¹H-NMR (400 MHz, CDCl₃): δ = 12.26 (s, 1H), 8.68 (dd, *J* = 8.4, 1.7 Hz, 1H), 8.37 (d, *J* = 8.0 Hz, 1H), 8.28 (dd, *J* = 6.7, 1.4 Hz, 1H), 7.39–7.30 (m, 2H), 7.28 (s, 1H), 7.00 (ddd, *J* = 8.4, 6.4, 1.7 Hz, 1H), 4.39 (q, *J* = 7.0 Hz, 2H), 1.73 (t, *J* = 7.0 Hz, 3H). ¹³C-NMR (125 MHz, CDCl₃): δ = 162.7 (C_q), 157.4 (C_q), 145.0 (C_q), 137.3 (CH), 135.6 (q, ²*J*_{C-F} = 33.3 Hz, C_q), 133.5 (CH), 127.8 (CH), 123.5 (C_q), 123.4

(q, $^1J_{C-F} = 280$ Hz, C_q), 118.9 (CH), 117.6 (q, $^3J_{C-F} = 3.8$ Hz, CH), 116.0 (q, $^3J_{C-F} = 4.0$ Hz, CH), 109.5 (CH), 66.1 (CH₂), 14.6 (CH₃). ^{19}F -NMR (282 MHz, CDCl₃): $d = -63.19$. IR (ATR): 3180, 3061, 1654, 1501, 1268, 1071, 760, 744 cm⁻¹. MS (EI) m/z (relative intensity): 326 (10) [M]⁺, 209 (19), 265 (31), 217 (40), 189 (100), 161 (28), 113 (10). HR-MS (EI) m/z calcd for C₁₅H₁₃F₃N₂O₃ [M]⁺: 326.0878, found: 326.0876.



2-(2-Ethoxy-4-methoxybenzamido)pyridine-1-oxide (150ca)

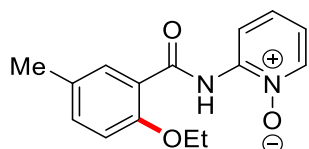
The general procedure **F** was followed using benzamide **117c** (123 mg, 0.50 mmol, 1.00 equiv) and ethanol (**149a**) (2 × 7.0 mL). Purification by column chromatography on silica gel (CH₂Cl₂/acetone 2:1) yielded **150ca** (106.3 mg, 369 μmol, 74%) as a white solid. M. p.: 191–193 °C. 1H -NMR (300 MHz, CDCl₃): $\delta = 12.13$ (s, 1H), 8.72 (d, $J = 7.9$ Hz, 1H), 8.28 (d, $J = 2.1$ Hz, 1H), 8.22 (d, $J = 9.3$ Hz, 1H), 7.29 (d, $J = 7.9$, 2.1 Hz, 1H), 6.96 (dd, $J = 7.4$, 7.1 Hz, 1H), 6.60 (dd, $J = 9.3$, 2.5 Hz, 1H), 6.53 (d, $J = 2.5$ Hz, 1H), 4.27 (q, $J = 7.0$ Hz, 2H), 3.84 (s, 3H), 1.64 (t, $J = 7.0$ Hz, 3H). ^{13}C -NMR (125 MHz, CDCl₃): $\delta = 164.5$ (C_q), 163.6 (C_q), 158.8 (C_q), 145.7 (C_q), 137.3 (CH), 134.3 (CH), 127.8 (CH), 117.7 (CH), 115.6 (CH), 113.6 (C_q), 105.7 (CH), 99.1 (CH), 65.4 (CH₂), 55.6 (CH₃), 14.7 (CH₃). IR (ATR): 3193, 3057, 2203, 2120, 1658, 1504, 1030, 727, 516 cm⁻¹. MS (EI) m/z (relative intensity): 288 (12) [M]⁺, 227 (10), 179 (100), 151 (82), 95 (15). HR-MS (EI) m/z calcd for C₁₅H₁₆N₂O₄ [M]⁺: 288.1110, found: 288.1120. The analytical data correspond with those reported in the literature.^[111b]



2-(4-Chloro-2-ethoxybenzamido)pyridine-1-oxide (150da)

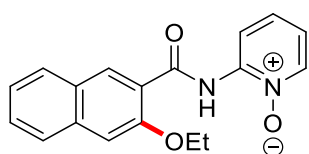
The general procedure **F** was followed using benzamide **117d** (125 mg, 0.50 mmol, 1.00 equiv) and ethanol (**149a**) (2 × 7.0 mL). Purification by column chromatography on silica gel (CH₂Cl₂/acetone 3:1) yielded **150da** (72.4 mg, 292 μmol, 58%) as a white solid. M. p.: 196–199 °C. 1H -NMR (300 MHz, CDCl₃): $\delta = 12.14$ (s, 1H), 8.68 (dd, $J = 7.9$, 1.8 Hz, 1H), 8.31 (dd, $J = 7.0$, 2.1 Hz, 1H), 8.17 (d, $J = 7.6$ Hz, 1H), 7.34 (dd, $J = 7.9$, 7.5, 2.1 Hz, 1H), 7.09–7.01 (m, 2H), 6.99 (dd, $J = 7.5$, 7.0, 1.8 Hz, 1H), 4.31 (q,

$J = 7.2$ Hz, 2H), 1.68 (t, $J = 7.2$ Hz, 3H). $^{13}\text{C-NMR}$ (125 MHz, CDCl_3): $\delta = 162.8$ (C_q), 157.7 (C_q), 145.1 (C_q), 140.1 (C_q), 137.3 (CH), 133.7 (CH), 128.0 (CH), 121.4 (CH), 119.1 (C_q), 118.5 (CH), 115.8 (CH), 113.0 (CH), 65.0 (CH_2), 14.6 (CH_3). IR (ATR): 3184, 3054, 1653, 1502, 1268, 760, 744 cm^{-1} . MS (EI) m/z (relative intensity): 294 (4) [$^{37}\text{Cl-M}$] $^+$, 292 (12) [$^{35}\text{Cl-M}$] $^+$, 277 (5), 275 (15), 185 (23), 183 (75), 157 (33), 155 (100), 127 (19), 99 (15). HR-MS (EI) m/z calcd for $\text{C}_{14}\text{H}_{13}\text{N}_2\text{O}_3^{35}\text{Cl}$ [M] $^+$: 292.0615, found: 292.0617. The analytical data correspond with those reported in the literature.^[111b]



2-(2-Ethoxy-5-methylbenzamido)pyridine-1-oxide (150ea)

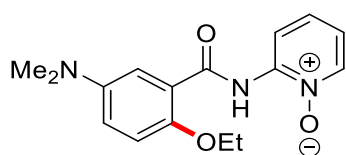
The general procedure **F** was followed using benzamide **117e** (114 mg, 0.50 mmol, 1.00 equiv) and ethanol (**149a**) (2 × 7.0 mL). Purification by column chromatography on silica gel (CH_2Cl_2 /acetone 3:1) yielded **150ea** (106 mg, 389 μmol , 78%) as a white solid. M. p.: 183–186 °C. $^1\text{H-NMR}$ (300 MHz, CDCl_3): $\delta = 12.27$ (s, 1H), 8.70 (dd, $J = 8.7, 2.3$ Hz, 1H), 8.27 (dd, $J = 7.2, 1.8$ Hz, 1H), 8.05 (d, $J = 2.0$ Hz, 1H), 7.35–7.26 (m, 2H), 7.00–6.97 (m, 2H), 4.29 (q, $J = 6.9$ Hz, 2H), 2.33 (s, 3H), 1.67 (t, $J = 6.9$ Hz, 3H). $^{13}\text{C-NMR}$ (125 MHz, CDCl_3): $\delta = 164.0$ (C_q), 155.3 (C_q), 145.4 (C_q), 137.3 (CH), 134.7 (CH), 132.6 (CH), 130.3 (CH), 127.7 (C_q), 120.0 (C_q), 118.2 (CH), 115.7 (CH), 112.3 (CH), 65.3 (CH_2), 20.4 (CH_3), 14.8 (CH_3). IR (ATR): 3176, 2918, 1657, 1508, 1278, 795, 511 cm^{-1} . MS (EI) m/z (relative intensity): 272 (19) [M] $^+$, 255 (23), 163 (87), 135 (100), 107 (26), 77 (21). HR-MS (EI) m/z calcd for $\text{C}_{15}\text{H}_{16}\text{N}_2\text{O}_3$ [M] $^+$: 272.1161, found: 272.1165. The analytical data correspond with those reported in the literature.^[111b]



2-(3-Ethoxy-2-naphthamido)pyridine-1-oxide (150fa)

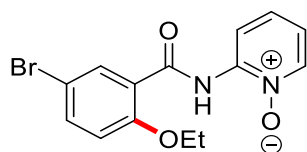
The general procedure **F** was followed using benzamide **117f** (132 mg, 0.50 mmol, 1.00 equiv) and ethanol (**149a**) (2 × 7.0 mL). Purification by column chromatography on silica gel (CH_2Cl_2 /acetone 3:1) yielded **150fa** (108 mg, 351 μmol , 70%) as a white solid. M. p.: 191–193 °C. $^1\text{H-NMR}$ (400 MHz, CDCl_3): $\delta = 12.39$ (s, 1H), 8.94 (s, 1H), 8.76 (dd, $J = 8.9, 1.5$ Hz, 1H), 8.30 (dd, $J = 6.8, 2.3$ Hz, 1H), 7.91 (dd, $J = 8.0, 0.9$ Hz,

1H), 7.74 (dd, $J = 9.2, 1.0$ Hz, 1H), 7.54 (dd, $J = 8.9, 6.9, 2.3$ Hz, 1H), 7.39 (dd, $J = 8.0, 7.7, 1.0$ Hz, 1H), 7.36 (dd, $J = 6.9, 6.8, 1.5$ Hz, 1H), 7.28 (s, 1H), 7.00 (dd, $J = 9.2, 7.7, 0.9$ Hz, 1H), 4.43 (q, $J = 7.1$ Hz, 2H), 1.80 (t, $J = 7.1$ Hz, 3H). $^{13}\text{C-NMR}$ (101 MHz, CDCl_3): $\delta = 163.9$ (C_q), 154.1 (C_q), 145.4 (C_q), 137.5 (CH), 136.5 (CH), 134.9 (CH), 129.3 (CH), 128.9 (CH), 127.9 (CH), 126.3 (C_q), 124.7 (CH), 121.5 (CH), 118.6 (C_q), 116.0 (CH), 107.5 (CH), 65.4 (CH_2), 14.7 (CH_3). IR (ATR): 3189, 2918, 1652, 1507, 1278, 1200, 1038, 725 cm^{-1} . MS (EI) m/z (relative intensity): 308 (13) $[\text{M}]^+$, 291 (15), 247 (30), 199 (89), 171 (100), 155 (22), 127 (19), 115 (41). HR-MS (ESI) m/z calcd for $\text{C}_{18}\text{H}_{16}\text{N}_2\text{O}_3$ $[\text{M}]^+$: 308.1161, found: 308.1158.



2-[5-(Dimethylamino)-2-ethoxybenzamido]pyridine-1-oxide (150ga)

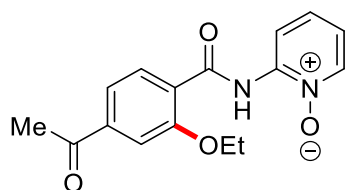
The general procedure **F** was followed using benzamide **117g** (128 mg, 0.50 mmol, 1.00 equiv) and ethanol (**149a**) (2 × 7.0 mL). Purification by column chromatography on silica gel ($\text{CH}_2\text{Cl}_2/\text{acetone}$ 3:1) yielded **150ga** (97.9 mg, 294 μmol , 59%) as a yellow solid. M. p.: 183–186 °C. $^1\text{H-NMR}$ (400 MHz, CDCl_3): $\delta = 12.35$ (s, 1H), 8.67 (dd, $J = 8.5, 2.3$ Hz, 1H), 8.22 (dd, $J = 8.0, 1.9$ Hz, 1H), 7.60 (d, $J = 2.3$ Hz, 1H), 7.27 (dd, $J = 8.0, 6.8, 2.3$ Hz, 1H), 6.94–6.86 (m, 3H), 4.21 (q, $J = 7.4$ Hz, 2H), 2.87 (s, 6H), 1.59 (t, $J = 7.4$ Hz, 3H). $^{13}\text{C-NMR}$ (125 MHz, CDCl_3): $\delta = 164.4$ (C_q), 149.6 (C_q), 145.7 (C_q), 145.4 (C_q), 137.5 (CH), 127.8 (CH), 120.5 (C_q), 119.3 (CH), 118.2 (CH), 116.2 (CH), 115.7 (CH), 113.8 (CH), 65.6 (CH_2), 41.3 (CH_3), 14.8 (CH_3). IR (ATR): 3196, 3057, 2931, 1657, 1502, 1426, 1204, 725 cm^{-1} . MS (ESI) m/z (relative intensity): 324 (19) $[\text{M}+\text{Na}]^+$, 302 (100), $[\text{M}+\text{H}]^+$, 288 (7), 209 (25), 192 (47). HR-MS (ESI) m/z calcd for $\text{C}_{16}\text{H}_{19}\text{N}_3\text{O}_3$ $[\text{M}+\text{H}]^+$: 302.1499, found: 302.1497. The analytical data correspond with those reported in the literature.^[11b]



2-(5-Bromo-2-ethoxybenzamido)pyridine-1-oxide (150ha)

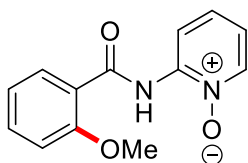
The general procedure **F** was followed using benzamide **117h** (146 mg, 0.50 mmol, 1.00 equiv) and ethanol (**149a**) (2 × 7.0 mL). Purification by column chromatography

on silica gel (CH₂Cl₂/acetone 3:1) yielded **150ha** (96.3 mg, 286 μmol, 57%) as a white solid. M. p.: 224–226 °C. ¹H-NMR (300 MHz, CDCl₃): δ = 12.22 (s, 1H), 8.67 (dd, *J* = 8.1, 2.5 Hz, 1H), 8.37 (d, *J* = 3.0 Hz, 1H), 8.27 (dd, *J* = 7.5, 2.3 Hz, 1H), 7.58 (dd, *J* = 8.1, 3.0 Hz, 1H), 7.34 (ddd, *J* = 8.1, 6.8, 2.3 Hz, 1H), 7.00 (ddd, *J* = 7.5, 6.8, 2.5 Hz, 1H), 6.93 (d, *J* = 8.1 Hz, 1H), 4.23 (q, *J* = 7.2 Hz, 2H), 1.68 (t, *J* = 7.2 Hz, 3H). ¹³C-NMR (125 MHz, CDCl₃): δ = 162.4 (C_q), 156.3 (C_q), 145.1 (C_q), 137.2 (CH), 136.7 (CH), 135.1 (CH), 127.7 (CH), 122.2 (C_q), 118.7 (CH), 115.8 (CH), 114.3 (CH), 113.5 (C_q), 65.9 (CH₂), 14.7 (CH₃). IR (ATR): 3163, 2924, 1656, 1562, 1508, 1238, 1028, 747 cm⁻¹. MS (ESI) *m/z* (relative intensity): 361 (29) [⁸¹Br-M+Na]⁺, 359 (31) [⁷⁹Br-M+Na]⁺, 339 (39) [⁸¹Br-M+H]⁺, 337 (29) [⁷⁹Br-M+H]⁺, 242 (100), 227 (10). HR-MS (ESI) *m/z* calcd for C₁₄H₁₃N₂O₃⁷⁹Br [⁷⁹Br-M+H]⁺: 337.0182, found: 337.0184.



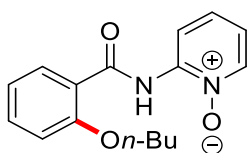
2-(4-Acetyl-2-ethoxybenzamido)pyridine-1-oxide (**150ia**)

The general procedure **F** was followed using benzamide **117i** (129 mg, 0.50 mmol, 1.00 equiv) and ethanol (**149a**) (2 × 7.0 mL). Purification by column chromatography on silica gel (CH₂Cl₂/acetone 3:1) yielded **150ia** (92.1 mg, 307 μmol, 61%) as a white solid. M. p.: 131–133 °C. ¹H-NMR (300 MHz, CDCl₃): δ = 12.27 (s, 1H), 8.70 (dd, *J* = 8.7, 2.1 Hz, 1H), 8.34 (d, *J* = 8.8 Hz, 1H), 8.30 (dd, *J* = 8.0, 2.3 Hz, 1H), 7.63 (d, *J* = 1.4 Hz, 1H), 7.52 (dd, *J* = 8.8, 1.4 Hz, 1H), 7.32 (dd, *J* = 8.7, 7.7, 2.3 Hz, 1H), 7.01 (dd, *J* = 8.0, 7.7, 2.1 Hz, 1H), 4.40 (q, *J* = 6.8 Hz, 2H), 2.62 (s, 3H), 1.71 (t, *J* = 6.8 Hz, 3H). ¹³C-NMR (125 MHz, CDCl₃): δ = 197.2 (C_q), 162.9 (C_q), 157.4 (C_q), 145.3 (C_q), 141.4 (C_q), 137.5 (CH), 133.1 (CH), 127.9 (CH), 124.2 (C_q), 121.0 (CH), 118.7 (CH), 115.8 (CH), 111.4 (CH), 65.8 (CH₂), 26.8 (CH₃), 14.6 (CH₃). IR (ATR): 3183, 2924, 1683, 1608, 1503, 1428, 1207, 756 cm⁻¹. MS (EI) *m/z* (relative intensity): 300 (15) [M]⁺, 283 (23), 256 (21), 191 (93), 163 (100), 147 (85), 119 (249, 91 (20), 43 (57). HR-MS (EI) *m/z* calcd for C₁₆H₁₆N₂O₄ [M]⁺: 300.1110, found: 300.1111. The analytical data correspond with those reported in the literature.^[111b]



2-(2-Methoxybenzamido)pyridine-1-oxide (**150ab**)

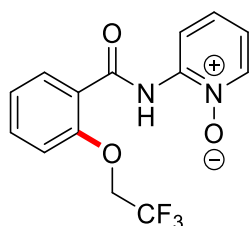
The general procedure **F** was followed using benzamide **117a** (107 mg, 0.50 mmol, 1.00 equiv) and methanol (**150b**) (2 × 7.0 mL). Purification by column chromatography on silica gel (CH₂Cl₂/acetone 2:1) yielded **150ab** (86.8 mg, 256 μmol, 71%) as a white solid. M. p.: 121–124 °C. ¹H-NMR (400 MHz, CDCl₃): δ = 12.41 (s, 1H), 8.67 (dd, *J* = 8.3, 1.7 Hz, 1H), 8.28–8.25 (m, 2H), 7.53 (ddd, *J* = 7.9, 7.0, 1.7 Hz, 1H), 7.35 (ddd, *J* = 8.3, 7.0, 1.4 Hz, 1H), 7.10 (ddd, *J* = 8.5, 7.5, 2.1 Hz, 1H), 7.05 (dd, *J* = 8.5, 1.0 Hz, 1H), 6.97 (ddd, *J* = 8.0, 7.5, 1.0 Hz, 1H), 4.13 (s, 3H). ¹³C-NMR (101 MHz, CDCl₃): δ = 163.5 (C_q), 157.9 (C_q), 145.4 (C_q), 137.3 (CH), 134.3 (CH), 132.4 (CH), 128.3 (CH), 121.3 (CH), 120.4 (C_q), 118.3 (CH), 115.5 (CH), 111.6 (CH), 56.3 (CH₃). IR (ATR): 3175, 1671, 1564, 1479, 1238, 1043, 744 cm⁻¹. MS (EI) *m/z* (relative intensity): 244 (18) [M]⁺, 227 (11), 197 (10), 135 (100), 110 (15), 92 (22), 77 (25). HR-MS (ESI) *m/z* calcd for C₁₄H₁₃N₂O₃⁷⁹Br [M]⁺: 244.0848, found 244.0851. The analytical data correspond with those reported in the literature.^[11b]



2-(2-*n*-Butoxybenzamido)pyridine-1-oxide (**150ac**)

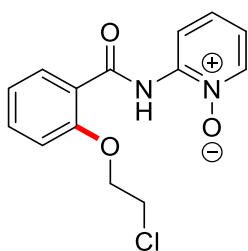
The general procedure **F** was followed using benzamide **117a** (107 mg, 0.50 mmol, 1.00 equiv), tetra-*n*-butylammonium acetate (150 mg, 0.50 mmol, 1.00 equiv in each cell) and *n*-butanol (**149c**) (2 × 7.0 mL). Purification by column chromatography on silica gel (CH₂Cl₂/acetone 4:1) yielded **150ac** (74.8 mg, 262 μmol, 52%) as a white solid. M. p.: 73–75 °C. ¹H-NMR (400 MHz, CDCl₃): δ = 12.41 (s, 1H), 8.84 (dd, *J* = 9.3, 1.6 Hz, 1H), 8.41 (dd, *J* = 7.4, 2.3 Hz, 1H), 8.33 (dd, *J* = 7.7, 2.1 Hz, 1H), 7.55 (ddd, *J* = 9.3, 8.0, 2.3 Hz, 1H), 7.29 (ddd, *J* = 8.0, 7.4, 1.6 Hz, 1H), 7.17–7.07 (m, 2H), 7.00 (ddd, *J* = 7.7, 7.5, 1.8 Hz, 1H), 4.35 (t, *J* = 7.4 Hz, 2H), 2.19–2.09 (m, 2H), 1.65–1.55 (m, 2H), 1.06 (q, *J* = 7.2 Hz, 3H). ¹³C-NMR (101 MHz, CDCl₃): δ = 164.0 (C_q), 157.6

(C_q), 138.1 (C_q), 134.2 (CH), 132.6 (CH), 129.0 (CH), 128.1 (CH), 121.0 (CH), 120.6 (C_q), 118.0 (CH), 115.4 (CH), 112.5 (CH), 69.6 (CH₂), 30.5 (CH₂), 19.2 (CH₂), 13.7 (CH₃). IR (ATR): 3164, 1673, 1561, 1502, 1204, 796, 741 cm⁻¹. MS (ESI) *m/z* (relative intensity): 309 (21) [M+Na]⁺, 287 (100) [M+H]⁺, 237 (19), 215 (13), 177 (45), 121 (19). HR-MS (ESI) *m/z* calcd for C₁₆H₁₈N₂O₃ [M+H]⁺: 287.1390, found: 287.1389. The analytical data correspond with those reported in the literature.^[11b]



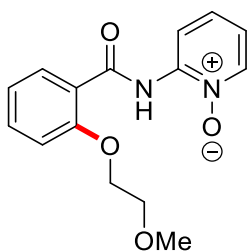
2-[2-(2,2,2-Trifluoroethoxy)benzamido]pyridine-1-oxide (**150ad**)

The general procedure **F** was followed using benzamide **117a** (107 mg, 0.50 mmol, 1.00 equiv) and trifluoroethanol (**149d**) (2 × 7.0 mL) at 60 °C. Purification by column chromatography on silica gel (CH₂Cl₂/acetone 4:1) yielded **150ad** (97.6 mg, 312 μmol, 62%) as a white solid. M. p.: 152–154 °C. ¹H-NMR (300 MHz, CDCl₃): δ = 11.93 (s, 1H), 8.68 (dd, *J* = 7.8, 2.2 Hz, 1H), 8.33 (dd, *J* = 6.6, 1.2 Hz, 1H), 8.27 (dd, *J* = 7.9, 1.6 Hz, 1H), 7.59 (ddd, *J* = 7.9, 7.8, 2.2 Hz, 1H), 7.38 (ddd, *J* = 8.1, 6.6, 1.7 Hz, 1H), 7.29 (ddd, *J* = 8.1, 6.6, 1.2 Hz, 1H), 7.12 (dd, *J* = 8.1, 1.7 Hz, 1H), 7.03 (ddd, *J* = 7.9, 7.8, 1.6 Hz, 1H), 4.76 (t, *J* = 8.6 Hz, 2H). ¹³C-NMR (125 MHz, CDCl₃): δ = 163.0 (C_q), 155.6 (C_q), 144.9 (C_q), 137.2 (CH), 134.1 (CH), 132.8 (CH), 127.6 (CH), 123.3 (CH), 123.0 (q, ¹*J*_{CF} = 258 Hz, C_q), 122.3 (C_q), 118.7 (CH), 115.5 (CH), 113.5 (CH), 66.5 (q, ²*J*_{CF} = 34.5 Hz, CH₂). ¹⁹F-NMR (282 MHz, CDCl₃): *d* = -72.81. IR (ATR): 3172, 1669, 1563, 1504, 1452, 1092, 670 cm⁻¹. MS (EI) *m/z* (relative intensity): 312 (16) [M]⁺, 203 (100), 197 (35), 183 (10), 155 (5), 120 (6), 92 (12). HR-MS (ESI) *m/z* calcd for C₁₄H₁₂F₃N₂O₃ [M+H]⁺: 313.0795, found: 313.0791.



2-[2-(2-Chloroethoxy)benzamido]pyridine-1-oxide (**150ae**)

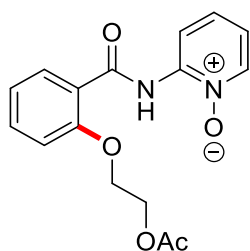
The general procedure **F** was followed using benzamide **117a** (107 mg, 0.50 mmol, 1.00 equiv) and 2-chloroethanol (**149e**) (2 × 7.0 mL). Purification by column chromatography on silica gel (CH₂Cl₂/acetone 4:1) yielded **150ae** (111 mg, 381 μmol, 76%) as a white solid. M. p.: 142–144 °C. ¹H-NMR (400 MHz, CDCl₃): δ = 12.18 (s, 1H), 8.69 (dd, *J* = 8.0, 2.0 Hz, 1H), 8.29–8.25 (m, 2H), 7.53 (ddd, *J* = 7.2, 6.8, 2.0 Hz, 1H), 7.33 (ddd, *J* = 8.0, 6.8, 1.7 Hz, 1H), 7.14 (ddd, *J* = 7.7, 7.0, 1.9 Hz, 1H), 7.06–6.94 (m, 2H), 4.49 (t, *J* = 7.9 Hz, 2H), 4.17 (t, *J* = 7.9 Hz, 2H). ¹³C-NMR (125 MHz, CDCl₃): δ = 163.3 (C_q), 156.5 (C_q), 145.2 (C_q), 137.2 (CH), 134.3 (CH), 132.7 (CH), 128.9 (C_q), 127.7 (CH), 121.9 (CH), 120.6 (C_q), 118.5 (CH), 115.6 (CH), 112.6 (CH), 69.5 (CH₂), 41.2 (CH₂). IR (ATR): 3168, 1565, 1508, 1178, 1021, 741 cm⁻¹. MS (ESI) *m/z* (relative intensity): 317 (30) [³⁷Cl-M+Na]⁺, 315 (94) [³⁵Cl-M+Na]⁺, 295 (35) [³⁷Cl-M+H]⁺, 293 (100) [³⁵Cl-M+H]⁺, 242 (5), 183 (56), 121 (12). HR-MS (ESI) *m/z* calcd for C₁₄H₁₃N₂O₃³⁵Cl [³⁵Cl-M+H]⁺: 293.0687, found: 293.0687.



2-(2-(2-Methoxyethoxy)benzamido)pyridine-1-oxide (**150af**)

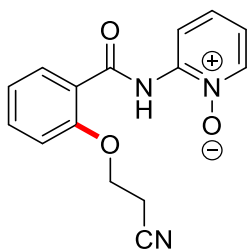
The general procedure **F** was followed using benzamide **117a** (107 mg, 0.50 mmol, 1.00 equiv) and 2-methoxyethanol (**149f**) (2 × 7.0 mL). Purification by column chromatography on silica gel (CH₂Cl₂/acetone 2:1) yielded **150af** (92.3 mg, 320 μmol, 64%) as a white solid. M. p.: 107–109 °C. ¹H-NMR (300 MHz, CDCl₃): δ = 12.21 (s, 1H), 8.70 (dd, *J* = 7.9, 1.3 Hz, 1H), 8.29–8.23 (m, 2H), 7.51 (ddd, *J* = 8.3, 7.2, 1.3 Hz, 1H), 7.31 (ddd, *J* = 7.9, 7.2, 2.0 Hz, 1H), 7.14–7.07 (m, 2H), 6.97 (ddd, *J* = 8.0, 6.5, 2.3 Hz, 1H), 4.41 (t, *J* = 5.1 Hz, 2H), 4.06 (t, *J* = 5.1 Hz, 2H), 3.45 (s, 3H). ¹³C-NMR

(125 MHz, CDCl₃): δ = 163.8 (C_q), 157.4 (C_q), 145.4 (C_q), 137.3 (CH), 134.3 (CH), 132.6 (CH), 127.7 (CH), 124.5 (CH), 120.8 (C_q), 118.4 (CH), 115.7 (CH), 112.8 (CH), 70.4 (CH₂), 69.0 (CH₂), 59.0 (CH₃). IR (ATR): 3171, 1656, 1560, 1422, 1251, 904, 747 cm⁻¹. MS (ESI) *m/z* (relative intensity): 311 (62) [M+Na]⁺, 289 (100) [M+H]⁺, 179 (37), 147 (6), 123 (9). HR-MS (ESI) *m/z* calcd for C₁₅H₁₆N₂O₄ [M+H]⁺: 289.1183, found: 289.1184. The analytical data correspond with those reported in the literature.^[111b]



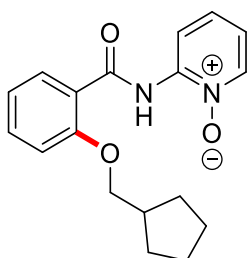
2-[2-(2-Acetoxyethoxy)benzamido]pyridine-1-oxide (**150ag**)

The general procedure **G** was followed using benzamide **117a** (53.5 mg, 0.25 mmol, 1.00 equiv) and 2-hydroxyethylacetate (**149g**) (2.3 mL) in MeCN (0.9 mL). Purification by column chromatography on silica gel (CH₂Cl₂/acetone 3:1) yielded **150ag** (42.5 mg, 136 μ mol, 54%) as a white solid. M. p.: 125–127 °C. ¹H-NMR (300 MHz, CDCl₃): δ = 12.11 (s, 1H), 8.67 (dd, *J* = 7.4, 2.2 Hz, 1H), 8.27–8.22 (m, 2H), 7.51 (ddd, *J* = 8.2, 7.4, 2.0 Hz, 1H), 7.32 (ddd, *J* = 8.2, 7.4, 2.2 Hz, 1H), 7.13 (dd, *J* = 8.2, 2.0 Hz, 1H), 7.04 (dd, *J* = 8.4, 1.3 Hz, 1H), 6.96 (ddd, *J* = 8.2, 8.0, 1.3 Hz, 1H), 4.71 (t, *J* = 5.6 Hz, 2H), 4.45 (t, *J* = 5.6 Hz, 2H), 2.01 (s, 3H). ¹³C-NMR (125 MHz, CDCl₃): δ = 170.9 (C_q), 163.4 (C_q), 156.8 (C_q), 145.1 (C_q), 137.1 (CH), 134.1 (CH), 132.6 (CH), 127.4 (CH), 121.7 (CH), 121.0 (C_q), 118.4 (CH), 115.5 (CH), 112.7 (CH), 67.6 (CH₂), 62.4 (CH₂), 20.9 (CH₃). IR (ATR): 3241, 2924, 1730, 1671, 1599, 1505, 1222, 1046, 860, 721 cm⁻¹. MS (EI) *m/z* (relative intensity): 316 (5) [M]⁺, 230 (41), 197 (53), 165 (100), 121 (81), 87 (45) 43 (67). HR-MS (ESI) *m/z* calcd for C₁₆H₁₆N₂O₅ [M+H]⁺: 317.1132, found: 317.1140.



2-[2-(2-Cyanoethoxy)benzamido]pyridine-1-oxide (**150ah**)

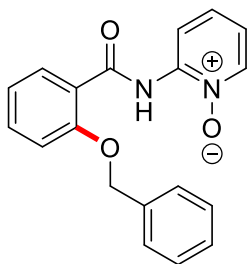
The general procedure **G** was followed using benzamide **117a** (53.5 mg, 0.25 mmol, 1.00 equiv) and 3-hydroxypropionitrile (**149h**) (2.3 mL) in MeCN (0.9 mL). Purification by column chromatography on silica gel (CH₂Cl₂/acetone 2:1) yielded **150ah** (43.5 mg, 153 μmol, 61%) as a white solid. M. p.: 183–185 °C. ¹H-NMR (300 MHz, CDCl₃): δ = 12.07 (s, 1H), 8.70 (dd, *J* = 8.4, 1.8 Hz, 1H), 8.32–8.25 (m, 2H), 7.57 (ddd, *J* = 8.4, 7.9, 2.1 Hz, 1H), 7.32 (ddd, *J* = 8.2, 7.4, 2.2 Hz, 1H), 7.13 (dd, *J* = 8.2, 2.0 Hz, 1H), 7.04 (dd, *J* = 8.4, 1.3 Hz, 1H), 7.04–6.99 (m, 2H), 4.71 (t, *J* = 5.6 Hz, 2H), 4.45 (t, *J* = 5.6 Hz, 2H), 2.01 (s, 3H). ¹³C-NMR (75 MHz, CDCl₃): δ = 163.1 (C_q), 151.1 (C_q), 145.1 (C_q), 137.2 (CH), 134.5 (CH), 132.9 (CH), 128.0 (CH), 122.4 (CH), 120.9 (C_q), 118.7 (CH), 117.1 (C_q), 115.6 (CH), 112.4 (CH), 64.3 (CH₂), 18.4 (CH₂). IR (ATR): 3191, 2930, 2257, 1662, 1599, 1428, 1267, 1205, 741 cm⁻¹. MS (EI) *m/z* (relative intensity): 283 (13) [M]⁺, 264 (8), 230 (44), 214 (17), 174 (69), 121 (100), 110 (53), 93 (27), 65 (25). HR-MS (ESI) *m/z* calcd for C₁₅H₁₃N₃O₃ [M]⁺: 284.1030, found: 284.1036.



2-[2-(Cyclopentylmethoxy)benzamido]pyridine-1-oxide (**150ai**)

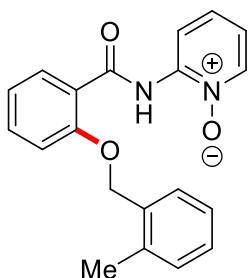
The general procedure **G** was followed using benzamide **117a** (53.7 mg, 0.25 mmol, 1.00 equiv) and cyclopentylmethanol (**149i**) (2.3 mL) in MeCN (0.9 mL). Purification by column chromatography on silica gel (CH₂Cl₂/acetone 4:1) yielded **150ai** (61.3 mg, 196 μmol, 78%) as a white solid. M. p.: 124–126 °C. ¹H-NMR (400 MHz, CDCl₃): δ = 12.17 (s, 1H), 8.71 (dd, *J* = 7.7, 1.9 Hz, 1H), 8.33–8.27 (m, 2H), 7.50 (ddd, *J* = 8.0, 7.6, 1.9 Hz, 1H), 7.32 (dd, *J* = 8.0, 2.2 Hz, 1H), 7.10–7.03 (m, 2H), 6.97 (ddd, *J* = 8.0, 6.5,

2.2 Hz, 1H), 4.13 (d, $J = 8.0$ Hz, 2H), 2.82–2.74 (m, 1H), 2.00–1.92 (m, 2H), 1.66–1.54 (m, 4H), 1.40–1.31 (m, 2H). ^{13}C -NMR (125 MHz, CDCl_3): $\delta = 164.1$ (C_q), 157.6 (C_q), 145.4 (C_q), 137.4 (CH), 134.2 (CH), 132.6 (CH), 127.5 (CH), 121.0 (CH), 120.6 (C_q), 118.4 (CH), 115.8 (CH), 112.6 (CH), 74.3 (CH_2), 38.3 (CH), 29.8 (CH_2), 24.4 (CH_2). IR (ATR): 3170, 2955, 1662, 1500, 1264, 1206, 1047, 746 cm^{-1} . MS (EI) m/z (relative intensity): 312 (4) $[\text{M}]^+$, 295 (10), 230 (37), 203 (819), 197 (44), 121 (100), 110 (15). HR-MS (ESI) m/z calcd for $\text{C}_{18}\text{H}_{21}\text{N}_2\text{O}_3$ $[\text{M}+\text{H}]^+$: 313.1547, found: 313.1543.



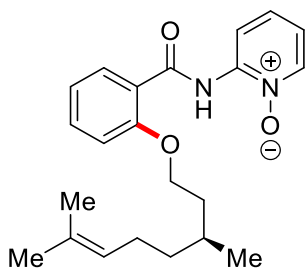
2-[2-(Benzyloxy)benzamido]pyridine-1-oxide (**150aj**)

The general procedure **G** was followed using benzamide **117a** (53.9 mg, 0.25 mmol, 1.00 equiv) and benzylalcohol (**149j**) (2.3 mL) in MeCN (0.9 mL). Purification by column chromatography on silica gel ($\text{CH}_2\text{Cl}_2/\text{acetone}$ 6:1) yielded **150aj** (58.9 mg, 184 μmol , 74%) as a white solid. M. p.: 121–122 $^\circ\text{C}$. ^1H -NMR (400 MHz, CDCl_3): $\delta = 12.59$ (s, 1H), 8.79 (dd, $J = 7.9, 1.7$ Hz, 1H), 8.28 (dd, $J = 8.2, 1.3$ Hz, 1H), 8.22 (dd, $J = 8.5, 2.0$ Hz, 1H), 7.49 (d, $J = 7.9$ Hz, 2H), 7.41–7.32 (m, 4H), 7.26 (ddd, $J = 8.2, 7.9, 1.7$ Hz, 1H), 7.06 (ddd, $J = 8.2, 7.9, 1.3$ Hz, 1H), 7.01–6.98 (m, 2H), 5.53 (s, 2H). ^{13}C -NMR (125 MHz, CDCl_3): $\delta = 163.7$ (C_q), 156.6 (C_q), 145.4 (C_q), 137.3 (CH), 135.8 (C_q), 134.0 (CH), 132.4 (CH), 128.7 (CH), 128.1 (CH), 128.0 (CH), 127.2 (CH), 121.4 (CH), 121.2 (C_q), 118.4 (CH), 115.6 (CH), 113.7 (CH), 71.2 (CH_2). IR (ATR): 3135, 1671, 1599, 1504, 1422, 1196, 999, 732, 684 cm^{-1} . MS (ESI) m/z (relative intensity): 320 (8) $[\text{M}]^+$, 303 (15), 211 (27), 197 (20), 183 (33), 121 (11), 91 (100), 65 (17). HR-MS (ESI) m/z calcd for $\text{C}_{19}\text{H}_{16}\text{N}_2\text{O}_3$ $[\text{M}]^+$: 320.1161, found: 320.1162. The analytical data correspond with those reported in the literature.^[111b]



2-{2-[(2-Methylbenzyl)oxy]benzamido}pyridine-1-oxide (150ak)

The general procedure **G** was followed using benzamide **117a** (53.2 mg, 0.25 mmol, 1.00 equiv) and 2-methylbenzylalcohol (**149k**) (2.3 mL) in MeCN (0.9 mL). Purification by column chromatography on silica gel (CH₂Cl₂/acetone 3:1) yielded **150ak** (58.9 mg, 184 μmol, 68%) as a white solid. M. p.: 161–162 °C. ¹H-NMR (400 MHz, CDCl₃): δ = 12.50 (s, 1H), 8.69 (dd, *J* = 7.6, 1.5 Hz, 1H), 8.24 (dd, *J* = 8.2, 1.9 Hz, 2H), 8.41–8.36 (m, 2H), 8.33 (ddd, *J* = 8.0, 7.6, 2.1 Hz, 1H), 7.21–7.14 (m, 3H), 7.08 (ddd, *J* = 7.6, 6.8, 2.2 Hz, 1H), 6.98 (ddd, *J* = 8.0, 7.6, 1.5 Hz, 1H), 6.91 (dd, *J* = 7.9, 1.7 Hz, 1H), 5.53 (s, 2H), 2.42 (s, 3H). ¹³C-NMR (125 MHz, CDCl₃): δ = 163.7 (C_q), 156.0 (C_q), 145.4 (C_q), 137.3 (CH), 135.4 (C_q), 134.0 (CH), 133.8 (C_q), 132.4 (CH), 130.4 (CH), 127.9 (CH), 127.6 (CH), 127.1 (CH), 126.1 (CH), 121.6 (CH), 121.1 (C_q), 118.3 (CH), 115.5 (CH), 113.7 (CH), 70.0 (CH₂) 19.1 (CH₃). IR (ATR): 3173, 2952, 1662, 1561, 1469, 1236, 841, 748, 601 cm⁻¹. MS (ESI) *m/z* (relative intensity): 334 (11) [M]⁺, 317 (7), 230 (20), 197 (26), 121 (15), 105 (100), 79 (16). HR-MS (EI) *m/z* calcd for C₂₀H₁₈N₂O₃ [M]⁺: 334.1317, found: 334.1325.



(S)-2-{2-[(3,7-Dimethyloct-6-en-1-yl)oxy]benzamido}pyridine-1-oxide (150al)

The general procedure **G** was followed using benzamide **117a** (53.5 mg, 0.25 mmol, 1.00 equiv) and (*S*)-citronellol (**149l**) (2.3 mL) in MeCN (0.9 mL). Purification by column chromatography on silica gel (CH₂Cl₂/acetone 8:1) yielded **150al** (48.9 mg, 133 μmol, 52%) as a yellow oil. ¹H-NMR (400 MHz, CDCl₃): δ = 12.22 (s, 1H), 8.69 (dd, *J* = 7.8, 2.2 Hz, 1H), 8.29–8.22 (m, 2H), 7.50 (ddd, *J* = 8.0, 7.8, 2.2 Hz, 1H), 7.32 (ddd, *J* = 8.0,

7.8, 1.7 Hz, 1H), 7.09–7.04 (m, 2H), 6.96 (ddd, $J = 7.9, 6.9, 2.0$ Hz, 1H), 5.07–5.04 (m, 1H), 4.35–4.24 (m, 2H), 2.17–2.11 (m, 1H), 2.03–1.90 (m, 2H), 1.72–1.65 (m, 2H), 1.62 (s, 3H), 1.55 (s, 3H), 1.41–1.33 (m, 1H), 1.27–1.20 (m, 1H), 0.98 (d, $J = 7.9$ Hz, 3H). ^{13}C -NMR (125 MHz, CDCl_3): $\delta = 163.9$ (C_q), 157.4 (C_q), 145.3 (C_q), 137.2 (CH), 135.1 (CH), 132.1 (CH), 131.2 (C_q), 127.4 (CH), 124.6 (CH), 120.9 (CH), 120.6 (C_q), 118.3 (CH), 115.7 (CH), 112.5 (CH), 68.3 (CH_2), 37.3 (CH_2), 35.5 (CH_2), 29.9 (CH_3), 25.7 (CH_3), 25.5 (CH_2), 19.5 (CH), 17.7 (CH_3). IR (ATR): 3168, 2917, 1669, 1600, 1505, 1426, 1207, 687 cm^{-1} . MS (ESI) m/z (relative intensity): 368 (23) $[\text{M}]^+$, 351 (11), 299 (10), 230 (21), 214 (19) 197 (16), 147 (12), 121 (100), 110 (25), 95 (28), 81 (33), 69 (53), 55 (33), 41 (44). HR-MS (EI) m/z calcd for $\text{C}_{22}\text{H}_{28}\text{N}_2\text{O}_3$ $[\text{M}]^+$: 368.2100, found: 368.2099.

Gram-Scale Synthesis of 150na

In a three-neck flask fitted with a Pt-plate electrode (2.5 cm \times 5 cm \times 0.25 mm) and a RVC electrode (2.5 cm \times 5 cm \times 0.6 cm), $\text{Co}(\text{OAc})_2 \cdot 4 \text{H}_2\text{O}$ (257 mg, 1.00 mmol, 20 mol %), NaOPiv (2.41 g, 20.0 mmol, 4.00 equiv) and benzamide **117n** (1.45 g, 5.00 mmol, 1.00 equiv) were dissolved in ethanol (**149a**) (70 mL) under N_2 atmosphere. Electrolysis was started at ambient temperature and a constant current of 16 mA maintained for 36 h. Evaporation of the solvent and subsequent column chromatography using $\text{CH}_2\text{Cl}_2/\text{Acetone}$ (3:1 \rightarrow 1:1) yielded **150na** (1.02 g, 3.12 mmol, 61%).

5.6.2 Mechanistic Studies

Studies on the Potential Racemization of 150al

A racemic sample of **150al** was synthesized following general procedure **B** using *rac*-Citronellol. Analysis by chiral HPLC showed that no racemization took place. HPLC chromatograms were recorded on an Agilent 1290 Infinity instrument using CHIRALPAK ® IA-1 column and *n*-hexane/*i*-PrOH (95:5, 0.5 mL/min, detection at 250 nm).

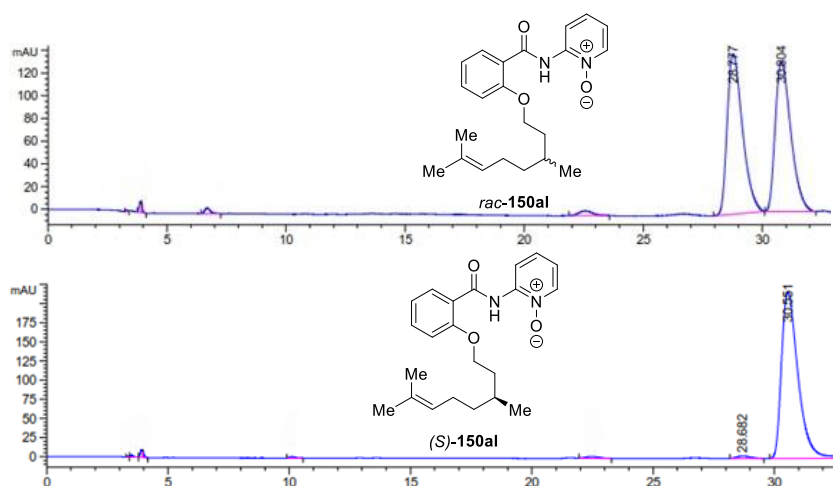
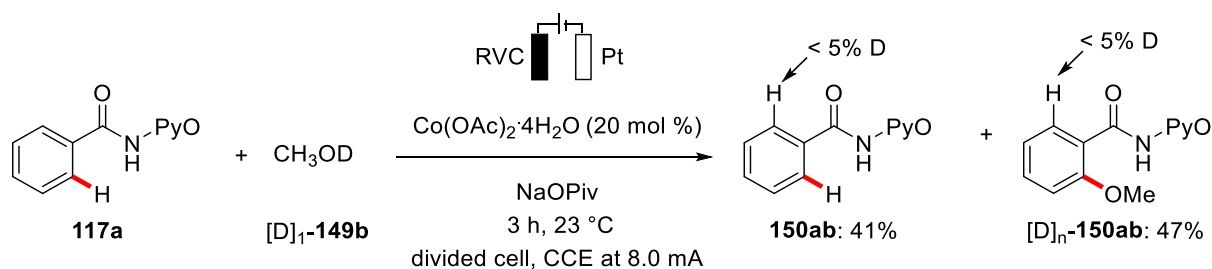


Figure 5.9. HPLC Chromatograms of *rac*-150al and (*S*)-150al.

H/D Exchange Experiment



Scheme 5.13. H/D exchange in the presence of [D]₁-149b.

In a divided cell with P4 sintered glass membrane, NaOPiv (122 mg, 1.00 mmol) was added in one cell, fitted with a Pt-plate electrode and dissolved in CH₃OD (7.0 mL). In the other half cell Co(OAc)₂·4 H₂O (25.7 mg, 0.10 mmol, 20 mol %), NaOPiv (122 mg, 1.00 mmol) and benzamide **117aa** (107 mg, 0.50 mmol) were dissolved in CH₃OD (7.0 mL) and fitted with a RVC electrode. Electrolysis was performed at ambient temperature and a constant current of 8 mA maintained for 3 h. Evaporation of the solvent and subsequent column chromatography (CH₂Cl₂/acetone 2:1) yielded the desired product (57.8 mg, 235 μmol, 47%) as a white solid and the reisolated starting material (43.9 mg, 206 μmol, 41%) as a white solid. No deuteration could be detected in either compound by ¹H-NMR spectroscopy and MS spectrometry.

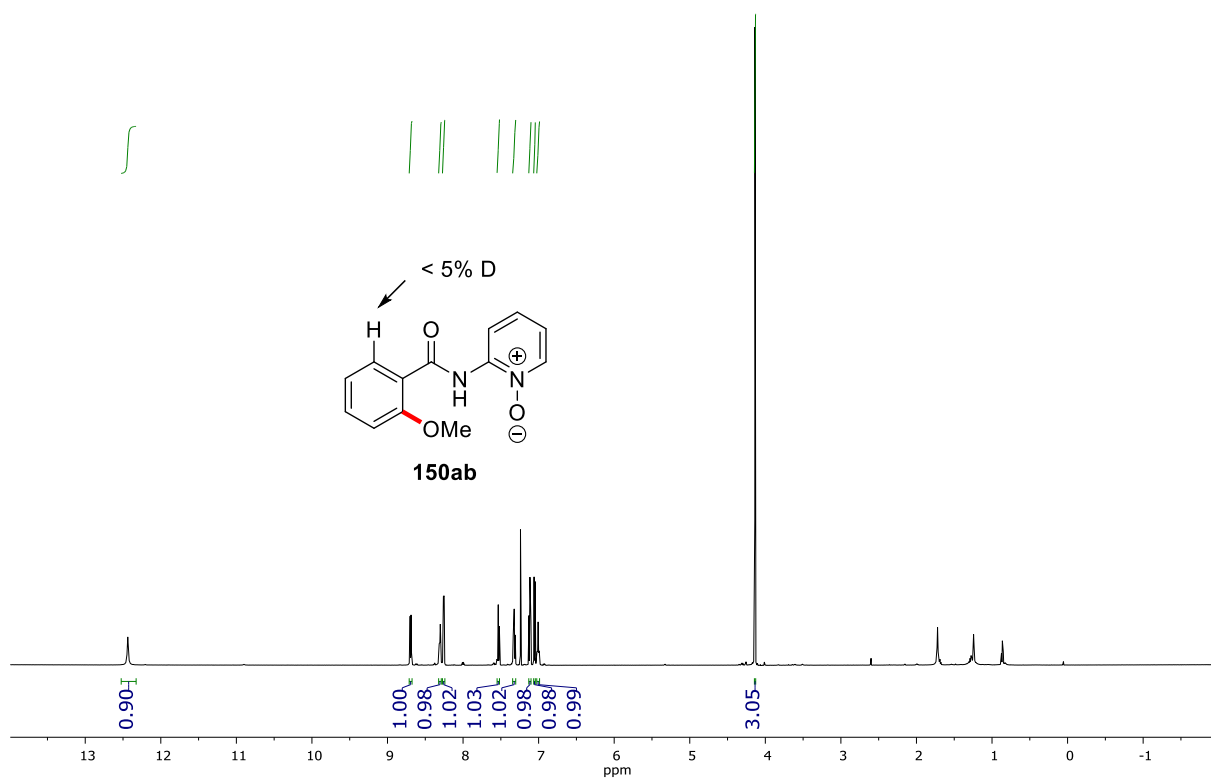


Figure 5.10. $^1\text{H-NMR}$ of **150ab** from the H/D exchange experiment.

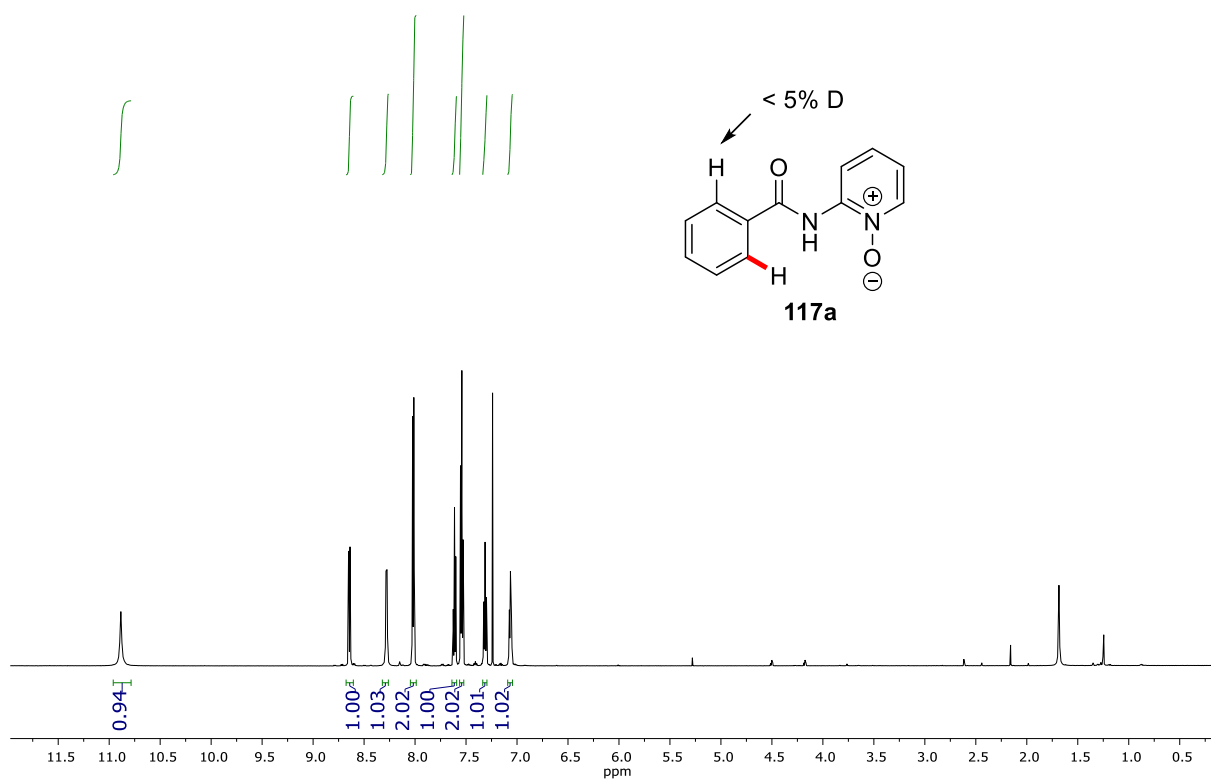
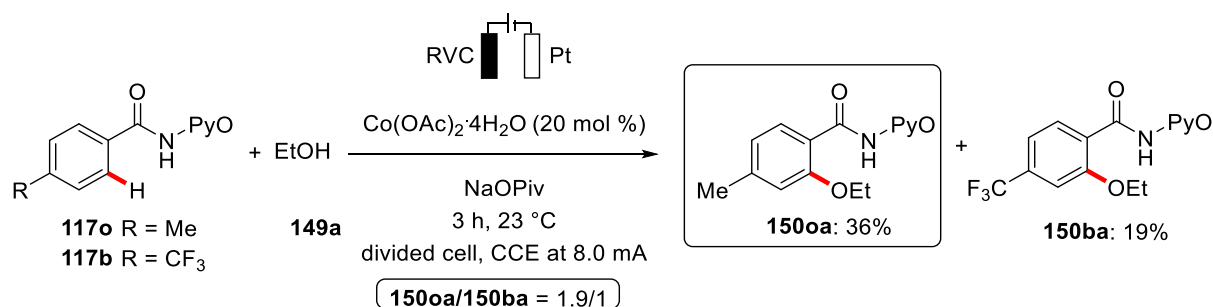


Figure 5.11. $^1\text{H-NMR}$ of **117a** from the H/D exchange experiment.

Competition Experiments



Scheme 5.14. Competition experiment between arenes **117o** and **117b**.

In a divided cell with P4 sintered glass membrane, NaOPiv (122 mg, 1.00 mmol, 4.00 equiv) was added in one cell, fitted with a Pt-plate electrode and dissolved in alcohol **149a** (7.0 mL). In the other half cell Co(OAc)₂·4H₂O (25.7 mg, 0.10 mmol, 20 mol %), NaOPiv (123 mg, 1.00 mmol, 4.00 equiv), benzamide **117o** (57.3 mg, 0.25 mmol, 1.00 equiv) and benzamide **117b** (70.5 mg, 0.25 mmol, 1.00 equiv) were dissolved in ethanol (**149a**) (7.0 mL) and fitted with a RVC electrode. Electrolysis was started at ambient temperature and a constant current of 8 mA maintained for 3 h. Evaporation of the solvent and subsequent column chromatography using CH₂Cl₂/acetone 3:1 yielded a mixture of products. Analysis by ¹H-NMR using CH₂Br₂ as the internal standard showed a product distribution of 1.9:1 in favor of **150oa**.

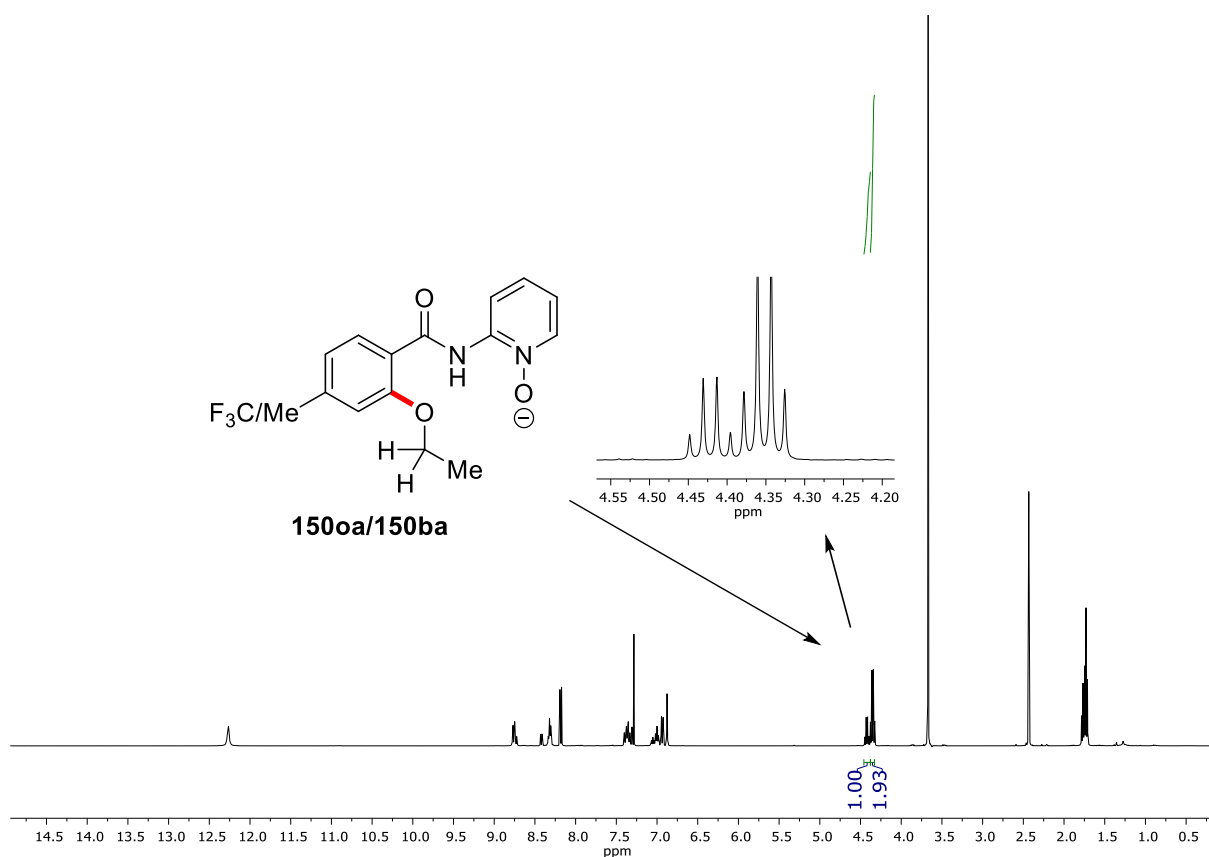


Figure 5.12. $^1\text{H-NMR}$ of the isolated mixture of **150oa** and **150ba**.

The relative kinetic studies were conducted with **150oa** and **150ba** using LC-MS measurements with an internal standard. Two independent reactions under standard conditions were carried out using substrates **117o** and **117b** (0.50 mmol each). After 10 minutes to reach a stable constant current of 8 mA aliquots of 0.3 mL were removed from the anodic chamber every five minutes. The mixture was diluted using MeCN (1.5 mL) and filtered. After addition of a stock solution (60 μL) of 1,3,5-trimethoxybenzene (84.1 mg, 0.5 mmol) in MeCN (10 mL) each sample was analyzed by RP-LCMS using $\text{H}_2\text{O}/\text{MeCN}$ 1:1 as the eluent.

Time [min]	5	10	15	20	25	30
150oa [%]	0.4	2.3	4.6	7.3	10.4	14.0
150ba [%]	-	0.4	1.6	3.3	4.7	6.7

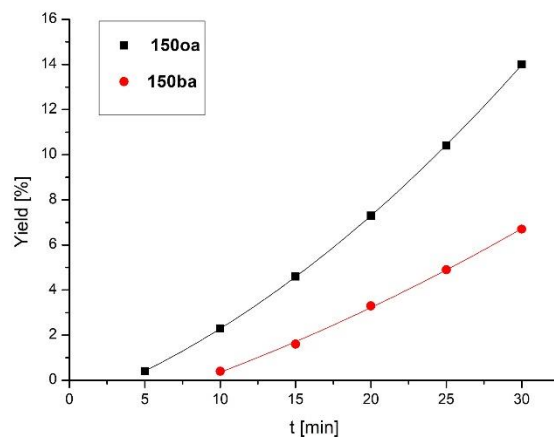
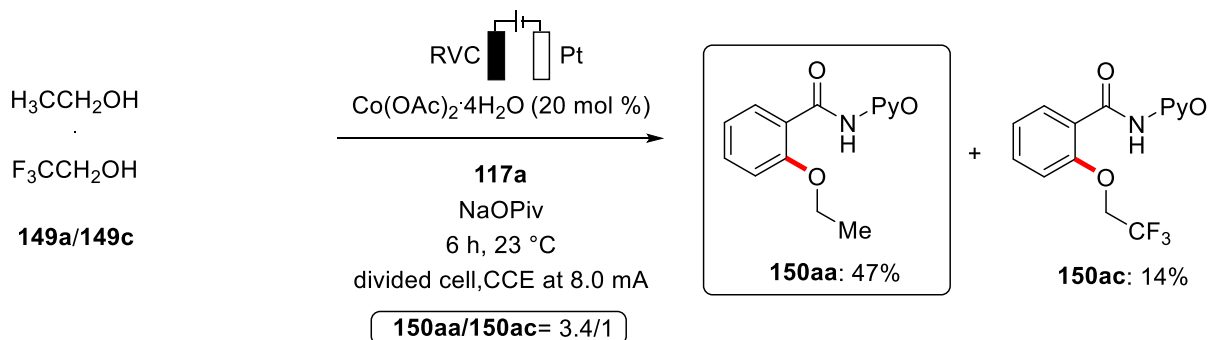


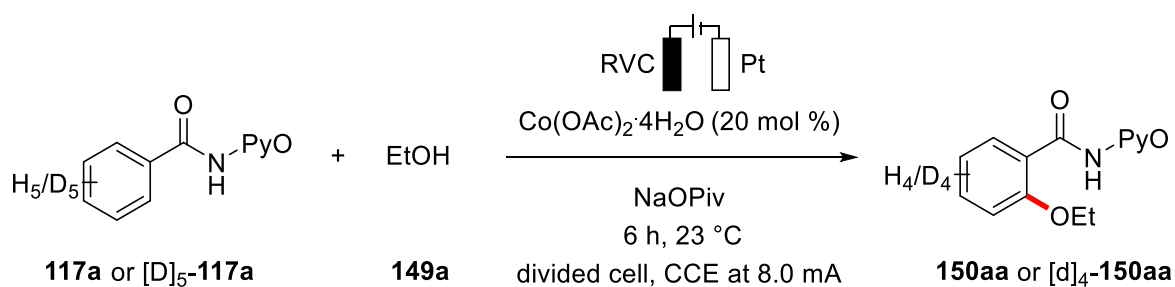
Figure 5.13. Relative initial rates of **150 oa** and **150ba**.



Scheme 5.15. Competition experiment between alcohols **149a** and **149c**.

In a divided cell with P4 sintered glass membrane, NaOPiv (124 mg, 1.00 mmol, 2.00 equiv) was added in one cell, fitted with a Pt-plate electrode and dissolved in a mixture of TFE/ethanol (1:1, 7.0 mL). In the other half cell $\text{Co}(\text{OAc})_2 \cdot 4\text{H}_2\text{O}$ (25.6 mg, 0.10 mmol, 20 mol %), NaOPiv (122 mg, 1.00 mmol, 12.00 equiv), benzamide **117a** (107 mg, 0.50 mmol, 1.00 equiv) were fitted with a RVC electrode and dissolved in a mixture of TFE **149c**/ethanol (**149a**) (1:1, 7.0 mL). Electrolysis was started at ambient temperature and a constant current of 8 mA maintained for 6 h. Evaporation of the solvent and subsequent column chromatography using CH_2Cl_2 /acetone 3:1 yielded **150aa** (60.4 mg, 236 μmol , 47%) and **150ac** (21.9 mg, 71.2 μmol , 14%).

KIE studies



Scheme 5.16. KIE study of the cobalt-catalyzed C–H oxygenation.

Two independent reactions under standard conditions were carried out using substrates **117a** and $[\text{D}_5]$ -**117a** (0.50 mmol each). After 10 minutes to reach a stable constant current of 8 mA aliquots of 0.3 mL were removed from the anodic chamber every five minutes. The mixture was diluted using MeCN (1.5 mL) and filtered. After addition of a stock solution (60 μL) of 1,3,5-trimethoxybenzene (84.1 mg, 0.5 mmol) in MeCN (10 mL) each sample was analyzed by RP-LCMS using $\text{H}_2\text{O}/\text{MeCN}$ 1:1 as the eluent.

Time [min]	5	10	15	20	25	30
150aa [%]	1.2	3.8	8.4	11.8	16.2	21.2
$[\text{D}_5]$ - 150aa [%]	-	1.7	5.3	8.3	13.0	16.9

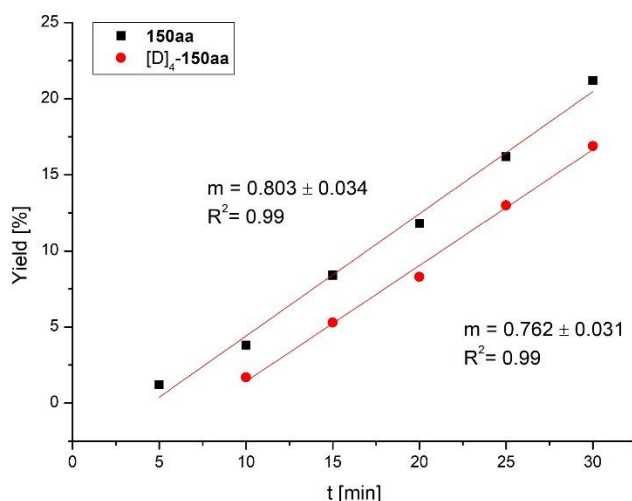
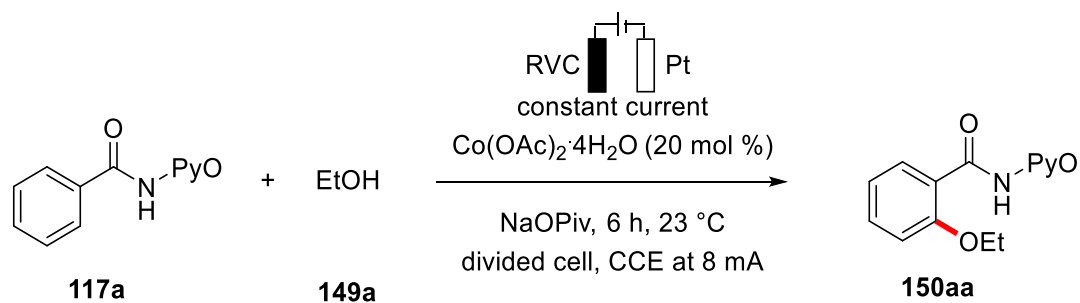


Figure 5.14. Initial rates of **150aa** and $[\text{D}]_4$ -**150aa**.

Kinetic Profile (Electrochemical Oxidation)



Scheme 5.17. C–H oxygenation under electrochemical conditions.

The general procedure **F** was followed using **117a** and **149a**. After 10 minutes to reach a stable constant current of 8 mA aliquots of 0.1 mL were removed from the anodic chamber every 10 minutes (first 3 h) and every 30 min (last 3 h). The mixture was diluted using MeCN (1.5 mL) and filtered. After addition of a stock solution (60 μL) of 1,3,5-trimethoxybenzene (84.1 mg, 0.5 mmol) in MeCN (10 mL) each sample was analyzed by RP-LCMS using $\text{H}_2\text{O}/\text{MeCN}$ 1:1 as the eluent.

Time [min]	10	20	30	40	50	60	70	80	90	100	110
150aa [%]	0.3	3.0	6.2	11.2	14.8	18.3	22.3	26.5	30.4	34.6	37.2
Time [min]	120	140	160	180	210	240	270	300	330	360	
150aa [%]	40.6	46.6	51.5	55.9	58.8	61.1	64.2	66.1	68.0	70.1	

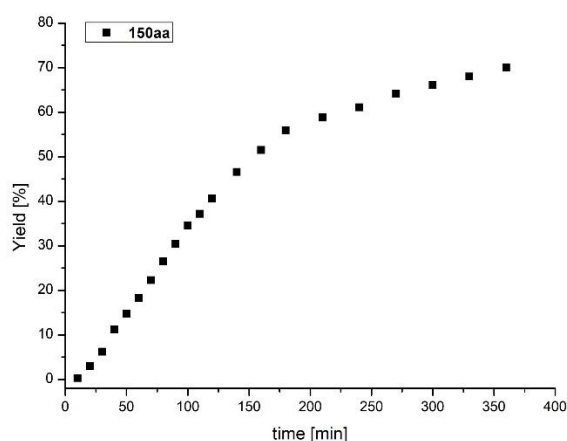
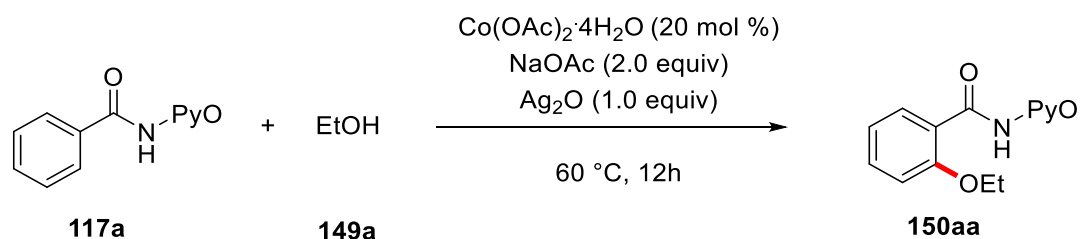


Figure 5.15. Lifetime of the catalyst under electrochemical oxidation.

Kinetic Profile (Chemical Oxidation)



Scheme 5.18. C–H oxygenation under chemical conditions.

A reaction was carried out using substrate **117a** (107 mg, 0.50 mmol, 1.00 equiv), $\text{Co(OAc)}_2 \cdot 4\text{H}_2\text{O}$ (25.6 mg, 0.10 mmol, 20 mol %), NaOAc (82.2 mg, 1.00 mmol, 2.00 equiv), Ag_2O (232 mg, 1.00 mmol, 1.00 equiv) and ethanol (**149a**) (4.0 mL). Aliquots of 0.1 mL were removed from the reaction mixture every 10 minutes (first 160 min) and every hour (last 9h). The mixture was diluted using MeCN (1.5 mL) and filtered. After addition of a stock solution (60 μL) of 1,3,5-trimethoxybenzene (84.1 mg, 0.5 mmol) in MeCN (10 mL) each sample was analyzed by RP-LCMS using $\text{H}_2\text{O}/\text{MeCN}$ 1:1 as the eluent.

Time [min]	10	20	30	40	50	60	70	80	90	100	110
150aa [%]	0.3	3.1	4.8	6.1	9.2	12.3	15.5	18.5	20.2	24.2	27.5
Time [min]	120	130	140	150	160	180	240	300	360	420	480
150aa [%]	33.6	37.4	43.7	51.2	59.8	64.2	67.4	68.8	69.9	71.4	72.4
Time [min]	540	600	660	720							
150aa [%]	73.0	74.1	75.2	76.0							

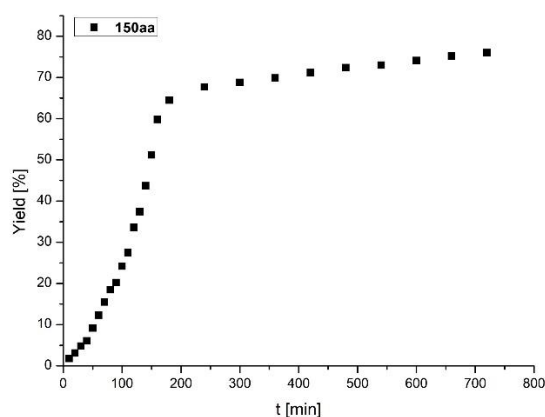


Figure 5.16. Lifetime of the catalyst under electrochemical oxidation.

Cyclic Voltammetry

The cyclic voltammetry was carried out with a Metrohm Autolab PGSTAT204 workstation and following analysis was performed with Nova 2.0 software. A glassy-carbon electrode (3 mm-diameter, disc-electrode) was used as the working electrode, a Pt wire as auxiliary electrode and a SCE electrode was used as the reference. The measurements were carried out at a scan rate of 100 mVs^{-1}

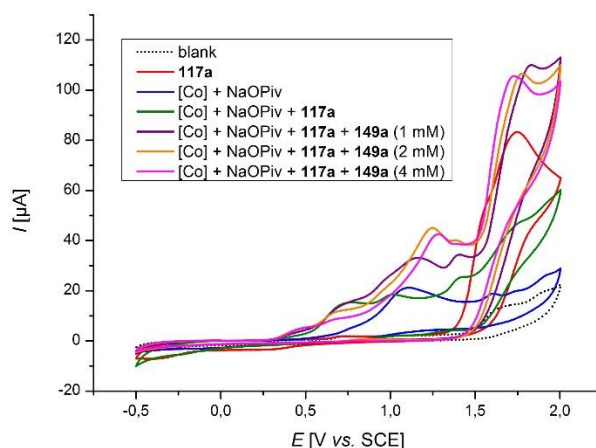


Figure 5.17. Cyclic voltammograms at 100 mVs^{-1} : $n\text{-Bu}_4\text{NPF}_6$ (1 M in MeCN), concentration of substrates 1 mM (NaOPiv 4 mM). (black) blank; (red) substrate **117a**; (blue) $\text{Co}(\text{OAc})_2 \cdot 4\text{H}_2\text{O}$ and NaOPiv; (green) $\text{Co}(\text{OAc})_2 \cdot 4\text{H}_2\text{O}$, NaOPiv and **117a**; (purple) $\text{Co}(\text{OAc})_2 \cdot 4\text{H}_2\text{O}$, NaOPiv, **117a** and EtOH (1 mM); (orange) $\text{Co}(\text{OAc})_2 \cdot 4\text{H}_2\text{O}$, NaOPiv and **117a** and EtOH (2 mM); (magenta) $\text{Co}(\text{OAc})_2 \cdot 4\text{H}_2\text{O}$, NaOPiv and **1a** and EtOH (4 mM).

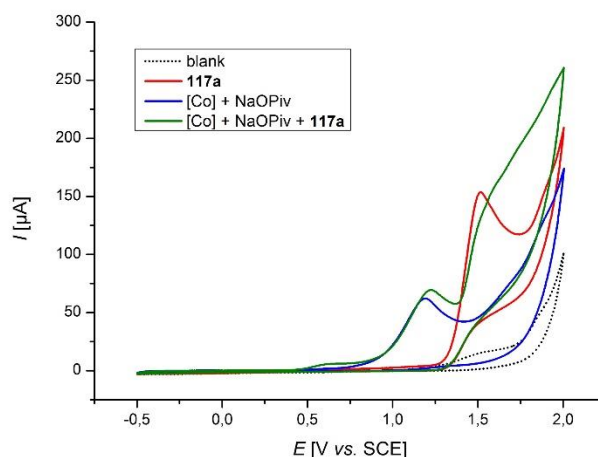
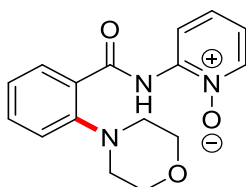


Figure 5.18. Cyclic voltammograms at 100 mVs⁻¹: *n*-Bu₄NPF₆ (1 M in MeOH), concentration of substrates 1 mM (NaOPiv 4 mM). (black) blank; (red) substrate **117a**; (blue) Co(OAc)₂·4H₂O and NaOPiv; (green) Co(OAc)₂·4H₂O, NaOPiv and **117a**.

5.7 Electrochemical Cobalt-catalyzed C–H Amination

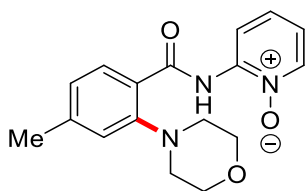
5.7.1 Analytical Data and Experimental Procedures



2-(2-Morpholinobenzamido)pyridine-1-oxide (**148aa**)

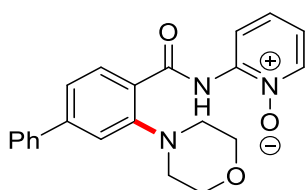
The general procedure **H** was followed using benzamide **117a** (107 mg, 0.50 mmol, 1.00 equiv) and morpholine (**146a**) (87.0 mg, 1.00 mmol, 2.00 equiv). Purification by column chromatography on silica gel (CH₂Cl₂/acetone 3:1→1:1) yielded **148aa** (115 mg, 384 μmol, 77%) as a white solid. M. p.: 153–155 °C. ¹H-NMR (500 MHz, CDCl₃): δ = 13.62 (s, 1H), 8.75 (dd, *J* = 8.4, 1.8 Hz, 1H), 8.26 (dd, *J* = 6.4, 2.0 Hz, 1H), 8.19 (dd, *J* = 7.7, 1.8 Hz, 1H), 7.54 (ddd, *J* = 8.4, 2.0, 1.8 Hz 1H), 7.35–7.23 (m, 3H), 6.99 (ddd, *J* = 6.4, 2.0, 1.8 Hz, 1H), 4.08–4.05 (m, 4H), 3.05–3.02 (m, 4H). ¹³C-NMR (125 MHz, CDCl₃): δ = 166.3 (C_q), 151.9 (C_q), 145.3 (C_q), 137.5 (CH), 133.5 (CH), 132.2 (CH), 127.5 (CH), 127.2 (C_q), 125.1 (CH), 120.8 (CH), 118.6 (CH), 116.0 (CH), 66.1 (CH₂), 54.1 (CH₂). IR (ATR): 2833, 1667, 1502, 1281, 1109, 764 cm⁻¹. MS (ESI)

m/z (relative intensity): 322 (88) [M+Na]⁺, 300 (100 [M+H]⁺, 242 (62), 205 (14), 190 (15), 169 (5). HR-MS (ESI) *m/z* calcd for C₁₆H₁₇N₃O₃ [M+H]⁺: 300.1343, found: 300.1348. The analytical data correspond with those reported in the literature.^[110b]



2-(4-Methyl-2-morpholinobenzamido)pyridine-1-oxide (148oa)

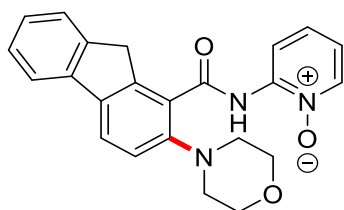
The general procedure **H** was followed using benzamide **117o** (114 mg, 0.50 mmol, 1.00 equiv) and morpholine (**146a**) (87.2 mg, 1.00 mmol, 2.00 equiv). Purification by column chromatography on silica gel (CH₂Cl₂/acetone 3:1→1:1) yielded **148oa** (129 mg, 416 μmol, 83%) as a white solid. M. p.: 197–199 °C. ¹H-NMR (500 MHz, CDCl₃): δ = 13.54 (s, 1H), 8.72 (dd, *J* = 8.0, 2.1 Hz, 1H), 8.24 (dd, *J* = 7.4, 1.9 Hz, 1H), 8.08 (d, *J* = 7.7 Hz, 1H), 7.34 (ddd, *J* = 8.0, 2.1, 1.9 Hz, 1H), 7.11 (d, *J* = 1.0 Hz, 1H), 7.07 (dd, *J* = 7.7, 1.0 Hz, 1H), 6.95 (ddd, *J* = 7.4, 2.1, 1.9 Hz, 1H), 4.10–4.05 (m, 4H), 3.05–3.00 (m, 4H), 2.38 (s, 3H). ¹³C-NMR (100 MHz, CDCl₃): δ = 165.3 (C_q), 152.0 (C_q), 145.4 (C_q), 144.4 (C_q), 137.5 (CH), 132.2 (CH), 127.4 (CH), 126.0 (CH), 124.5 (C_q), 121.6 (CH), 118.5 (CH), 116.1 (CH), 66.2 (CH₂), 54.2 (CH₂), 21.7 (CH₃). IR (ATR): 2832, 16665, 1558, 1502, 1311, 1210, 1115, 847, 755 cm⁻¹. MS (ESI) *m/z* (relative intensity): 334 (87) [M+Na]⁺, 314 (100) [M+H]⁺, 296 (5), 242 (44), 204 (76), 174 (11). HR-MS (EI) *m/z* calcd for C₁₇H₁₉N₃O₃ [M+H]⁺: 314.1499, found: 314.1489. The analytical data correspond with those reported in the literature.^[110b]



2-[3-Morpholino-(1,1'-biphenyl)-4-carboxamido]pyridine-1-oxide (148na)

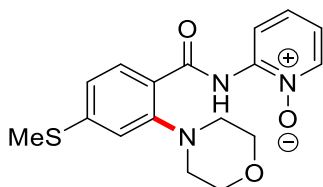
The general procedure **H** was followed using benzamide **117n** (146 mg, 0.50 mmol, 1.00 equiv) and morpholine (**146a**) (86.4 mg, 1.00 mmol, 2.00 equiv). Purification by column chromatography on silica gel (CH₂Cl₂/acetone 5:1→2:1) yielded **148na** (117.5 mg, 313 μmol, 62%) as a white solid. M. p.: 183–185 °C. ¹H-NMR (400 MHz, CDCl₃): δ = 13.72 (s, 1H), 8.70 (dd, *J* = 8.2, 2.0 Hz, 1H), 8.33–8.27 (m, 2H), 7.68–7.62

(m, 2H), 7.57–7.28 (m, 6H), 7.03 (ddd, $J = 7.4, 2.3, 2.0$ Hz, 1H), 4.20–4.12 (m, 4H), 3.17–3.12 (m, 4H). ^{13}C -NMR (101 MHz, CDCl_3): $\delta = 166.1$ (C_q), 152.1 (C_q), 146.5 (C_q), 145.3 (C_q), 139.7 (C_q), 137.5 (CH), 132.8 (CH), 129.0 (CH), 128.4 (CH), 127.9 (CH), 127.6 (CH), 125.1 (C_q), 123.8 (CH), 119.6 (CH), 118.7 (CH), 116.1 (CH), 66.2 (CH_2), 54.1 (CH_2). IR (ATR): 2833, 1669, 1560, 1505, 1260, 1111, 759, 700 cm^{-1} . MS (EI) m/z (relative intensity): 398 (100) $[\text{M}+\text{Na}]^+$, 381 (70), 376 (45) $[\text{M}+\text{H}]^+$, 336 (10). HR-MS (EI) m/z calcd for $\text{C}_{22}\text{H}_{21}\text{N}_3\text{O}_3$ $[\text{M}+\text{H}]^+$: 367.1656, found: 367.1657. The analytical data correspond with those reported in the literature.^[110b]



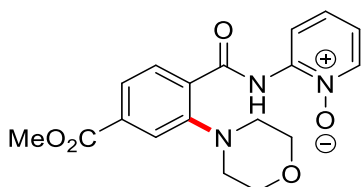
2-(2-Morpholino-9H-fluorene-1-carboxamido)pyridine-1-oxide (**148pa**)

The general procedure **H** was followed using benzamide **117p** (151 mg, 0.50 mmol, 1.00 equiv) and morpholine (**146a**) (86.0 mg, 1.00 mmol, 2.00 equiv). Purification by column chromatography on silica gel ($\text{CH}_2\text{Cl}_2/\text{acetone}$ 3:1→1:1) yielded **148pa** (97.2 mg, 254 μmol , 51%) as a white solid. M. p.: 163–165 °C. ^1H -NMR (400 MHz, CDCl_3): $\delta = 13.13$ (s, 1H), 8.63 (dd, $J = 8.1, 2.3$ Hz, 1H), 8.26 (dd, $J = 8.4, 2.0$ Hz, 1H), 7.79 (d, $J = 8.9$ Hz, 1H), 7.63 (dd, $J = 8.9, 2.3$ Hz, 1H), 7.47 (ddd, $J = 8.1, 2.3, 2.0$ Hz, 1H), 7.25–7.15 (m, 4H), 6.88 (ddd, $J = 8.4, 2.3, 2.0$ Hz, 1H), 4.19 (s, 2H), 3.98–3.90 (m, 4H), 2.97–2.88 (m, 4H). ^{13}C -NMR (100 MHz, CDCl_3): $\delta = 166.0$ (C_q), 150.5 (C_q), 147.7 (C_q), 145.3 (C_q), 143.5 (C_q), 140.2 (C_q), 139.7 (C_q), 137.5 (CH), 127.6 (CH), 127.0 (CH), 126.7 (CH), 124.8 (CH), 124.4 (C_q), 123.6 (CH), 119.6 (CH), 119.1 (CH), 118.5 (CH), 115.6 (CH), 66.2 (CH_2), 54.4 (CH_2), 39.4 (CH_2). IR (ATR): 2831, 1665, 1559, 1503, 1264, 1107, 846, 753, 701 cm^{-1} . MS (ESI) m/z (relative intensity): 410 (100) $[\text{M}+\text{Na}]^+$, 388 (87) $[\text{M}+\text{H}]^+$, 339 (18), 276 (9), 244 (68), 222 (23). HR-MS (ESI) m/z calcd for $\text{C}_{23}\text{H}_{21}\text{N}_3\text{O}_3$ $[\text{M}+\text{H}]^+$: 388.1656, found: 388.1661.



2-[4-(Methylthio)-2-morpholinobenzamido]pyridine-1-oxide (**148qa**)

The general procedure **H** was followed using benzamide **117q** (176 mg, 0.50 mmol, 1.00 equiv) and morpholine (**146a**) (87.2 mg, 1.00 mmol, 2.00 equiv). Purification by column chromatography on silica gel (CH₂Cl₂/acetone 3:1→1:1) yielded **148qa** (124 mg, 358 μmol, 72%) as a white solid. M. p.: 229–237 °C. ¹H-NMR (400 MHz, CDCl₃): δ = 13.51 (s, 1H), 8.74 (dd, *J* = 8.2, 2.2 Hz, 1H), 8.31 (dd, *J* = 8.0, 1.5 Hz, 1H), 8.15 (dd, *J* = 8.5 Hz, 1H), 7.36 (ddd, *J* = 8.2, 2.2, 1.5 Hz, 1H), 7.17 (d, *J* = 0.7 Hz, 1H), 7.11 (dd, *J* = 8.5, 0.7 Hz, 1H), 7.02 (ddd, *J* = 8.0, 2.2, 1.5 Hz, 1H) 4.15–4.08 (m, 4H), 3.02–2.97 (m, 4H), 2.57 (s, 3H). ¹³C-NMR (100 MHz, CDCl₃): δ = 164.9 (C_q), 152.5 (C_q), 146.2 (C_q), 145.3 (C_q), 137.5 (CH), 132.5 (CH), 127.6 (CH), 123.4 (C_q), 121.4 (CH), 118.6 (CH), 117.8 (CH), 116.0 (CH), 66.1 (CH₂), 54.1 (CH₂), 14.9 (CH₃). IR (ATR): 2826, 1663, 1560, 1503, 1260, 1106, 890, 724 cm⁻¹. MS (ESI) *m/z* (relative intensity): 368 (83) [M+Na]⁺, 346 (100) [M+H]⁺, 324 (28), 242 (73), 210 (55), 188 (44). HR-MS (ESI) *m/z* calcd for C₁₇H₁₉N₃O₃S [M]⁺: 346.1220, found: 346.1211.



2-[4-(Methoxycarbonyl)-2-morpholinobenzamido]pyridine-1-oxide (**148ra**)

The general procedure **H** was followed using benzamide **117r** (135 mg, 0.50 mmol, 1.00 equiv) and morpholine (**146a**) (87.8 mg, 1.00 mmol, 2.00 equiv). Purification by column chromatography on silica gel (CH₂Cl₂/acetone 3:1→1:1) yielded **148ra** (116.1 mg, 325 μmol, 65%) as a white solid. M. p.: 173–175 °C. ¹H-NMR (400 MHz, CDCl₃): δ = 13.50 (s, 1H), 8.71 (dd, *J* = 8.1, 1.7 Hz, 1H), 8.32 (dd, *J* = 8.0, 1.6 Hz, 1H), 8.15 (d, *J* = 8.1 Hz, 1H), 8.16 (dd, *J* = 8.1, 0.8 Hz, 1H), 8.0 (d, *J* = 0.8 Hz, 1H), 7.99 (dd, *J* = 8.1, 0.8 Hz, 1H), 7.33 (ddd, *J* = 8.0, 2.2, 1.5 Hz, 1H), 7.01 (ddd, *J* = 8.0, 2.2, 1.5 Hz, 1H), 4.06–4.04 (m, 4H), 3.91 (s, 3H), 3.12–3.08 (m, 4H). ¹³C-NMR (101 MHz, CDCl₃): δ = 166.0 (C_q), 164.5 (C_q), 151.9 (C_q), 145.0 (C_q), 137.5 (CH), 134.5 (CH), 132.4 (CH), 131.0 (CH), 130.8 (C_q), 127.5 (C_q), 125.7 (CH), 119.0 (CH), 116.1 (CH),

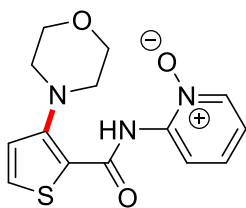
66.0 (CH₂), 54.1 (CH₂), 52.6 (CH₃). IR (ATR): 2954, 2833, 1722, 1671, 1504, 1278, 1110, 757 cm⁻¹. MS (ESI) *m/z* (relative intensity): 380 (100) [M+Na]⁺, 358 (49) [M+H]⁺, 305 (17), 248 (27), 214 (5). HR-MS (ESI) *m/z* calcd for C₁₈H₁₃N₃O₅ [M+H]⁺: 358.1397, found: 358.1398.



2-(5-Iodo-2-morpholinobenzamido)pyridine-1-oxide (**148ha**)

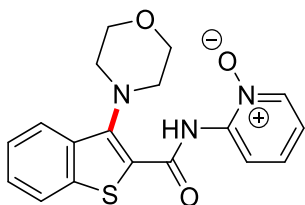
2-(3-Iodo-2-morpholinobenzamido)pyridine-1-oxide (**148ha'**)

The general procedure **H** was followed using benzamide **117h** (176 mg, 0.50 mmol, 1.00 equiv) and morpholine (**146a**) (87.0 mg, 1.00 mmol, 2.00 equiv). Purification by column chromatography on silica gel (CH₂Cl₂/acetone 3:1→1:1) yielded **148ha** (124 mg, 293 μmol, 59%) as a white solid, the ratio of **148ha** and **148ha'** (81:19) was determined by ¹H-NMR, in the following are the analytical data for **148ha**. M. p.: 200–204 °C. ¹H-NMR (400 MHz, CDCl₃): δ = 13.39 (s, 1H), 8.72 (dd, *J* = 7.6, 2.0 Hz, 1H), 8.51 (d, *J* = 0.9 Hz, 1H), 8.31 (dd, *J* = 8.2, 2.0 Hz, 1H), 7.85 (dd, *J* = 8.8, 0.9 Hz, 1H), 7.38 (ddd, *J* = 7.6, 2.0, 2.0 Hz, 1H), 7.10 (d, *J* = 8.8 Hz, 1H), 7.05 (ddd, *J* = 8.2, 2.0, 2.0 Hz, 1H) 4.19–4.12 (m, 4H), 3.06–3.03 (m, 4H). ¹³C-NMR (100 MHz, CDCl₃): δ = 163.7 (C_q), 151.6 (C_q), 145.3 (C_q), 142.2 (CH), 140.9 (CH), 137.5 (CH), 127.7 (CH), 125.1 (C_q), 122.6 (CH), 118.6 (CH), 116.1 (CH), 88.9 (C_q), 66.0 (CH₂), 54.0 (CH₂). IR (ATR): 2843, 1669, 1562, 1504, 1258, 1110, 925, 759 cm⁻¹. MS (ESI) *m/z* (relative intensity): 448 (100) [M+Na]⁺, 426 (55) [M+H]⁺, 397 (24), 322 (55), 300 (9), 188 (22) 170 (5). HR-MS (ESI) *m/z* calcd for C₁₆H₁₆N₃O₃I [M+H]⁺: 426.0309, found: 426.0315. The analytical data correspond with those reported in the literature.^[110b]



2-(3-Morpholinothiophene-2-carboxamido)pyridine-1-oxide (148ka)

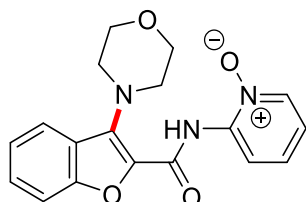
The general procedure **H** was followed using benzamide **117k** (110 mg, 0.50 mmol, 1.00 equiv) and morpholine (**146a**) (87.2 mg, 1.00 mmol, 2.00 equiv). Purification by column chromatography on silica gel (CH₂Cl₂/acetone 3:1→1:1) yielded **148ka** (104 mg, 336 μmol, 67%) as a white solid. M. p.: 212–214 °C. ¹H-NMR (400 MHz, CDCl₃): δ = 12.99 (s, 1H), 8.56 (dd, *J* = 8.3, 1.7 Hz, 1H), 8.12 (dd, *J* = 7.9, 2.1 Hz, 1H), 7.45 (d, *J* = 5.5 Hz, 1H), 7.21 (ddd, *J* = 8.3, 2.1, 1.7 Hz, 1H), 7.09 (d, *J* = 5.5 Hz, 1H), 6.88 (ddd, *J* = 7.9, 2.1, 1.7 Hz, 1H), 4.01–3.95 (m, 4H), 2.92–2.88 (m, 4H). ¹³C-NMR (100 MHz, CDCl₃): δ = 160.3 (C_q), 153.5 (C_q), 145.0 (C_q), 137.5 (CH), 131.7 (CH), 128.8 (C_q), 127.6 (CH), 122.7 (CH), 118.6 (CH), 115.9 (CH), 66.7 (CH₂), 54.3 (CH₂). IR (ATR): 2837, 1661, 1606, 1517, 1433, 1102, 920, 769, 671 cm⁻¹. MS (ESI) *m/z* (relative intensity): 328 (100) [M+Na]⁺, 306 (15) [M+H]⁺, 237 (17), 159 (24). HR-MS (ESI) *m/z* calcd for C₁₄H₁₅N₃O₃S [M+H]⁺: 306.0907, found: 306.0911. The analytical data correspond with those reported in the literature.^[110b]



2-(3-Morpholinobenzo[*b*]thiophene-2-carboxamido)pyridine-1-oxide (148sa)

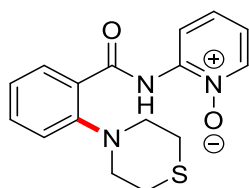
The general procedure **H** was followed using benzamide **117s** (135 mg, 0.50 mmol, 1.00 equiv) and morpholine (**146a**) (87.0 mg, 1.00 mmol, 2.00 equiv). Purification by column chromatography on silica gel (CH₂Cl₂/acetone 3:1→1:1) yielded **148sa** (108 mg, 310 μmol, 62%) as a white solid. M. p.: decomposed at 234 °C. ¹H-NMR (400 MHz, CDCl₃): δ = 12.88 (s, 1H), 8.71 (dd, *J* = 8.3, 1.7 Hz, 1H), 8.28 (dd, *J* = 7.4, 2.2 Hz, 1H), 7.87 (dd, *J* = 8.2, 2.1 Hz, 1H), 7.61 (dd, *J* = 7.4, 1.6 Hz, 1H), 7.45 (ddd, *J* = 7.4, 2.1, 1.3 Hz, 1H), 7.37–7.27 (m, 2H), 7.01 (ddd, *J* = 7.4, 2.2, 1.7 Hz, 1H), 4.16–4.08 (m, 4H), 3.42–3.34 (m, 4H). ¹³C-NMR (100 MHz, CDCl₃): δ = 157.4 (C_q), 154.5 (C_q), 144.9 (C_q), 139.7 (C_q), 137.6 (CH), 132.0 (C_q), 127.9 (CH), 127.8 (CH), 124.1

(C_q), 123.5 (CH), 122.5 (CH), 118.8 (CH), 115.8 (CH), 113.4 (CH), 67.0 (CH₂), 52.7 (CH₂). IR (ATR): 2854, 1622, 1501, 1433, 1114, 961, 846, 752 cm⁻¹. MS (ESI) *m/z* (relative intensity): 378 (100) [M+Na]⁺, 356 (82) [M+H]⁺, 300 (13), 210 (34), 188 (15). HR-MS (ESI) *m/z* calcd for C₁₈H₁₇N₃O₃S [M+H]⁺: 356.1053, found: 356.1063.



2-(3-Morpholinobenzofuran-2-carboxamido)pyridine-1-oxide (148ta)

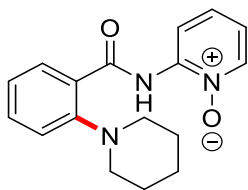
The general procedure **H** was followed using benzamide **117t** (127 mg, 0.50 mmol, 1.00 equiv) and morpholine (**146a**) (86.2 mg, 1.00 mmol, 2.00 equiv). Purification by column chromatography on silica gel (CH₂Cl₂/acetone 3:1→1:1) yielded **148ta** (94 mg, 282 μmol, 57%) as a white solid. M. p.: decomposed at 225 °C. ¹H-NMR (400 MHz, CDCl₃): δ = 13.50 (s, 1H), 8.72 (dd, *J* = 8.3, 1.7 Hz, 1H), 8.30 (dd, *J* = 7.4, 2.2 Hz, 1H), 8.22 (dd, *J* = 8.0, 2.1 Hz, 1H), 7.87 (dd, *J* = 7.9, 1.4 Hz, 1H), 7.47–7.36 (m, 2H), 7.33 (ddd, *J* = 8.3, 2.2, 1.7 Hz, 1H), 7.00 (ddd, *J* = 7.4, 2.2, 1.7 Hz, 1H), 4.28–4.13 (m, 4H), 3.52–3.56 (m, 4H). ¹³C-NMR (100 MHz, CDCl₃): δ = 161.1 (C_q), 145.6 (C_q), 144.9 (C_q), 139.8 (C_q), 137.6 (CH), 135.6 (CH), 133.0 (C_q), 127.6 (CH), 126.7 (CH), 124.9 (CH), 124.3 (CH), 124.1 (C_q), 119.1 (CH), 116.3 (CH), 66.8 (CH₂), 51.4 (CH₂). IR (ATR): 2847, 1631, 1501, 1427, 1261, 1109, 1025, 752 cm⁻¹. MS (ESI) *m/z* (relative intensity): 362 (100) [M+Na]⁺, 340 (75) [M+H]⁺, 301 (8), 242 (14), 188 (15). HR-MS (ESI) *m/z* calcd for C₁₈H₁₇N₃O₄ [M+H]⁺: 340.1297, found: 340.1294.



2-(2-Thiomorpholinobenzamido)pyridine-1-oxide (148ab)

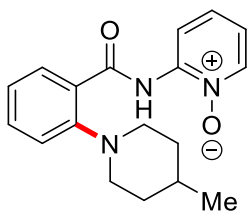
The general procedure **H** was followed using benzamide **117a** (107 mg, 0.50 mmol, 1.00 equiv) and thiomorpholine (**146b**) (100 mg, 1.00 mmol, 2.00 equiv). Purification by column chromatography on silica gel (CH₂Cl₂/acetone 3:1→1:1) yielded **148ab** (96.5 mg, 307 μmol, 61%) as a white solid. M. p.: 123–124 °C. ¹H-NMR (400 MHz, CDCl₃): δ = 13.68 (s, 1H), 8.69 (dd, *J* = 8.3, 2.0 Hz, 1H), 8.28 (dd, *J* = 7.7, 2.1 Hz, 1H),

8.21 (dd, $J = 7.5, 1.8$ Hz, 1H), 7.50 (ddd, $J = 8.3, 2.1, 2.0$ Hz 1H), 7.35–7.23 (m, 3H), 6.97 (ddd, $J = 7.7, 2.1, 2.0$ Hz, 1H), 3.27–3.25 (m, 4H), 3.06–3.01 (m, 4H). ^{13}C -NMR (101 MHz, CDCl_3): $\delta = 166.1$ (C_q), 153.1 (C_q), 145.3 (C_q), 137.6 (CH), 133.5 (CH), 132.1 (CH), 127.3 (CH), 127.2 (C_q), 125.4 (CH), 121.8 (CH), 118.6 (CH), 116.1 (CH), 56.3 (CH_2), 27.3 (CH_2). IR (ATR): 2832, 1665, 1695, 1500, 1382, 1209, 1115, 845, 746 cm^{-1} . MS (EI) m/z (relative intensity): 315 (8) $[\text{M}]^+$, 298 (100), 242 (21). 204 (100), 176 (27), 158 (52), 146 (68), 132 (87), 95 (63). HR-MS (ESI) m/z calcd for $\text{C}_{16}\text{H}_{17}\text{N}_3\text{O}_2\text{S}$ $[\text{M}+\text{H}]^+$: 316.1114, found: 316.1109. The analytical data correspond with those reported in the literature.^[110b]



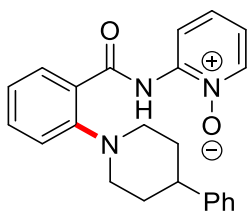
2-[2-(Piperidin-1-yl)benzamido]pyridine-1-oxide (**148ac**)

The general procedure **H** was followed using benzamide **117a** (107 mg, 0.50 mmol, 1.00 equiv) and piperidine (**146c**) (78.2 mg, 1.00 mmol, 2.00 equiv). Purification by column chromatography on silica gel ($\text{CH}_2\text{Cl}_2/\text{acetone}$ 10:1→8:1) yielded **148ac** (109 mg, 370 μmol , 74%) as a white solid. M. p.: 140–142 °C. ^1H -NMR (500 MHz, CDCl_3): $\delta = 13.63$ (s, 1H), 8.74 (dd, $J = 7.9, 2.0$ Hz, 1H), 8.25 (dd, $J = 7.8, 1.9$ Hz, 1H), 8.15 (dd, $J = 7.0, 2.0$ Hz, 1H), 7.49 (ddd, $J = 7.9, 2.0, 1.9$ Hz 1H), 7.32–7.29 (m, 2H), 7.20 (ddd, $J = 7.0, 2.5, 1.9$ Hz 1H), 6.95 (ddd, $J = 7.7, 2.1, 2.0$ Hz, 1H), 2.98–2.94 (m, 4H), 1.94–1.90 (m, 4H), 1.66–1.63 (m, 2H). ^{13}C -NMR (125 MHz, CDCl_3): $\delta = 166.8$ (C_q), 153.6 (C_q), 145.4 (C_q), 137.6 (CH), 133.2 (CH), 131.9 (CH), 127.3 (CH), 127.0 (C_q), 124.3 (CH), 120.7 (CH), 118.5 (CH), 116.2 (CH), 55.6 (CH_2), 25.3 (CH_2), 24.1 (CH_2). IR (ATR): 2941, 2799, 1666, 1501, 1284, 1207, 1098, 753 cm^{-1} . MS (ESI) m/z (relative intensity): 320 (70) $[\text{M}+\text{Na}]^+$, 298 (100) $[\text{M}+\text{H}]^+$, 242 (15), 204 (12), 188 (21). HR-MS (EI) m/z calcd for $\text{C}_{17}\text{H}_{19}\text{N}_3\text{O}_2$ $[\text{M}+\text{H}]^+$: 298.1550, found: 298.1555. The analytical data correspond with those reported in the literature.^[110b]



2-[2-(4-Methylpiperidin-1-yl)benzamido]pyridine-1-oxide (**148ad**)

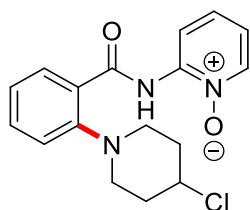
The general procedure **H** was followed using benzamide **117a** (107 mg, 0.50 mmol, 1.00 equiv) and 4-methylpiperidine (**146d**) (93.1 mg, 1.00 mmol, 2.00 equiv). Purification by column chromatography on silica gel (CH₂Cl₂/acetone 12:1→8:1) yielded **148ad** (111 mg, 355 μmol, 71%) as a white solid. M. p.: 179–181 °C. ¹H-NMR (400 MHz, CDCl₃): δ = 13.53 (s, 1H), 8.71 (dd, *J* = 8.0, 2.4 Hz, 1H), 8.30 (dd, *J* = 7.2, 1.9 Hz, 1H), 8.14 (dd, *J* = 7.1, 1.9 Hz, 1H), 7.47 (ddd, *J* = 8.0, 2.4, 1.9 Hz 1H), 7.32–7.28 (m, 2H), 7.17 (ddd, *J* = 7.1, 2.0, 1.9 Hz 1H), 6.98 (ddd, *J* = 7.2, 2.4, 2.0 Hz, 1H), 3.21–3.17 (m, 2H), 2.83–2.75 (m, 2H), 1.91–1.81 (m, 2H), 1.71–1.64 (m, 2H), 1.55–1.43 (m, 1H), 1.01 (d, *J* = 8.8 Hz, 3H). ¹³C-NMR (101 MHz, CDCl₃): δ = 166.8 (C_q), 153.3 (C_q), 145.4 (C_q), 137.5 (CH), 133.1 (CH), 131.8 (CH), 127.1 (C_q), 126.9 (CH), 124.1 (CH), 120.5 (CH), 118.4 (CH), 116.0 (CH), 54.9 (CH₂), 33.3 (CH₂), 30.4 (CH), 21.6 (CH₃). IR (ATR): 3049, 2832, 1664, 1593, 1505, 1269, 1122, 866, 759 cm⁻¹. MS (ESI) *m/z* (relative intensity): 334 (52) [M+Na]⁺, 312 (100) [M+H]⁺, 241 (8), 218 (18), 202 (22). HR-MS (EI) *m/z* calcd for C₁₈H₂₁N₃O₂ [M+H]⁺: 312.1707, found: 312.1709.



2-[2-(4-Phenylpiperidin-1-yl)benzamido]pyridine-1-oxide (**148ae**)

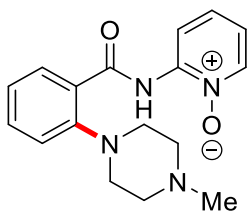
The general procedure **H** was followed using benzamide **117a** (107 mg, 0.50 mmol, 1.00 equiv) and 4-phenylpiperidine (**146d**) (164 mg, 1.00 mmol, 2.00 equiv). Purification by column chromatography on silica gel (CH₂Cl₂/acetone 12:1→8:1) yielded **148ad** (124 mg, 342 μmol, 69%) as a white solid. M. p.: 194–196 °C. ¹H-NMR (600 MHz, CDCl₃): δ = 13.64 (s, 1H), 8.78 (dd, *J* = 7.8, 2.2 Hz, 1H), 8.30 (dd, *J* = 7.9, 1.6 Hz, 1H), 8.16 (dd, *J* = 7.5, 2.2 Hz, 1H), 7.51 (ddd, *J* = 7.8, 2.2, 1.6 Hz 1H), 7.48–7.46 (m, 2H), 7.34–7.28 (m, 4H), 7.24–7.19 (m, 2H), 6.97 (ddd, *J* = 7.9, 2.2, 1.6 Hz, 1H), 3.37–3.32 (m, 2H), 2.95–2.91 (m, 2H), 2.64–2.58 (m, 1H), 2.55–2.47 (m, 2H),

1.86–1.82 (m, 1H). ^{13}C -NMR (125 MHz, CDCl_3): δ = 166.6 (C_q), 152.9 (C_q), 146.3 (C_q), 145.3 (C_q), 137.1 (CH), 133.1 (CH), 131.9 (CH), 128.3 (CH), 127.3 (CH), 127.1 (C_q), 126.9 (CH), 126.0 (CH), 124.2 (CH), 120.3 (CH), 118.4 (CH), 115.9 (CH), 55.4 (CH_2), 42.9 (CH), 32.8 (CH_2). IR (ATR): 2917, 2932, 1666, 1501, 1282, 1212, 1108, 756, 699 cm^{-1} . MS (ESI) m/z (relative intensity): 396 (33) $[\text{M}+\text{Na}]^+$, 374 (100) $[\text{M}+\text{H}]^+$, 358 (8), 264 (12), 242 (23), 123 (10). HR-MS (EI) m/z calcd for $\text{C}_{23}\text{H}_{23}\text{N}_3\text{O}_2$ $[\text{M}+\text{H}]^+$: 374.1863, found: 374.1864.



2-[2-(4-Chloropiperidin-1-yl)benzamido]pyridine-1-oxide (**148af**)

The general procedure **H** was followed using benzamide **117a** (107 mg, 0.50 mmol, 1.00 equiv) and 4-chloropiperidine (**146f**) (110 mg, 1.00 mmol, 2.00 equiv). Purification by column chromatography on silica gel ($\text{CH}_2\text{Cl}_2/\text{acetone}$ 12:1 \rightarrow 8:1) yielded **148af** (89.0 mg, 269 μmol , 54%) as a white solid. M. p.: 132–134 $^\circ\text{C}$. ^1H -NMR (300 MHz, CDCl_3): δ = 13.75 (s, 1H), 8.87 (dd, J = 7.8, 2.0 Hz, 1H), 8.35–8.27 (m, 2H), 8.16 (dd, J = 7.5, 2.2 Hz, 1H), 7.57 (ddd, J = 7.8, 2.1, 2.0 Hz 1H), 7.45–7.29 (m, 3H), 7.01 (ddd, J = 7.6, 2.1, 2.0 Hz, 1H), 4.60–4.48 (m, 2H), 3.40–3.29 (m, 2H), 3.06–2.96 (m, 2H), 2.77–2.61 (m, 2H), 2.23–2.10 (m, 1H). ^{13}C -NMR (75 MHz, CDCl_3): δ = 166.4 (C_q), 152.6 (C_q), 146.4 (C_q), 137.6 (CH), 133.5 (CH), 132.1 (CH), 127.6 (C_q), 127.0 (CH), 125.0 (CH), 121.2 (CH), 118.6 (CH), 116.2 (CH), 57.2 (CH_2), 50.2 (CH), 33.8 (CH_2). IR (ATR): 2835, 1667, 1560, 1500, 1424, 1209, 1112, 757, 723 cm^{-1} . MS (ESI) m/z (relative intensity): 354 (100) $[\text{M}+\text{Na}]^+$, 332 (84) $[\text{M}+\text{H}]^+$, 305 (15), 242 (71), 222 (55), 165 (34). HR-MS (EI) m/z calcd for $\text{C}_{17}\text{H}_{18}\text{N}_3\text{O}_2\text{Cl}$ $[\text{M}+\text{H}]^+$: 332.1160, found: 332.1164.

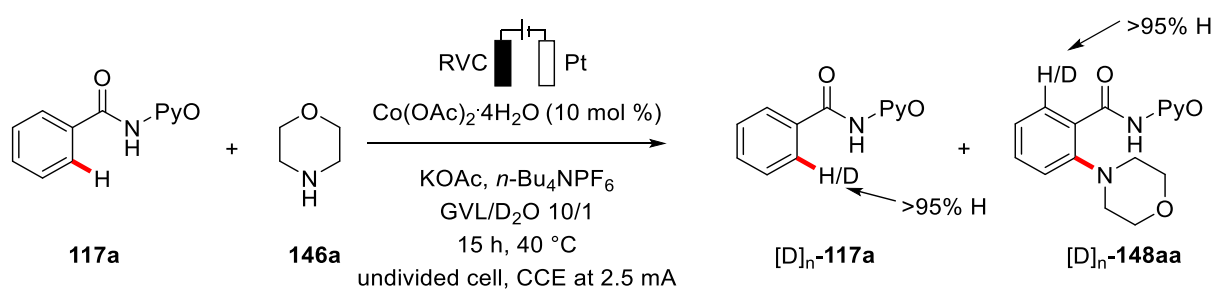


2-[2-(4-Methylpiperazin-1-yl)benzamido]pyridine-1-oxide (148ag)

The general procedure **H** was followed using benzamide **117a** (107 mg, 0.50 mmol, 1.00 equiv) and 4-methylpiperazine (**146f**) (94.7 mg, 1.00 mmol, 2.00 equiv). Purification by column chromatography on silica gel (CH₂Cl₂/acetone 1:1→0:1) yielded **148ag** (85.9 mg, 276 μmol, 55%) as a white solid. M. p.: 185–186 °C. ¹H-NMR (500 MHz, CDCl₃): δ = 13.47 (s, 1H), 8.74 (dd, *J* = 8.2, 2.4 Hz, 1H), 8.27 (dd, *J* = 7.7, 1.8 Hz, 1H), 8.14 (dd, *J* = 7.2, 2.1 Hz, 1H), 7.57 (ddd, *J* = 8.2, 2.4, 1.8 Hz 1H), 7.34–7.28 (m, 2H), 7.26–7.22 (m, 1H), 6.97 (ddd, *J* = 7.7, 2.4, 1.8 Hz, 1H), 3.13–3.05 (m, 4H), 2.88–2.79 (m, 4H), 2.41 (s, 3H). ¹³C-NMR (125 MHz, CDCl₃): δ = 166.5 (C_q), 152.2 (C_q), 145.3 (C_q), 137.5 (CH), 133.4 (CH), 132.0 (CH), 127.6 (C_q), 127.2 (CH), 124.8 (CH), 120.7 (CH), 118.5 (CH), 116.1 (CH), 53.9 (CH₂), 53.9 (CH₂), 45.9 (CH₃). IR (ATR): 2841, 1667, 1559, 1500, 1425, 1264, 1108, 758, 724 cm⁻¹. MS (EI) *m/z* (relative intensity): 335 (10) [M+Na]⁺, 313 (100) [M+H]⁺, 219 (8), 203 (21). HR-MS (EI) *m/z* calcd for C₁₇H₂₀N₄O₂ [M+H]⁺: 313.1659, found: 313.1661.

5.7.2 Mechanistic Studies

Deuteration Experiment



Scheme 5.19. H/D exchange experiment using D₂O as the co-solvent.

The general procedure **H** was followed using benzamide **117a** (107 mg, 0.50 mmol, 1.00 equiv) and morpholine (**146a**) (82.7 mg, 1.00 mmol, 2.00 equiv) using a mixture of GVL and D₂O (10/1, 2.2 mL) as solvent. Electrolysis was performed at 40 °C and a constant current of 2.5 mA was maintained for 15 h. Column chromatography (CH₂Cl₂/acetone 2:1) yielded the desired product [D]_n-**148aa** (83.8 mg, 275 μmol,

55%) as a white solid and the reisolated starting material [D]_n-**117a** (40.9 mg, 191 μmol, 38%) as a white solid. Deuteration could not be detected in neither of the two compounds **117a** and **148aa** as determined by ¹H-NMR spectroscopy.

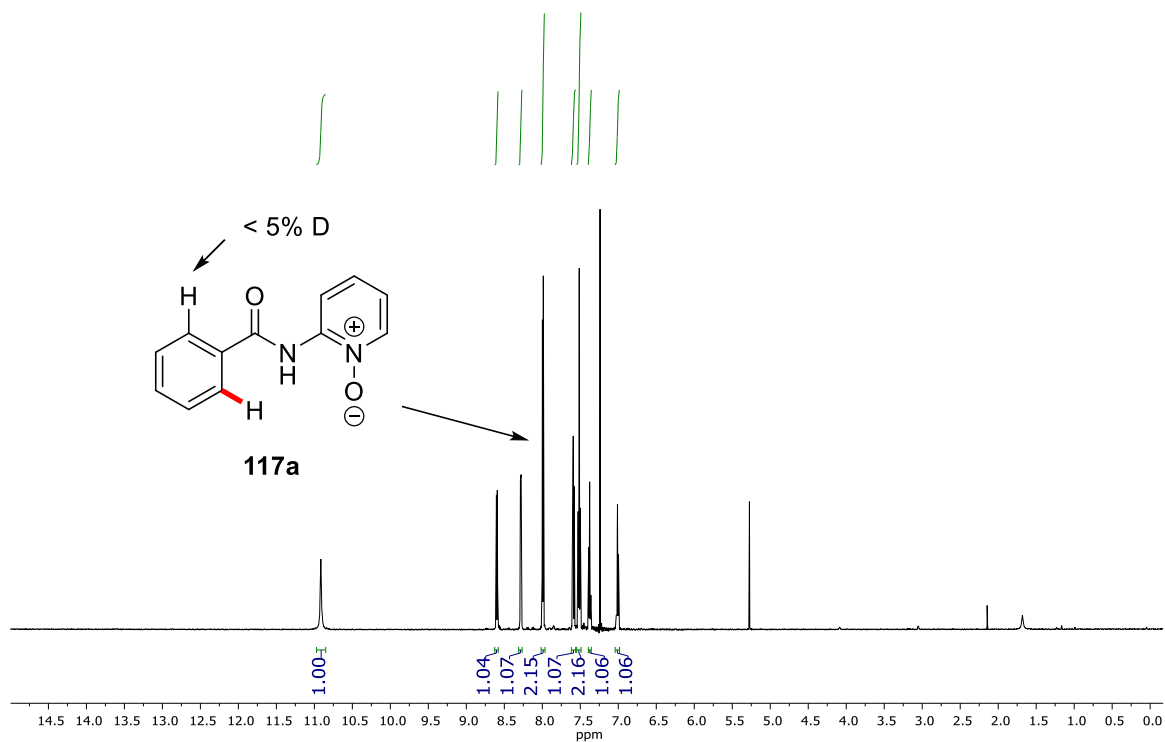


Figure 5.19. ¹H-NMR spectra of **117a** from the H/D exchange experiment.

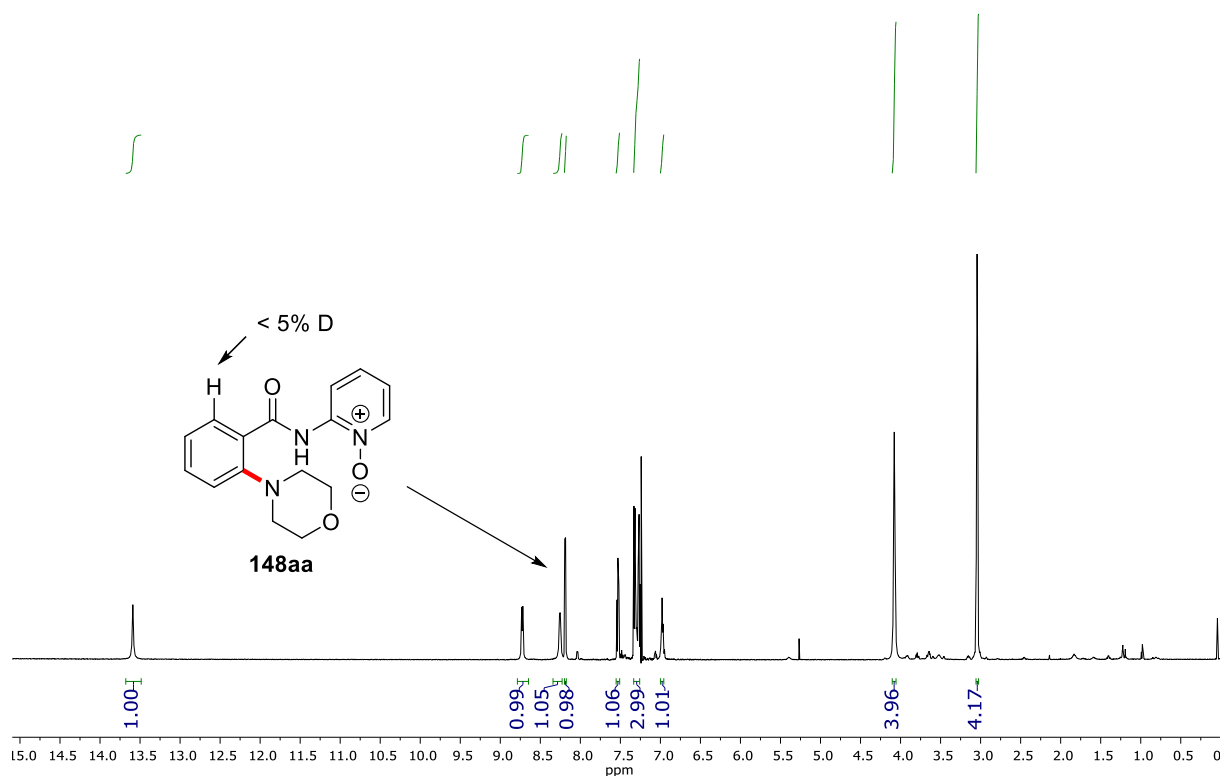
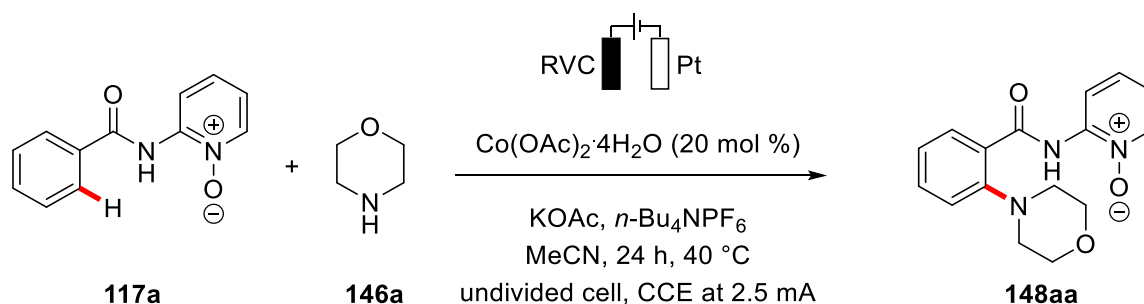


Figure 5.20. $^1\text{H-NMR}$ spectra of **150aa** from the H/D exchange experiment.

Reaction Profile



Scheme 5.20. Cobalt-catalyzed C–H amination.

A solution of benzamide **117a** (214 mg, 1.00 mmol, 1.00 equiv), $\text{Co(OAc)}_2 \cdot 4\text{H}_2\text{O}$ (51.4 mg, 20 mol %), KOAc (301 mg, 1.50 mmol, 1.50 equiv), $n\text{-Bu}_4\text{NPF}_6$ (386 mg, 0.50 mmol, 0.50 equiv) and morpholine (**146a**) (176 mg, 2.00 mmol, 2.00 equiv) in MeCN (20 mL) was fitted with a carbon mesh electrode, a platinum electrode and a diamond probe connected to a Mettler Toledo ReactIR and heated for 20 min to 40 °C to achieve a stable temperature. Then, electrolysis was started using a constant current of 5.0 mA. Every minute (first 4 h) and every 2 minutes (next 20 h) an IR spectrum was

recorded. Peaks at 1096 cm^{-1} and 1115 cm^{-1} were identified to belong to the starting material and the product, respectively. After 24 h, **148aa** (82.0 mg, 274 μmol , 55 %) and **117a** (44.3 mg, 207 μmol 41%) were isolated to scale the peak intensities.

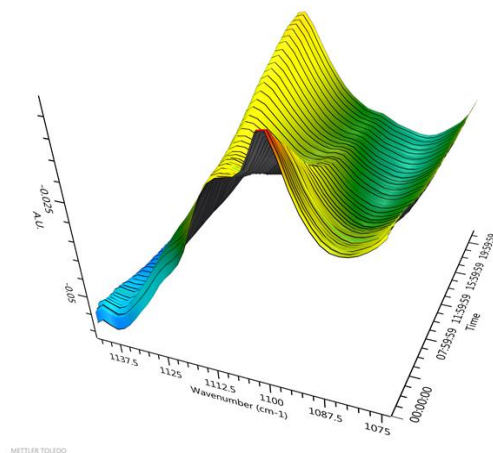


Figure 5.21. 3D-Surface plot of the observed vibrations at 1115 cm^{-1} and 1096 cm^{-1} .

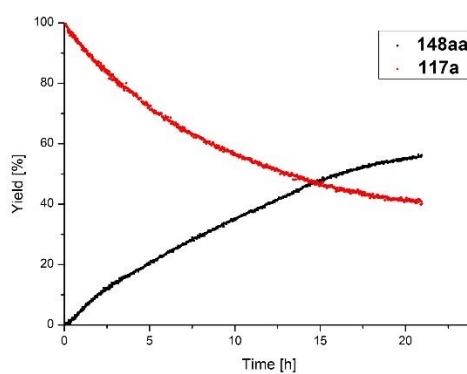
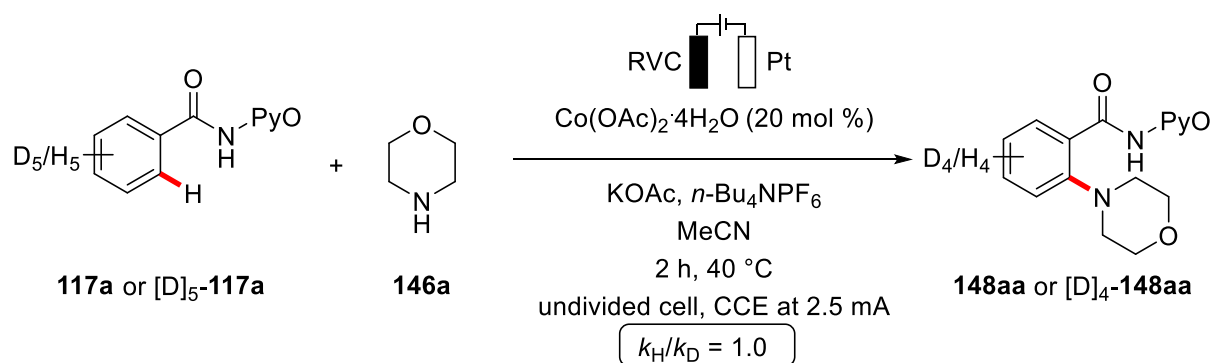


Figure 5.22. Plot of the observed vibrations over time.

KIE Studies



Scheme 5.21. KIE studies for the cobalt-catalyzed C–H amination.

Two independent reactions were carried out following the above procedure for the ReactIR studies using substrates **117aa** (1.00 mmol) and **[D]₅-117aa** (1.00 mmol). For the first 4 h every minute an IR spectrum was recorded, then every 2 min for the following 18 h. The KIE was determined by measuring the initial rates from the increase of the peak at 1115 cm⁻¹. After the reaction, the products **148aa** and **[D]₄-148aa** were isolated to correlate the peak intensity. Then, the measured yields for the first 2 h were plotted to analyze the initial rates of the reaction and a linear fit revealed a KIE of $k_{\text{H}}/k_{\text{D}} \approx 1.0$ (See Figures S-5 and S-6).

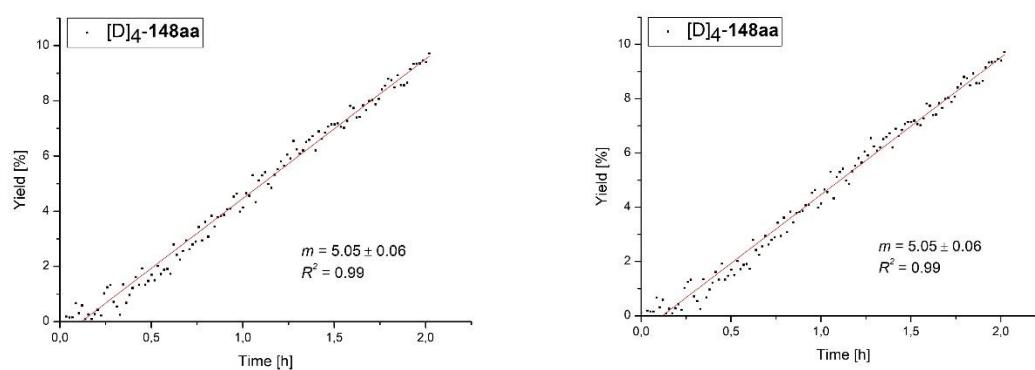
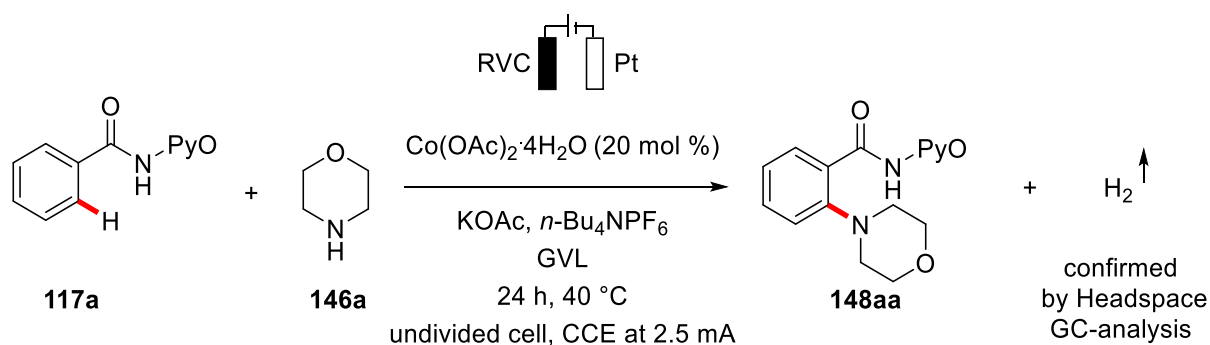


Figure 5.23. Initial rates of **148aa** and **[D]₄-148aa**.

Headspace Analysis



Scheme 5.22. Headspace analysis of the reaction mixture.

Following the general procedure **H**, a reaction was performed under N_2 in a two-neck flask, tightly sealed with two septa. After 24 h, the gas-phase above the solution was analyzed by headspace GC analysis using a Shimadzu S 2014 gas chromatograph equipped with a 5\AA MS column (column length: 2 m, column width: 2 mm, column temp. $100\text{ }^\circ\text{C}$), carrier gas Argon, 25 mL/min, 1 mL volume was injected. The sample was analyzed by a temperature conductivity detector at $110\text{ }^\circ\text{C}$.

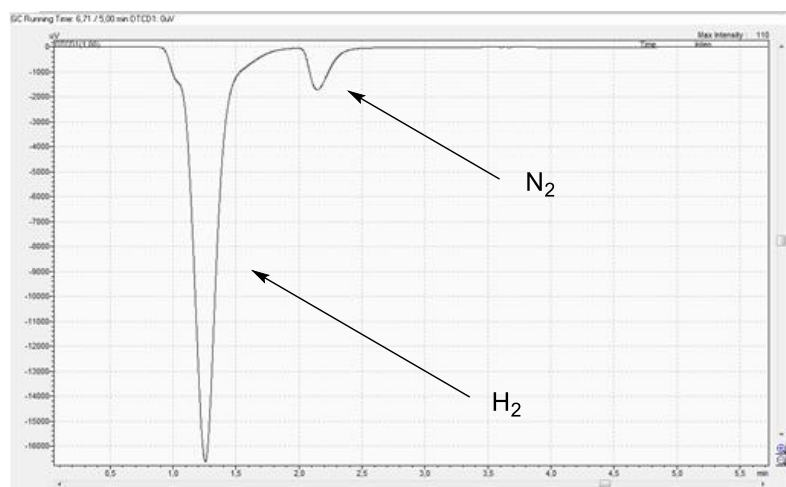


Figure 5.24. Chromatogram of the gas phase of the reaction mixture.

Cyclic Voltammetry

The cyclic voltammetry was carried out with a Metrohm Autolab PGSTAT204 workstation and following analysis was performed with Nova 2.0 software. A glassy-carbon electrode (3 mm-diameter, disc-electrode) was used as the working electrode, a Pt wire as auxiliary electrode and a SCE electrode was used as the reference. The measurements were carried out at a scan rate of 100 mVs^{-1} .

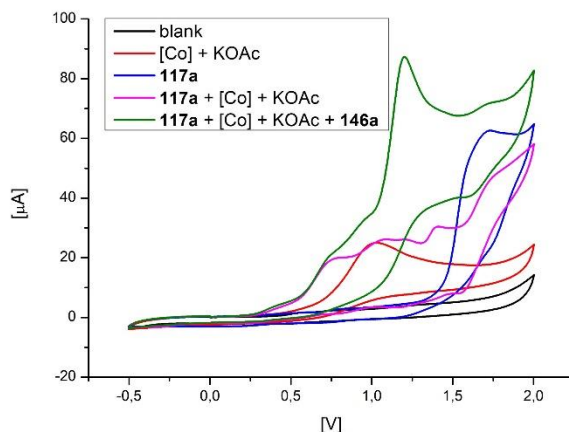
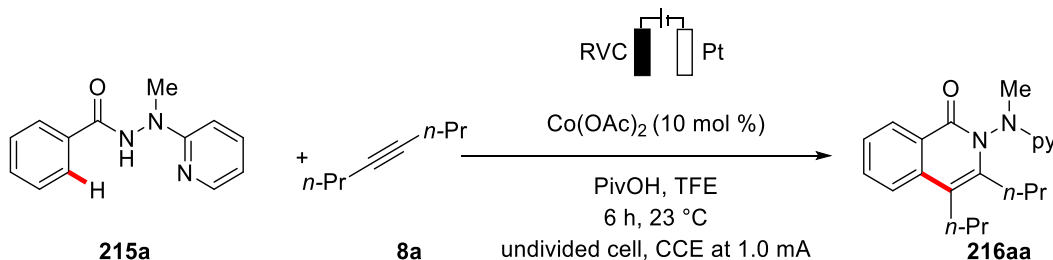


Figure 5.25. Cyclic voltammograms at 100 mVs^{-1} : $n\text{-Bu}_4\text{NPF}_6$ (0.1 M in MeCN), concentration of substrates 1 mM (KOAc 4 mM). (black) blank; (blue) substrate **117a**; (red) $\text{Co}(\text{OAc})_2 \cdot 4\text{H}_2\text{O}$ and KOAc; (purple) $\text{Co}(\text{OAc})_2 \cdot 4\text{H}_2\text{O}$, KOAc and **117a**; (green) $\text{Co}(\text{OAc})_2 \cdot 4\text{H}_2\text{O}$, KOAc, **117a** and **146a**.

5.8 Mechanistic Experiments for Electrochemical C–H Activation

Time-resolved UV/Vis measurements



Scheme 5.23. Time resolved UV/Vis measurements.

In a 5 mL vial, hydrazide **215a** (113 mg, 0.50 mmol, 1.00 equiv), **8a** (66.7 mg, 0.60 mmol, 1.20 equiv), $\text{Co}(\text{OAc})_2$ (7.8 mg, 0.05 mmol, 10 mol %) and PivOH (101 mg, 1.00 mmol, 2.00 equiv) were dissolved in TFE (2 mL), and stirred for 5 min. Then, 0.2 mL of the prepared solution were transferred to a three-neck flask fitted with the UV/Vis probe and Pt (5.0 × 2.5 cm) and RVC (5.0 × 2.5 cm) electrodes containing PivOH (2.04 g, 20 mmol, 20 equiv) in TFE (200 mL). After start of the electrolysis, spectra were obtained every 2 min for 6 h in a range of 220 to 800 nm.

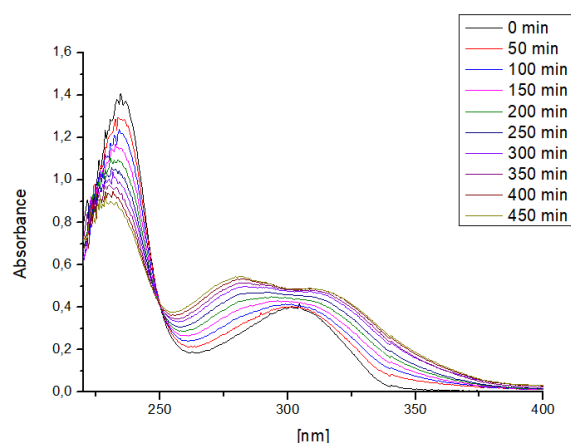
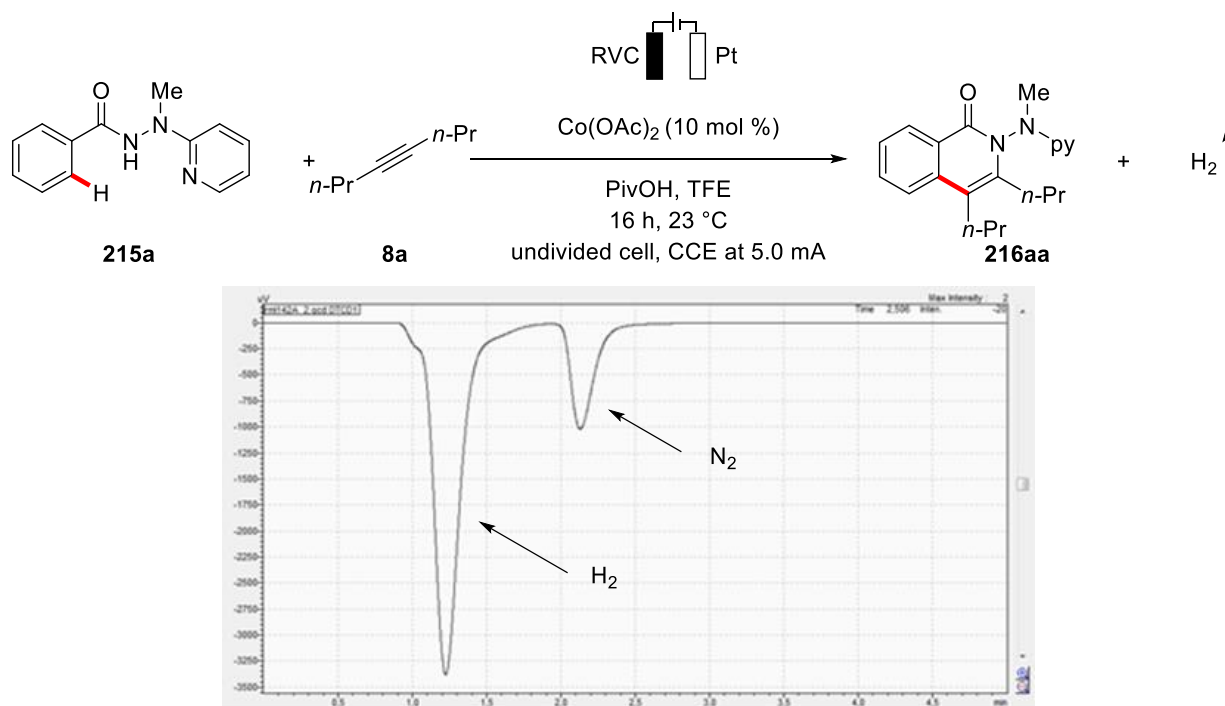


Figure 5.26. Time-resolved UV/Vis spectra for the cobalt-catalyzed annulation (region from 400-800 nm omitted for clarity).

Headspace Analysis



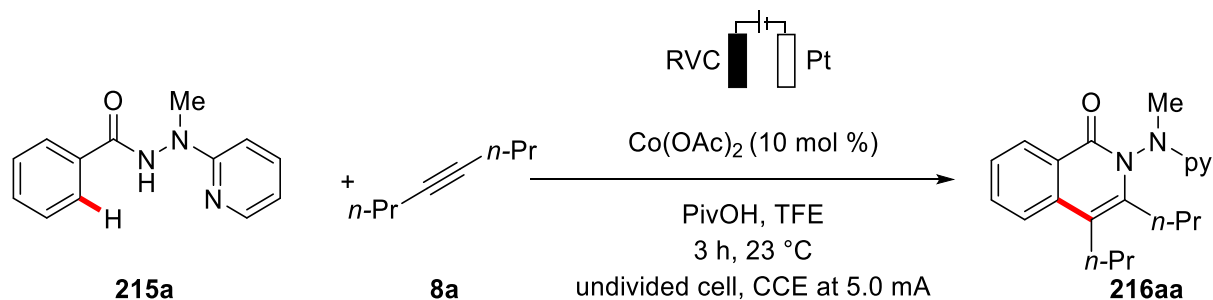
Scheme 5.24. Headspace analysis for the cobalt-catalyzed C–H/N–H annulation.

A reaction was performed under nitrogen in tightly sealed flask using hydrazide **215a** (113 mg, 0.50 mmol, 1.00 equiv), **8a** (66.9 mg, 0.60 mmol, 1.20 equiv), Co(OAc)₂ (7.8 mg, 0.05 mmol, 10 mol %) and PivOH (101 mg, 1.00 mmol, 2.00 equiv) in TFE (3.0 mL). Electrolysis was carried out at a constant current of 5.0 mA. After 16 h, the gas-phase above the solution was analyzed by headspace GC analysis using a Shimadzu S 2014 gaschromatograph equipped with a 5Å MS column (column length:

2 m, column width: 2 mm, column temp. 100 °C), carrier gas Argon, 25 mL/min, 1 mL volume was injected. The sample was analyzed by a temperature conductivity detector at 110 °C.

ESI-MS studies on reaction intermediates

ESI-MS of the reaction mixture



Scheme 5.25. Reaction mixture for ESI-MS analysis.

A reaction was conducted using **215a** (56.8 mg, 0.25 mmol, 1.00 equiv), **8a** (45.7 mg, 0.28 mmol, 1.10 equiv), Co(OAc)_2 (8.9 mg, 20 mol %) and PivOH (51.0 mg, 0.50 mmol, 2.00 equiv) in TFE (3 mL) at 5.0 mA for 3 h. Then 0.1 mL of the solution was removed and analyzed by ESI-MS. Furthermore, the ion observed at m/z 495.1 was isolated and fragmented by MS/MS.

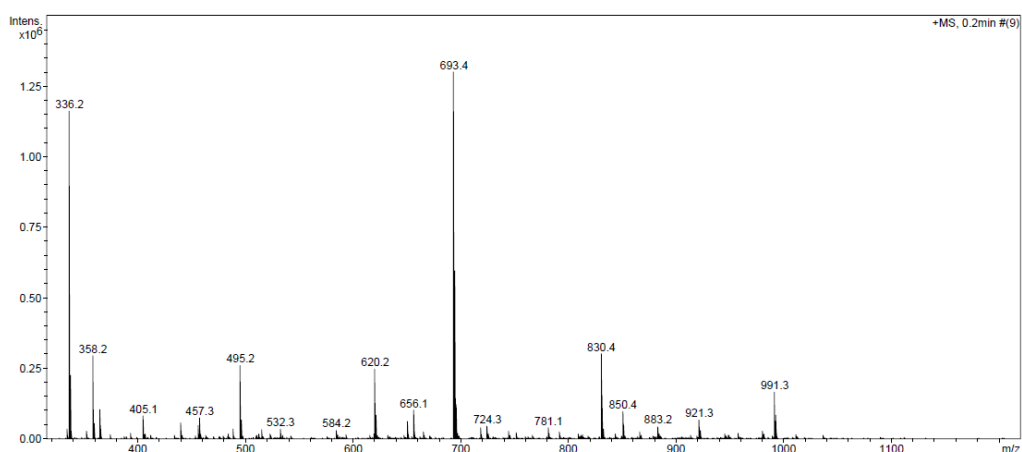


Figure 5.27. ESI-MS spectra of the reaction mixture.

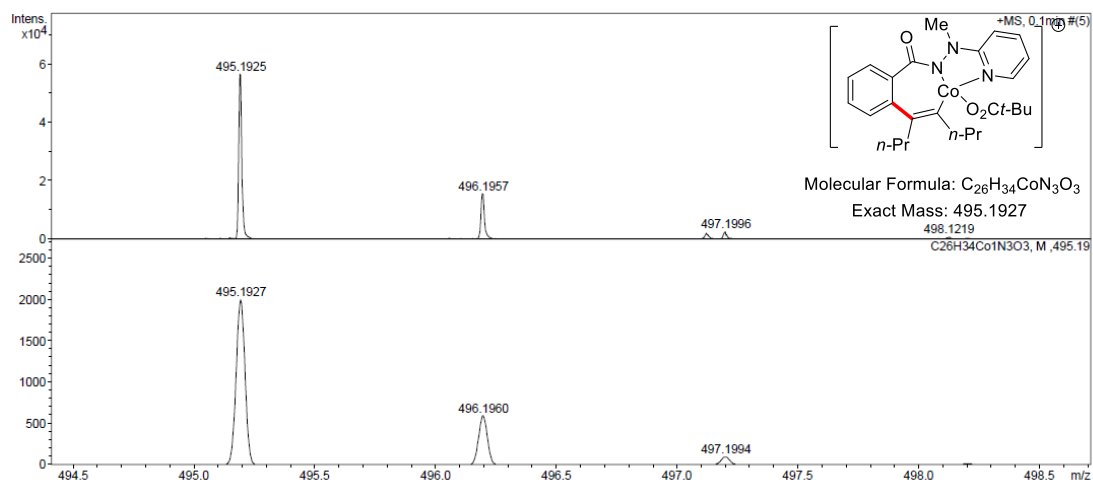


Figure 5.28. ESI-HRMS of the Peak at m/z 495.2.

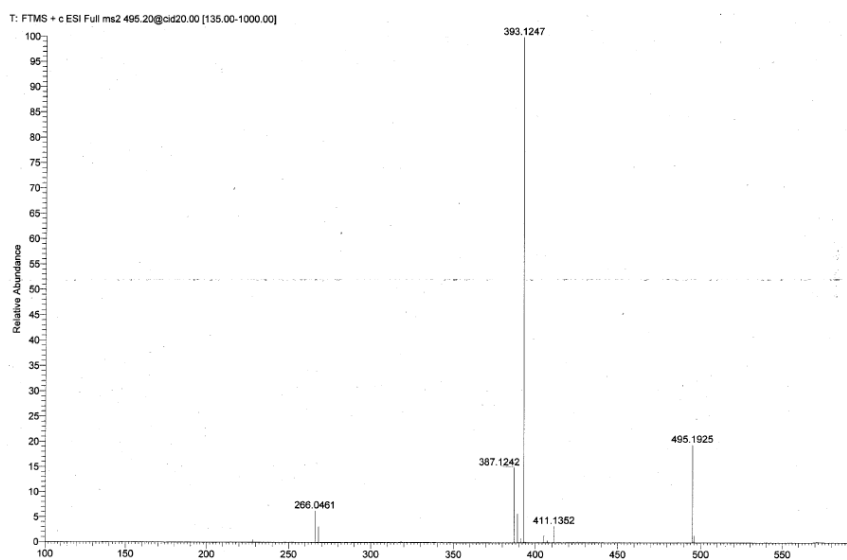
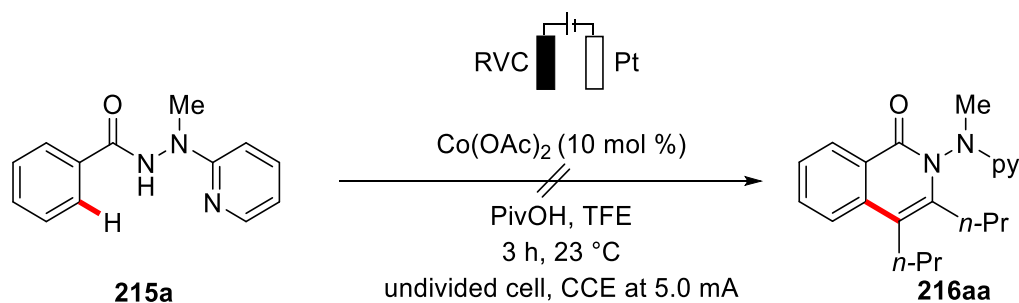


Figure 5.29. MS/MS spectra of the Ion observed at m/z 495.1925.

ESI-MS of the Reaction Mixture without Alkyne **8a**



Scheme 5.26. Reaction mixture for ESI-MS analysis in the absence of alkyne **8a**.

A reaction was conducted using **215a** (56.9 mg, 0.25 mmol, 1.00 equiv), Co(OAc)_2 (8.9 mg, 20 mol %) and PivOH (50.3 mg, 0.50 mmol, 2.00 equiv) in TFE (3 mL) at 5.0 mA for 3 h. Then 0.1 mL of the solution was removed and analyzed by ESI-MS.

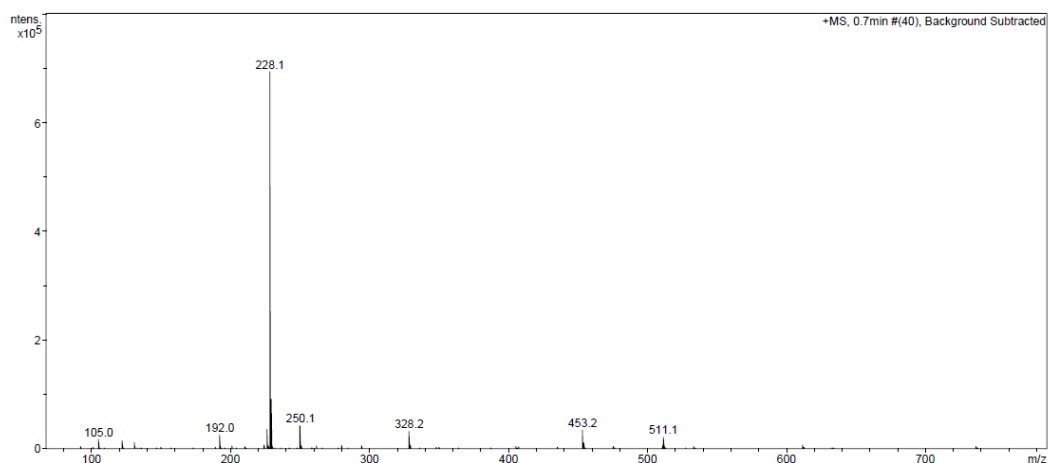


Figure 5.30. ESI-MS spectra of the reaction mixture.

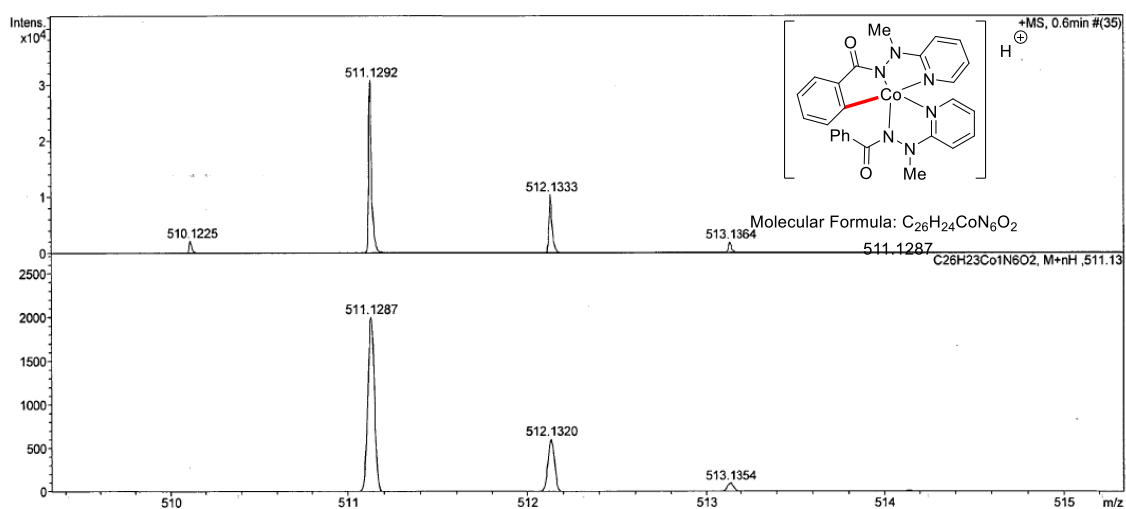
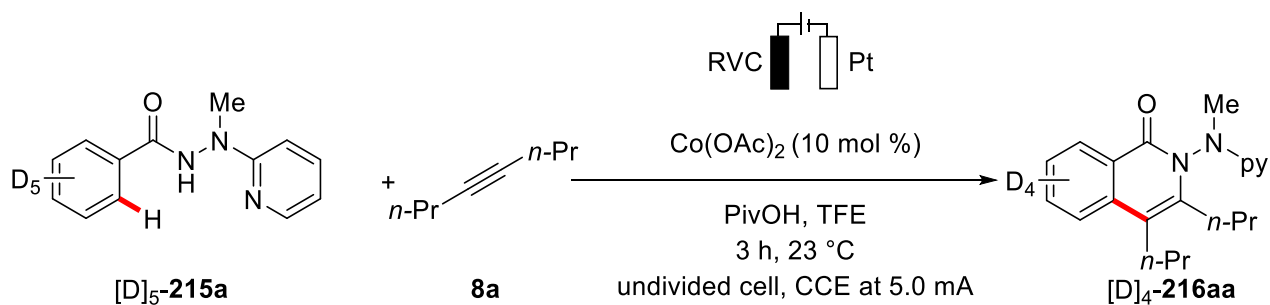


Figure 5.31. ESI-HRMS of the Peak at m/z 511.1.

ESI-MS of the Reaction Mixture using [D]₅-215a



Scheme 5.27. Reaction mixture for ESI-MS analysis of the reaction using [D]₅-215a.

A reaction was conducted using [D]₅-1a (57.2 mg, 0.25 mmol, 1.00 equiv), **8a** (46.0 mg, 0.28 mmol, 1.10 equiv), Co(OAc)₂ (8.9 mg, 20 mol %) and PivOH (50.3 mg, 0.50 mmol, 2.00 equiv) in TFE (3 mL) at 5.0 mA for 3 h. Then 0.1 mL of the solution was removed and analyzed by ESI-MS.

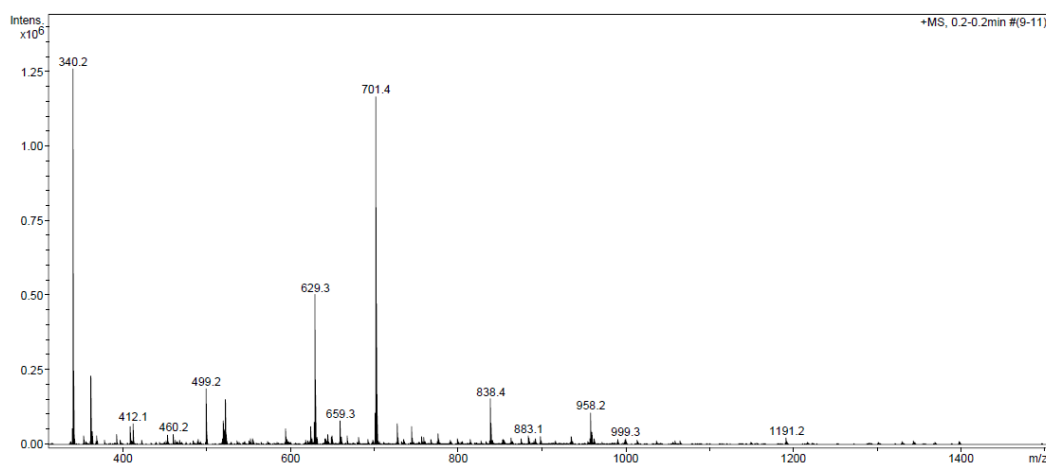


Figure 5.32. ESI-MS spectra of the reaction mixture.

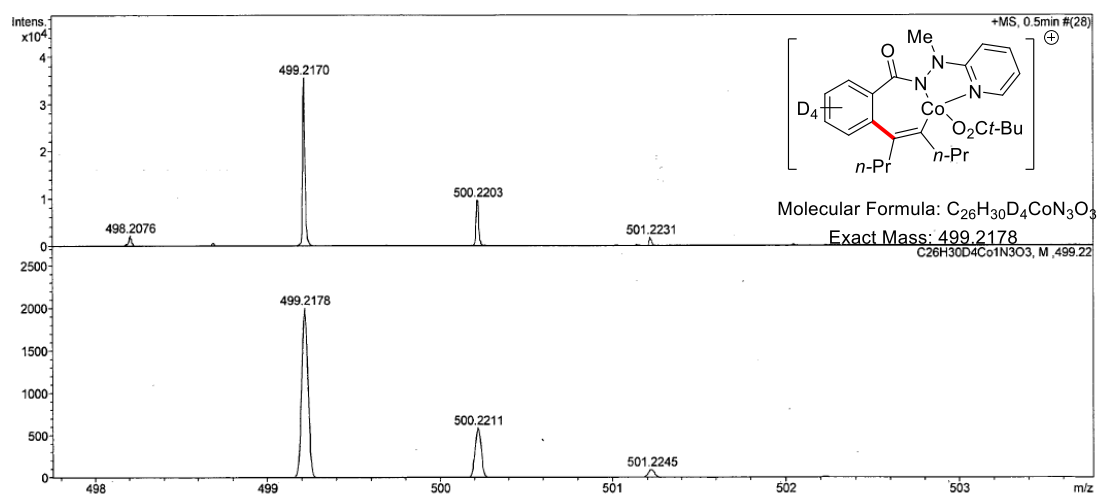


Figure 5.33. ESI-HRMS of the Peak at m/z 499.2.

Cyclic Voltammetry

The cyclic voltammetry was carried out with a Metrohm Autolab PGSTAT204 workstation and following analysis was performed with Nova 2.0 software. A glassy-carbon electrode (3 mm-diameter, disc-electrode) was used as the working electrode, a Pt wire as auxiliary electrode and a SCE electrode was used as the reference. The measurements were carried out at a scan rate of 100 mVs⁻¹.

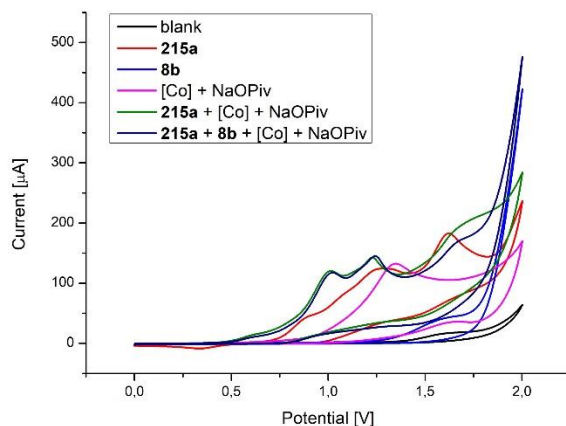


Figure 5.34. Cyclic voltammograms at 100 mVs⁻¹: *n*-Bu₄NPF₆ (0.1 M in MeOH), concentration of substrates 1 mM (NaOPiv 4 mM). (black) blank; (blue) substrate **8a**; (red) substrate **215a**; (purple) Co(OAc)₂ and NaOPiv; (green) Co(OAc)₂, **215a** and NaOPiv; (dark blue) Co(OAc)₂, **215a**, **8a** and NaOPiv.

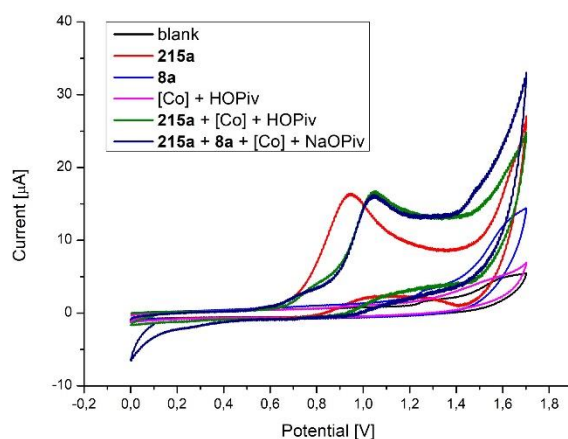


Figure 5.35. Cyclic voltammograms at 100 mVs⁻¹: *n*-Bu₄NPF₆ (0.1 M in TFE), concentration of substrates 1 mM (NaOPiv 4 mM). (black) blank; (blue) substrate **8a**; (red) substrate **215a**; (purple) Co(OAc)₂ and NaOPiv; (green) Co(OAc)₂, **215a** and NaOPiv; (dark blue) Co(OAc)₂, **215a**, **8a** and NaOPiv.

Cyclic Voltammetry

The cyclic voltammetry was carried out with a Metrohm Autolab PGSTAT204 workstation and following analysis was performed with Nova 2.0 software. A glassy-carbon electrode (3 mm-diameter, disc-electrode) was used as the working electrode, a Pt wire as auxiliary electrode and a SCE electrode was used as the reference. The measurements were carried out at a scan rate of 100 mVs⁻¹.

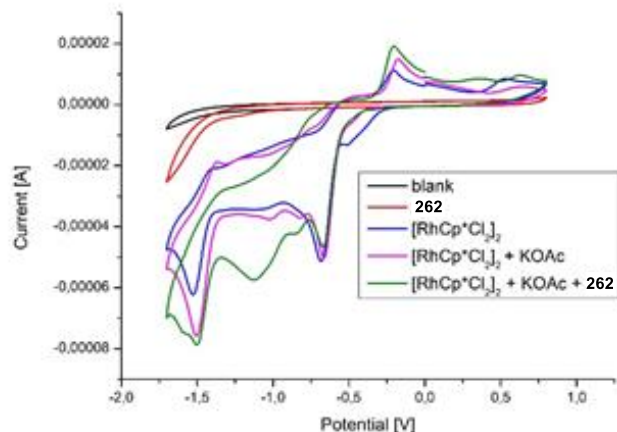


Figure 5.36. Cyclic voltammograms at 100 mV/s in MeCN: *n*-Bu₄NPF₆ (0.1 M in MeCN), concentration of substrates 1mM (KOAc 4 mM). (black) blank; (red) **262**; (blue) [RhCp*Cl₂]₂; (pink) [RhCp*Cl₂]₂ + KOAc; (green) [RhCp*Cl₂]₂ + KOAc + **262**.

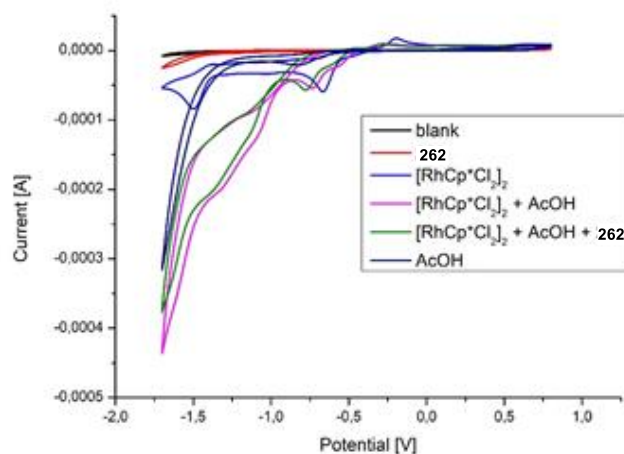


Figure 5.37. Cyclic voltammograms at 100 mV/s in MeCN. *N*-Bu₄NPF₆ (0.1 M in MeCN), concentration of substrates 1mM (HOAc 4 mM). (black) blank; (red) **262**; (blue) [RhCp*Cl₂]₂; (pink) [RhCp*Cl₂]₂ + HOAc; (green) [RhCp*Cl₂]₂ + HOAc + **262**; (dark blue) HOAc.

6 References

- [1] a) P. Ruiz-Castillo, S. L. Buchwald, *Chem. Rev.* **2016**, *116*, 12564-12649; b) S. D. Roughley, A. M. Jordan, *J. Med. Chem.* **2011**, *54*, 3451-3479; c) S. Tasler, J. Mies, M. Lang, *Adv. Synth. Catal.* **2007**, *349*, 2286-2300; d) J.-P. Corbet, G. Mignani, *Chem. Rev.* **2006**, *106*, 2651-2710.
- [2] a) E. B. Pinxterhuis, M. Giannerini, V. Hornillos, B. L. Feringa, *Nat. Commun.* **2016**, *7*, 11698; b) B. H. Lipshutz, N. A. Isley, J. C. Fennewald, E. D. Slack, *Angew. Chem. Int. Ed.* **2013**, *52*, 10952-10958; c) B. H. Lipshutz, A. R. Abela, Ž. V. Bošković, T. Nishikata, C. Duplais, A. Krasovskiy, *Top. Catal.* **2010**, *53*, 985-990.
- [3] *Green Chemistry, Theory and Practice* (Eds.: P. T. Anastas, J. C. Warner), Oxford Universal Press, Oxford, **1998**.
- [4] *Modern Arylation Methods* (Ed.: L. Ackermann), Wiley VCH, Weinheim, **2009**.
- [5] C. Glaser, *Ber. Dtsch. Chem. Ges.* **1869**, *2*, 422-424.
- [6] F. Ullmann, J. Bielecki, *Ber. Dtsch. Chem. Ges.* **1901**, *34*, 2174-2185.
- [7] a) C. C. C. Johansson Seechurn, M. O. Kitching, T. J. Colacot, V. Snieckus, *Angew. Chem. Int. Ed.* **2012**, *51*, 5062-5085; b) K. C. Nicolaou, P. G. Bulger, D. Sarlah, *Angew. Chem. Int. Ed.* **2005**, *44*, 4442-4489.
- [8] a) N. Miyaura, A. Suzuki, *Chem. Rev.* **1995**, *95*, 2457-2483; b) N. Miyaura, K. Yamada, A. Suzuki, *Tetrahedron Lett.* **1979**, *20*, 3437-3440; c) N. Miyaura, A. Suzuki, *J. Chem. Soc. Chem. Comm.* **1979**, 866-867.
- [9] A. O. King, N. Okukado, E.-i. Negishi, *J. Chem. Soc. Chem. Comm.* **1977**, 683-684.
- [10] a) K. Tamao, K. Sumitani, M. Kumada, *J. Am. Chem. Soc.* **1972**, *94*, 4374-4376; b) R. J. P. Corriu, J. P. Masse, *J. Chem. Soc. Chem. Comm.* **1972**, 144a.
- [11] Y. Hatanaka, T. Hiyama, *J. Org. Chem.* **1988**, *53*, 918-920.
- [12] a) J. K. Stille, *Angew. Chem. Int. Ed.* **1986**, *25*, 508-524; b) D. Milstein, J. K. Stille, *J. Am. Chem. Soc.* **1978**, *100*, 3636-3638.
- [13] a) K. Sonogashira, *J. Organomet. Chem.* **2002**, *653*, 46-49; b) K. Sonogashira, Y. Tohda, N. Hagihara, *Tetrahedron Lett.* **1975**, *16*, 4467-4470.
- [14] a) R. F. Heck, J. P. Nolley, *J. Org. Chem.* **1972**, *37*, 2320-2322; b) M. Tsutomu, M. Kunio, O. Atsumu, *Bull. Chem. Soc. Jap.* **1971**, *44*, 581-581.
- [15] a) F. Paul, J. Patt, J. F. Hartwig, *J. Am. Chem. Soc.* **1994**, *116*, 5969-5970; b) A. S. Guram, S. L. Buchwald, *J. Am. Chem. Soc.* **1994**, *116*, 7901-7902.
- [16] The Nobel prize in Chemistry 2010 - Press Release https://www.nobelprize.org/nobel_prizes/chemistry/laureates/2010/press.html accessed 20.04.2018.
- [17] a) T. L. Mako, J. A. Byers, *Inorg. Chem. Front.* **2016**, *3*, 766-790; b) W. M. Czaplik, M. Mayer, J. Cvengroš, A. Jacobi von Wangelin, *ChemSusChem* **2009**, *2*, 396-417; c) J. K. Kochi, M. Tamura, *J. Am. Chem. Soc.* **1971**, *93*, 1485-1487.
- [18] a) J. Yamaguchi, K. Muto, K. Itami, *Eur. J. Org. Chem.* **2013**, *2013*, 19-30; b) B. M. Rosen, K. W. Quasdorf, D. A. Wilson, N. Zhang, A.-M. Resmerita, N. K. Garg, V. Percec, *Chem. Rev.* **2011**, *111*, 1346-1416; c) D. G. Morrell, J. K. Kochi, *J. Am. Chem. Soc.* **1975**, *97*, 7262-7270.
- [19] S. Santoro, F. Ferlin, L. Luciani, L. Ackermann, L. Vaccaro, *Green. Chem.* **2017**, *19*, 1601-1612.
- [20] L. Ackermann, A. R. Kapdi, H. K. Potukuchi, S. I. Kozhushkov, in *Handbook of Green chemistry* (Ed.: C.-J. Li), Wiley-VCH, Weinheim, **2012**, 259-305.
- [21] a) S. I. Kozhushkov, H. K. Potukuchi, L. Ackermann, *Catal. Sci. Technol.* **2013**, *3*, 562-571; b) L. Ackermann, *Chem. Commun.* **2010**, *46*, 4866-4877.
- [22] F. Kakiuchi, S. Murai, in *Activation of Unreactive Bonds and Organic Synthesis* (Eds.: S. Murai, H. Alper, R. A. Gossage, V. V. Grushin, M. Hidai, Y. Ito, W. D. Jones, F. Kakiuchi, G. van Koten, Y. S. Lin, Y. Mizobe, S. Murai, M. Murakami, T. G. Richmond, A. Sen, M. Suginome, A. Yamamoto), Springer Berlin, Heidelberg, **1999**, 47-79.
- [23] L. Ackermann, in *Directed Metallation* (Ed.: N. Chatani), Springer Berlin, Heidelberg, **2007**, 35-60.

- [24] P. Gandeepan, L. Ackermann, *Chem* **2018**, *4*, 199–222.
- [25] a) L. Ackermann, *Chem. Rev.* **2011**, *111*, 1315–1345; b) D. Balcells, E. Clot, O. Eisenstein, *Chem. Rev.* **2010**, *110*, 749–823; c) J. A. Labinger, J. E. Bercaw, *Nature* **2002**, *417*, 507.
- [26] J. Oxgaard, W. J. Tenn, R. J. Nielsen, R. A. Periana, W. A. Goddard, *Organometallics* **2007**, *26*, 1565–1567.
- [27] a) S. I. Gorelsky, D. Lapointe, K. Fagnou, *J. Am. Chem. Soc.* **2008**, *130*, 10848–10849; b) D. García-Cuadrado, A. A. C. Braga, F. Maseras, A. M. Echavarren, *J. Am. Chem. Soc.* **2006**, *128*, 1066–1067; c) L.-C. Campeau, M. Parisien, A. Jean, K. Fagnou, *J. Am. Chem. Soc.* **2006**, *128*, 581–590; d) L.-C. Campeau, M. Parisien, M. Leblanc, K. Fagnou, *J. Am. Chem. Soc.* **2004**, *126*, 9186–9187.
- [28] a) Y. Boutadla, D. L. Davies, S. A. Macgregor, A. I. Poblador-Bahamonde, *Dalton Trans.* **2009**, 5820–5831; b) Y. Boutadla, D. L. Davies, S. A. Macgregor, A. I. Poblador-Bahamonde, *Dalton Trans.* **2009**, 5887–5893.
- [29] a) E. Tan, O. Quinero, M. E. de Orbe, A. M. Echavarren, *ACS Catal.* **2018**, *8*, 2166–2172; b) D. Zell, M. Bursch, V. Müller, S. Grimme, L. Ackermann, *Angew. Chem. Int. Ed.* **2017**, *56*, 10378–10382; c) H. Wang, M. Moselage, M. J. González, L. Ackermann, *ACS Catal.* **2016**, *6*, 2705–2709; d) D. Santrač, S. Cella, W. Wang, L. Ackermann, *Eur. J. Org. Chem.* **2016**, *2016*, 5429–5436; e) R. Mei, J. Loup, L. Ackermann, *ACS Catal.* **2016**, *6*, 793–797; f) W. Ma, R. Mei, G. Tenti, L. Ackermann, *Chem. Eur. J.* **2014**, *20*, 15248–15251.
- [30] a) T. G. Saint-Denis, R.-Y. Zhu, G. Chen, Q.-F. Wu, J.-Q. Yu, *Science* **2018**, *359*; b) W. Ma, P. Gandeepan, J. Li, L. Ackermann, *Org. Chem. Front* **2017**, *4*, 1435–1467; c) Y. Segawa, T. Maekawa, K. Itami, *Angew. Chem. Int. Ed.* **2015**, *54*, 66–81; d) J. Wencel-Delord, F. Glorius, *Nat. Chem.* **2013**, *5*, 369; e) L. McMurray, F. O'Hara, M. J. Gaunt, *Chem. Soc. Rev.* **2011**, *40*, 1885–1898; f) O. Baudoin, *Chem. Soc. Rev.* **2011**, *40*, 4902–4911; g) R. G. Bergman, *Nature* **2007**, *446*, 391.
- [31] a) K. Shin, H. Kim, S. Chang, *Acc. Chem. Res.* **2015**, *48*, 1040–1052; b) N. Kuhl, N. Schröder, F. Glorius, *Adv. Synth. Catal.* **2014**, *356*, 1443–1460; c) D. A. Colby, A. S. Tsai, R. G. Bergman, J. A. Ellman, *Acc. Chem. Res.* **2012**, *45*, 814–825; d) D. A. Colby, R. G. Bergman, J. A. Ellman, *Chem. Rev.* **2010**, *110*, 624–655.
- [32] a) T. Sperger, I. A. Sanhueza, I. Kalvet, F. Schoenebeck, *Chem. Rev.* **2015**, *115*, 9532–9586; b) S. Pan, T. Shibata, *ACS Catal.* **2013**, *3*, 704–712; c) I. A. I. Mkhaliid, J. H. Barnard, T. B. Marder, J. M. Murphy, J. F. Hartwig, *Chem. Rev.* **2010**, *110*, 890–931.
- [33] a) J. He, M. Wasa, K. S. L. Chan, Q. Shao, J. Q. Yu, *Chem. Rev.* **2017**, *117*, 8754–8786; b) A. Dey, S. Agasti, D. Maiti, *Org. Biomol. Chem.* **2016**, *14*, 5440–5453; c) T. W. Lyons, M. S. Sanford, *Chem. Rev.* **2010**, *110*, 1147–1169; d) X. Chen, K. M. Engle, D. H. Wang, J. Q. Yu, *Angew. Chem. Int. Ed.* **2009**, *48*, 5094–5115.
- [34] a) J. A. Leitch, C. G. Frost, *Chem. Soc. Rev.* **2017**, *46*, 7145–7153; b) D. J. Burns, S. I. Kozhushkov, L. Ackermann, in *Catalytic Hydroarylation of Carbon-Carbon Multiple Bonds* (Eds.: L. G. Habgood, T. B. Gunnoe, L. Ackermann), Wiley VCH, Weinheim, **2017**; c) L. Ackermann, *Acc. Chem. Res.* **2014**, *47*, 281–295; d) P. B. Arockiam, C. Bruneau, P. H. Dixneuf, *Chem. Rev.* **2012**, *112*, 5879–5918; e) L. Ackermann, R. Vicente, in *C-H Activation* (Eds.: J.-Q. Yu, Z. Shi), Springer Berlin Heidelberg, Berlin, Heidelberg, **2010**, 211–229.
- [35] *CRC Handbook of Chemistry and Physics* (Ed.: D. R. Lide), CRC Press/Taylor and Francis, Boca Raton, **2010**.
- [36] www.infomine.com/investment/ accessed on 20.04.2018.
- [37] M. Beller, B. Cornils, C. D. Frohning, C. W. Kohlpaintner, *J. Mol. Catal. A* **1995**, *104*, 17–85.
- [38] a) H. Bönemann, *Angew. Chem.* **1978**, *90*, 517–526; b) W. Reppe, N. V. Kutepow, A. Margin, *Angew. Chem.* **1969**, *81*, 717–723.
- [39] a) I. U. Khand, G. R. Knox, P. L. Pauson, W. E. Watts, M. I. Foreman, *J. Chem. Soc. Perkin Trans.* **1973**, 977–981; b) I. U. Khand, G. R. Knox, P. L. Pauson, W. E. Watts, *J. Chem. Soc. Perkin Trans.* **1973**, 975–977.
- [40] M. Tokunaga, J. F. Larrow, F. Kakiuchi, E. N. Jacobsen, *Science* **1997**, *277*, 936–938.

- [41] M. S. Kharasch, E. K. Fields, *J. Am. Chem. Soc.* **1941**, *63*, 2316–2320.
- [42] a) S. Murahashi, S. Horie, *J. Am. Chem. Soc.* **1956**, *78*, 4816–4817; b) S. Murahashi, *J. Am. Chem. Soc.* **1955**, *77*, 6403–6404.
- [43] a) S. Camadanli, R. Beck, U. Florke, H.-F. Klein, *Dalton Trans.* **2008**, 5701–5704; b) R. Beck, H. Sun, X. Li, S. Camadanli, H.-F. Klein, *Eur. J. Inorg. Chem.* **2008**, *2008*, 3253–3257; c) H.-F. Klein, S. Camadanli, R. Beck, D. Leukel, U. Flörke, *Angew. Chem. Int. Ed.* **2005**, *44*, 975–977; d) H.-F. Klein, R. Beck, U. Flörke, H.-J. Haupt, *Eur. J. Inorg. Chem.* **2003**, *2003*, 1380–1387; e) H.-F. Klein, S. Schneider, M. He, U. Flörke, H.-J. Haupt, *Eur. J. Inorg. Chem.* **2000**, 2295–2301; f) H.-F. Klein, M. Hellwig, U. Koch, U. Flörke, H.-J. Haupt, *Z. Naturforsch. B* **1993**, *48*, 778–784.
- [44] C. P. Lenges, M. Brookhart, B. E. Grant, *J. Organomet. Chem.* **1997**, *528*, 199–203.
- [45] G. Halbritter, F. Knoch, A. Wolski, H. Kisch, *Angew. Chem. Int. Ed.* **1994**, *33*, 1603–1605.
- [46] a) B. J. Fallon, E. Derat, M. Amatore, C. Aubert, F. Chemla, F. Ferreira, A. Perez-Luna, M. Petit, *Org. Lett.* **2016**, *18*, 2292–2295; b) B. J. Fallon, J.-B. Garsi, E. Derat, M. Amatore, C. Aubert, M. Petit, *ACS Catal.* **2015**, *5*, 7493–7497; c) B. J. Fallon, E. Derat, M. Amatore, C. Aubert, F. Chemla, F. Ferreira, A. Perez-Luna, M. Petit, *J. Am. Chem. Soc.* **2015**, *137*, 2448–2451.
- [47] L. Ilies, Q. Chen, X. Zeng, E. Nakamura, *J. Am. Chem. Soc.* **2011**, *133*, 5221–5223.
- [48] a) M. Moselage, J. Li, L. Ackermann, *ACS Catal.* **2016**, *6*, 498–525; b) Y. Naohiko, *Bull. Chem. Soc. Jap.* **2014**, *87*, 843–857; c) K. Gao, N. Yoshikai, *Acc. Chem. Res.* **2014**, *47*, 1208–1219; d) L. Ackermann, *J. Org. Chem.* **2014**, *79*, 8948–8954.
- [49] B. Punji, W. Song, G. A. Shevchenko, L. Ackermann, *Chem. Eur. J.* **2013**, *19*, 10605–10610.
- [50] K. Gao, N. Yoshikai, *J. Am. Chem. Soc.* **2013**, *135*, 9279–9282.
- [51] Prices of chlorocyclohexane (17.26€/mol) and bromo-2,2-dimethylpropane (936,41€/mol) calculated based on the largest available unit from sigma aldrich, prices obtained on 16.05.2018.
- [52] W. Song, L. Ackermann, *Angew. Chem. Int. Ed.* **2012**, *51*, 8251–8254.
- [53] J. Li, L. Ackermann, *Chem. Eur. J.* **2015**, *21*, 5718–5722.
- [54] R. Mei, L. Ackermann, *Adv. Synth. Catal.* **2016**, *358*, 2443–2448.
- [55] a) Y. Onishi, Y. Yoneda, Y. Nishimoto, M. Yasuda, A. Baba, *Org. Lett.* **2012**, *14*, 5788–5791; b) Y. Ding, W. Wang, Z. Liu, *Phosphorous Sulfur Relat. Elem.* **1996**, *118*, 113–116; c) M. G. Silvestri, M. P. Hanson, J. G. Pavlovich, L. F. Studen, M. S. DeClue, M. R. DeGraffenreid, C. D. Amos, *J. Org. Chem.* **1999**, *64*, 6597–6602; d) M. Boultadakis-Arapinis, M. N. Hopkinson, F. Glorius, *Org. Lett.* **2014**, *16*, 1630–1633.
- [56] M. Moselage, N. Sauermann, S. C. Richter, L. Ackermann, *Angew. Chem. Int. Ed.* **2015**, *54*, 6352–6355.
- [57] K. Gao, P.-S. Lee, T. Fujita, N. Yoshikai, *J. Am. Chem. Soc.* **2010**, *132*, 12249–12251.
- [58] Z. Ding, N. Yoshikai, *Angew. Chem. Int. Ed.* **2012**, *51*, 4698–4701.
- [59] P.-S. Lee, T. Fujita, N. Yoshikai, *J. Am. Chem. Soc.* **2011**, *133*, 17283–17295.
- [60] T. Yamakawa, N. Yoshikai, *Org. Lett.* **2013**, *15*, 196–199.
- [61] a) Z. Ding, N. Yoshikai, *Synthesis* **2011**, 2561–2566; b) Z. Ding, N. Yoshikai, *Org. Lett.* **2010**, *12*, 4180–4183.
- [62] K. Gao, N. Yoshikai, *J. Am. Chem. Soc.* **2011**, *133*, 400–402.
- [63] K. Gao, N. Yoshikai, *Angew. Chem. Int. Ed.* **2011**, *50*, 6888–6892.
- [64] P.-S. Lee, N. Yoshikai, *Org. Lett.* **2015**, *17*, 22–25.
- [65] a) W. Xu, J. H. Pek, N. Yoshikai, *Adv. Synth. Catal.* **2016**, *358*, 2564–2568; b) J. Yang, N. Yoshikai, *J. Am. Chem. Soc.* **2014**, *136*, 16748–16751.
- [66] U. Koelle, B. Fuss, M. V. Rajasekharan, B. L. Ramakrishna, J. H. Ammeter, M. C. Boehm, *J. Am. Chem. Soc.* **1984**, *106*, 4152–4160.
- [67] T. Yoshino, H. Ikemoto, S. Matsunaga, M. Kanai, *Angew. Chem. Int. Ed.* **2013**, *52*, 2207–2211.
- [68] T. Yoshino, H. Ikemoto, S. Matsunaga, M. Kanai, *Chem. Eur. J.* **2013**, *19*, 9142–9146.
- [69] T. Yoshino, S. Matsunaga, in *Advances in Organometallic Chemistry, Vol. 68* (Ed.: P. J. Pérez), Academic Press, **2017**, 197–247.

- [70] H. Ikemoto, T. Yoshino, K. Sakata, S. Matsunaga, M. Kanai, *J. Am. Chem. Soc.* **2014**, *136*, 5424–5431.
- [71] H. Ikemoto, R. Tanaka, K. Sakata, M. Kanai, T. Yoshino, S. Matsunaga, *Angew. Chem. Int. Ed.* **2017**, *56*, 7156–7160.
- [72] R. Tanaka, H. Ikemoto, M. Kanai, T. Yoshino, S. Matsunaga, *Org. Lett.* **2016**, *18*, 5732–5735.
- [73] S. Nakanowatari, R. Mei, M. Feldt, L. Ackermann, *ACS Catal.* **2017**, *7*, 2511–2515.
- [74] Z. Zhang, S. Han, M. Tang, L. Ackermann, J. Li, *Org. Lett.* **2017**, *19*, 3315–3318.
- [75] J. R. Hummel, J. A. Ellman, *J. Am. Chem. Soc.* **2015**, *137*, 490–498.
- [76] a) J. Li, M. Tang, L. Zang, X. Zhang, Z. Zhang, L. Ackermann, *Org. Lett.* **2016**, *18*, 2742–2745; b) H. Wang, J. Koeller, W. Liu, L. Ackermann, *Chem. Eur. J.* **2015**, *21*, 15525–15528; c) B. Sun, T. Yoshino, M. Kanai, S. Matsunaga, *Angew. Chem. Int. Ed.* **2015**, *54*, 12968–12972; d) M. Sen, D. Kalsi, B. Sundararaju, *Chem. Eur. J.* **2015**, *21*, 15529–15533.
- [77] H. Wang, M. M. Lorion, L. Ackermann, *Angew. Chem. Int. Ed.* **2016**, *55*, 10386–10390.
- [78] Z.-Z. Zhang, B. Liu, C.-Y. Wang, B.-F. Shi, *Org. Lett.* **2015**, *17*, 4094–4097.
- [79] a) M. Moselage, N. Sauermaun, J. Koeller, W. Liu, D. Gelman, L. Ackermann, *Synlett* **2015**, *26*, 1596–1600; b) D.-G. Yu, T. Gensch, F. de Azambuja, S. Vásquez-Céspedes, F. Glorius, *J. Am. Chem. Soc.* **2014**, *136*, 17722–17725.
- [80] a) M. R. Sk, S. S. Bera, M. S. Maji, *Org. Lett.* **2018**, *20*, 134–137; b) K. Ramachandran, P. Anbarasan, *Eur. J. Org. Chem.* **2017**, *2017*, 3965–3968; c) L. Kong, S. Yu, G. Tang, H. Wang, X. Zhou, X. Li, *Org. Lett.* **2016**, *18*, 3802–3805.
- [81] H. Wang, M. M. Lorion, L. Ackermann, *ACS Catal.* **2017**, *7*, 3430–3433.
- [82] a) Y. Bunno, N. Murakami, Y. Suzuki, M. Kanai, T. Yoshino, S. Matsunaga, *Org. Lett.* **2016**, *18*, 2216–2219; b) Y. Suzuki, B. Sun, K. Sakata, T. Yoshino, S. Matsunaga, M. Kanai, *Angew. Chem. Int. Ed.* **2015**, *54*, 9944–9947.
- [83] T. Gensch, S. Vásquez-Céspedes, D.-G. Yu, F. Glorius, *Org. Lett.* **2015**, *17*, 3714–3717.
- [84] J. Li, L. Ackermann, *Angew. Chem. Int. Ed.* **2015**, *54*, 3635–3638.
- [85] A. B. Pawar, S. Chang, *Org. Lett.* **2015**, *17*, 660–663.
- [86] A. B. Pawar, D. M. Lade, *Org. Biomol. Chem.* **2016**, *14*, 3275–3283.
- [87] B. Sun, T. Yoshino, S. Matsunaga, M. Kanai, *Adv. Synth. Catal.* **2014**, *356*, 1491–1495.
- [88] Y. Liang, Y.-F. Liang, C. Tang, Y. Yuan, N. Jiao, *Chem. Eur. J.* **2015**, *21*, 16395–16399.
- [89] P. Patel, S. Chang, *ACS Catal.* **2015**, *5*, 853–858.
- [90] V. G. Zaitsev, D. Shabashov, O. Daugulis, *J. Am. Chem. Soc.* **2005**, *127*, 13154–13155.
- [91] Q. Gu, H. Al Mamari Hamad, K. Graczyk, E. Diers, L. Ackermann, *Angew. Chem. Int. Ed.* **2014**, *53*, 3868–3871.
- [92] F.-J. Chen, S. Zhao, F. Hu, K. Chen, Q. Zhang, S.-Q. Zhang, B.-F. Shi, *Chem. Sci.* **2013**, *4*, 4187–4192.
- [93] X.-Q. Hao, L.-J. Chen, B. Ren, L.-Y. Li, X.-Y. Yang, J.-F. Gong, J.-L. Niu, M.-P. Song, *Org. Lett.* **2014**, *16*, 1104–1107.
- [94] L. Grigorjeva, O. Daugulis, *Angew. Chem. Int. Ed.* **2014**, *53*, 10209–10212.
- [95] L. Grigorjeva, O. Daugulis, *Org. Lett.* **2014**, *16*, 4684–4687.
- [96] T. T. Nguyen, L. Grigorjeva, O. Daugulis, *ACS Catal.* **2015**, *6*, 551–554.
- [97] T. T. Nguyen, L. Grigorjeva, O. Daugulis, *Angew. Chem. Int. Ed.* **2018**, *57*, 1688–1691.
- [98] W. Ma, L. Ackermann, *ACS Catal.* **2015**, *5*, 2822–2825.
- [99] R. Mei, H. Wang, S. Warratz, S. A. Macgregor, L. Ackermann, *Chem. Eur. J.* **2016**, *22*, 6759–6763.
- [100] N. Thrimurtulu, A. Dey, D. Maiti, C. M. R. Volla, *Angew. Chem. Int. Ed.* **2016**, *55*, 12361–12365.
- [101] a) D. Kalsi, B. Sundararaju, *Org. Lett.* **2015**, *17*, 6118–6121; b) O. Planas, C. J. Whiteoak, A. Company, X. Ribas, *Adv. Synth. Catal.* **2015**, *357*, 4003–4012.
- [102] L. Grigorjeva, O. Daugulis, *Org. Lett.* **2014**, *16*, 4688–4690.
- [103] V. G. Landge, G. Jaiswal, E. Balaraman, *Org. Lett.* **2016**, *18*, 812–815.
- [104] Q. Li, Y. Li, W. Hu, R. Hu, G. Li, H. Lu, *Chem. Eur. J.* **2016**, *22*, 12286–12289.
- [105] T. Yamaguchi, Y. Komagalla, Y. Aihara, N. Chatani, *Chem. Commun.* **2016**, *52*, 10129–10132.

- [106] L. Grigorjeva, O. Daugulis, *Org. Lett.* **2015**, *17*, 1204–1207.
- [107] C. Du, P. X. Li, X. Zhu, J. F. Suo, J. L. Niu, M. P. Song, *Angew. Chem. Int. Ed.* **2016**, *55*, 13571–13575.
- [108] a) G. Tan, S. He, X. Huang, X. Liao, Y. Cheng, J. You, *Angew. Chem. Int. Ed.* **2016**, *55*, 10414–10418; b) L. Hu, Q. Gui, X. Chen, Z. Tan, G. Zhu, *Org. Biomol. Chem.* **2016**, *14*, 11070–11075.
- [109] X. Zhu, J. H. Su, C. Du, Z. L. Wang, C. J. Ren, J. L. Niu, M. P. Song, *Org. Lett.* **2017**, *19*, 596–599.
- [110] a) C. Du, P.-X. Li, X. Zhu, J.-N. Han, J.-L. Niu, M.-P. Song, *ACS Catal.* **2017**, *7*, 2810–2814; b) L. B. Zhang, S. K. Zhang, D. Wei, X. Zhu, X. Q. Hao, J. H. Su, J. L. Niu, M. P. Song, *Org. Lett.* **2016**, *18*, 1318–1321; c) Q. Yan, T. Xiao, Z. Liu, Y. Zhang, *Adv. Synth. Catal.* **2016**, *358*, 2707–2711.
- [111] a) R. Ueno, S. Natsui, N. Chatani, *Org. Lett.* **2018**, *20*, 1062–1065; b) L. B. Zhang, X. Q. Hao, S. K. Zhang, Z. J. Liu, X. X. Zheng, J. F. Gong, J. L. Niu, M. P. Song, *Angew. Chem. Int. Ed.* **2015**, *54*, 272–275.
- [112] Y. Kommagalla, K. Yamazaki, T. Yamaguchi, N. Chatani, *Chem. Commun.* **2018**, *54*, 1359–1362.
- [113] X. Wu, K. Yang, Y. Zhao, H. Sun, G. Li, H. Ge, *Nat. Commun.* **2015**, *6*, 6462.
- [114] J. Zhang, H. Chen, C. Lin, Z. Liu, C. Wang, Y. Zhang, *J. Am. Chem. Soc.* **2015**, *137*, 12990–12996.
- [115] a) L. Zeng, S. Tang, D. Wang, Y. Deng, J. L. Chen, J. F. Lee, A. Lei, *Org. Lett.* **2017**, *19*, 2170–2173; b) P. Williamson, A. Galvan, M. J. Gaunt, *Chem. Sci.* **2017**, *8*, 2588–2591; c) N. Barsu, S. K. Bolli, B. Sundararaju, *Chem. Sci.* **2017**, *8*, 2431–2435.
- [116] a) D. S. Avila, R. L. Puntel, M. Aschner, in *Interrelations between Essential Metal Ions and Human Diseases* (Eds.: A. Sigel, H. Sigel, R. K. O. Sigel), Springer Netherlands, Dordrecht, **2013**, 199–227; b) P. B. Tchounwou, C. G. Yedjou, A. K. Patlolla, D. J. Sutton, in *Molecular, Clinical and Environmental Toxicology: Volume 3: Environmental Toxicology* (Ed.: A. Luch), Springer Basel, Basel, **2012**, 133–164; c) N. A. Law, M. T. Caudle, V. L. Pecoraro, in *Advances in Inorganic Chemistry, Vol. 46* (Ed.: A. G. Sykes), Academic Press, **1998**, 305–440.
- [117] a) A. S. Borovik, *Chem. Soc. Rev.* **2011**, *40*, 1870–1874; b) A. Gunay, K. H. Theopold, *Chem. Rev.* **2010**, *110*, 1060–1081.
- [118] a) S. M. Paradine, J. R. Griffin, J. Zhao, A. L. Petronico, S. M. Miller, M. C. White, *Nat. Chem.* **2015**, *7*, 987–994; b) X. Huang, T. M. Bergsten, J. T. Groves, *J. Am. Chem. Soc.* **2015**, *137*, 5300–5303; c) D. Shen, C. Miao, S. Wang, C. Xia, W. Sun, *Org. Lett.* **2014**, *16*, 1108–1111; d) X. Huang, W. Liu, H. Ren, R. Neelamegam, J. M. Hooker, J. T. Groves, *J. Am. Chem. Soc.* **2014**, *136*, 6842–6845; e) W. Liu, J. T. Groves, *Angew. Chem. Int. Ed.* **2013**, *52*, 6024–6027; f) R. V. Ottenbacher, D. G. Samsonenko, E. P. Talsi, K. P. Bryliakov, *Org. Lett.* **2012**, *14*, 4310–4313; g) W. Liu, X. Huang, M.-J. Cheng, R. J. Nielsen, W. A. Goddard, J. T. Groves, *Science* **2012**, *337*, 1322–1325; h) W. Liu, J. T. Groves, *J. Am. Chem. Soc.* **2010**, *132*, 12847–12849; i) S. Das, C. D. Incarvito, R. H. Crabtree, G. W. Brudvig, *Science* **2006**, *312*, 1941–1943; j) R. Breslow, X. Zhang, Y. Huang, *J. Am. Chem. Soc.* **1997**, *119*, 4535–4536.
- [119] a) Y. Hu, B. Zhou, C. Wang, *Acc. Chem. Res.* **2018**, *51*, 816–827; b) W. Liu, L. Ackermann, *ACS Catal.* **2016**, *6*, 3743–3752.
- [120] a) C. Zhu, J. C. A. Oliveira, Z. Shen, H. Huang, L. Ackermann, *ACS Catal.* **2018**, *8*, 4402–4407; b) T. Sato, T. Yoshida, H. H. Al Mamari, L. Ilies, E. Nakamura, *Org. Lett.* **2017**, *19*, 5458–5461; c) W. Liu, G. Cera, J. C. A. Oliveira, Z. Shen, L. Ackermann, *Chem. Eur. J.* **2017**, *23*, 11524–11528.
- [121] M. I. Bruce, M. Z. Iqbal, F. G. A. Stone, *J. Chem. Soc. A.* **1970**, 3204–3209.
- [122] R. F. Heck, *J. Am. Chem. Soc.* **1968**, *90*, 313–317.
- [123] a) G. J. Depree, L. Main, B. K. Nicholson, N. P. Robinson, G. B. Jameson, *J. Organomet. Chem.* **2006**, *691*, 667–679; b) J. Albert, J. M. Cadena, J. Granell, X. Solans, M. Font-Bardia, *J. Organomet. Chem.* **2004**, *689*, 4889–4896; c) M. A. Leeson, B. K. Nicholson, M. R. Olsen, *J. Organomet. Chem.* **1999**, *579*, 243–251; d) J.-P. Djukic, A. Maise, M. Pfeffer, *J. Organomet. Chem.* **1998**, *567*, 65–74; e) J.-P. Djukic, A. Maise, M. Pfeffer, A. de Cian, J. Fischer, *Organometallics* **1997**, *16*, 657–667; f) J. M. Cooney, L. H. P. Gommans, L. Main, B. K. Nicholson, *J. Organomet. Chem.* **1988**, *349*, 197–207; g) M. I. Bruce, B. L. Goodall, M. Z. Iqbal, F. G. A. Stone, R. J. Doedens, R. G. Little, *J. Chem. Soc. D.* **1971**, 1595–1596.
- [124] Y. Kuninobu, Y. Nishina, T. Takeuchi, K. Takai, *Angew. Chem. Int. Ed.* **2007**, *46*, 6518–6520.

- [125] a) B. Zhou, Y. Hu, T. Liu, C. Wang, *Nat. Commun.* **2017**, *8*, 1169; b) B. Zhou, Y. Hu, C. Wang, *Angew. Chem. Int. Ed.* **2015**, *54*, 13659–13663; c) B. Zhou, P. Ma, H. Chen, C. Wang, *Chem. Commun.* **2014**, *50*, 14558–14561; d) B. Zhou, H. Chen, C. Wang, *J. Am. Chem. Soc.* **2013**, *135*, 1264–1267.
- [126] a) Y. F. Liang, L. Massignan, L. Ackermann, *ChemCatChem* **2018**, DOI: 10.1002/cctc.201800144; b) H. Wang, F. Pesciaioli, J. C. A. Oliveira, S. Warratz, L. Ackermann, *Angew. Chem. Int. Ed.* **2017**, *56*, 15063–15067; c) W. Liu, D. Zell, M. John, L. Ackermann, *Angew. Chem. Int. Ed.* **2015**, *54*, 4092–4096; d) W. Liu, J. Bang, Y. Zhang, L. Ackermann, *Angew. Chem. Int. Ed.* **2015**, *54*, 14137–14140; e) H. Wang, M. M. Lorion, L. Ackermann, *Angew. Chem. Int. Ed.* **2017**, *56*, 6339–6342; f) T. H. Meyer, W. Liu, M. Feldt, A. Wuttke, R. A. Mata, L. Ackermann, *Chem. Eur. J.* **2017**, *23*, 5443–5447.
- [127] a) C. Wang, A. Wang, M. Rueping, *Angew. Chem. Int. Ed.* **2017**, *56*, 9935–9938; b) S. Y. Chen, Q. Li, H. Wang, *J. Org. Chem.* **2017**, *82*, 11173–11181; c) S. Y. Chen, X. L. Han, J. Q. Wu, Q. Li, Y. Chen, H. Wang, *Angew. Chem. Int. Ed.* **2017**, *56*, 9939–9943; d) L. Shi, X. Zhong, H. She, Z. Lei, F. Li, *Chem. Commun.* **2015**, *51*, 7136–7139; e) Q. Lu, F. J. R. Klauck, F. Glorius, *Chem. Sci.* **2017**, *8*, 3379–3383.
- [128] a) Y. F. Liang, R. Steinbock, A. Münch, D. Stalke, L. Ackermann, *Angew. Chem. Int. Ed.* **2018**, *57*, 5384–5388. b) Q. Lu, S. Gressies, S. Cembellin, F. J. R. Klauck, C. G. Daniliuc, F. Glorius, *Angew. Chem. Int. Ed.* **2017**, *56*, 12778–12782; c) Y. F. Liang, V. Muller, W. Liu, A. Munch, D. Stalke, L. Ackermann, *Angew. Chem. Int. Ed.* **2017**, *56*, 9415–9419; d) S. Y. Chen, Q. Li, X. G. Liu, J. Q. Wu, S. S. Zhang, H. Wang, *ChemSusChem* **2017**, *10*, 2360–2364; e) S. Sueki, Z. Wang, Y. Kuninobu, *Org. Lett.* **2016**, *18*, 304–307.
- [129] W. Liu, S. C. Richter, Y. Zhang, L. Ackermann, *Angew. Chem. Int. Ed.* **2016**, *55*, 7747–7750.
- [130] W. Liu, S. C. Richter, R. Mei, M. Feldt, L. Ackermann, *Chem. Eur. J.* **2016**, *22*, 17958–17961.
- [131] Q. Lu, S. Gressies, F. J. R. Klauck, F. Glorius, *Angew. Chem. Int. Ed.* **2017**, *56*, 6660–6664.
- [132] a) H. Amii, K. Uneyama, *Chem. Rev.* **2009**, *109*, 2119–2183; b) J. L. Kiplinger, T. G. Richmond, C. E. Osterberg, *Chem. Rev.* **1994**, *94*, 373–431.
- [133] D. Zell, U. Dhawa, V. Müller, M. Bursch, S. Grimme, L. Ackermann, *ACS Catal.* **2017**, *7*, 4209–4213.
- [134] S. H. Cai, L. Ye, D. X. Wang, Y. Q. Wang, L. J. Lai, C. Zhu, C. Feng, T. P. Loh, *Chem. Commun.* **2017**, *53*, 8731–8734.
- [135] www.bmwi/Redaktion/EN/Dossier/renewable-energy.html accessed on 30.03.2018.
- [136] a) J. Collins, G. Gourdin, D. Qu, in *Green. Chem.*, Elsevier, **2018**, 771–860; b) W. Leitner, E. A. Quadrelli, R. Schlogl, *Green. Chem.* **2017**, *19*, 2307–2308.
- [137] Average prices calculated on the prices for the largest unit available at abcr, sigma-aldrich and fisher scientific, obtained on 20.04.2018.
- [138] a) H. Kolbe, *Liebigs. Ann. Chem.* **1849**, *69*, 257–294; b) H. Kolbe, *Liebigs. Ann. Chem.* **1848**, *68*, 339–341; c) M. Faraday, *Phil. Trans. R. Soc. Lond.* **1832**, *122*, 125–162; d) A. Volta, *Phil. Trans. R. Soc. Lond.* **1800**, *90*, 403–431.
- [139] a) P. Alfonso-Suárez, A. V. Koliopoulos, J. P. Smith, C. E. Banks, A. M. Jones, *Tetrahedron Lett.* **2015**, *56*, 6863–6867; b) A. M. Jones, C. E. Banks, *Beilstein J. Org. Chem.* **2014**, *10*, 3056–3072.
- [140] a) S. Möhle, M. Zirbes, E. Rodrigo, T. Gieshoff, A. Wiebe, S. R. Waldvogel, *Angew. Chem. Int. Ed.* **2018**, *57*, 6018–6041; b) A. Wiebe, T. Gieshoff, S. Möhle, E. Rodrigo, M. Zirbes, S. R. Waldvogel, *Angew. Chem. Int. Ed.* **2018**, *57*, 5594–5619; c) M. Yan, Y. Kawamata, P. S. Baran, *Angew. Chem. Int. Ed.* **2017**, *57*, 4149–4155; d) E. J. Horn, B. R. Rosen, P. S. Baran, *ACS Central Science* **2016**, *2*, 302–308; e) R. Francke, R. D. Little, *Chem. Soc. Rev.* **2014**, *43*, 2492–2521; f) J.-i. Yoshida, K. Kataoka, R. Horcajada, A. Nagaki, *Chem. Rev.* **2008**, *108*, 2265–2299.
- [141] a) A. Wiebe, S. Lips, D. Schollmeyer, R. Franke, S. R. Waldvogel, *Angew. Chem. Int. Ed.* **2017**, *56*, 14727–14731; b) L. Schulz, M. Enders, B. Elsler, D. Schollmeyer, K. M. Dybala, R. Franke, S. R. Waldvogel, *Angew. Chem. Int. Ed.* **2017**, *56*, 4877–4881; c) T. Gieshoff, A. Kehl, D. Schollmeyer, K. D. Moeller, S. R. Waldvogel, *J. Am. Chem. Soc.* **2017**, *139*, 12317–12324; d) A. Wiebe, D. Schollmeyer, K. M. Dybala, R. Franke, S. R. Waldvogel, *Angew. Chem. Int. Ed.* **2016**,

- 55, 11801–11805; e) B. Elsler, D. Schollmeyer, K. M. Dyballa, R. Franke, S. R. Waldvogel, *Angew. Chem. Int. Ed.* **2014**, *53*, 5210–5213.
- [142] a) C. Li, Y. Kawamata, H. Nakamura, J. C. Vantourout, Z. Liu, Q. Hou, D. Bao, J. T. Starr, J. Chen, M. Yan, P. S. Baran, *Angew. Chem. Int. Ed.* **2017**, *56*, 13088–13093; b) Y. Kawamata, M. Yan, Z. Liu, D.-H. Bao, J. Chen, J. T. Starr, P. S. Baran, *J. Am. Chem. Soc.* **2017**, *139*, 7448–7451; c) E. J. Horn, B. R. Rosen, Y. Chen, J. Tang, K. Chen, M. D. Eastgate, P. S. Baran, *Nature* **2016**, *533*, 77; d) B. R. Rosen, E. W. Werner, A. G. O'Brien, P. S. Baran, *J. Am. Chem. Soc.* **2014**, *136*, 5571–5574; e) A. G. O'Brien, A. Maruyama, Y. Inokuma, M. Fujita, P. S. Baran, D. G. Blackmond, *Angew. Chem. Int. Ed.* **2014**, *53*, 11868–11871.
- [143] a) R. Hayashi, A. Shimizu, J.-i. Yoshida, *J. Am. Chem. Soc.* **2016**, *138*, 8400–8403; b) T. Morofuji, A. Shimizu, J.-i. Yoshida, *J. Am. Chem. Soc.* **2015**, *137*, 9816–9819; c) T. Morofuji, A. Shimizu, J.-i. Yoshida, *J. Am. Chem. Soc.* **2014**, *136*, 4496–4499; d) T. Morofuji, A. Shimizu, J.-i. Yoshida, *J. Am. Chem. Soc.* **2013**, *135*, 5000–5003; e) Y. Ashikari, A. Shimizu, T. Nokami, J.-i. Yoshida, *J. Am. Chem. Soc.* **2013**, *135*, 16070–16073; f) T. Morofuji, A. Shimizu, J. i. Yoshida, *Angew. Chem. Int. Ed.* **2012**, *51*, 7259–7262.
- [144] a) P. Xiong, H.-H. Xu, J. Song, H.-C. Xu, *J. Am. Chem. Soc.* **2018**, *140*, 2460–2464; b) H. B. Zhao, Z. J. Liu, J. Song, H. C. Xu, *Angew. Chem. Int. Ed.* **2017**, *56*, 12732–12735; c) P. Xiong, H.-H. Xu, H.-C. Xu, *J. Am. Chem. Soc.* **2017**, *139*, 2956–2959; d) Z. W. Hou, Z. Y. Mao, Y. Y. Melcamu, X. Lu, H. C. Xu, *Angew. Chem. Int. Ed.* **2017**, *57*, 1636–1639; e) L. Zhu, P. Xiong, Z. Y. Mao, Y. H. Wang, X. Yan, X. Lu, H. C. Xu, *Angew. Chem. Int. Ed.* **2016**, *55*, 2226–2229; f) H. B. Zhao, Z. W. Hou, Z. J. Liu, Z. F. Zhou, J. Song, H. C. Xu, *Angew. Chem. Int. Ed.* **2016**, *56*, 587–590; g) Z. W. Hou, Z. Y. Mao, H. B. Zhao, Y. Y. Melcamu, X. Lu, J. Song, H. C. Xu, *Angew. Chem. Int. Ed.* **2016**, *55*, 9168–9172.
- [145] a) K.-Y. Ye, G. Pombar, N. Fu, G. S. Sauer, I. Keresztes, S. Lin, *J. Am. Chem. Soc.* **2018**, *140*, 2438–2441; b) P. Wang, S. Tang, P. Huang, A. Lei, *Angew. Chem. Int. Ed.* **2017**, *56*, 3009–3013; c) O. Koleda, T. Broese, J. Noetzel, M. Roemelt, E. Suna, R. Francke, *J. Org. Chem.* **2017**, *82*, 11669–11681; d) N. Fu, G. S. Sauer, A. Saha, A. Loo, S. Lin, *Science* **2017**, *357*, 575–579; e) N. Fu, G. S. Sauer, S. Lin, *J. Am. Chem. Soc.* **2017**, *139*, 15548–15553; f) M. J. Llorente, B. H. Nguyen, C. P. Kubiak, K. D. Moeller, *J. Am. Chem. Soc.* **2016**, *138*, 15110–15113; g) L.-S. Kang, M.-H. Luo, C. M. Lam, L.-M. Hu, R. D. Little, C.-C. Zeng, *Green. Chem.* **2016**, *18*, 3767–3774; h) J. Chen, W.-Q. Yan, C. M. Lam, C.-C. Zeng, L.-M. Hu, R. D. Little, *Org. Lett.* **2015**, *17*, 986–989; i) H.-C. Xu, J. M. Campbell, K. D. Moeller, *J. Org. Chem.* **2014**, *79*, 379–391; j) W. C. Li, C. C. Zeng, L. M. Hu, H. Y. Tian, R. D. Little, *Adv. Synth. Catal.* **2013**, *355*, 2884–2890.
- [146] M. S. Freund, J. A. Labinger, N. S. Lewis, J. E. Bercaw, *J. Mol. Catal.* **1994**, *87*, L11–L15.
- [147] M. Khenkin Alexander, M. Somekh, R. Carmieli, R. Neumann, *Angew. Chem. Int. Ed.* **2018**, *57*, 4503–4507.
- [148] C. Amatore, C. Cammoun, A. Jutand, *Adv. Synth. Catal.* **2007**, *349*, 292–296.
- [149] a) Y. Fujiwara, I. Moritani, S. Danno, R. Asano, S. Teranishi, *J. Am. Chem. Soc.* **1969**, *91*, 7166–7169; b) Y. Fujiwara, I. Moritani, M. Matsuda, S. Teranishi, *Tetrahedron Lett.* **1968**, *9*, 633–636; c) I. Moritani, Y. Fujiwara, *Tetrahedron Lett.* **1967**, *8*, 1119–1122.
- [150] F. Kakiuchi, T. Kochi, H. Mutsutani, N. Kobayashi, S. Urano, M. Sato, S. Nishiyama, T. Tanabe, *J. Am. Chem. Soc.* **2009**, *131*, 11310–11311.
- [151] H. Aiso, T. Kochi, H. Mutsutani, T. Tanabe, S. Nishiyama, F. Kakiuchi, *J. Org. Chem.* **2012**, *77*, 7718–7724.
- [152] A. E. Proctor, L. A. Thompson, C. L. O'Bryant, *Ann. Pharmacother.* **2014**, *48*, 99–106.
- [153] M. Konishi, K. Tsuchida, K. Sano, T. Kochi, F. Kakiuchi, *J. Org. Chem.* **2017**, *82*, 8716–8724.
- [154] F. Saito, H. Aiso, T. Kochi, F. Kakiuchi, *Organometallics* **2014**, *33*, 6704–6707.
- [155] Y. B. Dudkina, D. Y. Mikhaylov, T. V. Gryaznova, A. I. Tufatullin, O. N. Kataeva, D. A. Vicic, Y. H. Budnikova, *Organometallics* **2013**, *32*, 4785–4792.
- [156] a) T. V. Grayaznova, Y. B. Dudkina, D. R. Islamov, O. N. Kataeva, O. G. Sinyashin, D. A. Vicic, Y. H. Budnikova, *J. Organomet. Chem.* **2015**, *785*, 68–71; b) T. Gryaznova, Y. Dudkina, M.

- Khrizanforov, O. Sinyashin, O. Kataeva, Y. Budnikova, *J. Solid State. Electr.* **2015**, *19*, 2665–2672.
- [157] a) M. Khrizanforov, S. Strekalova, V. Khrizanforova, V. Grinenko, K. Kholin, M. Kadirov, T. Burganov, A. Gubaidullin, T. Gryaznova, O. Sinyashin, L. Xu, D. A. Vicic, Y. Budnikova, *Dalton Trans.* **2015**, *44*, 19674–19681; b) D. Mikhaylov, T. Gryaznova, Y. Dudkina, M. Khrizanphorov, S. Latypov, O. Kataeva, D. A. Vicic, O. G. Sinyashin, Y. Budnikova, *Dalton Trans.* **2012**, *41*, 165–172; c) Y. B. Dudkina, D. Y. Mikhaylov, T. V. Gryaznova, O. G. Sinyashin, D. A. Vicic, Y. H. Budnikova, *Eur. J. Org. Chem.* **2012**, *2012*, 2114–2117.
- [158] a) M. N. Khrizanforov, S. O. Strekalova, V. V. Grinenko, V. V. Khrizanforova, T. V. Gryaznova, Y. H. Budnikova, *Russ. Chem. Bull.* **2017**, *66*, 1446–1449; b) M. N. Khrizanforov, S. V. Fedorenko, S. O. Strekalova, K. V. Kholin, A. R. Mustafina, M. Y. Zhilkin, V. V. Khrizanforova, Y. N. Osin, V. V. Salnikov, T. V. Gryaznova, Y. H. Budnikova, *Dalton Trans.* **2016**, *45*, 11976–11982; c) Y. B. Dudkina, D. Y. Mikhailov, T. V. Gryaznova, S. G. Fattakhov, Y. G. Budnikova, O. G. Sinyashin, *Russ. Chem. Bull.* **2013**, *62*, 2362–2366.
- [159] Q.-L. Yang, Y.-Q. Li, C. Ma, P. Fang, X.-J. Zhang, T.-S. Mei, *J. Am. Chem. Soc.* **2017**, *139*, 3293–3298.
- [160] Y.-Q. Li, Q.-L. Yang, P. Fang, T.-S. Mei, D. Zhang, *Org. Lett.* **2017**, *19*, 2905–2908.
- [161] A. Shrestha, M. Lee, A. L. Dunn, M. S. Sanford, *Org. Lett.* **2018**, *20*, 204–207.
- [162] C. Ma, C.-Q. Zhao, Y.-Q. Li, L.-P. Zhang, X.-T. Xu, K. Zhang, T.-S. Mei, *Chem. Commun.* **2017**, *53*, 12189–12192.
- [163] L. Ackermann, A. V. Lygin, *Org. Lett.* **2012**, *14*, 764–767.
- [164] F. Xu, Y.-J. Li, C. Huang, H.-C. Xu, *ACS Catal.* **2018**, 3820–3824.
- [165] Y. Qiu, C. Tian, L. Massignan, T. Rogge, L. Ackermann, *Angew. Chem. Int. Ed.* **2018**, *57*, 5818–5822.
- [166] S. De Sarkar, W. Liu, S. I. Kozhushkov, L. Ackermann, *Adv. Synth. Catal.* **2014**, *356*, 1461–1479.
- [167] a) P. Gomes, C. Gosmini, J. Périchon, *J. Org. Chem.* **2003**, *68*, 1142–1145; b) P. Gomes, C. Gosmini, J. Périchon, *Tetrahedron* **2003**, *59*, 2999–3002; c) P. Gomes, C. Gosmini, J.-Y. Nédélec, J. Périchon, *Tetrahedron Lett.* **2002**, *43*, 5901–5903; d) E. Le Gall, C. Gosmini, J.-Y. Nédélec, J. Périchon, *Tetrahedron Lett.* **2001**, *42*, 267–269; e) H. Fillon, C. Gosmini, J.-Y. Nédélec, J. Périchon, *Tetrahedron Lett.* **2001**, *42*, 3843–3846; f) C. Gosmini, Y. Rollin, J. Y. Nédélec, J. Périchon, *J. Org. Chem.* **2000**, *65*, 6024–6026; g) P. Gomes, C. Gosmini, J.-Y. Nédélec, J. Périchon, *Tetrahedron Lett.* **2000**, *41*, 3385–3388.
- [168] C. Tian, L. Massignan, T. H. Meyer, L. Ackermann, *Angew. Chem. Int. Ed.* **2018**, *57*, 2383–2387.
- [169] S. Tang, D. Wang, Y. Liu, L. Zeng, A. Lei, *Nat. Commun.* **2018**, *9*, DOI:10.1038/s41467-41018-03246-41464.
- [170] G. Cera, L. Ackermann, *Top. Curr. Chem.* **2016**, *374*, 57–91.
- [171] Y. Kommagalla, N. Chatani, *Coord. Chem. Rev.* **2017**, *350*, 117–135.
- [172] a) D. M. Flanigan, F. Romanov-Michailidis, N. A. White, T. Rovis, *Chem. Rev.* **2015**, *115*, 9307–9387; b) O. Schuster, L. Yang, H. G. Raubenheimer, M. Albrecht, *Chem. Rev.* **2009**, *109*, 3445–3478.
- [173] a) L. Raibaut, N. Ollivier, O. Melnyk, *Chem. Soc. Rev.* **2012**, *41*, 7001–7015; b) P. Tam James, J. Xu, D. Eom Khee, *Peptide Science* **2004**, *60*, 194–205; c) C. W. Tornøe, C. Christensen, M. Meldal, *J. Org. Chem.* **2002**, *67*, 3057–3064.
- [174] C.-J. Li, *Acc. Chem. Res.* **2009**, *42*, 335–344.
- [175] K. Gao, P.-S. Lee, C. Long, N. Yoshikai, *Org. Lett.* **2012**, *14*, 4234–4237.
- [176] a) G. Wittig, A. Krebs, *Chem. Ber.* **1961**, *94*, 3260–3275; b) G. Wittig, A. Krebs, R. Pohlke, *Angew. Chem.* **1960**, *72*, 324–324.
- [177] V. R. Yatham, W. Harnying, D. Kootz, J.-M. Neudörfl, N. E. Schlörer, A. Berkessel, *J. Am. Chem. Soc.* **2016**, *138*, 2670–2677.
- [178] a) X. Bugaut, F. Glorius, *Chem. Soc. Rev.* **2012**, *41*, 3511–3522; b) D. Enders, O. Niemeier, A. Henseler, *Chem. Rev.* **2007**, *107*, 5606–5655.

- [179] a) J. P. Wagner, P. R. Schreiner, *Angew. Chem. Int. Ed.* **2015**, *54*, 12274–12296; b) L. Schweighauser, M. A. Strauss, S. Bellotto, H. A. Wegner, *Angew. Chem. Int. Ed.* **2015**, *54*, 13436–13439; c) S. Grimme, P. R. Schreiner, *Angew. Chem. Int. Ed.* **2011**, *50*, 12639–12642; d) S. Grimme, R. Huenerbein, S. Ehrlich, *ChemPhysChem* **2011**, *12*, 1258–1261.
- [180] *Strategic Applications of Named Reactions in Organic synthesis*, Elsevier Academic Press, London, **2005**.
- [181] G. Cahiez, A. Moyeux, *Chem. Rev.* **2010**, *110*, 1435–1462.
- [182] *C–H and C–C Activation by Cobalt and Ruthenium Catalysis*, M. Moselage, PhD Thesis, Georg-August-Universität Göttingen (Göttingen), **2017**.
- [183] a) A. H. Hoveyda, A. R. Zhugralin, *Nature* **2007**, *450*, 243; b) A. K. Chatterjee, T.-L. Choi, D. P. Sanders, R. H. Grubbs, *J. Am. Chem. Soc.* **2003**, *125*, 11360–11370; c) A. Fürstner, *Angew. Chem. Int. Ed.* **2000**, *39*, 3012–3043.
- [184] a) N. A. Butt, W. Zhang, *Chem. Soc. Rev.* **2015**, *44*, 7929–7967; b) B. M. Trost, M. L. Crawley, *Chem. Rev.* **2003**, *103*, 2921–2944.
- [185] *Modern Heterocyclic Chemistry*, Wiley-VCH, Weinheim, **2011**.
- [186] *Cobalt(III)-Catalyzed Allylation and Alkyne Annulation*, J. Koeller, Master Thesis, Georg August Universität Göttingen (Göttingen), **2015**.
- [187] J. F. Daeuble, C. McGettigan, J. M. Stryker, *Tetrahedron Lett.* **1990**, *31*, 2397–2400.
- [188] a) R. Chinchilla, C. Najera, *Chem. Soc. Rev.* **2011**, *40*, 5084–5121; b) R. Chinchilla, C. Najera, *Chem. Rev.* **2007**, *107*, 874–922.
- [189] H. C. Kolb, M. G. Finn, K. B. Sharpless, *Angew. Chem. Int. Ed.* **2001**, *40*, 2004–2021.
- [190] a) N. Jin, C. Pan, H. Zhang, P. Xu, Y. Cheng, C. Zhu, *Adv. Synth. Catal.* **2015**, *357*, 1149–1153; b) C. Feng, T. P. Loh, *Angew. Chem. Int. Ed.* **2014**, *53*, 2722–2726; c) C. Feng, D. Feng, T.-P. Loh, *Chem. Commun.* **2014**, *50*, 9865–9868.
- [191] Y. Wu, Y. Yang, B. Zhou, Y. Li, *J. Org. Chem.* **2015**, *80*, 1946–1951.
- [192] a) J. Kaschel, D. B. Werz, *Angew. Chem. Int. Ed.* **2015**, *54*, 8876–8878; b) D. Fernández González, J. P. Brand, R. Mondière, J. Waser, *Adv. Synth. Catal.* **2013**, *355*, 1631–1639; c) P. Brand Jonathan, J. Charpentier, J. Waser, *Angew. Chem. Int. Ed.* **2009**, *48*, 9346–9349.
- [193] I. Crossing, I. Raabe, *Angew. Chem. Int. Ed.* **2004**, *43*, 2066–2090.
- [194] N. Sauermann, M. J. González, L. Ackermann, *Org. Lett.* **2015**, *17*, 5316–5319.
- [195] H. K. Grover, T. P. Lebold, M. A. Kerr, *Org. Lett.* **2011**, *13*, 220–223.
- [196] D. R. Stuart, M. Bertrand-Laperle, K. M. N. Burgess, K. Fagnou, *J. Am. Chem. Soc.* **2008**, *130*, 16474–16475.
- [197] N. Okamoto, K. Takeda, R. Yanada, *Org. Synth.* **2014**, *91*, 27–38.
- [198] L. Ackermann, H. K. Potukuchi, D. Landsberg, R. Vicente, *Org. Lett.* **2008**, *10*, 3081–3084.
- [199] *C–H Alkylations and Alkynylations Using Ruthenium, Nickel and Manganese Complexes*, Z. Ruan, PhD Thesis, Georg-August-Universität Göttingen (Göttingen), **2017**.
- [200] L. Ackermann, A. V. Lygin, *Org. Lett.* **2011**, *13*, 3332–3335.
- [201] Z. Ruan, N. Sauermann, E. Manoni, L. Ackermann, *Angew. Chem. Int. Ed.* **2017**, *56*, 3172–3176.
- [202] R. J. Sundberg, in *Heterocyclic Scaffolds II: Reactions and Applications of Indoles* (Ed.: G. W. Gribble), Springer Berlin Heidelberg, Berlin, Heidelberg, **2010**, 47–115.
- [203] a) J. B. Lambert, Y. Zhao, R. W. Emblidge, L. A. Salvador, X. Liu, J.-H. So, E. C. Chelius, *Acc. Chem. Res.* **1999**, *32*, 183–190. b) J. B. Lambert, G. T. Wang, R. B. Finzel, D. H. Teramura, *J. Am. Chem. Soc.* **1987**, *109*, 7838–7845. c) S. G. Wierschke, J. Chandrasekhar, W. L. Jorgensen, *J. Am. Chem. Soc.* **1985**, *107*, 1496–1500.
- [204] N. Sauermann, T. H. Meyer, Y. Qiu, L. Ackermann, *ACS Catal.* **2018**, submitted.
- [205] C. Stang, F. Harnisch, *ChemSusChem* **2015**, *9*, 50–60.
- [206] N. Sauermann, T. H. Meyer, C. Tian, L. Ackermann, *J. Am. Chem. Soc.* **2017**, *139*, 18452–18455;
- [207] a) C.-C. Chang, L.-C. Chen, S.-J. Liu, Chang, *J. Phys. Chem. B* **2006**, *110*, 19426–19432; b) O. R. Brown, S. Chandra, J. A. Harrison, *J. Electroanal. Chem. Interfacial Electrochem.* **1972**, *38*, 185–190.
- [208] T. H. Meyer, ongoing PhD Thesis, Georg-August-Universität (Göttingen), **2017**.

- [209] S. Santoro, A. Marrocchi, D. Lanari, L. Ackermann, L. Vaccaro, *Chem. Eur. J.* **2018**, *20*, DOI: 10.1039/C8G01115J.
- [210] W.-J. Gao, W.-C. Li, C.-C. Zeng, H.-Y. Tian, L.-M. Hu, R. D. Little, *J. Org. Chem.* **2014**, *79*, 9613–9618.
- [211] R. Mei, N. Sauermann, J. C. A. Oliveira, L. Ackermann, *J. Am. Chem. Soc.* **2018**, *140*, DOI: 10.1021/jacs.8b03521.
- [212] Y. Qiu, W. J. Kong, J. Struwe, N. Sauermann, T. Rogge, A. Scheremetjew, L. Ackermann, *Angew. Chem. Int. Ed.* **2018**, 5828–5832.
- [213] a) G. Song, X. Li, *Acc. Chem. Res.* **2015**, *48*, 1007–1020; b) T. Satoh, M. Miura, *Chem. Eur. J.* **2010**, *16*, 11212–11222; c) K. Fagnou, M. Lautens, *Chem. Rev.* **2003**, *103*, 169–196.
- [214] a) T. J. Hansen, D. A. Crowl, *Process Saf. Prog.* **2010**, 209–215; b) T. H. Pratt, *Process Saf. Prog.* **1993**, *12*, 203–205.
- [215] a) Y. Lu, H.-W. Wang, J. E. Spangler, K. Chen, P.-P. Cui, Y. Zhao, W.-Y. Sun, J.-Q. Yu, *Chem. Sci.* **2015**, *6*, 1923–1927; b) A. Archambeau, T. Rovis, *Angew. Chem. Int. Ed.* **2015**, *54*, 13337–13340; c) G. Zhang, H. Yu, G. Qin, H. Huang, *Chem. Commun.* **2014**, *50*, 4331–4334; d) G. Zhang, L. Yang, Y. Wang, Y. Xie, H. Huang, *J. Am. Chem. Soc.* **2013**, *135*, 8850–8853; e) D.-G. Yu, M. Suri, F. Glorius, *J. Am. Chem. Soc.* **2013**, *135*, 8802–8805; f) D. R. Stuart, P. Alsabeh, M. Kuhn, K. Fagnou, *J. Am. Chem. Soc.* **2010**, *132*, 18326–18339.
- [216] E. Kudo, Y. Shibata, M. Yamazaki, K. Masutomi, Y. Miyauchi, M. Fukui, H. Sugiyama, H. Uekusa, T. Satoh, M. Miura, K. Tanaka, *Chem. Eur. J.* **2016**, *22*, 14190–14194.
- [217] N. Sauermann, J. Loup, D. Kootz, V. R. Yatham, A. Berkessel, L. Ackermann, *Synthesis* **2017**, *49*, 3476–3484.
- [218] Q. L. Yang, P. Fang, T. S. Mei, *Chinese Journal of Chemistry* **2018**, *36*, 338–352.
- [219] N. Sauermann, R. Mei, L. Ackermann, *Angew. Chem. Int. Ed.* **2018**, *57*, 5090–5094.
- [220] B. Sun, T. Yoshino, S. Matsunaga, M. Kanai, *Chem. Commun.* **2015**, *51*, 4659–4661.
- [221] X. Y. Chen, L. Wang, M. Frings, C. Bolm, *Org. Lett.* **2014**, *16*, 3796–3799.
- [222] S. Petrova, E. Jager, R. Konefal, A. Jager, C. G. Venturini, J. Spevacek, E. Pavlova, P. Stepanek, *Polym. Chem.* **2014**, *5*, 3884–3893.
- [223] *Chemical Kinetics and Reaction Mechanisms*, 2nd ed. (Ed.: J. H. Espenson), McGraw-Hill, New York, **1995**.

Erklärung

Ich versichere, dass ich die vorliegende Dissertation im Zeitraum von November 2014 bis Juni 2018 am Institut für organische und biomolekulare Chemie der Georg-August-Universität Göttingen

Auf Anregung und unter Anleitung von

Prof. Dr. Lutz Ackermann

Selbstständig durchgeführt und keine anderen als die angegebenen Hilfsmittel und Quellen verwendet habe.

Göttingen, den
